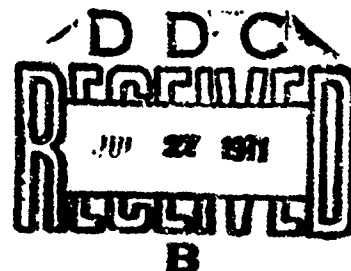




AD 726764

SER-611344

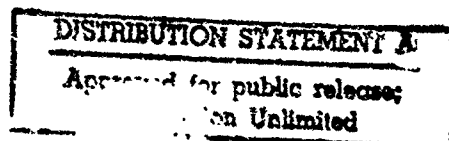
FINAL REPORT NH-3A  
(SIKORSKY S-61F)  
FLIGHT TEST PROGRAM



"Distribution of this Document is unlimited"

"This report has been reviewed by the Naval Air Systems Command. The findings in this report are those of the contractor and not those of the Naval Air Systems Command or the Department of the Navy."

Reproduced by  
NATIONAL TECHNICAL  
INFORMATION SERVICE  
Springfield, Va. 22151



Unclassified

Security Classification

DOCUMENT CONTROL DATA - R & D

Security classification of title, body of abstract and indexing annotation must be entered when the overall report is classified

1. ORIGINATING ACTIVITY (Corporate author) Sikorsky Aircraft United Aircraft Corp., Stratford, Conn.		2a. REPORT SECURITY CLASSIFICATION Unclassified	
3. REPORT TITLE Final Report - NH-3A (Sikorsky S-61F) Flight Test Program		2b. GROUP	
4. DESCRIPTIVE NOTES (Type of report and inclusive dates) Final Report			
5. AUTHOR(S) (first name, middle initial, last name) R. M. Segel, D. S. Jenney, W. Gerdes			
6. REPORT DATE March 20, 1969		7a. TOTAL NO. OF PAGES 167	7b. NO. OF REFS 7
8a. CONTRACT OR GRANT NO. Contract N0w-64-0528-f		9. ORIGINATOR'S REPORT NUMBER(S) SER-611344	
b. PROJECT NO.		9a. OTHER REPORT NO(S) (i.e., if this report) or numbers that may be assigned	
10. DISTRIBUTION STATEMENT Distribution of this Document is unlimited.			
11. SUPPLEMENTARY NOTES		12. SPONSORING MILITARY ACTIVITY Naval Air Systems Command	
13. ABSTRACT <p>&gt;This report summarizes a flight test evaluation of the effects of auxiliary propulsion, wings, rotor solidity, and blade twist on a modified SH-3A helicopter airframe with standard S-61 dynamic components. A total of 88 hours of tests explored performance, handling qualities, stresses, vibrations and control loads for eight different configurations.</p> <p>The primary objective of the program, to extend tests of the compound configuration to a maximum safe speed of not less than 200 knots, was achieved. Level flight and dive speeds of 211 and 230 knots, respectively, were reached. At 200 knots, rotor lift was varied from 25 to 75% of gross weight.</p> <p>Throughout the expanded flight envelope, handling qualities and structural loads confirmed predictions with few exceptions. The tests confirmed the ability of the articulated rotor system to operate satisfactorily in this flight regime and provided a basis for future aircraft design and for extrapolation to higher speed.</p>			

DD FORM 1473

(PAGE 1)

1 NOV 65  
54 0102-214-6600

Unclassified

Security Classification

Unclassified

Security Classification

KEY WORDS	LINK A		LINK B		LINK C	
	ROLE	WT	ROLE	WT	ROLE	WT
SH-3A, S-61F, Compound Helicopter Flight Tests Sikorsky Performance Load Sharing Handling Qualities Vibratory Stress						

Unclassified

Security Classification

# Sikorsky Aircraft DIVISION OF UNITED AIRCRAFT CORPORATION

U  
A

**TITLE:** Final Report - NH-3A (Sikorsky S-61F)  
Flight Test Program

**REPORT NUMBER:** SER-611344

**PREPARED UNDER:** Item 3(g), Contract NOW-64-0528-F

**REPORT DATE:** March 20, 1969

**REPORT PERIOD:**

This report is applicable to the following aircraft model(s) and contract(s):

**MODEL**

**CONTRACT**

NH-3A

NOW-64-0528-F

Distribution of this Document is unlimited.

This report has been reviewed by the Naval Air Systems Command. The findings in this report are those of the contractor and not those of the Naval Air Systems Command or the Department of the Navy.

Prepared by R. M. Segel, D. S. Jenney, W. Gerdes, et al.

Approved by E. A. Fradenburgh, Assistant Chief of Advanced Research

## REVISIONS

REV.	CHANGED BY	REVISED PAGE(S)	ADDED PAGE(S)	DELETED PAGE(S)	DESCRIPTION	DATE	APPROVAL
1	DSJ/ RKB	All	--	155 thru 160	To comply with AVLABS request.	11/3/70	<i>[Signature]</i>

REVISIONS CONTINUED ON NEXT PAGE



## ABSTRACT

This report summarizes a flight test evaluation of the effects of auxiliary propulsion, wings, rotor solidity, and blade twist on a modified SH-3A helicopter airframe with standard S-61 dynamic components. A total of 88 hours of tests explored performance, handling qualities, stresses, vibrations and control loads for eight different configurations.

The primary objective of the program, to extend tests of the compound configuration to a maximum safe speed of not less than 200 knots, was achieved. Level flight and dive speeds of 211 and 230 knots, respectively, were reached. At 200 knots, rotor lift was varied from 25 to 75% of gross weight.

Throughout the expanded flight envelope, handling qualities and structural loads confirmed predictions with few exceptions. The tests confirmed the ability of the articulated rotor system to operate satisfactorily in this flight regime and provided a basis for future aircraft design and for extrapolation to higher speed.

## FOREWORD

This report summarizes the results of a compound helicopter flight investigation conducted by Sikorsky Aircraft. The program was jointly funded and monitored by the U. S. Naval Air Systems Command (NAVAIRSYSCOM), and U. S. Army Aviation Materiel Laboratories (AVLABS). Due to the large number of configurations and test conditions and the duration of the flight investigation many individuals contributed to the program.

The program was monitored for NAVAIRSYSCOM by Messrs. Frank O'Brimski and John Snoderly. and for AVLABS by Messrs. Richard Adams and Richard Dumond.

NH-3A project engineers at Sikorsky were Messrs. F. de Sibert and J. E. Nedin. Program technical direction was provided by Mr. E. A. Fradenburgh. Additional Sikorsky Aircraft personnel closely associated with the program were Messrs. G. B. Chesley, G. M. Chuga, T. M. Coonan, P. J. D'Ostilio, R. R. Fenaughty, W. Gerdes, B. Graham, Jr., D. S. Jenney, W. H. Kimes, J. Kotkowski, D. F. Perrault, C. M. Reine, A. J. Ruddell, R. M. Segel, and P. VonHardenberg.

# TABLE OF CONTENTS

	<u>Page</u>
ABSTRACT . . . . .	ii
FOREWORD . . . . .	iii
LIST OF ILLUSTRATIONS . . . . .	v
LIST OF TABLES . . . . .	ix
LIST OF SYMBOLS . . . . .	x
INTRODUCTION . . . . .	1
DESCRIPTION OF VEHICLE . . . . .	3
DIMENSIONS AND GENERAL DATA . . . . .	5
TEST PROCEDURES . . . . .	8
RESULTS AND DISCUSSION . . . . .	11
. Operating Envelopes - Aircraft . . . . .	11
. Hover Performance . . . . .	14
. Aircraft Drag . . . . .	15
. Differential Wing Lift . . . . .	16
. Operating Limits - Main Rotor . . . . .	17
. Structural Loads . . . . .	22
. Flying Qualities . . . . .	30
CONCLUSIONS . . . . .	35
RECOMMENDATIONS . . . . .	36
REFERENCES . . . . .	37
APPENDIX	
I 1/12 Scale Model Wind Tunnel Data . . . . .	123
II Test Instrumentation . . . . .	131
III Typical Flight Test Data . . . . .	144

## LIST OF ILLUSTRATIONS

<u>Figure</u>	<u>Page</u>
1. Production SH-3A Helicopter . . . . .	46
2. NH-3A - Helicopter With Jets . . . . .	47
3. NH-3A - Helicopter With Jets - General Arrangement . . . . .	48
4. NH-3A Compound Helicopter Configuration . . . . .	49
5. NH-3A Compound Helicopter - General Arrangement . . . . .	50
6. NH-3A Helicopter - General Arrangement. . . . .	51
7. NH-3A Level Flight Envelope for Various Aircraft Configurations, Elevator Settings and Horizontal Stabilizer Incidences . . . . .	52
8. Hover Performance - Effect of Blade Twist (Basic Helicopter, Five Main Rotor Blades) . . . . .	60
9. Hover Performance - Effect of Rotor Solidity ( -4 Degrees Twist, With Jet Pods) . . . . .	61
10. Hover Performance - Effect of Wing Installation (Five Main Rotor Blades, -4 Degrees Twist) . . . . .	62
11. Lift Drag Polars . . . . .	63
12. Lateral Control Position Versus Airspeed . . . . .	65
13. Differential Wing Lift Test Installation . . . . .	66
14. Wing Lift Distribution . . . . .	67
15. Rotor Operating Envelope for Various Airspeeds and Rotor Configurations and 660 FPS Rotor Tip Speed . . . . .	69
16. Compressibility Mapping Conditions . . . . .	78
17. Dynamic Behavior During Blade Tip Excursion at 190 Knots . . . . .	79
18. Blade Pitching Moment Coefficient Versus Angle of Attack and Mach Number . . . . .	80
19. Analytical Reproduction of Blade Spread . . . . .	81
20. Control Loads at Points Below Theoretical Lower Stall Limit . . . . .	82

<u>Figure</u>		<u>Page</u>
21.	Change in Control Loads at Points Above Theoretical Stall Limit . . . . .	83
22.	Control Loads Correlation With CH-53A . . . . .	84
23.	Control Loads Correlation With CH-3C . . . . .	85
24.	Control System Load Contours at 175 Knots (Five Main Rotor Blades, -8 Degrees Twist) . . . . .	86
25.	Main Rotor Rotating Scissors, Vibratory Load (With Wings and Jets, Five Main Rotor Blades, -4 Degrees Twist) . . . . .	87
26.	Main Rotor Stationary Scissors, Vibratory Load (Without Wings, Six Main Rotor Blades, -4 Degrees Twist) . . . . .	88
27.	Blade Stresses at 70 Percent Radius Versus Airspeed (Five Main Rotor Blades, -4 Degrees Twist) . . . . .	89
28.	Effect of Rotor Lift and Airspeed on Blade Stress at 70 Percent Radius, (Five Blades, -4 Degrees Twist) . . . . .	90
29.	Effect of Number of Blades on Blade Stress With Auxiliary Propulsion, (-4 Degrees Twist) . . . . .	91
30.	Effect of Twist on Maximum Stress, (With Auxiliary Propulsion, Six Main Rotor Blades) . . . . .	92
31.	Effect of Rudder Deflection on Tail Rotor Stresses . . . . .	93
32.	Effect of Number of Blades and Blade Twist on Fuselage Vibration . . . . .	94
33.	NH-3A Cockpit Response Versus Frequency . . . . .	95
34.	Effect of Number of Blades on Transmission Support Stresses at Left Forward Fitting . . . . .	96
35.	Effect of Rotor Unloading on Cockpit Vibration . . . . .	97
36.	V-N Diagram for Various Aircraft Configurations . . . . .	98
37.	Lateral Directional Static Stability at 125 Knots (Five Main Rotor Blades, -8 Degrees, Zero Degree $i_{HT}$ ) . . . . .	101
38.	Correlation of Steady State Flight Parameters, (With Wings and Jets, Five Main Rotor Blades, -4 Degrees Twist, -15 Degrees $\delta_e$ , Zero Degree $\delta_f$ , 5 Degrees $i_{HT}$ ) . . . . .	102

# Figure

# Page

39.	Effect of Drag Reduction on Steady State Flight Parameters, (With Wings and Jets, Five Main Rotor Blades, -4 Degrees Twist, Zero Degree $\delta_e$ , 4 Degrees $\delta_f$ , Zero Degree $i_{HT}$ ) . . . . .	105
40.	Effect of Speed on Horizontal Tail Loading . . . . .	107
41.	Effect of Wing on Steady State Flight Parameters, (With Jets, Five Main Rotor Blades, -4 Degrees Twist, Zero Degree $\delta_e$ , -15 Degrees $\delta_f$ , 5 Degrees $i_{HT}$ ) . . . . .	108
42.	Effect of Wings on NH-3A Dynamic Response of Fuselage Attitude to a Longitudinal Pull and Return at 120 Knots, (With Jets, Five Main Rotor Blades, -8 Degrees Twist, Zero Degree $\delta_e$ , Zero Degree $i_{HT}$ ) . . . . .	110
43.	Correlation of Dynamic Response of Fuselage Attitude to a Longitudinal Pull and Return at 120 Knots, (With Jets, Five Main Rotor Blades, -8 Degrees Twist, Zero Degree $\delta_e$ , Zero Degree $i_{HT}$ ) . . . . .	111
44.	Effect of Solidity on Steady State Flight Parameters, Without Wings and Jets, -8 Degrees Twist, Zero Degree $\delta_e$ , Zero Degree $i_{HT}$ ) . . . . .	113
45.	Correlation of Dynamic Response of Fuselage Attitude to a Longitudinal Pull and Return at 120 Knots, (Without Wings, With Jets, Six Main Rotor Blades, -8 Degrees Twist, Zero Degree $\delta_e$ , Zero Degree $i_{HT}$ ) . . . . .	115
46.	Comparison of NH-3A and SH-3A Dynamic Response . . . . .	116
47.	Effect of Elevator Deflection on Steady State Flight Parameters, (With Wings and Jets, Five Main Rotor Blades, -8 Degrees Twist, 4 Degrees $\delta_f$ , Zero Degree $i_{HT}$ ) . . . . .	117
48.	Effect of Rudder Deflection on Steady State Flight Parameters, (With Wings and Jets, Five Main Rotor Blades, -4 Degrees Twist, Zero Degree $\delta_e$ , Zero Degree $\delta_f$ , Zero Degree $i_{HT}$ ) . . . . .	121
49.	1/12 Scale Wind Tunnel Model - NH-3A . . . . .	125
50.	Effect of Configuration on Longitudinal Characteristics, 1/12 Scale Airframe Model . . . . .	126
51.	Effect of Flap Deflection on Longitudinal Characteristics, 1/12 Scale Airframe Model . . . . .	127
52.	Effect of Elevator Deflection on Longitudinal Characteristics, 1/12 Scale Airframe Model . . . . .	128

<u>Figure</u>		<u>Page</u>
53.	Effect of Horizontal Tail Incidence on Longitudinal Characteristics, 1/12 Scale Airframe Model . . . .	129
54.	Effect of Fuselage Attitude on Lateral and Roll Characteristics, 1/12 Scale Airframe Model . . . .	130
55.	Airspeed Calibrations . . . . .	134

# LIST OF TABLES

<u>Table</u>	<u>Page</u>
I Data Flights . . . . .	38
II NH-3A Parasite Drag Breakdown . . . . .	45
III Control Rigging . . . . .	135
IV Oscillograph Measurements . . . . .	136
V Photopanel Measurements . . . . .	140
VI Instrumentation Accuracies . . . . .	141
VII Typical Flight Test Data . . . . .	144



# LIST OF SYMBOLS

A	rotor disc area, square feet
A <sub>ls</sub>	lateral cyclic control, degrees
a <sub>ls</sub>	longitudinal flapping, degrees
b	number of blades
B <sub>ls</sub>	longitudinal cyclic control, degrees
b <sub>ls</sub>	lateral flapping, degrees
c	chord, feet
$\bar{C}_D$	drag/dynamic pressure, square feet
$\bar{C}_L$	lift/dynamic pressure, square feet
$\bar{C}_\ell$	rolling moment/dynamic pressure, feet cubed
$\bar{C}_m$	pitching moment/dynamic pressure, feet cubed
C <sub>mb</sub>	control load coefficient

$$C_{mb} = \frac{2P \cdot l}{\rho R c^2 (\Omega R)^2 \cdot v \cdot t}$$

C <sub>P</sub>	power coefficient
----------------	-------------------

$$C_P = \frac{550 \text{ SHP}}{\rho A (\Omega R)^3}$$

C <sub>Q</sub>	torque coefficient
----------------	--------------------

$$C_Q = \frac{Q}{\rho A (\Omega R)^2}$$

C <sub>QD</sub>	drag torque coefficient
-----------------	-------------------------

$$C_{QD} = \frac{Q_D}{\rho A (\Omega R)^2}$$

$C_W$  weight coefficient

$$C_W = \frac{G.W.}{\rho A (\Omega R)^2}$$

CAS calibrated airspeed, knots

CG center of gravity, inches

CPM cycles per minute

$D_V$  vertical drag (download) on airframe due to rotor downwash

$f$  equivalent flat plate area, square feet

fps feet per second

$g$  acceleration of gravity

G.W. gross weight, pounds

$H_D$  density altitude, feet

$i_{HT}$  stabilizer incidence, degrees

IAS indicated airspeed, knots

KN nautical miles per hour, knots

$L$  lift, pounds

$L_R$  rotor lift, pounds

$l_t$  blade control horn arm length, feet

$M$  Mach number

$m$  blade root pitching moment

$N$  flight load factor

$N_R$  rotor speed, RPM or percent 100% = 203 RPM

PSI pounds per square inch

$P_V$  main rotor push rod vibratory control load, pounds

$q$  dynamic pressure

$$q = \frac{1}{2} \rho V^2$$

Q	torque, foot pounds
R	rotor radius, feet
RPM	revolutions per minute
SHP	shaft horsepower
SHP <sub>MR</sub>	main rotor shaft horsepower
V	true airspeed, feet per second
V <sub>T</sub>	true airspeed (TAS), knots
$\alpha_f$	fuselage angle of attack, degrees
$\delta_f$	flap deflection, degrees
$\delta_e$	elevator deflection, degrees
$\delta_R$	rudder deflection, degrees
$\theta_o$	collective pitch at the blade cuff, degrees
$\theta_{.75}$	collective pitch at the 75% blade radius, degrees
$\theta_l$	linear blade twist, degrees
$\mu$	advance ratio $\mu = \frac{V}{\Omega R}$
$\rho$	air density
$\sigma$	rotor solidity $\sigma = \frac{bc}{\pi R}$
$\Omega R$	tip speed, feet per second

## INTRODUCTION

Sikorsky Aircraft, with the support of the U. S. Naval Air Systems Command and U. S. Army Aviation Materiel Laboratories, has conducted a flight research program to demonstrate an expanded flight envelope for rotorcraft.

The conventional pure helicopter has limitations in forward flight caused by stall on the retreating blade. Both the lifting and propulsive capabilities of the rotor decrease with increasing speed. Compounding the helicopter, by adding a fixed wing and auxiliary propulsion is, therefore, a logical means of increasing speed potential. Theoretical research and wind tunnel tests of articulated rotors have shown that compound helicopters should be capable of practical speeds at least 100 knots faster than the pure helicopter. The NH-3A research program was prompted by the need for an aircraft of operationally useful gross weight to demonstrate these improved capabilities and to confirm the theoretical work under full-scale conditions.

The Navy/Sikorsky SH-3A, which was chosen as the base aircraft for the research program, was designed for a cruise speed of approximately 135 knots. It was known, however, that the rotor system of this aircraft was capable of much higher speeds. In February 1962, the SH-3A, with a special skid landing gear to reduce drag and weight, set a world's absolute speed record of 210 miles per hour, or 183 knots. This was an impressive achievement for a pure helicopter, surpassed as of the date of this report only by the SUD/Super Frelon using a similar system designed by Sikorsky Aircraft. The speed record set by the SH-3A, however, did not represent actual mission capability. The aircraft was stripped of all equipment unnecessary for the flight, and payload was nearly zero. Aircraft vibration, blade vibratory stresses, flying qualities, and maneuvering capability at maximum speed were satisfactory for establishing the record, but they were not satisfactory for operational use.

The major objectives of the NH-3A flight research program were:

- (1) Demonstration of improved aircraft capability. Speeds of at least 200 knots were desired with good useful load, low vibration, low stresses, improved flying qualities, and good maneuverability.
- (2) Determination of the effect of a number of design variables on aircraft characteristics. Eight aircraft configurations were tested. The variables included the number of rotor blades (five and six), two values of blade twist ( $-4^{\circ}$  and  $-8^{\circ}$ ), a wing (on and off), and auxiliary jet engines (on and off).
- (3) Experimental determination of rotor capability at high speed. The aircraft was designed to be used as a flying wind tunnel. The wing and auxiliary propulsion permitted operation of the main rotor over a wide range of conditions so that envelopes of rotor lift, propulsive force, and power loading capability could be established. This also permitted determination of rotor control power, flapping, dynamic behavior, and rotor-wing interference over a wide range of flight conditions.

The NH-3A research program has been successful in demonstrating an improved capability for rotary wing aircraft. Valuable research data were generated to permit the design of future high performance helicopters and compounds. All of the major objectives of the program were achieved.

## DESCRIPTION OF VEHICLE

The NH-3A (Sikorsky model S-61F) high-speed research helicopter is a modified SH-3A helicopter, Bureau No. 148033. A production SH-3A is shown in Figure 1.

The military electronics, sonar, armament, shackles, hoist, sonar seats, and automatic flight control system were removed from the aircraft, and the following changes were made:

WING: A wing of 170 square feet was installed in the "shoulder" position, with the aerodynamic center slightly aft of the rotor centerline. A full-span plain flap, capable of up or down deflection, was provided to trim the wing lift independently of fuselage angle of attack. The flap is controllable in flight through a "beeper" arrangement, with a normal rate of 3 degrees/second and an emergency "up" rate of 30 degrees/second.

AUXILIARY PROPULSION: Two Pratt & Whitney J-60-P2 turbojets, mounted in T-39 "Sabreliner" nacelles, were installed on either side of the fuselage, outboard of the landing gear sponsons.

TAIL CONE: A streamlined tail cone replaced the SH-3A aft fuselage. This modification provides a 17 degrees flapping clearance between the main rotor and the tail cone compared with 13 degrees for the SH-3A.

HORIZONTAL TAIL: A Cessna T-37 stabilizer with an added constant chord center section was installed. The incidence was ground adjustable. A "beeper" arrangement provided in-flight elevator control with a rate of 2 degrees/second.

VERTICAL TAIL: A large vertical tail with rudder was provided. The rudder deflection was controlled in-flight by a "beeper" with a rate of 2 degrees/second.

ROTOR HEAD: The automatic blade folding hardware was removed to reduce drag. A "beanie" fairing was installed on the rotor head.

OIL COOLER: A CH-3C/VH-3A oil cooler system was incorporated in the main rotor pylon area.

FUSELAGE: The aft cargo door, sonar well hole, and doppler antenna were eliminated and skinned over. An emergency exit panel was provided on the right-hand side of the cabin. The cockpit side windows were made fixed but jettisonable. The cockpit glass was reinforced or, in some areas, skinned over. The chin lines of the flying boat hull were rounded to provide a better streamlined nose shape.

LANDING GEAR: The open-well sponsons on the SH-3A were replaced with more streamlined sponsons with doors which completely enclose the main gear in the up position. The landing gear tread was reduced from 13 to 10 feet.

The following table gives dimensional information pertinent to the NH-3A (S-61F).

## DIMENSIONS AND GENERAL DATA

### Main Rotor:

Diameter	62 feet
Normal tip speed (100% $N_R$ )	660 fps.
Disc area	3019 ft. <sup>2</sup>
Blade chord	18.25 in.
Airfoil section	NACA 0012
Number of blades	5 or 6
Solidity, $\frac{bc}{\pi R}$	.0775 or 0.0937
Blade twist (center of rotation to tip)	-.4° or -8°
Root cutout (% radius of first blade pocket)	15%
Hinge offset	1.05 ft.
Articulation	Full flapping and lag
Blade weight moment about flap hinge	2876.1 ft. lb.
Blade moment of inertia about flap hinge	1703.5 ft-lb-sec <sup>2</sup>

### Tail Rotor:

Diameter	10 ft. 4 in.
Normal tip speed	660 fps.
Blade chord	7.34 in.
Airfoil section	NACA 0012
Number of blades	5
Solidity	.188
Blade twist	0°
Hinge offset	.323 ft.
Articulation	flapping only
Pitch flap coupling (delta-three angle)	45°

### Wing:

Span	32 ft. 0 in.
Area	170 ft. <sup>2</sup>
Exposed area	137 ft. <sup>2</sup>
Taper ratio (tip chord/theoretical root chord)	0.5



Wing (continued):

Tip chord	42.5 in.
Mean aerodynamic chord	72.8 in.
Twist	0°
Dihedral	0°
Sweep of 26% chord line	10°
Aspect ratio	6.04
Flap area (aft of hinge line)	29.8 ft. <sup>2</sup>
Flap chord (aft of hinge line)	26% wing chord
Airfoil section	NACA 63 <sub>2</sub> A 415

Tail Surfaces:

Horizontal tail area	76.2 ft. <sup>2</sup>
Horizontal tail span	20 ft. 0 in.
Elevator area	10.8 ft. <sup>2</sup>
Horizontal tail airfoil section	NACA 0010 modified
Vertical tail area (above WL 158)	44 ft. <sup>2</sup>
Rudder area	8.6 ft. <sup>2</sup>

Fuselage:

Length	56 ft. 0 in.
Cabin width	7 ft. 0 in.
Landing gear tread	10 ft. 0 in.
Wheel base	34 ft. 7.5 in.
Rotor head height	15 ft. 5.5 in.

Weights:

	<u>5 Blades</u>	<u>6 Blades</u>
	<u>lbs.</u>	<u>lbs.</u>
Rotor group (6 blades)		2517.5
Rotor group (5 blades)	2097.9	
Wing group $\frac{1}{4}$ chord Sta. 278.0	1014.0	1014.0
Tail group	350.9	350.9
Body group	2520.6	2520.6
Alighting gear	811.2	811.2
Eng. section (T-58)	141.7	141.7

Weights (continued):

	<u>5 Blades</u>	<u>6 Blades</u>
	<u>lbs.</u>	<u>lbs.</u>
Eng. section (J-60)	421.4	421.4
Powerplant group	2608.6	2608.6
Fixed equipment group	2910.5	2910.5
Weight empty	12876.8	13296.4
Useful load	6123.2	5703.6
Design gross weight	19000.0	19000.0

Powerplants:

Main propulsion unit

Two General Electric T58-GE-3B turboshaft engines with the following ratings at sea level standard day conditions:

<u>Ratings, Shaft hp</u>	<u>Power Shaft Output R.P.M.</u>	<u>Max. SFC lbs/SHP/hr</u>
Military - 1250	19,500	0.61
Normal - 1050	19,500	0.64

Auxiliary propulsion unit

Two Pratt & Whitney J-60P-2 turbojet engines with the following static ratings at sea level standard day conditions:

<u>Ratings</u>	<u>Jet Thrust lbs.</u>	<u>Maximum R.P.M.</u>	<u>Max. SFC lbs/hr/lb</u>
Military	2,900	16,400	0.930
Normal	2,570	15,750	0.905

## TEST PROCEDURES

Flight testing of the S-61F research aircraft was initiated on May 21, 1965, following satisfactory completion of proof load, shake, and tie-down tests. A total of 113 flights involving 88.2 hours of flight were completed during the test program which terminated on May 8, 1967. Flights were conducted at a density altitude of 3000 feet, except for the hovering, autorotation, and airspeed calibration flights, which required specific altitudes. A summary of the flights accomplished during the program is given in Table I.

### PRELIMINARY EVALUATION

For the initial phase of the test program the aircraft was configured as follows: two J-60 turbojet engines, a horizontal stabilizer with +5 degrees of incidence, and five main rotor blades with -4 degrees of twist. A photograph of this configuration is presented in Figure 2 and a general arrangement in Figure 3.

Initial flights were conducted without auxiliary jet thrust to provide pilot familiarization and preliminary evaluation of the basic characteristics of the helicopter, including handling qualities, performance, stress, and vibration levels.

### THRUST AUGMENTATION

Following the preliminary flight test phase, jet thrust augmentation was used to investigate higher speeds. Jet thrust augmentation was applied by the following "standard" procedure.

1. Set the J-60 jets at idle.
2. Trim the aircraft in level flight at a specified forward speed, 100 percent  $N_R$ , with the main rotor collective pitch control as required.
3. Lock the collective pitch.
4. Increase jet thrust as necessary to attain higher forward speeds.

When this procedure was followed, a high collective pitch and high rotor shaft power level resulted from an initial high speed trim condition,

and a medium collective pitch and rotor power resulted from an initial trim speed near the minimum power speed of the helicopter (70-80 knots). To establish a low collective pitch, low rotor power condition, the aircraft was first trimmed at 80 knots, and then the collective pitch was lowered to the prescribed value while increasing jet thrust as required to maintain speed and altitude.

#### COMPOUND CONFIGURATION

A photograph and general arrangement of the compound configuration are shown in Figures 4 and 5. After initial flights in this configuration for aircraft familiarization, several combinations of elevator and flap settings were investigated to vary rotor/wing load sharing, and establish the maximum speed of the configuration. A stabilizer incidence of zero degrees was selected and used for the remainder of the program. A maximum true airspeed of 221.6 knots (212.2 knots CAS) was achieved with a rate of descent of 1300 feet/minute. The basic test procedure was the "standard" procedure described above. During testing of the compound configuration with -4 degree twist blades, several additional evaluations were completed, including the following:

1. Investigations of a blade tip excursion phenomenon associated with advancing blade Mach number and low frequency vertical response characteristics of the fuselage.
2. Evaluation of asymmetric wing lift including in-flight photographs of tufts installed forward of the leading edge of the wing.
3. Two stages of drag reduction at Flight No. 30 and Flight No. 40 with improved wing root fairing, sealing of the gaps in the wing flaps, and general clean-up. A maximum level flight true airspeed of 210.9 knots (199.3 knots CAS) was achieved with this configuration.

#### BLADE TWIST EVALUATION

The effects of blade twist on rotor stall characteristics, blade

stress levels, advancing blade compressibility, and aircraft performance were investigated through tests of both -4 degree and -8 degree twist main rotor blades. The aircraft configuration remained unchanged except for the rigging changes necessary with the increased blade twist. Twist effects were evaluated on both the helicopter and compound configuration and with both 5 and 6 blades.

#### ROTOR SOLIDITY EVALUATION

The thrust augmented helicopter (without wings) was tested with both five and six-bladed rotors to determine the effects of increased solidity ratio on aircraft performance, handling qualities, vibration, and stress levels.

In addition to establishing the boundary limits for the six-bladed configuration, static and dynamic stability maneuvers as well as coordinated turns were accomplished. Hover performance data were also recorded with both the -4 degree and -8 degree twist main rotor blades.

#### PURE HELICOPTER CONFIGURATION

The aircraft was configured for the pure helicopter tests to provide baseline data by removing the jet engine pods and installing an aerodynamic fairing outboard of the sponsons. The general arrangement is shown in Figure 6. Flight testing provided baseline data in the areas of aircraft performance, handling qualities, vibration, and structural loads with both the -4 degree and -8 degree twist rotor blades. Flight conditions included level flight, autorotation, and dynamic stability maneuvers. Hover performance data were also recorded with both the -4 degree and -8 degree twist main rotor blades.

## RESULTS AND DISCUSSION

### OPERATING ENVELOPES-AIRCRAFT

The achieved operating envelopes of the eight aircraft configurations are shown in Figure 7a through 7h in terms of airspeed and rotor shaft horsepower. In each case, the helicopter flight mode (jets idle or removed as applicable) is presented as a solid curve. In addition, Figures 7a through 7f show points achieved with jet thrust augmentation at various main rotor collective pitch settings. These data are also listed with values of jet thrust and rotor lift and rotor drag in Table VII. Factors which limited the aircraft operating envelopes are discussed in the succeeding paragraphs.

### Helicopter With Thrust Augmentation

#### a. Five Blades, -4 Degrees Twist

The envelope for this configuration is shown in Figure 7a. With collective pitch settings at the 80 knot value or lower, the high speed boundary was defined by available jet thrust. The aircraft was flown in level flight autorotation at full low collective at 162.3 knots CAS and 5200 pounds of jet thrust.

At collective pitch settings above the 80 knot value, forward speed was limited by retreating blade stall, indicated by aircraft roughness and elevated control loads. Main rotor transmission support stresses indicated elevated levels at high shaft horsepower, but this condition was considered acceptable for short periods of operation.

#### b. Five Blades, -8 Degrees Twist

The envelope for this configuration is shown in Figure 7b.

The increased blade twist provided a greater rotor propulsive force capability, permitting a slight expansion of the high power portion of the envelope. A maximum speed of 196.2 knots (207.0 knots TAS) was attained at the 100 knot collective pitch setting. Further increases in collective pitch were limited by aircraft roughness, high main rotor control system loads, and high stress levels at the forward transmission support fitting. The aircraft was also flown as an autogyro with full low collective, at speeds from 85 to 167 knots CAS.

#### Compound Configuration

a. Five Blades, -4 Degrees and -8 Degrees Twist

The envelopes for these configurations are shown in Figures 7c and 7d. A maximum level flight calibrated airspeed of 199.3 knots (210.9 knots TAS) was achieved at the 130 knot collective pitch setting, utilizing 5485 pounds of jet thrust and 1668 main rotor shaft horsepower with the -4 degree twist blades.

In the compound configuration, the upper portion of the speed boundary was extended to higher speeds compared to the wingless configuration. This expansion was possible because of the additional lift produced by the wing. Reduced rotor lift requirements permitted additional rotor propulsive force for a comparable degree of rotor stall. Main rotor control loads and vibratory stress levels at the transmission attachment fittings showed considerable reduction in magnitudes as the main rotor loading was decreased. Available jet thrust was the limiting factor in establishing the level flight speed boundary for the compound configuration.

### Six-Bladed Helicopter With Thrust Augmentation

The envelopes established for this configuration with -4 degree and -8 degree twist blades are presented in Figures 7e and 7f. The n/rev. aircraft vibration levels and transmission attachment stress levels were considerably reduced with the six-bladed configuration and presented no problem at high main rotor shaft horsepower. However, the stationary scissors link of the main rotor control system exhibited higher loads than with the five-bladed rotor at high collective pitch settings.

Full jet thrust was utilized with the 120 knot collective pitch setting to achieve a maximum calibrated airspeed of 204.5 knots (215.0 knots true airspeed) with -4 degree twist blades. This condition was obtained utilizing 5690 pounds of jet thrust and 1390 shaft horsepower. Further increases in collective pitch were limited by the high stationary scissors loads. With lower values of collective pitch, maximum forward speeds decreased and jet thrust became the limiting factor.

### Pure Helicopter

Figures 7g and 7h present the level flight performance of the pure helicopter configuration. Data points are shown for zero stabilizer incidence and elevator settings of zero and -2 degrees. As illustrated in Figure 7g, a power-limited maximum level flight calibrated airspeed of 152.0 knots (160.2 knots true airspeed) was obtained with the -8 degree twist rotor blades while utilizing 2440 shaft horsepower from the T-58 engines. Under similar flight conditions with the -4 degree twist blades installed, a speed of 144.0 knots



calibrated airspeed (152.3 knots true airspeed) was obtained using 2390 shaft horsepower.

#### HOVER PERFORMANCE

In addition to accomplishing the primary investigation of high speed flight, a limited study was conducted to determine the effect of each of the configuration changes on NH-3A hover performance.

The effect of blade twist is shown in Figure 8, which compares the hover performance of five bladed rotors, having -4 degrees and -8 degrees twist. The lower (solid) curve was derived from Sikorsky main rotor test stand data for -8 degree twist blades. Experimentally determined tail rotor power, fixed losses, and 3 percent vertical drag have been added. This curve correlates well with the NH-3A hover data for -8 degree twist blades.

The Goldstein-Lock method (Reference 1) was used to estimate the increment in power due to the change in twist. This increment of 2% in power was applied to the -8 degree data to predict the performance of the -4 degree twist rotor shown in the upper curve. The test results appear to confirm the predicted penalty.

A comparison of the NH-3A hover data with 5 and 6 blades (of -4 degrees twist) is shown in Figure 9. The performance increment due to the change in solidity, estimated by the Goldstein-Lock method, is also shown. The five blade data were acquired in ground effect and corrected to the OGE conditions. With six blades, the aircraft was flown at a lower gross weight in order to hover OGE.

The vertical drag effect of the wing and sponson/engine installation is shown in Figure 10, which compares hover data for the pure helicopter (from Figure 8) and compound configurations. At constant power, a 6 percent reduction was required in the compound helicopter gross weight. This increment is the vertical drag contribution of the wing and sponson/engine installation.

#### AIRCRAFT DRAG

Aircraft drag has been estimated using measured values of jet thrust, main rotor thrust and torque, and main rotor drag calculated by the method of Reference 2. The lift-drag polars resulting from this procedure are shown in Figures 11a and b for the jet augmented helicopter and the full compound configuration respectively. The improvement at 160 knots due to the drag reduction program is approximately two to three square feet. The drag reduction modifications performed after flight number 39 included the following items:

1. Enlarged wing-fuselage junction fairings.
2. Reworked landing gear fairing.
3. Streamlined tail rotor gear box nose section.
4. Covered various openings on the aircraft.
5. Elimination of various antennae.

Equivalent parasite area was found to increase with forward speed, particularly in the full compound configuration. The reason for this speed dependency has not been firmly established, but a probable source of the drag increase is spillage from the T-58 engine air intakes. A decrease in accuracy of the rotor performance calculations with forward speed may also contribute to the apparent drag increase. Correlation of the full-scale wind tunnel tests of an H-34 rotor system, reported in Reference 3, indicated that at lift and torque coefficients similar to NH-3A flight test values, the theory was increasingly optimistic with forward speed. This would result in an apparent increase in airframe parasite area.

Table II presents the estimated parasite drag breakdown of the full compound configuration at 160 knots. These data are based on flight tests of the SH-3A and wind tunnel investigations, with analytical corrections where applicable.

The J-60 nacelles as-installed were found to be producing nearly three times the estimated drag. In addition, local separated flow, which was observed on the wing and landing gear pod fillets and on the wing

flap, is believed to have caused penalties as shown. It is notable that the drag of the pure helicopter (without wings and J-60's) was reduced 20 percent below that of the SH-3A even though the rotorhead was unmodified except for removal of blade fold parts, and the cockpit canopy shape and engine inlets were left unchanged. Improvements in these areas would be particularly fruitful at speeds above 200 knots.

#### DIFFERENTIAL WING LIFT

During initial tests of the compound configuration, wing instrumentation indicated that the left wing lift was higher than the right. This finding was substantiated by examination of lateral cyclic pitch data. Figure 12 shows that with the wing installed an increment of left lateral stick, which increased with forward speed, was required to balance the wing rolling moment.

To further define the wing lift distribution, tufts were installed on a wire mounted 8 inches forward of the wing leading edge. The test installation is shown in Figure 13. Local angle of attack was determined from film records of these tufts, taken in various flight conditions. Wing lift distributions were then determined from the experimental angle-of-attack and two-dimensional characteristics of the wing airfoil (NACA 63<sub>2</sub>A415). While there was some scatter in the data, it was generally found that very low angles of attack were developed on the inboard portion of the wing (above the sponson). In addition angles of attack on the right wing were lower than on the left. The aircraft was flown with wings level in a slight right sideslip. This resulted in a higher lift on the right sponson, which probably caused the greater lift interference on the right wing.

Sikorsky Aircraft recently conducted a U. S. Army AVLABS sponsored investigation of rotor-wing fuselage aerodynamic interference effects, Reference 4. The results of that program were reviewed and spanwise lift distributions are compared for two flight conditions with the NH-3A data in Figure 14. As in the flight test data, the wind tunnel results indicate a slightly reduced right wing lift, although the effect is less pronounced.

It was concluded from the flight and wind tunnel tests that lower right wing lift is caused by rotor induced velocity producing a higher downwash under the advancing blade. In addition, on the NH-3A, a large interference effect occurs on the inboard portion of both wings due to the close proximity of the sponson (located directly below and forward). The effect of differential wing lift on overall performance and control characteristics is small, but it should be considered in the design of an optimized compound helicopter.

#### OPERATING LIMITS - MAIN ROTOR

The envelope of achievable main rotor lift and propulsion (or drag) at a given speed is bounded by allowable limits of collective pitch, cyclic pitch, and blade flapping, and by allowable levels of rotor stall and aircraft vibration. The operating regime for the rotor was predicted in advance of flight test, using the theory of Reference 2.

In order to compare actual performance with predicted performance, theoretically derived boundary plots have been constructed at three forward speeds: 156 knots ( $\mu = .40$ ), 175 knots ( $\mu = .45$ ), and 195 knots ( $\mu = .50$ ). For flight test data points near these three speeds ( $\pm 9$  knots), main rotor lift and drag have been determined using measured values of main rotor torque, rotor thrust, and jet thrust. The measured quantities from representative flights, were used in combination with the theory of Reference 2, to derive the aircraft wing/body lift-drag polars presented in Figure 11. Using these polars, rotor propulsive force could be determined for all data points by subtracting jet thrust from aircraft drag. For most flights, a direct measurement of rotor thrust was available. This was checked against gross weight less wing/body lift derived from wind tunnel data presented in Appendix I.

The flight test program was arranged to test the theoretical rotor envelope as far as possible, using jet thrust to achieve speed points up to maximum speed and changes in wing flap and elevator settings to vary wing/body lift. Figure 15 shows the predicted envelopes and the points at which data were obtained at 156, 175, and 195 knots. Numerical

values of the data are also listed in Table VII. Experimentally determined vibration and jet thrust limits are also shown.

The basic envelope of the rotor is determined by retreating blade stall, indicated by the upper stall limits, and by the zero horsepower (autorotation) line. Additional limits peculiar to the NH-3A aircraft are the transmission rating of 2300 horsepower, collective pitch limits of 14.5 degrees maximum and 1.0 degree minimum. The jet thrust limit, determined by the installed thrust and airframe parasite drag, is also shown, because it constitutes a basic limit of the NH-3A in level flight. With more thrust, or reduced drag, this limit would shift to the right. The experimentally determined vibration limit is shown, when encountered, on a number of envelopes.

Further limits including main rotor flapping and longitudinal cyclic pitch, may be predicted. However, these quantities are dependent upon fuselage attitude, in addition to rotor lift and drag, and, consequently are not shown in Figure 15 which is valid for any fuselage attitude.

As speed increases, the predicted envelope shrinks due to the decreasing lift and propulsive force capability of the rotor. The flight test data follow this trend, covering most of the area within the theoretical rotor envelopes, and lend validity to the use of the charts of Reference 2 for predicting rotor operating envelopes. Those areas of the predicted envelopes which were not covered by flight data were limited by factors beyond the scope of the theoretical analysis. These factors are discussed in the following sections.

### Flapping

The design flapping limit for the NH-3A rotor system is  $\pm 8$  degrees relative to the shaft. This value is based on structural criteria for satisfactory life of the main rotor shaft.

At most flight conditions flapping values were well below the design limit. The only exceptions occurred when the rotor angle of attack was excessively negative at relatively high fuselage attitudes. Such conditions occurred when the rotor generated large amounts of propulsive force necessary to overcome parasite drag at high speeds. Large amounts of forward cyclic stick were then required, resulting in high forward flapping relative to the shaft to maintain steady level flight.

### Control Limits

The control margins of the NH-3A were adequate in all configurations. No control limits were encountered, except under the conditions described in the preceding paragraph, when the longitudinal stick forward limit was reached at high nose-up attitudes. This condition was corrected by applying 2 degrees of down elevator. A more detailed discussion of control characteristics is contained under FLYING QUALITIES.

### Blade Spread Phenomenon

During flight testing of the NH-3A under some conditions at high advancing tip Mach numbers, the main rotor tip path split into two distinct planes. The characteristics of this phenomenon were the following:

1. The tip path plane spread was observed by the pilots and was felt as a vertical bounce.
2. The spread was a maximum over the nose and was seen as two distinct tip path planes.
3. Blade tip excursions between the two planes of approximately  $2\frac{1}{2}$  to 3 feet were noted.
4. The blade spread increased with increasing Mach number.
5. A normal acceleration of the aircraft center of gravity was recorded at  $2\frac{1}{2}$  per rev.
6. Blade stress levels remained generally unchanged except for a small amount of  $2\frac{1}{2}$  per rev flatwise stress and  $\frac{1}{2}$  per rev torsional stress peaking at azimuth  $\psi = 90$  degrees.
7. There was no deterioration in control power or any tendency for the aircraft to rotate about any axis.
8. On reducing rotor rpm rapidly, the tip path plane spread ceased almost immediately.
9. No physical damage resulted from the blade spread.
10. The blade spread could not be eliminated by fine tuning of blade track or by close matching of tip caps.

The conditions under which blade spread occurred in the five-bladed rotor are shown in Figure 16. The major parameter is advancing tip Mach number, with blade spread occurring only at values above  $M = 0.92$ .

An example of the measured blade and airframe response under conditions of tip spread is shown for several revolutions in Figure 17. The reversal in the torsional stress peak at 90 degrees azimuth suggested the existence

of blade pitching moments of alternating sign at high Mach numbers. Although two dimensional data were not available for the C012 airfoil at these conditions, examination of data for other airfoils showed that a forward shift in airfoil center of pressure probably occurs at Mach numbers above 0.7. It was not possible to determine the exact form of the pitching moment characteristics, but the coefficients shown in Figure 18 were developed for use in the blade analysis.

With these data, the  $\frac{1}{2}$  per revolution characteristics of the S-61 blade was predicted analytically using the Sikorsky/UAC Research Laboratories Normal Mode Blade Aeroelastic Transient Analysis. Figure 19 clearly shows the large calculated tip deflection occurring on alternating revolutions. The angle of attack of the advancing tip alternates between plus and minus  $1\frac{1}{2}$  degrees on successive revolutions while the retreating tip angle of attack exceeds 20 degrees, and is thus stalled. As anticipated, the pitching moment at the advancing tip is positive for one revolution and partly negative in the following revolution.

The reversal in sign of the advancing tip angle of attack during successive revolutions appears to be due to the first flatwise blade mode which has a frequency of approximately  $2\frac{1}{2}$  per revolution at normal rotor speed. This frequency is approximately coincident with the NH-3A fuselage first vertical bending mode. Therefore the measured  $2\frac{1}{2}$  per revolution vertical acceleration of the fuselage center of gravity was due to the combined response of the blade flatwise mode and the fuselage bending mode at that frequency.

Analytical studies showed that the blade spread could be eliminated, either by decreasing the positive moments at high Mach numbers, or by increasing the blade first flatwise natural frequency to remove it from proximity to  $2\frac{1}{2}$  per revolution. In addition it was found that the occurrence of stall on the retreating blade was not significant in the mechanism of blade spread. A more detailed analysis of the phenomenon is presented in Reference 5.

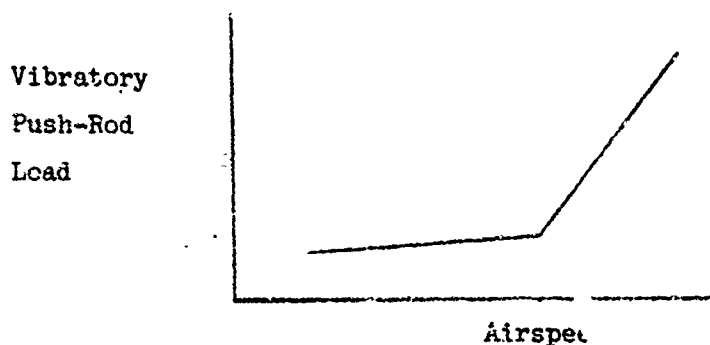


## STRUCTURAL LOADS

### Control System Loads and Retreating Blade Stall

During the NH-3A compound helicopter flight tests, control load data were obtained on an articulated rotor over a wide range of speed and rotor operating conditions. These data have been analyzed to establish the effects of high speed and rotor unloading on the level of vibratory control loads before stall and the rate of build-up beyond the onset of stall. From this study, an empirical method has been developed for predicting control loads.

The vibratory load in the rotating control system of conventional helicopters generally follows the pattern sketched below:



The level of pushrod load is nearly constant up to some airspeed and increases rapidly at higher speeds. Accurate prediction of the "knee" of this control load curve, and the load build-up beyond it, is important in order to define the load spectrum for control system design. In a pure helicopter, this curve is generated at one value of rotor lift (aircraft gross weight), and the knee of the curve has been found to correspond reasonably to the onset of stall defined by the lower stall limit criterion of Reference 2 ( $bC_{QD/c} = .004$ ).

In a compound helicopter such as the NH-3A, the rotor can be unloaded to the degree necessary to delay or avoid retreating blade stall. A large number of NH-3A control load data points were analyzed on the basis of the stall criterion, and the points below the theoretical lower stall limit have been plotted in Figure 20 as a function of advance ratio. The curve through the points shows an increase in vibratory load level with increasing

advance ratio. The points represent a wide range of unstalled rotor lift and propulsive force conditions, demonstrating the basic influence of advance ratio upon vibratory control loads.

Data obtained at conditions beyond the theoretical lower stall limit would fall above the curve of Figure 20. These loads have been analyzed in terms of the degree of stall penetration defined by the rise in rotor torque:

$$\Delta C_Q/\sigma = C_Q/\sigma_{Exp} - C_Q/\sigma_{CR}$$

where

$\Delta C_Q/\sigma$  is the measure of the degree of stall.

$C_Q/\sigma_{Exp}$  is the measure  $C_Q/\sigma$  at a specific test condition.

$C_Q/\sigma_{CR}$  is the value of  $C_Q/\sigma$  ( given by Reference 2 ) at the lower stall limit with the rotor operating at the advance ratio and  $C_D/\sigma$  values of the test point.

Under stalled conditions, the control load increment above the curve of Figure 21 is defined as  $\Delta C_{mb}$ . The effect of stall penetration upon  $\Delta C_{mb}$  is shown in Figure 21. These data encompass the entire high speed range and both -4-degree. and -8-degree twist blades. The fairing provides an approximation of the loads developed at high speed; over a wide range of rotor loadings. A value of  $C_{mb}$  can be defined at any operating condition from the value below stall in Figure 20, the degree of penetration,  $\Delta C_Q/\sigma$  from Reference 2 and the control load build-up beyond stall from Figure 21.

To verify this technique, it has been used to predict the control load characteristics of the CH-53A and CH-3C helicopters. The results are compared with flight test data in Figures 22 and 23. Good correlation has been obtained for both rotor systems.

This technique, when applied to the NH-3A rotor operating envelope, gives a set of control load contours which correspond to the test data. A sample envelope at 175 knots (equivalent to the envelope in Figure 15c is presented in Figure 24, which shows the effects of rotor lift and drag on the control loads. Below the  $\pm 465$  lb contour, equivalent to the lower stall limit, the loads are nearly constant. The higher contours indicate the load build-up as stall is penetrated. It is apparent that rotor lift level, and, to a lesser extent, the rotor drag have a strong influence on control loads when the rotor is operating beyond the theoretical lower stall limit. It should be noted that these loads correspond only to steady level flight. During most maneuvers, with the rotor out of equilibrium, control load levels are substantially lower than the values that would be predicted, extrapolating from steady-state values.

A limitation encountered with the five-bladed rotor system was the high vibratory load in the rotating scissors link of the main rotor control system. Loads above the endurance limit were encountered when operating at high forward speeds and high collective pitch settings. Rotating scissors loads obtained with the compound configuration and five-bladed rotor system are shown in Figure 25. The loads increased rapidly with airspeed when trimmed at the maximum 135 knot collective trim setting. This increase closely parallels the build-up of push-rod loads and was apparently due to blade stall. With the wing removed greater rotating scissors loads were obtained at an equivalent collective pitch setting since the rotor was more heavily loaded.

With the six-bladed rotor configuration increased loads on the rotating scissors were anticipated, and provisions were made for the installation of dual rotating scissors. Due to the load sharing between the two scissors, vibratory stresses were reduced to low levels for all flight conditions. The stationary scissors, however, which indicated lower loads with the five-bladed configuration showed a substantial increase in vibratory load for the six-bladed rotor system. This increase in load was noted both with and without auxiliary jet thrust and became a limiting factor when operating with high collective pitch at high forward speed. Figure 26 shows that load levels exceed the endurance limit of the scissors at high forward speeds with the 120

knots collective pitch setting. The approximate boundary imposed by these loads was shown in Figure 151. Since this limit did not severely restrict the flight envelope, no modifications were considered necessary.

### Blade Stress

The effect of rotor lift and drag upon blade stress characteristics was investigated over a wide range of airspeeds. In addition, main rotor blade twist and number of blades were varied to evaluate the effects of these parameters upon blade stress. Recent emphasis on high speed rotor operation has made reduction of blade stress particularly important, because stress, rather than power, may determine maximum allowable flight speeds.

In an articulated rotor, the maximum blade vibratory stress usually occurs at the bottom rear corner of the spar at 60 to 70 percent span (gage BR-7 for the NH-3A). Figure 27 is a composite plot showing the effect of wings and auxiliary propulsion on blade stress of the five blade, -4 degree twist rotor. The bands represent stress data from numerous flights over a range of rotor operating conditions. The band is widest for the full compound configurations due to the increased size of the available flight envelope.

Without wings or jet engines, the vibratory stress level approached 6,000 psi at 140 knots (CAS). The addition of auxiliary propulsion to the pure helicopter reduced the rate of stress increase with airspeed - apparently because of rotor unloading produced by the jet engine-sponson assembly which developed considerable lift at high speeds. The greatest stress reduction was obtained with the full compound configuration in which the addition of the wing permitted significant unloading of the rotor.

The effects of rotor lift and airspeed upon vibratory stress of the -4 degree twist blades are shown in Figure 28. Forty-six data points were examined for speeds between 149 and 194 knots, rotor lift values of 4,300 to 16,000 lbs., and rotor drag of 900 to -800 lbs. For this range of data, stress was determined to be a nearly linear function of speed and rotor lift, but not significantly affected by rotor drag. Consequently,

stress is seen to increase, linearly, with forward speed at a given lift value and to be strongly affected by the degree of unloading. This stress reducing effect of decreased rotor loading was shown in Figure 27 by the low stresses demonstrated in the compound configuration.

The insensitivity of blade stress level to rotor drag is not unexpected for the -4 degree twist blades. In full-scale wind tunnel tests of the H-34 (Sikorsky S-58) rotor system, Reference 3, stress was found to increase in zero degree twist blades with increased rotor propulsion, while -8 degree twist blades developed reduced stresses as rotor propulsion increased. Therefore, it may be concluded that -4 degree twist blades are relatively insensitive to rotor propulsive force.

The effects of number of blades and blade twist were also evaluated. Figure 29 shows that main rotor blade stress was lower with the six-bladed rotor than with the five-bladed rotor having identical blades as expected, because of the lower lift required per blade. The increase in twist from -4 degrees to -8 degrees shifted the location of maximum stress inboard (from BR-7 at 70 percent span to BR- at 60 percent span) and increased the maximum stress value. These data were measured with collective pitch at the 80 knot position which, at speeds above approximately 120 knots, resulted in the rotor operating at a drag condition. The increased stress measured on the higher twist rotor under such conditions is in agreement with the H-34 full scale wind tunnel test results discussed above.

#### Effects of Rudder Deflection on Tail Rotor Stresses

The effect of rudder deflection on tail rotor blade stress was evaluated as a function of airspeed. Figure 31 shows NB-R vibratory stress versus airspeed for 0, 10, and 20 degrees left rudder deflection. As speed increases, the effect of the rudder increases, and the tail rotor thrust requirement is reduced. Lower blade coning and flapping and, therefore, lower stresses on the semi-articulated rotor result. During the flight, main rotor power was reduced slightly between 0 and 10 degrees rudder settings. The data indicate, however, that a stress reduction of as much as 25-30 percent can be achieved at constant power. Camber or positive incidence on an adequately sized vertical tail should have the same effect.

## AIRFRAME VIBRATION

Prior to flight testing, the NH-3A was shake tested with and without wings. These tests, described in detail in Reference 6, indicated that the NH-3A vibration levels with a five-bladed rotor would be lower than other S-61 series aircraft (SH-3A and CH-3C), primarily because the NH-3A fuselage modes are further removed from 5 per rev. The response of the NH-3A with the six-bladed rotor was predicted to be even lower due to the lower rotor blade loads and the absence of fuselage resonances near 6 per rev operating speeds.

Flight tests confirmed that NH-3A cockpit vibration levels were in agreement with values predicted by analysis of shake test results. The effects of number of blades, blade twist, wings, and jet thrust on vibration are discussed in the following paragraphs.

### Effect of Number of Blades

Cockpit vibration levels of the five bladed and six-bladed configurations are compared in Figure 32 for a range of flight conditions. With the -4 degree twist blades, the six-bladed system reduced both vertical and lateral response. With the higher twist (-8 degrees) blades, the six-bladed system provided little reduction in vertical response, but lateral accelerations were reduced by 50 percent.

There are several reasons for the substantial improvement with the six-bladed rotor. First, blade airloads generally decrease with higher input harmonics. In addition, the blade response characteristics are such that the six-bladed rotor transmits less of the applied loads to the fuselage. The natural frequency of the second flatwise bending mode of the S-61 blade is near 5 per rev. Blade response at this frequency provides considerable fuselage vertical excitation in the five-bladed rotor, but does not feed through the rotor head in the six-bladed system.

Similarly, lateral and longitudinal fuselage excitations result from  $n-1$  and  $n+1$  edgewise blade response. Since the S-61 blades have a first edgewise resonance near 4 per rev, the five-bladed rotor passes high 5

per rev lateral and longitudinal loads to the fuselage. With the six-bladed rotor, the 4 per rev response is not transmitted through to the airframe.

Finally, Figure 33 shows that two of the three important modes of the NH-3A fuselage response are less sensitive at 6 per rev than at 5 per rev. The higher vertical response to longitudinal excitation at 6 per rev may explain the lack of difference in vertical vibration between the five- and six-bladed rotors with the -8 degree twist blades.

#### Effects of Blade Twist

Flight test results on -4 degree and -8 degree twist blades, also compared in Figure 32, indicate small changes in cockpit vertical vibration levels. However, the cockpit lateral levels, especially with the five-bladed configuration, are significantly higher for -8 degree twist.

#### Transmission Support Structure Stresses

The transmission support fittings transmit loads from the rotor system to the airframe. Consequently, stresses in this area are affected by the same parameters which influence airframe vibration. Transmission support fitting stresses are presented in Figure 34 which shows that the stress levels with the six-bladed rotor were only a fraction of those with the five-bladed configuration, especially at higher speeds. This behavior parallels the cockpit lateral vibration characteristics shown in Figure 32.

#### Rotor Unloading

Figure 35 shows the effect of rotor unloading upon cockpit vibration. The use of wings and auxiliary propulsion resulted in reduced cockpit vibration at high speeds, primarily because of the delay or elimination of retreating blade stall. Analysis predicted vibration levels at 180 knots in the compound configuration to be equivalent to those at 140 knots with the rotor carrying the full aircraft weight. The predictions were based on the assumption that vibration levels would be equal at the onset of stall in the two cases. The stall criterion of Reference 2 was utilized. Figure 35 confirms that this is a useful method for predicting the effect of compounding upon vibration levels.

### Tail Shake

Commencing with testing of the six-bladed rotor configuration, a lateral tail shake was encountered. The tail shake was defined as a low frequency, high displacement, lateral oscillation of the tail assembly, believed to result from turbulent airflow generated by the main rotor impacting on the tail pylon area. Although the structural integrity of the aircraft was not seriously affected, the vibration level increased with speed and became objectionable at high forward speeds.

In an attempt to reduce the tail shake vibration level several possible solutions were considered. Previous testing with the five-bladed rotor system had been accomplished using a main rotor head "beanie" fairing to streamline the airflow from the main rotor and deflect it downward away from the tail rotor. As an initial step this fairing was modified and installed on the aircraft. However, due to the damper installation, the fairing was installed approximately seven inches higher on the six-bladed rotor system than the original installation. Since the effectiveness of the fairing is a function of several factors including its diameter, thickness and distance above the rotor head, no significant reduction in the tail shake was accomplished. As an additional modification a skirt was installed around the circumference of the fairing to effectively lower the installation. Subsequent flights revealed that only a small reduction in the tail shake could be accomplished with this configuration.

Simultaneously, the effect of fuselage trim attitude on the tail shake problem was investigated in an attempt to remove the tail pylon from the turbulent airflow. A c.g. change to 265.7 inches or an elevator setting of + 4 degrees was found sufficient to eliminate the tail shake problem. The latter solution was used for the remainder of the six-bladed flights.

It is apparent that to avoid tail shake in a high speed helicopter or compound, the turbulent wake of the rotor head/pylon should be reduced as much as possible, and that, further, the tail rotor and tail surfaces should be located outside the rotor head wake if at all possible.



### FLYING QUALITIES

The NH-3A compound helicopter was designed to provide a stable aircraft for research and data acquisition purposes. To accomplish this the airframe was equipped with a large empennage. The result of this design was a stable aircraft, even without AFCS (which had been removed), and there was no unexpected loss of stability with speed. Flying qualities were generally as expected, and the influences of wing, jets, control surfaces and the different rotor configurations were predictable.

### V-N Envelopes

Although the full load factor capability of the NH-3A was not developed during this program, sufficient load factors were generated to indicate the maneuver potential of the aircraft. Load factors achieved with the jet augmented, five-bladed configuration are shown in Figure 36a. A maximum of 1.82g was obtained in a left turn at 120 knots indicated airspeed. The minimum load factor of .05g was obtained during an entry to autorotation at 120 knots. Addition of the wing expanded the envelope to a maximum load factor of 2.24g, shown in Figure 36 b. This was obtained in a climbing turn at 160 knots. The addition of a sixth main rotor blade (without the wing) also improved the load factor capability of the basic aircraft. Figure 36c shows that a maximum of 2.2g was obtained at 120 knots. This configuration achieved an indicated airspeed of 230 knots in a dive.

### Theoretical Correlation With Flight Test

Flight test values of control positions and aircraft attitude agreed well with theoretical predictions based on small scale wind tunnel tests. Figure 37 compares flight test data at 125 knots with predicted lateral directional characteristics from Reference 7. The effect of the differential wing lift is apparent in the lateral cyclic stick data. This effect was not considered in the preflight calculations and consequently near zero sideslip there was approximately  $1\frac{1}{2}$  degrees more left cyclic pitch than predicted. This difference had no adverse effect on the NH-3A, but it should be considered in the design of future compound aircraft.

At speeds below 150 knots aircraft attitude and control positions were predicted using a digital computer program based on linearized rotor aerodynamic theory. Figure 38 demonstrates the adequacy of this approach. For higher speeds a combined analog-digital ("hybrid") computer was used to obtain trim solutions. The hybrid computer program includes the aerodynamic analysis of the generalized rotor performance (GRP) program (Ref. 2) which considers the effects of Mach number and reverse flow, and has no small angle assumptions.

Figure 38 compares flight test with computed values of various parameters. In calculating these parameters on the hybrid computer, jet thrust, roll attitude, and collective pitch were specified as equal to the measured values. Discrepancies in the generally good correlation appear in longitudinal cyclic pitch, aircraft pitch attitude, and tail rotor pitch, at high speeds. There was considerable scatter in flight test values of the first two parameters, which could account for the differences. The discrepancy in tail rotor pitch at high speeds is probably due to a high prediction of main rotor torque and use of too low a lift curve slope in the linearized analysis of the tail rotor.

#### Effect of Various Parameters on Aircraft Attitude and Control Positions

##### Effect of Drag Reduction

The effect of drag reduction on control positions, aircraft attitude, and jet thrust is shown in Figure 39. There was a significant forward shift in longitudinal stick position and an increase in flapping which would produce a nose-down pitching moment. At 199 knots, two degrees of downward elevator displacement were required to produce an equivalent moment and return the stick to the position established prior to the drag reduction modifications. This shift in longitudinal characteristics is believed to be due to increased effectiveness of the horizontal stabilizer resulting from improved airflow characteristics over the wing root and landing gear fairing. A study of horizontal tail loading, determined from stabilizer bending moment measurements, (Figure 40) confirms that increased tail loads are the cause of the trim change. It was demonstrated, therefore, that improved stability is provided by putting the tail surfaces in a clean environment.

### Effect of the Wing

The NH-3A compound configuration included a high wing with a constant incidence angle of zero degrees (airfoil reference chord line). The wing aerodynamic center was located near to the basic aircraft c.g. in order to keep the wing-fuselage pitching moment changes caused by changes in wing lift to a minimum. Therefore the aircraft trim and dynamic response characteristics were not expected to change significantly with the addition of the wing.

Figure 41 shows the effect of wings on flight characteristics of the NH 3A. For all flights shown in this figure the aircraft was trimmed at 80 knots with jet thrust at idle. The collective remained fixed and jet thrust was increased to achieve higher speeds. In the full compound configuration, the wing was developing a positive lift at 80 knots, so less collective pitch was required than in the wingless configuration. The differential wing lift effect can be observed in these data. The differential lateral stick displacement required to counteract the positive rolling moment is approximately 18 percent at 180 knots.

Dynamic response to a longitudinal stick pulse was measured in flight with and without the wing. The results of a  $\frac{1}{2}$  inch longitudinal cyclic pull and return are shown in Figure 42. These data show little change in response due to the presence of the wing. The small differences may reflect the difference in actual control input during the maneuver. The measured response is compared with calculated values in Figure 43. The measured control input has been utilized in the analysis, and the results show good agreement both with and without the wing.

Although lateral characteristics were not directly investigated, pilots report that, with the wing, roll control power was somewhat diminished, but that lateral stability was improved.

### Solidity Effect

To determine the effect of solidity, the NH-3A was flown with both a

five-bladed and a six-bladed rotor system. The added blade increases rotor control power and damping, and reduces the collective pitch requirement at a given speed and angle of attack. Figure 44 is a comparison of aircraft attitudes and control positions for the five-bladed and six-bladed configurations. The added profile power of the sixth blade increased rotor torque at low speed so that more left pedal was required for trim.

Theoretical and experimental longitudinal response to a pull and return were compared for the five-bladed rotor in Figure 43. A similar comparison for the six-bladed rotor appears in Figure 45. Again the agreement is excellent for the first 10 seconds. Beyond that point, the matching of control inputs in the calculation was stopped.

#### Effect of Twist

Main rotor blades of both -4 and -8 degrees were tested on the five- and six-bladed rotors during the test program. The twist variation caused no changes in aircraft trim, control positions and stability, within the accuracy of the test data.

#### Effect of Horizontal Tail

The NH-3A horizontal stabilizer was designed to provide a stable pitching moment (Ma) slope, including the contribution of the rotor. With the tail initially set on this basis, wind tunnel tests revealed a serious reduction of tail effectiveness over a narrow range of angle of attack where the tip vortices from the J-60 installation impinged upon the stabilizer. To eliminate this problem the span of the stabilizer was increased to provide area outboard of the jet engines. The characteristics of the NH-3A and standard SH-3A stabilizers are as follows.

	<u>SH-3A</u>	<u>NH-3A</u>
Total Area	20 feet <sup>2</sup>	76.2 feet <sup>2</sup>
Aspect Ratio	1.8	5.25
Incidence	0 degrees	Ground Adjustable -5, 0, 5 degrees

The effect of the increased stabilizer area upon dynamic response is shown in Figure 46 for an aft stick pulse. The stick displacement was held for the NH-3A longer than that for the SH-3A but with less amplitude, giving a similar impulse. The maximum change in pitch attitude of the NH-3A was only 6 degrees, compared to 20 degrees for the SH-3A. In addition, changes in speed and vertical acceleration were smaller for the NH-3A.

Some problems were encountered with the larger empennage in hover, sideward and rearward flight. Pitch oscillations occurred in hover due to intermittent partial immersion of the horizontal tail in the main rotor downwash. This effect did not occur in calm air. The aircraft also had reduced speed capabilities in sideward and rearward flight due to abnormal airflows caused by the larger vertical and horizontal tails.

#### Effects of Elevator Deflection

The effectiveness of the large elevator is demonstrated in Figure 47, which shows the effects of changes in elevator setting upon steady state flight parameters. Figure 47a shows that a 2 degree negative (up) elevator increment produced a much more nose-up attitude. This resulted in a reduction of the rotor lift requirement at constant collective pitch. The combination of increased pitch attitude and increased rotor propulsive force resulted in a large forward stick motion and greatly increased flapping, limiting speed to 140 knots.

The effect of a positive (downward) elevator deflection is shown separately in Figure 47b. A 2 degree positive increment produced a nose-down moment, allowing the longitudinal stick to move aft to produce the required balancing moment. With the favorable stick position and reduced flapping, speed was limited only by available jet thrust.

#### Effect of Rudder Deflection ( $\delta_R$ )

The effect of rudder deflection on the compound helicopter flight parameters is shown in Figure 48. Deflection values of -10 and -20 degrees (left deflection) were chosen to counteract main rotor torque and provide tail rotor unloading. Rudder deflection did not significantly affect any flight parameters except rudder pedal.

## CONCLUSIONS

1. The NH-3A test program demonstrated that the fully articulated rotor system is well adapted to the environment of compound helicopter flight at speeds up to at least 230 knots, the maximum attained in this program.
2. Available methods of analysis of performance, stability, control requirements, blade stresses, and vibration can generally be applied up to at least 200 knots without significant loss of accuracy.
3. Anticipated results which were confirmed by test included the following:
  - a. Speeds in excess of 200 knots were achieved both with and without a wing through application of auxiliary propulsion.
  - b. Blade stresses at high speed were acceptable and were reduced by rotor unloading and by reduced blade twist.
  - c. Vibration levels at high speed were very acceptable and were markedly reduced with the six-bladed rotor.
  - d. Inherent aircraft stability without any type of artificial stabilization was provided by an adequately sized fixed horizontal stabilizer.
  - e. Blade stall and the associated build up of control loads was delayed by rotor unloading and by use of increased blade twist.
  - f. Tail rotor blade stresses at high speeds may be significantly reduced by providing anti-torque forces with a vertical tail.

## RECOMMENDATIONS

The following areas are recommended for further study, based on the results of this investigation.

1. The NH-3<sup>a</sup> research helicopter should be modified to permit testing to higher speeds. Modifications required to achieve speeds above 250 knots include the following:
  - a. Installation of integrated controls to augment the rotor when it is slowed and unloaded.\*
  - b. Reduction of airframe parasite drag by fairing of rotorhead, installation of new T-58 inlets and streamlining of aircraft nose, cockpit canopy and T-58 engine housing.
  - c. Installation of increased thrust jet engines.
2. Serious study should be made of application of the 200-250 knot articulated rotor compound helicopter to operational missions.
3. Study should be made of application of the six-bladed rotor to the H-3 family of aircraft as a result of the very favorable pilot reaction to the flight characteristics of that configuration.
4. Further study, including flight tests should be conducted to verify the findings of the tip spread analysis. Acquisition of two-dimensional airfoil pitching moment characteristics at Mach numbers from 0.7 to 1.0 is also desirable.

\* This has been accomplished at full rotor speed under U. S. Navy Contract N 00019-67-C-C513.

#### REFERENCES

1. Lock, G. N. H., The Application of Goldstein's Theory to the Practical Design of Airscrews, British ARC R&M No. 1377, 1931.
2. Tanner, W. H., Charts for Estimating Rotary Wing Performance in Hover and at High Forward Speeds, NASA CR-114, Sikorsky Engineering Report SER-50379, November 1964.
3. Paglino, V. M. and Logan, A. H., An Experimental Study of the Performance and Structural Loads of a Full-Scale Rotor at Extreme Operating Conditions, Sikorsky Engineering Report SER-50505, March 1968.
4. Bain, L. J. and Landgrebe, A. J., Investigation of Compound Helicopter Aerodynamic Interference Effects, USAAVLABS Technical Report 57-44, Sikorsky Engineering Report SER-50474, November 1967.
5. Paul, William F., A Self Excited Rotor Blade Oscillation at High Subsonic Mach Numbers, Paper presented at AHS 24th Annual National Forum, Washington, D. C., May 8-10, 1968.
6. Winter, W., NH-3A Ground Vibration Test Report, Sikorsky Engineering Report, SER-611100, April 9, 1965.
7. D'Ostilio, P. J., Jenney, D. S. and Segel, R. M., Flight Test Planning Report, Sikorsky Engineering Report SER-611065, January 21, 1965.



TABLE I NH-3A DATA FLIGHTS

5-Blades, -4 Degrees, No Wings, +5-Degree Stabilizer									
Flt. No.	Date	Test Plan	Elev. Pos.	Flap Pos.	J-60	Alt.	Comments	P/F	Oscil.
4	5/26*	-1	0	---	Off	3000	Level Flight Vmax = 135 knots, 70 knots autorotation, 120 knot 30° banks	x	2 x
6	5/28	-1	-5, -10	---	Off	3000	Level Flight, Vmax = 137 knots with -5° elevator, Vmax = 139 knots with -10 elevator	x	x
7	6/1	-1	0	---	On/Off	3000	Level Flight, 80, 100-knot trim	x	x
8	6/3	-3	0	---	On	3000	Level Flight, 80-knot trim, Vmax = 159 knots	x	x
10	6/4	-3	-7, -10	---	On	3000	-10 elevator, 80-knot trim, Vmax = 157 knots	x	x
11	6/8	-3	-10	---	On/Off	3000	-7.7 elevator, 80-knot trim, Vmax = 155 knots	x	x
12	6/8	-3	-15	---	On	3000	Autorota. and Dynamic Stability	x	x
14	6/29	-3	-15	---	On	3000	Autorota. at 85, 103 and 127 knots, jets off	x	x
16	7/6	-3	-15	---	On	3000	Level Flight, 80-knot trim, Vmax = 155 knots	x	x
18	7/8	-3	-15	---	On	3000	Level Flight, 80-knot trim, Vmax = 186 knots	x	x
20	7/9	-3	-15	---	On/Off	3000	Level Flight, Trim 80 knots -9% collective	x	x
22	7/21	-4	0	0	Off	3000	133 knot and 151 knot level flight autorotation, 28% collective	x	x
23	7/21	-4	-10	0	Off	3000	Level Flight, Trim 80 knots -21% collective, Vmax = 177 knots	x	x
24	7/22	-4	-10	0	On	3000	Level Flight, Trim 120 knots, Vmax = 167 knots, Also jets inop., Vmax = 135 knots	x	x
25	7/23	-4	-15	0	On	3000	Level Flight, Trim 120 knots, Vmax = 135 knots	x	x
5-Blades, -4 Degree Compound, +5-Degree Stabilizer									
22	7/21	-4	0	0	Off	3000	Level Flight Power required, jets inop., both oscil inop, Vmax = 121 knots	x	x
23	7/21	-4	-10	0	Off	3000	Level Flight and Autorota., Autorota. at 82 knots, Vmax = 128 knots	x	x
24	7/22	-4	-10	0	On	3000	Level Flight, Trim 80 knots, Vmax = 158 knots	x	x
25	7/23	-4	-15	0	On	3000	Level Flight, 160-knot turn, 30° bank, Trim 80 knots, elevator increased to -20° at 158 knots	x	x

TABLE I NH-3A DATA FLIGHTS (Continued)

<u>5-Blades, -4 Degree Compound, +5-Degree Stabilizer (Continued)</u>										
<u>Flt. No.</u>	<u>Date</u>	<u>Test Plan</u>	<u>Elev. in.</u>	<u>Flap Pos.</u>	<u>J-60</u>	<u>Alt.</u>	<u>Comments</u>	<u>P/P Tbl</u>	<u>Oscil. 1</u>	<u>Oscil. 2</u>
26	7/26	-4	-15	0	On	3000	Level Flight, +160-knot turns, 30° bank, Trim 80 knots, Vmax = 190	x	x	x
27	7/27	-6	Varied	Varied	On	3000	Level Flight, Single A/S 180 knots, Eval. of optimum high speed configuration	x	x	x
28	7/29	-7	Varied	Varied	On	3000	Level Flight, High A/S plus Lt and Rt turns, 4° bank, continued eval. of optimum high-speed configuration	x	x	x
<u>5 Blades, -4 Degree-Compound, 0° Stabilizer</u>										
30	8/6	-8	0,+3	+10	On/Off	3000	Level Flight, data for jets off only on P/P, jets off, Vmax = 130 knots, jets on, Trim 80 knots, Vmax = 167, also 45° and 60° banks	x	x	x
31	8/5	-9	0,+6	+10	On	3000	Level Flight, Trim 80 knots, high-speed data only, Vmax = 205 knots	x	x	x
34	8/24	-10	0,-5,+5	0,5,10,-10	Off	3000	Level Flight, jets inop to evaluate various flap and elevator settings	x	x	x
35	8/25	-10	0,-6	0,+11,-20	Off	3000	Level Flight and autorota. single A/S 125-knot level flight. 100-knot auto.	x	x	x
37	8/31	-10	0,+6	0,+4	On	3000	Level Flight, Trim 80 knots, Vmax +6 elev., 0 flap = 190 knots, Vmax 0 elev., +4 flap = 194 knots	x	x	x
38	9/2	-10	0	+4	On	3000	Level Flight and full lo coll. at 172 knots, Trim 80 knots -11% coll., Vmax = 188 knots	x	x	x
39	9/3	-10	0	+4	On/Off	3000	Level Flight, Vmax jets off = 134 knots, jets on Trim 125 knots, Vmax = 199 knots, full to lo coll. at 139 knot. jets on	x	x	x
45	10/20	-11	0,+2	+4	On/Off	3000	Level Flight jets off, Vmax = 139 knots, jets on Trim 130 knots, Vmax = 199 knots	x	x	x
47	10/26	-11	+2	+4	On	3000	Level Flight, Trim 135 knots, Vmax = 197	x	x	x

TABLE 1 NH-3A DATA FLIGHTS (Continued)

Flt. No.	Date	Test Plan	Elev. Pos.	Flap Pos.	J-60 Alt.	Comments	5 Blades, -8 Degree-Compound, 0° Stabilizer		
							P/P Tbl	Oscil. 1	Oscil. 2
56	12/27	-18	0 & +2	+4	On/Off	3000 Level Flight, jets off, Vmax = 149, Trim 80 knots, Vmax = 190, Trim 80 knots -8°, Vmax = 189, full lo coll. at 145 and 175 knots	x	x	x
57	1/4**	-18	+2	+4	On	3000 Level Flight, Trim 100 knots, Vmax = 194	x	x	x
58	1/7	-18	0 & +2	+4	On	3000 Level Flight, Trim 125 knots, Vmax = 195, Trim 80 knots -7% coll., Vmax = 171	x	x	
60	1/17	-18	+2, -2	+4	On	3000 Level Flight, Trim 80 knots -10% coll., Vmax = 189, Trim 80 knots -10% coll., Vmax = 140 knots	x	x	
64	1/25	-18	+2	+4, +10 -20, 1	On	3000 Level Flight and auto. full lo coll. at 90, 100, 110 knots, Trim 135 knots, Vmax = 198	x	x	
67	2/1	-18	+2, +4	+4, +10 +15	On	3000 Level Flight, Trim 80 knots with 3 various flap and elev. comb.	x	x	
68	2/2	-18	+6	+4	On	3000 Level Flight, Trim 80 knots, Vmax = 187	x	x	
69	2/8	-18	+2	+4	On	3000 Trim 80 knots, 120 and 180 knots, 60° banks	x	x	
70	2/10	-18	+2	+4	On	3000 Level Flight, Trim 125 knots, Vmax = 193	x	x	
5 Blades, -8 Degrees, No Wing, 0° Stabilizer									
71	2/18	-19	0, +2	---	On/Off	3000 Level Flight, jets inop, Vmax = 138, Trim 80 knots and 0 elev., Vmax = 186, Trim 80 knots and +2 elev., Vmax = 187	x	x	x
72	2/21	-19	+2	---	On	3000 Level Flight, Trim 120 knots, Vmax = 186, Trim 80 knots -8% coll., Vmax = 184	x	x	x
73	2/23	-19	0	---	On	3000 Level Flight, Trim 100, Vmax = 196, Trim 80 knots, vary elev. and hit lo and hi speed only	x	x	x
75	3/3	-19	0	---	On/Off	3000 Level Flight, jets inop, Vmax = 142, Trim 80 knots -9% coll., Trim 80 knots -20% coll.	x	x	x

TABLE I NH-3A DATA FLIGHTS (Continued)

5 Blades, -8 Degrees, No Wing, 0° Stabilizer (Continued)										
Flt. No.	Date	Test Plan	Elev. Pos.	Flap Pos.	J-60	Alt.	Comments	P/P Tbl	Oscil. 1	Oscil. 2
76	3/17	-19	0	---	On/Off	3000	Level Flight, full lo coll., Vmax = 167, Trim 120 knots, Vmax = 178	x	x	x
77	3/18	-19	+2	----	On	3000	Level Flight, Trim 80 knots -20% coll., Vmax = 165	x	x	x
79	3/31	-19	0,+2	----	On	3000	Level Flight, full lo coll., Vmax = 178, 160 knots static stability, 160 knots 10% coll. static stability, 120 and 160 knots, 45° banks	x	x	
6 Blades, -4 Degrees, No Wing, 0° Stabilizer										
82	4/25	-20	0	----	Off	3000	Level Flight, jets inop, no beanie			
83	4/29	-20	0, +2, +4	----	Off	3000	Level Flight, jets inop, Vmax 142 knots, 0 elev., vary elev. at 142, no beanie, repeat of Flight 82	x	x	x
84	5/2	-20	0	----	On/Off	3000	Level flight at 120 knots and rpm sweep, autorotation at 80, 100, 120 knots, no beanie		x	x
85	5/3	-20	0	----	On	3000	Level flight trim 80 knots, Vmax = 190, Trim 80 knots -10% coll., Vmax = 188	x	x	x
86	5/11	-20	0	----	On	3000	Level flight trim 80 knots and pulses at 120 knots Trim 80 knots to Vr, 1/2" steps at 120 knots		x	x
89	5/23	-20	+2,+4 0	----	On	3000	Level flight trim 90 knots, 0 elev., Vmax = 195 Trim 80 +2 elev., Vmax = 202 Trim 80 knots +4 elev., Vmax = 202	x		
90	5/31	-20	+4	----	On	3000	Level Flight trim 80 knots, Vmax = 197, Trim 80 knots -10% coll., Vmax = 191	x	x	x
91	6/3	-20	+4	----	On	3000	Level Flight trim 80 knots -20% coll., Vmax = 183, full lo coll., Vmax = 141	x	x	x

TABLE I NH-3A DATA FLIGHTS (Continued)

<u>6 Blades, -4 Degrees, No Wing, 0° Stabilizer (Continued)</u>								<u>Oscil. 1</u>			<u>Oscil. 2</u>		
<u>Fit.</u>	<u>Date</u>	<u>Test</u>	<u>Elev.</u>	<u>Flap</u>	<u>J-60</u>	<u>Alt.</u>	<u>Comments</u>	<u>P/P</u>	<u>Tbl</u>				
<u>No.</u>		<u>Plan</u>	<u>Pos.</u>	<u>Pos.</u>									
92	6/8	-20	0,+4	---	On	3000	Level Flight trim 100 knots, Vmax = 202, Full lo coll., Vmax = 164, 60° Lt and Rt banks	x	x		x	x	
93	6/14	-20	+4	---	On	3000	Level Flight trim 120 knots, Vmax = 205	x	x		x	x	
<u>6 Blades, -8 Degrees, No Wing, 0° Stabilizer</u>													
95	6/22	-22	0,+4	---	On/Off	3000	Level Flight, jets inop., 0 elev. Vmax = 136, Trim 80 knots, +4 elev., Vmax = 191	x	x		x	x	
96	6/23	-22	+4	---	On	3000	Level Flight trim 85 knots, -4% coll., Vmax = 192, Trim 100 knots, Vmax = 195	x	x		x	x	
97	6/28	-22	+4	---	On	3000	Level Flight trim 120 knots, Vmax = 201, Trim 80 knots, -20% coll., Vmax = 187	x	x		x	x	
99	6/30	-22	0,+4	---	On	3000	Level Flight, full lo coll., Vmax = 159, Trim 80 knots, 30° lt bank at 125, 160, 170 knots, aft steps and pulses at 120 and 180	x	x		x	x	
<u>Dynamic Stability, 5 Blades, -4 Degrees, No Wing</u>													
11	6/8	-3	-10	---	On/Off	3000	Autorota. and dynamic stability, aft step at 120, aft pulse at 120, jets inop.	x					
<u>Dynamic Stability, 5 Blades, -4 Degrees, Compound</u>													
<u>Dynamic Stability, 5 Blades, -8 Degrees, No Wing</u>													
59	1/13	-18	+2	+4	On/Off	3000	60° banks, 4 static dir. stability, dynamic stability steps and pulses 120, 160 knots (no data)	x	x		x	x	

TABLE I NH-3A DATA FLIGHTS (Continued)

Flt. No.	Date	Test Plan	Elev. Pos.	Flap Pos.	J-60	Alt.	Comments	P/P Tbl	Oscil. 1	Oscil. 2
<u>Dynamic Stability, 5 Blades, -8 Degrees, No Wing</u>										
76	2/18	-19	0,+2	---	On/Off	3000	Level Flight	x	x	x
79	3/17	-19	0	---	On/Off	3000	Level Flight, Dynamic Stability	x	x	x
80	3/31	-19	0,+2	---	On	3000	Level Flight	x		
	4/4	-19	0	---	On	3000	Level Flight pulses at 120, 140, 160			
<u>Dynamic Stability, 6 Blades, -4 Degrees, No Wing</u>										
86	5/11	-20	0	---	On	3000	Level Flight	x	x	x
92	6/8	-20	0,+4	---	On	3000	Level Flight, Turns at 120 knots	x	x	
<u>Dynamic Stability, 6 Blades, -8 Degrees, No Wing</u>										
95	6/22	-22	0,+4	---	On/Off	3000	Level Flight	x	x	x
99	6/30	-22	0,+4	---	On	3000	Level Flight	x	x	
<u>Static Directional Stability, 5 Blades, -8 Degrees, No Wing</u>										
62	1/19	-18	+2	+4	On	3000	Static and Static Directional Stability			
<u>Static Directional Stability, 5 Blades, -8 Degrees, Compound</u>										
80	4/4	-19	0	---	On	3000				
133		-29	---	---	---	---	Hover Data, 5 Blades, -4 Degrees, No Wing			x

TABLE I NH-3A DATA FLIGHTS (Continued)

<u>Hover Data, 5 Blades, -4 Degrees, Compound</u>										
<u>Flt.</u> <u>No.</u>	<u>Date</u>	<u>Test</u> <u>Plan</u>	<u>Elev.</u> <u>Pos.</u>	<u>Flap</u> <u>Pos.</u>	<u>J-60</u>	<u>Alt.</u>	<u>Comments</u>	<u>P/P Tbl</u>	<u>Oscil. 1</u>	<u>Oscil. 2</u>
119		-24	---	---	---	---			x	
<u>Hover Data, 5 Blades, -4 Degrees, Pure Helicopter</u>										
139		-32	---	---	---	---			x	
<u>Hover Data, 5 Blades, -8 Degrees, Pure Helicopter</u>										
138		-32	---	---	---	---			x	
<u>Hover Data, 6 Blades, -4 Degrees, No Wing</u>										
88	5/18	-21	0	---	Off	SL	Hover Power Required Data Available			
<u>Pure Helicopter Data, -4°, 5 Blades, 0° Stabilizer</u>										
139		-32	---	---	---	---			x	x
140	5/8	-33	0, -2	---	---	3000		x		
<u>Pure Helicopter Data, -4°, 5 Blades, 0° Stabilizer</u>										
136	4/13	-33	0, -2	---	---	3000				
138		-32	---	---	---	---		x	x	

\* 1965  
\*\* 1966

TABLE II

NH-3A PARASITE DRAG BREAKDOWN

V = 160 Knots

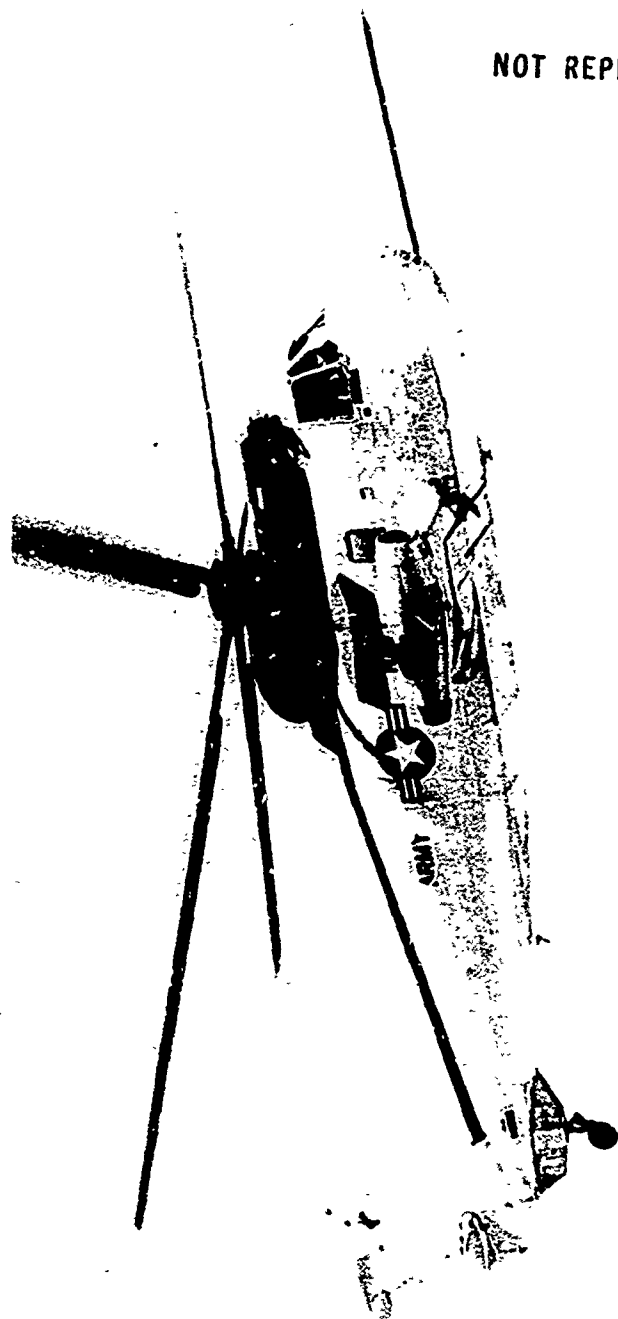
	<u>SH-3A</u>	<u>Design Est.</u>	<u>Present Est.</u>
Fuselage	5.12	4.00	4.00
Main Rotor Head	9.92	8.90	8.95
Main Rotor Pylon & T-58 Installation	2.36	2.36	2.36
Vertical Stabilizer Plus Interference	0.37	0.82	0.82
Horizontal Stabilizer	0.25	0.59	0.81
Tail Wheel	0.46	0.46	0.46
Landing Gear Pods	6.95	2.67	3.20
Tail Rotor Head	1.76	1.76	1.76
J-60 Nacelles	----	2.20	6.20
Wing installed	----	1.29	4.00 (4° Flaps)
Protuberances, Gaps, Joints and Miscellaneous	2.75	0.51	1.54
Momentum Losses, Spillage Drag	1.17	0.40	0.90
	<hr/>	<hr/>	<hr/>
	31.11	25.96	35.00
Without Wing & Jets	31.11	22.47	24.80





NOT REPRODUCIBLE

Figure 1. Production SH-3A Helicopter.



NOT REPRODUCIBLE

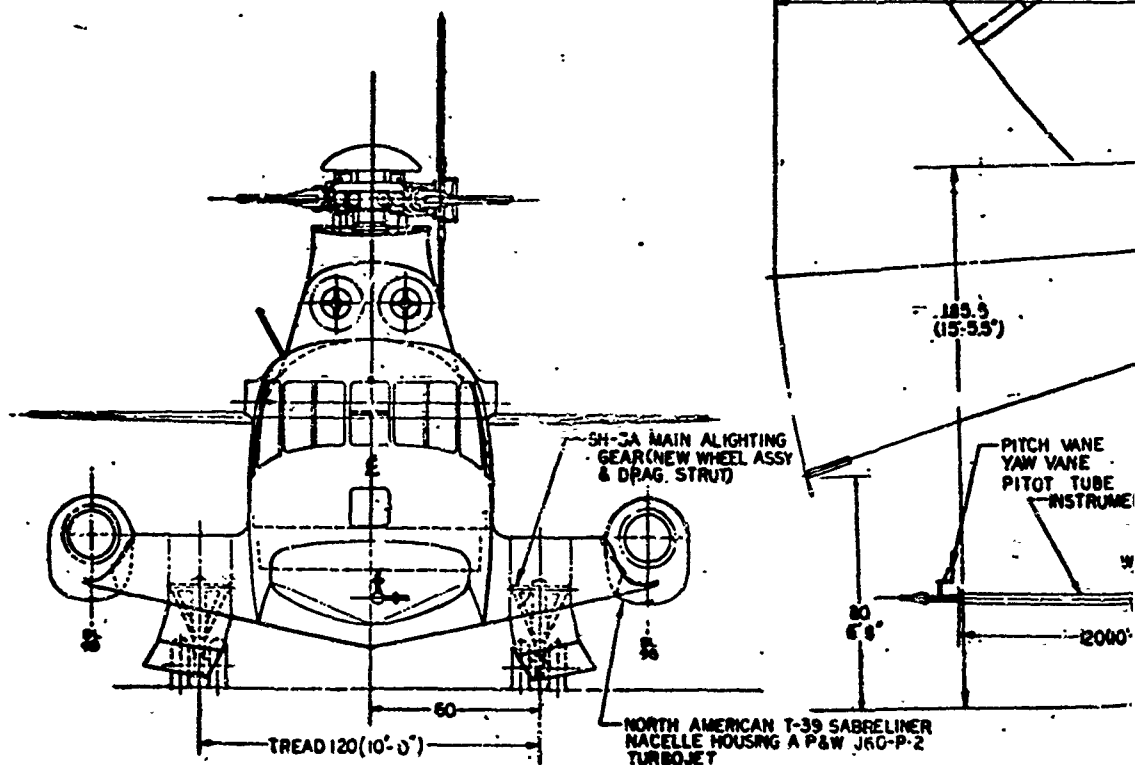


Figure 2. NH-3A - Helicopter With Jets.

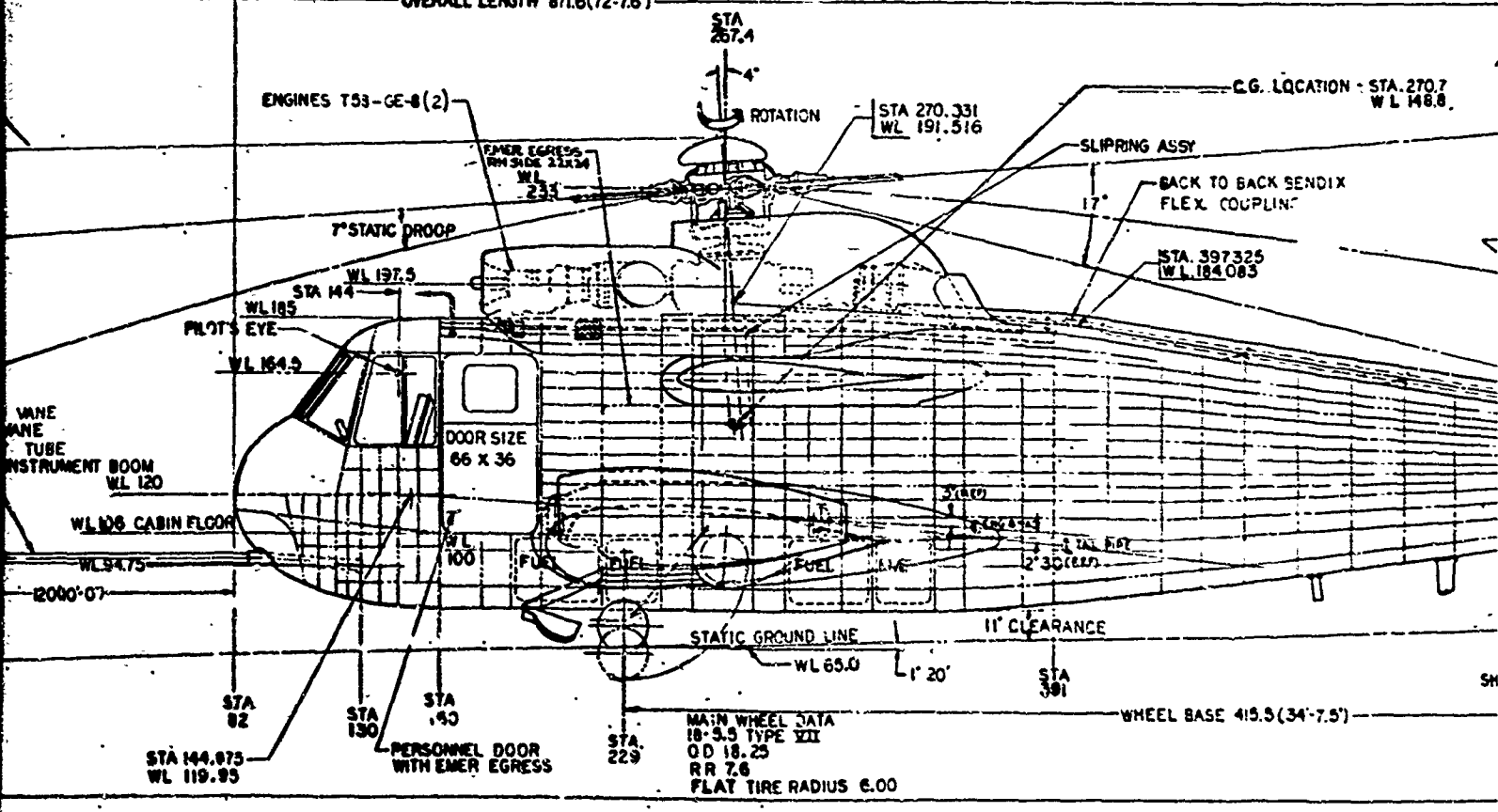
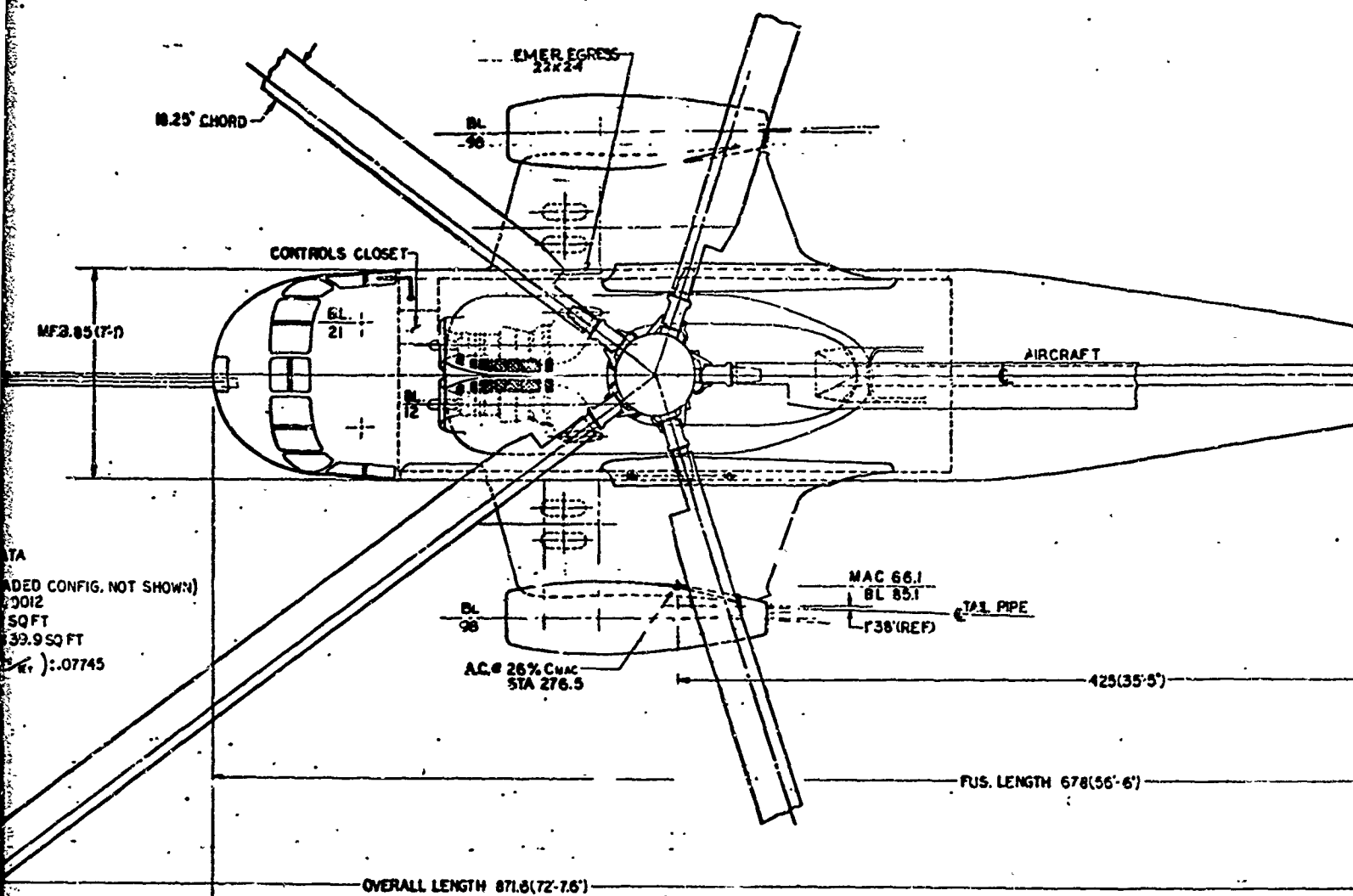
A

MFR. 85

MAIN ROTOR DATA  
 DIA: 62'  
 BLADES: 5 (6 BLADED CONF)  
 AIRFOIL: MOD. 0012  
 DISC AREA: 3019 SQ FT  
 BLADE AREA (EA): 39.9 SQ FT  
 SOLIDITY RATIO ( $\frac{C_L}{\sigma}$ ): .077  
 TWIST (LH): -8°  
 $\Omega R$ : 860  $\frac{FT}{SEC}$



18



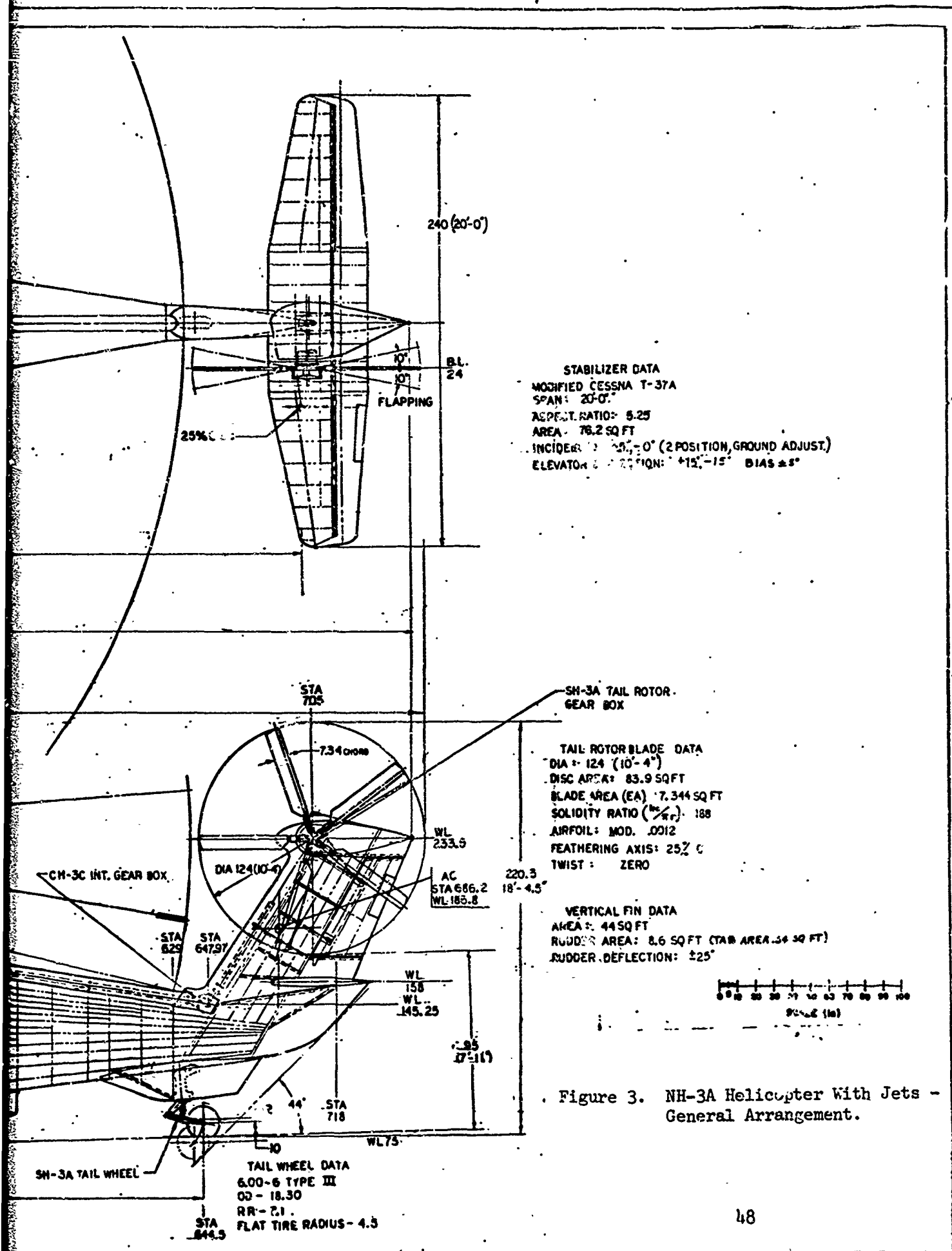


Figure 3. NH-3A Helicopter With Jets - General Arrangement.

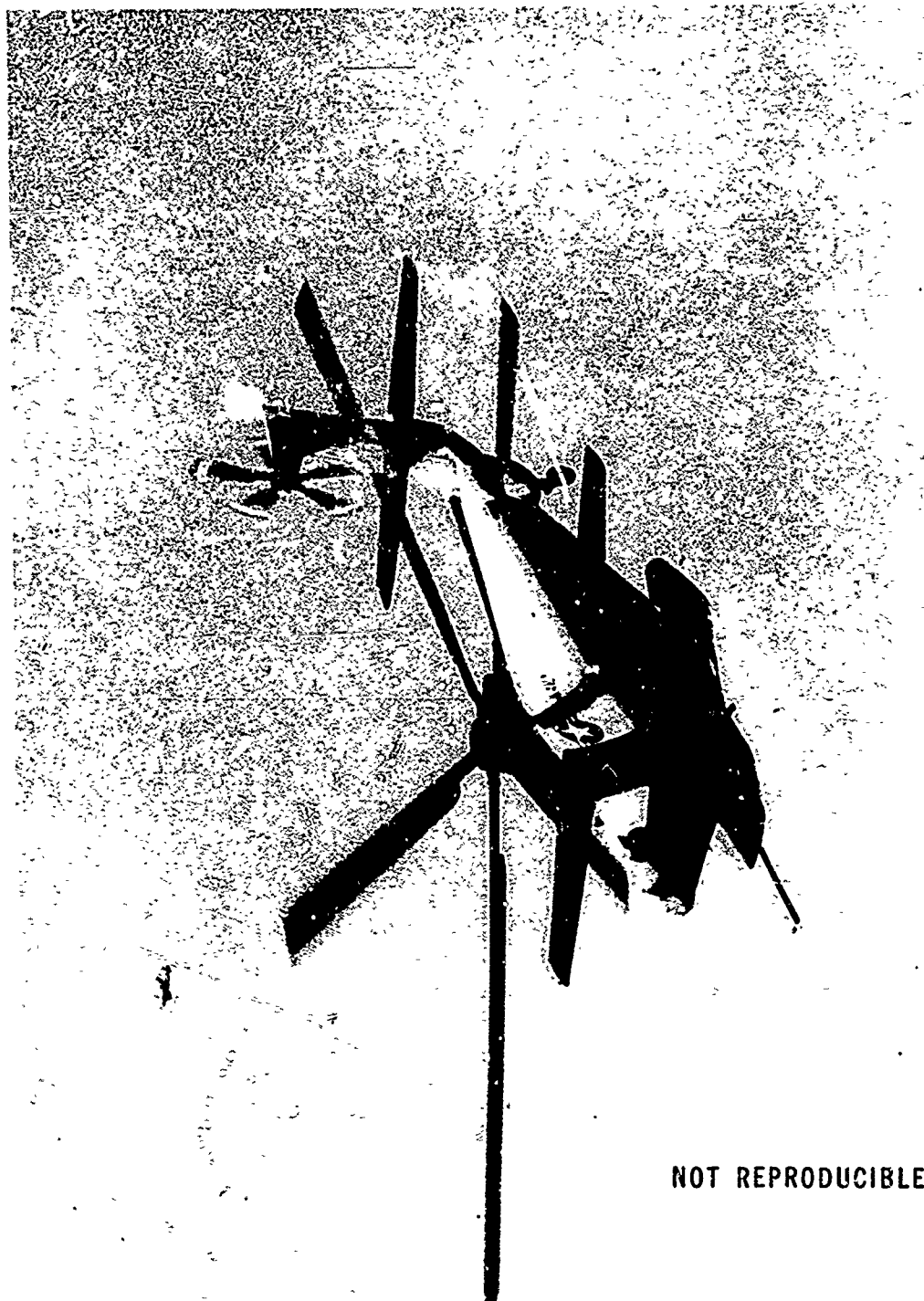
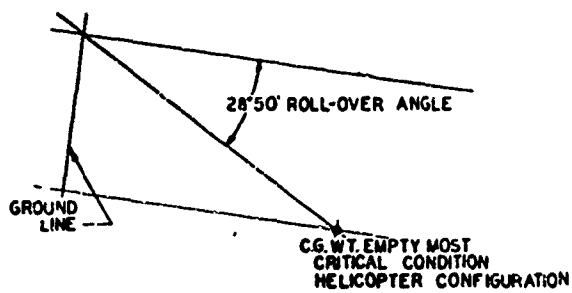


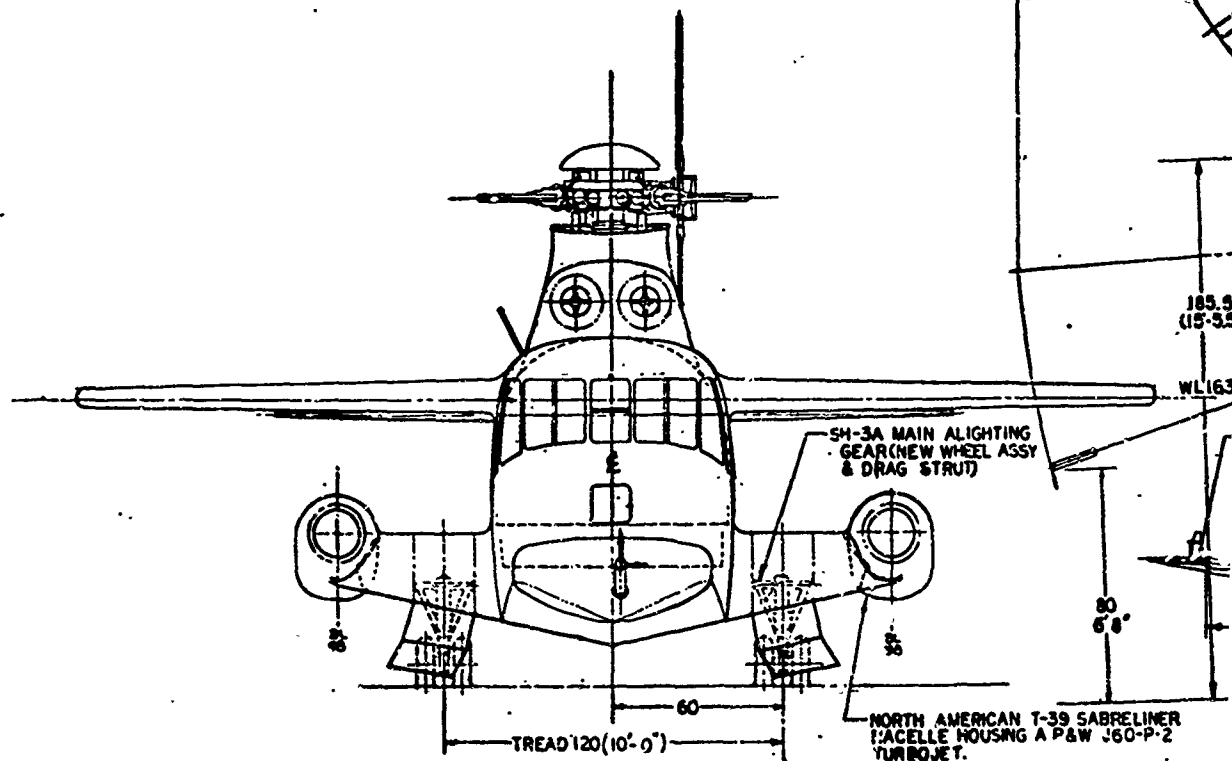
Figure 4. NH-3A Compound Helicopter Configuration.

A

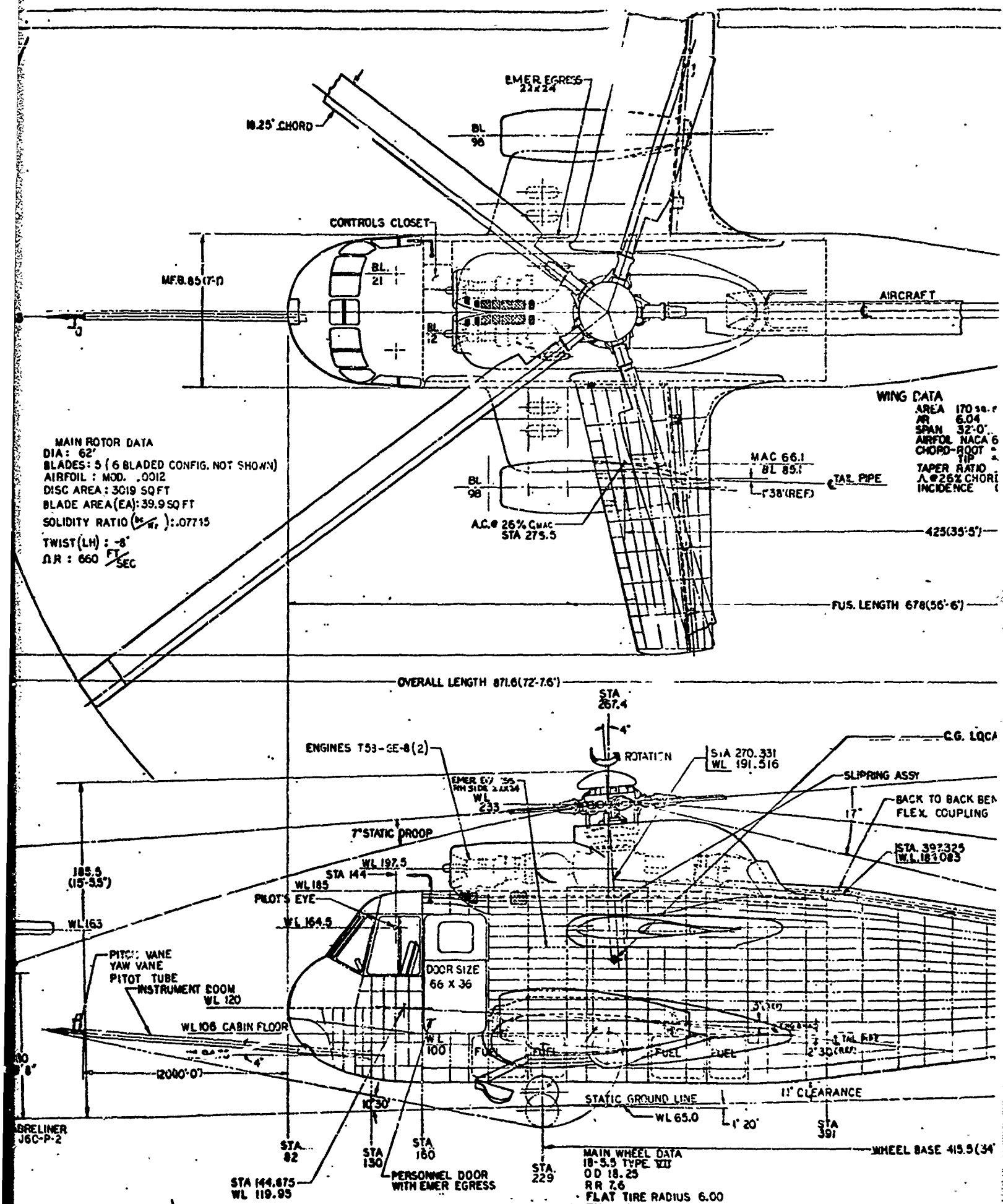


WING SPAN  
384 (32'-0")

MAIN ROTO  
DIA: 62'  
BLADES: 5  
AIRFOIL: M  
DISC AREA:  
BLADE AREA  
SOLIDITY RA  
TWIST (LH):  
AR: 860



١٣







A

10.25' CHORD

MF 8.65 (7-D)

BL 3

MAIN ROTOR DATA  
 DIA: 62'  
 BLADES: 5 (6 BLADED CONFIG. NOT SHOWN)  
 AIRFOIL: MOD. .0012  
 DISC AREA: 3019 SQ FT  
 BLADE AREA (EA): 39.9 SQ FT  
 SOLIDITY RATIO ( $\frac{c}{r}$ ): .07745  
 TWIST (LH): -8°  
 $\Omega R$ : 660  $\frac{FT}{SEC}$

ENG

185.5  
 (15-55°)

WL 101  
 PILOT'S EYE

WL 104

PITCH WAVE  
 YAW WAVE  
 PITOT TUBE

INSTRUMENT BOOM  
 WL 120

WL 106 CABIN FLOOR

WL 94.75

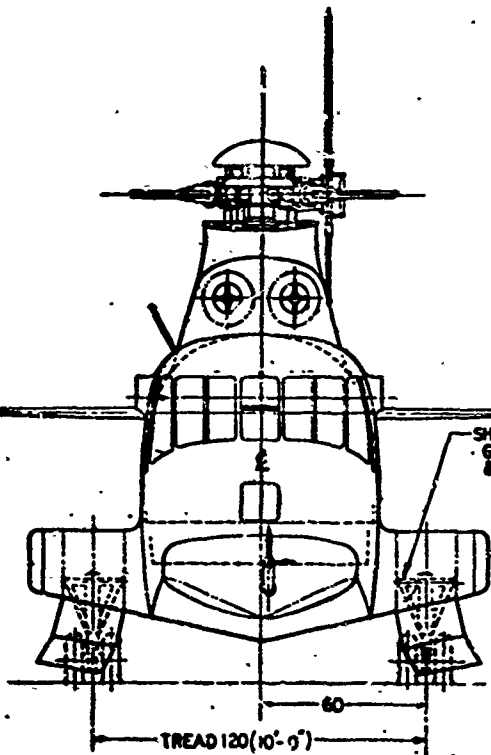
2000'-0"

30  
 6'-8"

STA  
 92

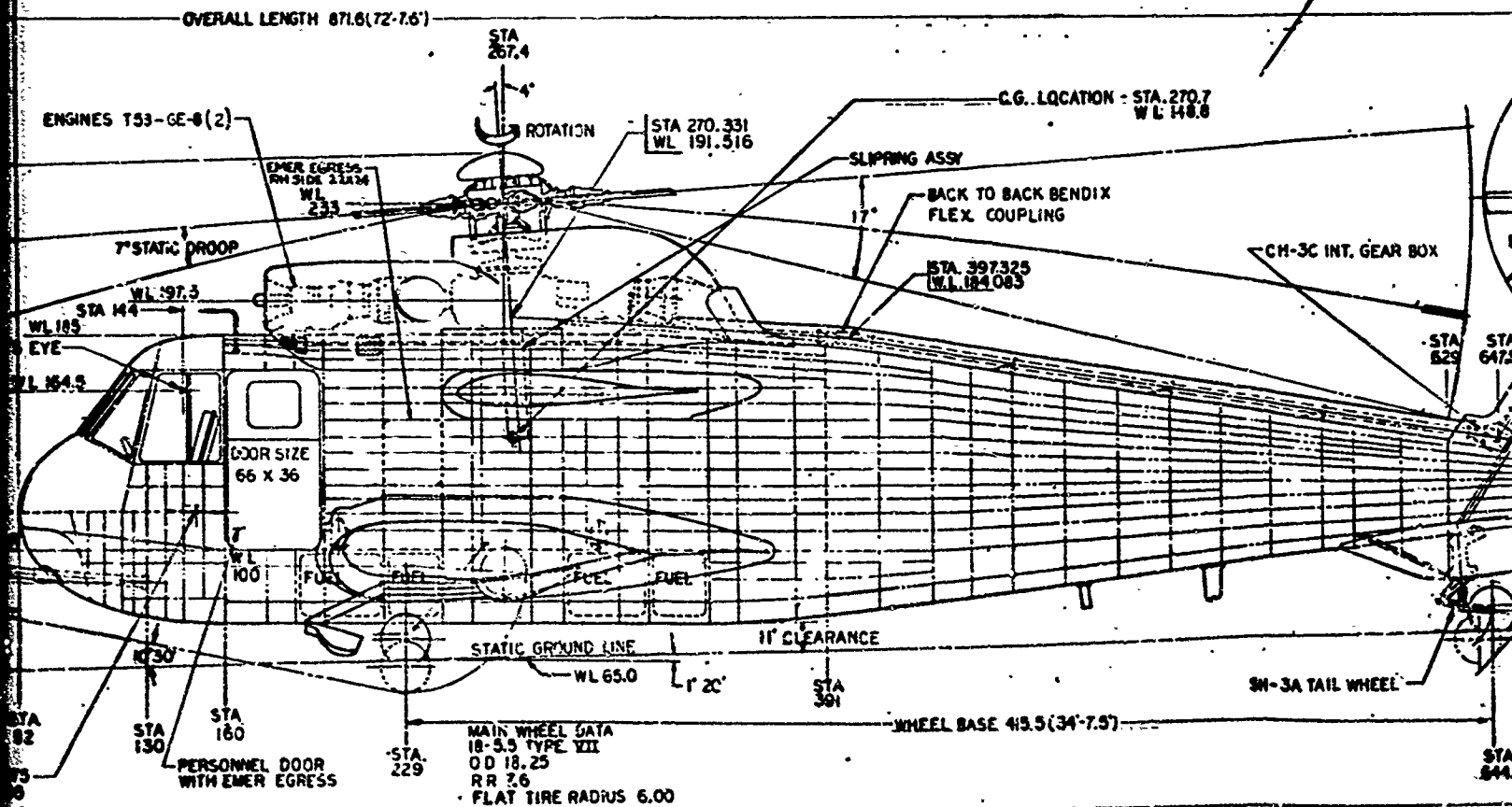
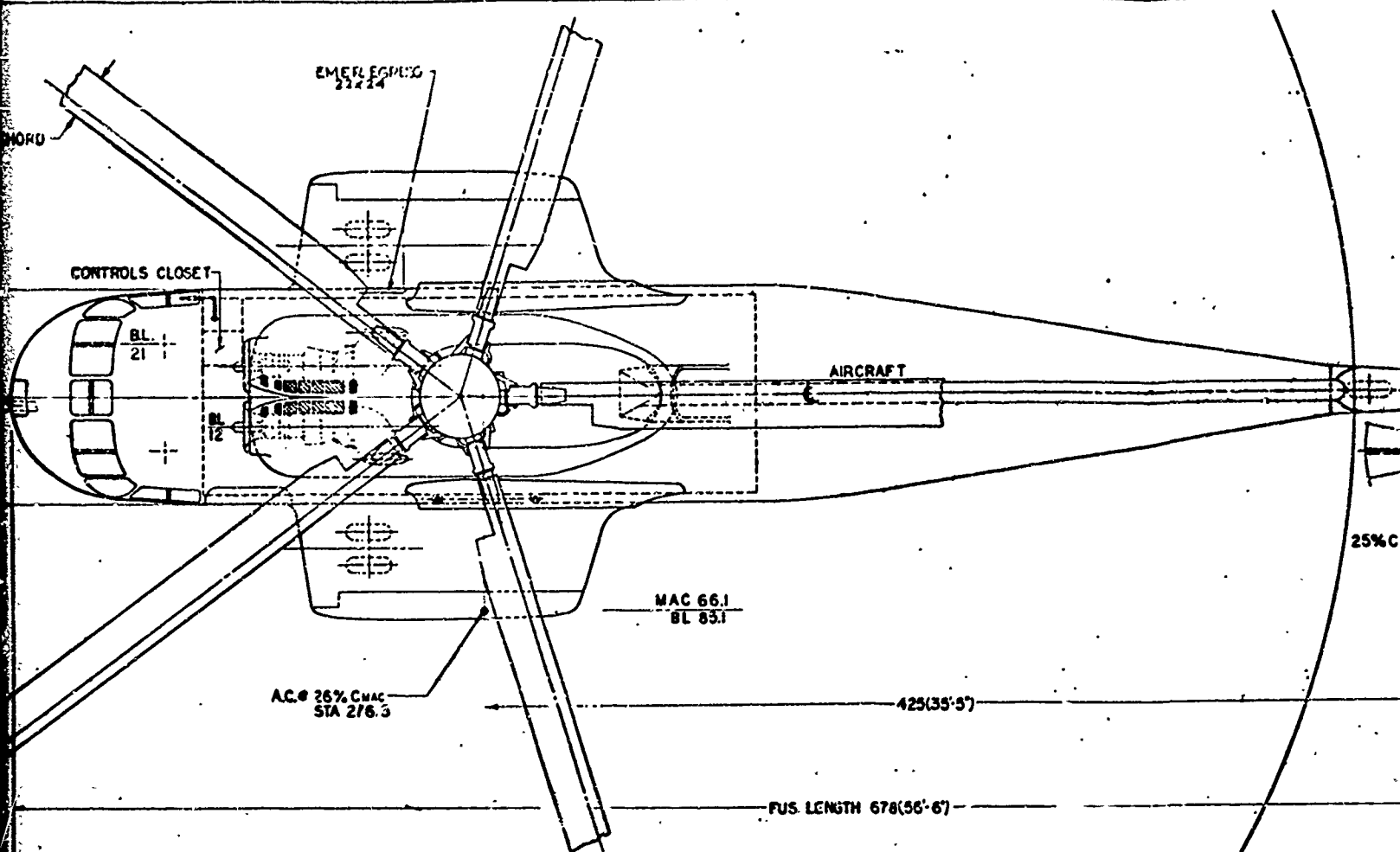
STA 144.875  
 WL 119.95

SH-3A MAIN ALIGHTING  
 GEAR (NEW WHEEL ASSY  
 & DRAG STRUT)



TREAD 120 (10'-0")

60



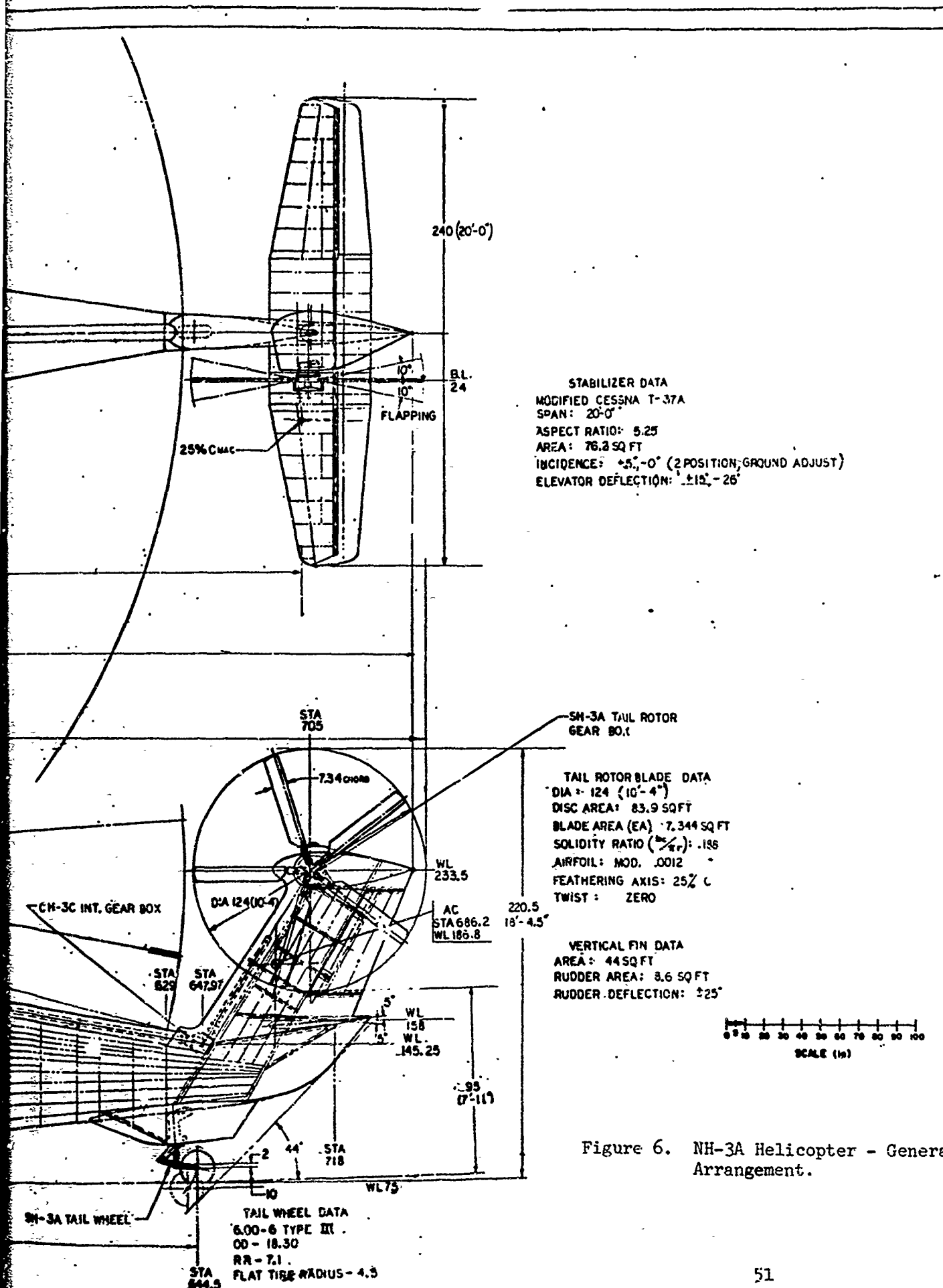
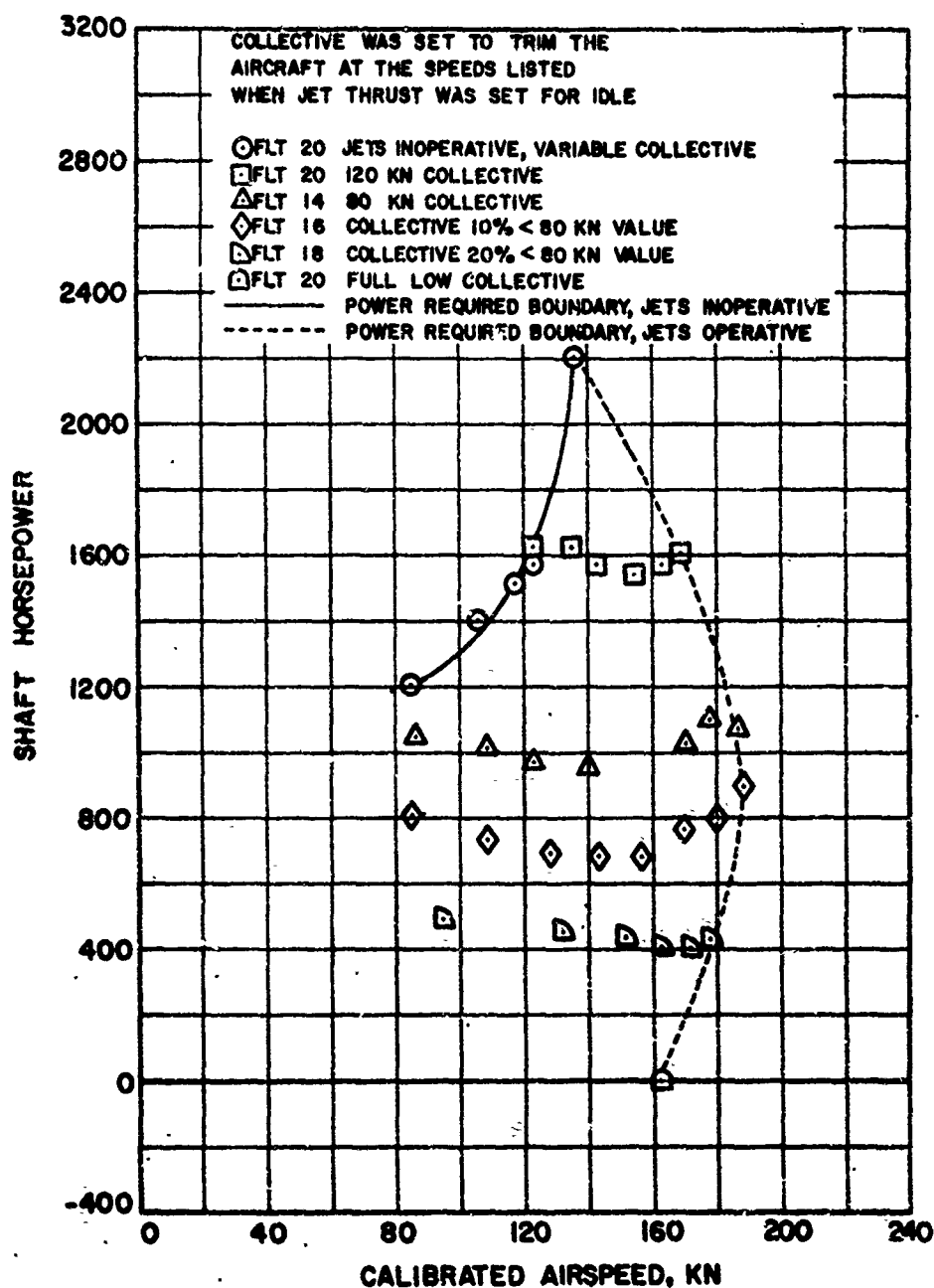
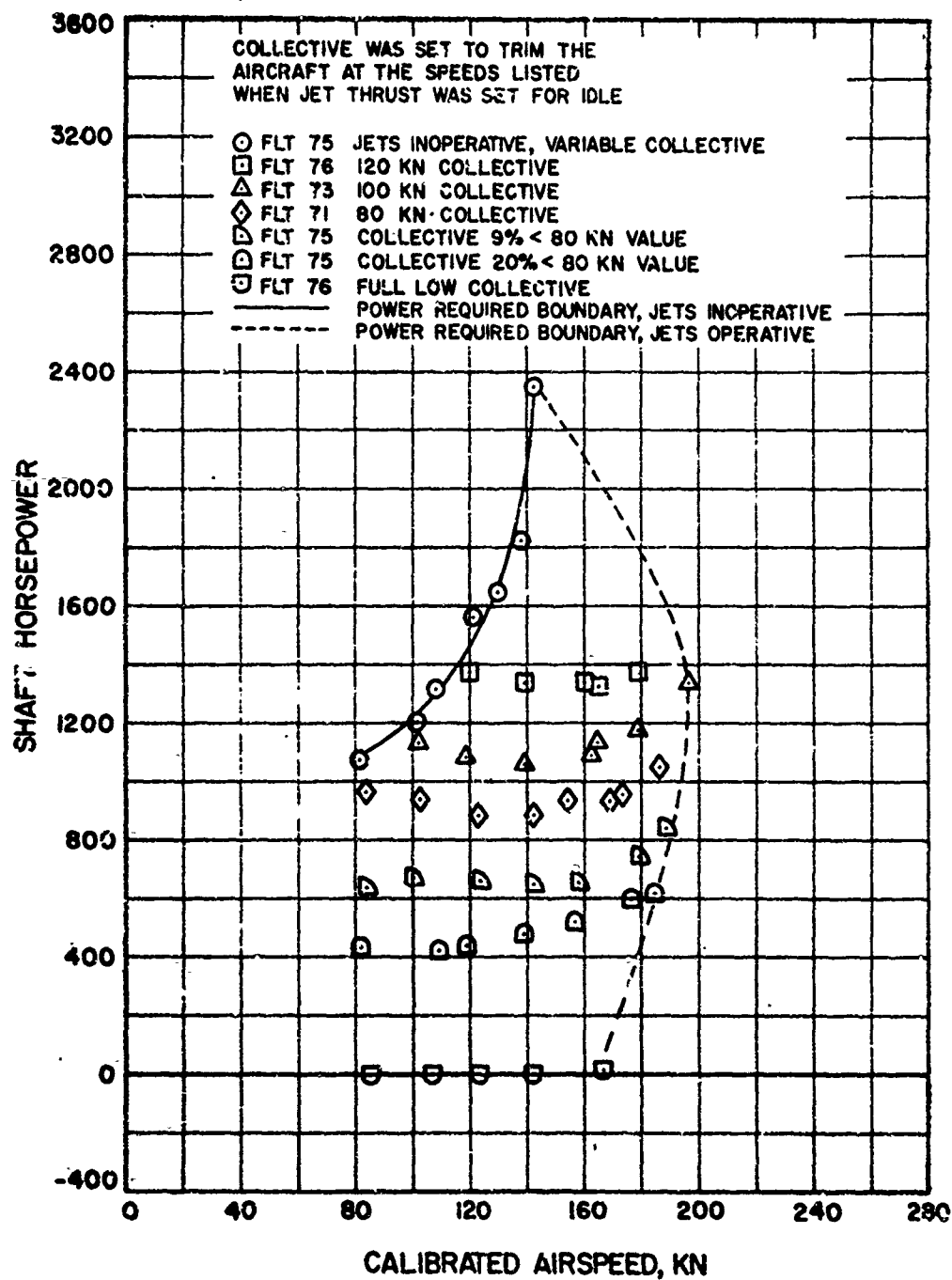


Figure 6. NH-3A Helicopter - General Arrangement.



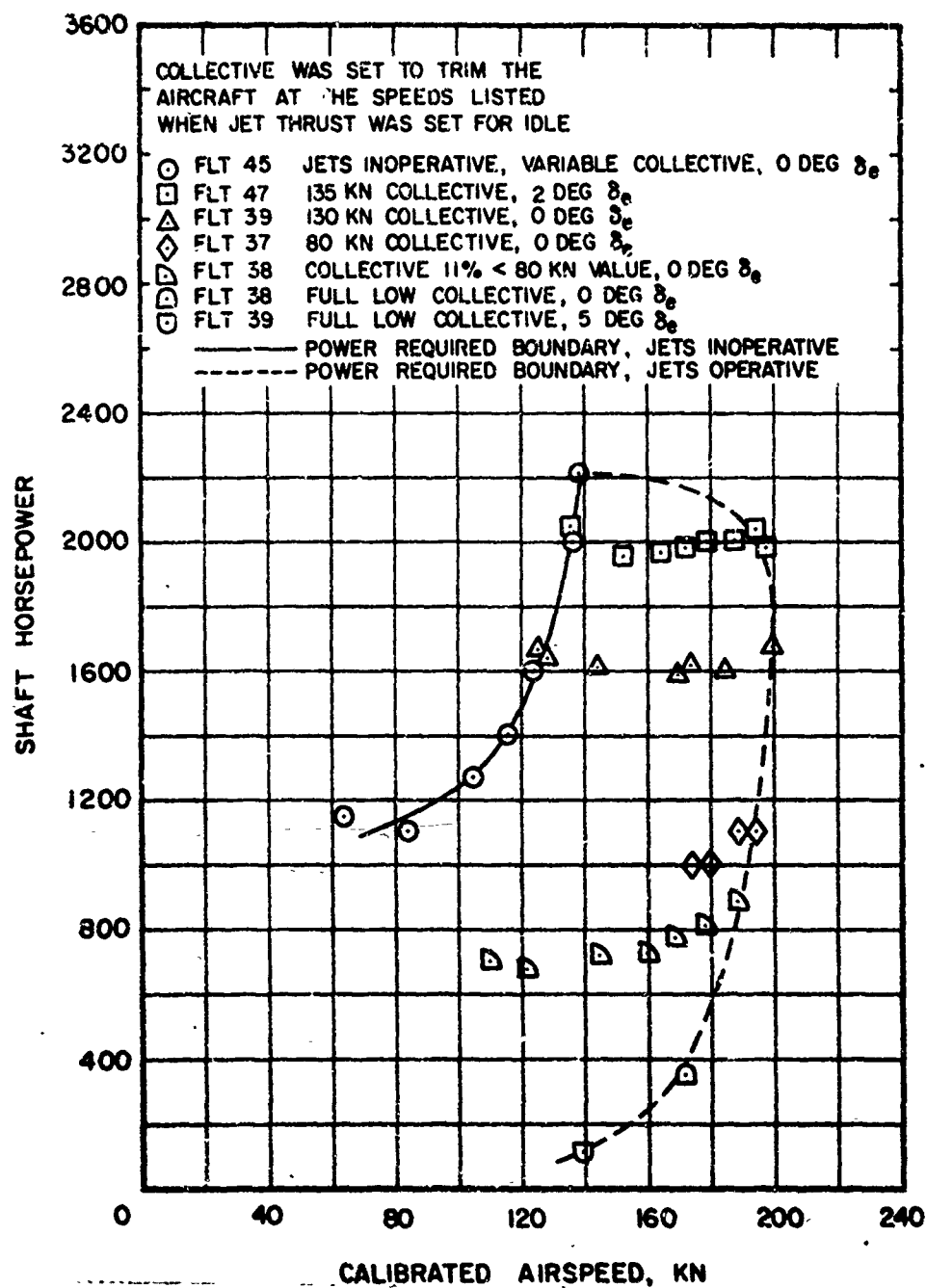
(a) WITHOUT WINGS, WITH JET PODS, FIVE MAIN ROTOR BLADES, -4 DEGREES TWIST, -15 DEGREES  $\delta_e$ , 5 DEGREES  $i_{HT}$

FIGURE 7. NH-3A LEVEL FLIGHT ENVELOPE FOR VARIOUS AIRCRAFT CONFIGURATIONS, ELEVATOR SETTINGS AND HORIZONTAL STABILIZER INCIDENCES.



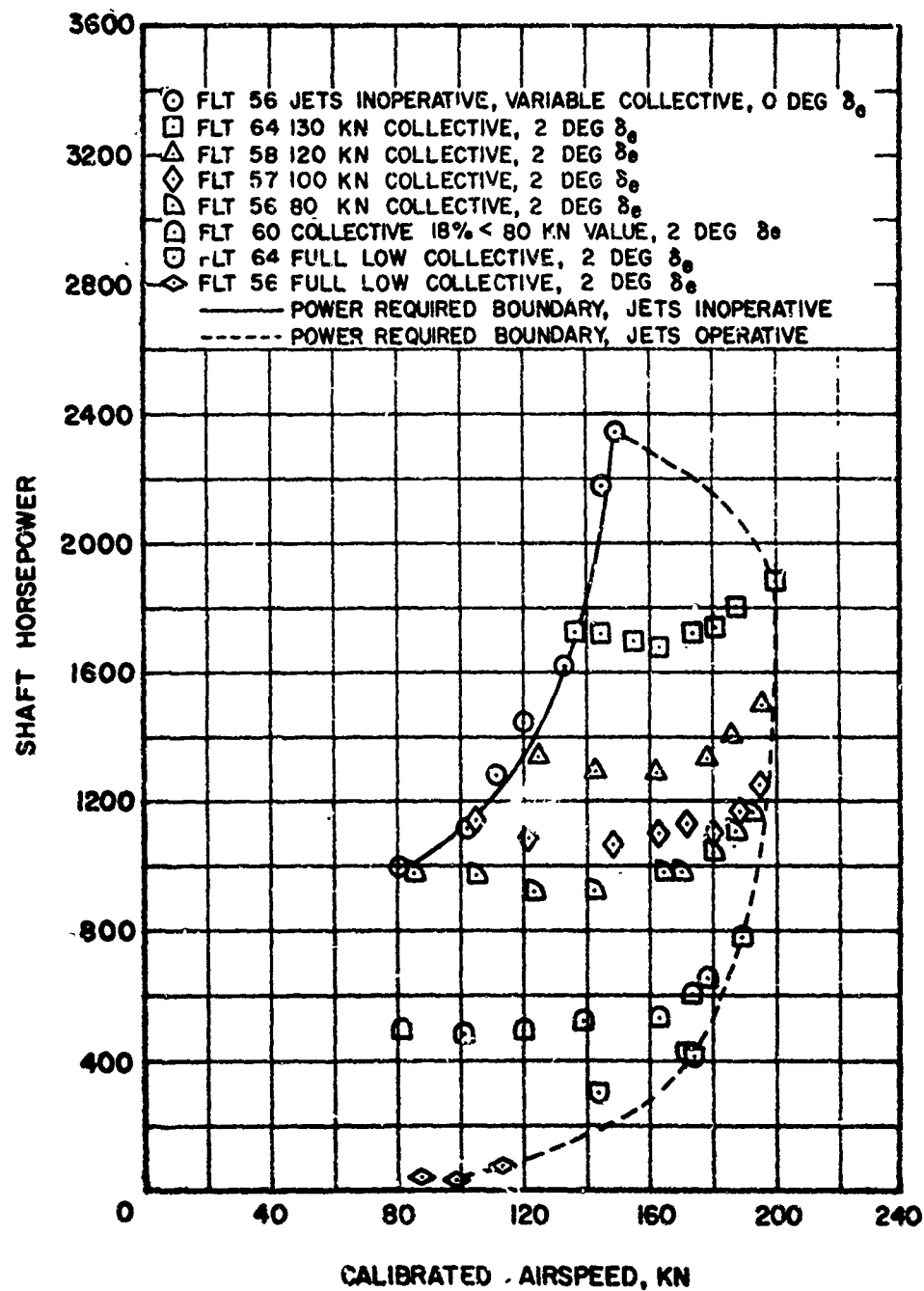
(b) WITHOUT WINGS, WITH JET PODS, FIVE MAIN ROTOR BLADES, -8 DEGREES TWIST, ZERO DEGREE  $\delta_e$ , ZERO DEGREE  $i_{HT}$

FIGURE 7. Continued.



(c) WITH WINGS, WITH JET PODS, FIVE MAIN ROTOR BLADES, -4 DEGREES TWIST, VARIOUS  $\delta_e$ , ZERO DEGREE  $i_{HT}$ , 4 DEGREES  $\delta_f$

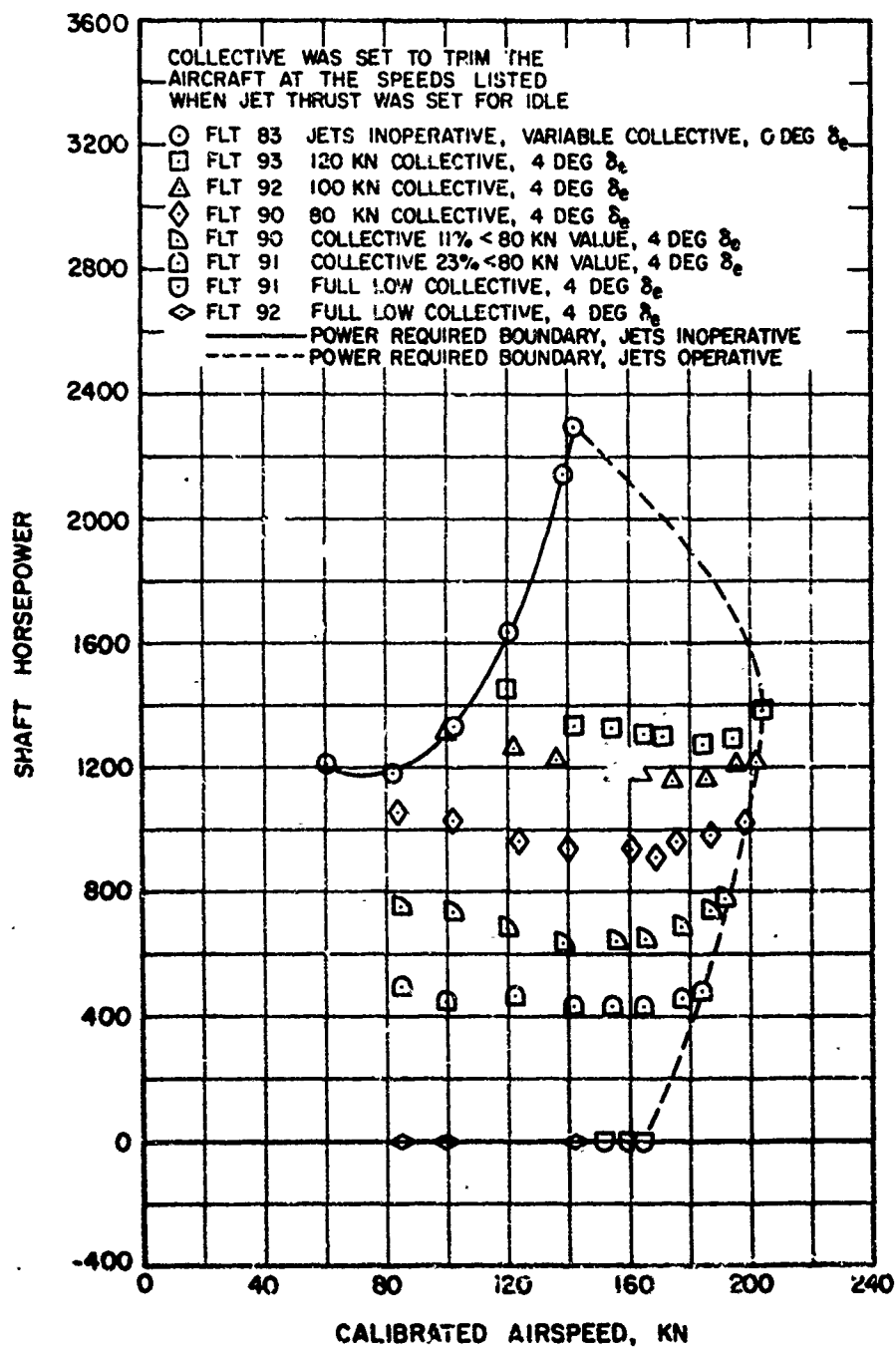
FIGURE 7. Continued.



(d) WITH WINGS, WITH JET PODS, FIVE MAIN ROTOR BLADES -8 DEGREES TWIST, VARIOUS  $\delta_e$ , ZERO DEGREE  $i_{HT}$ , 4 DEGREES  $\delta_f$

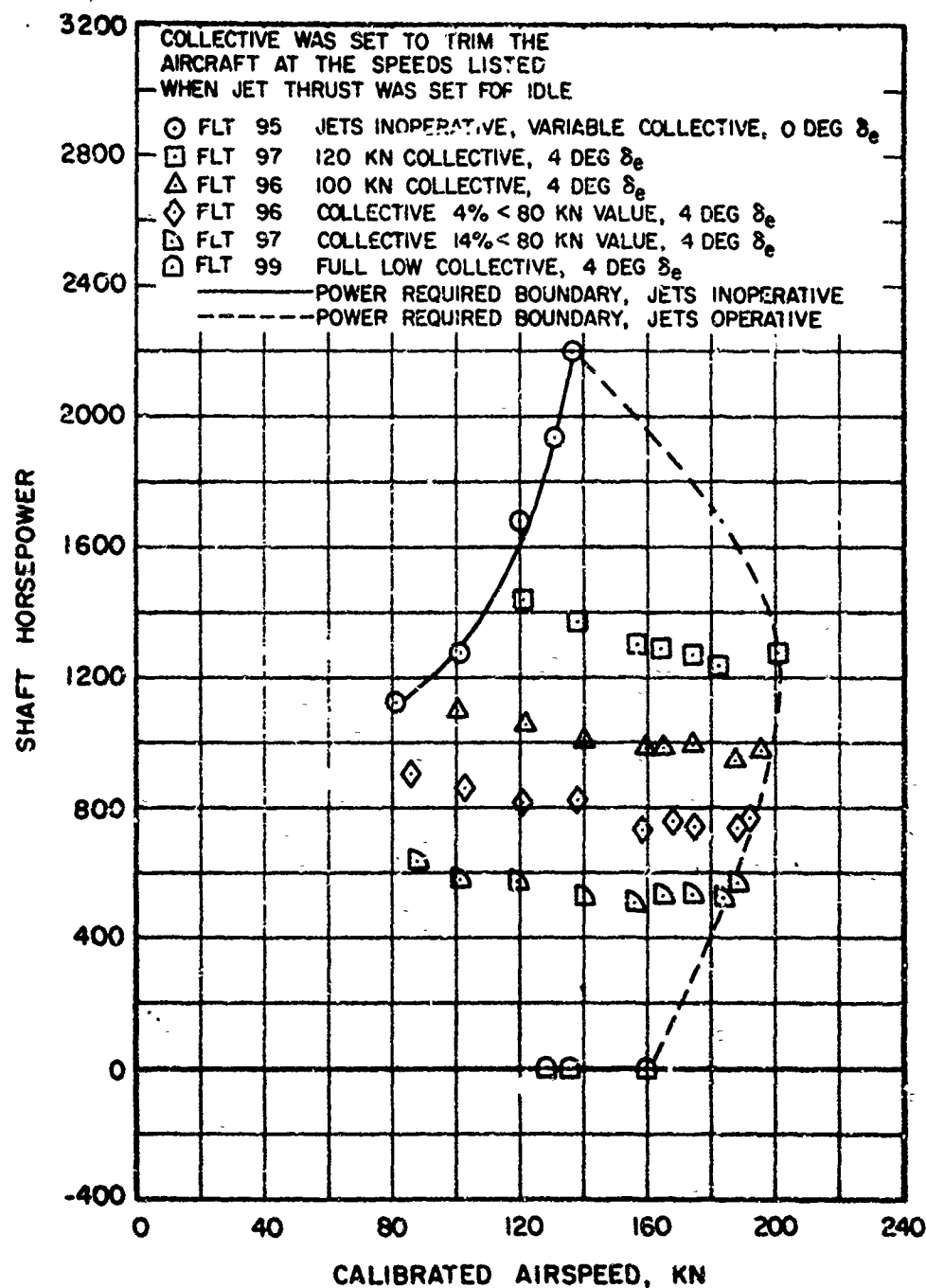
FIGURE 7. Continued.





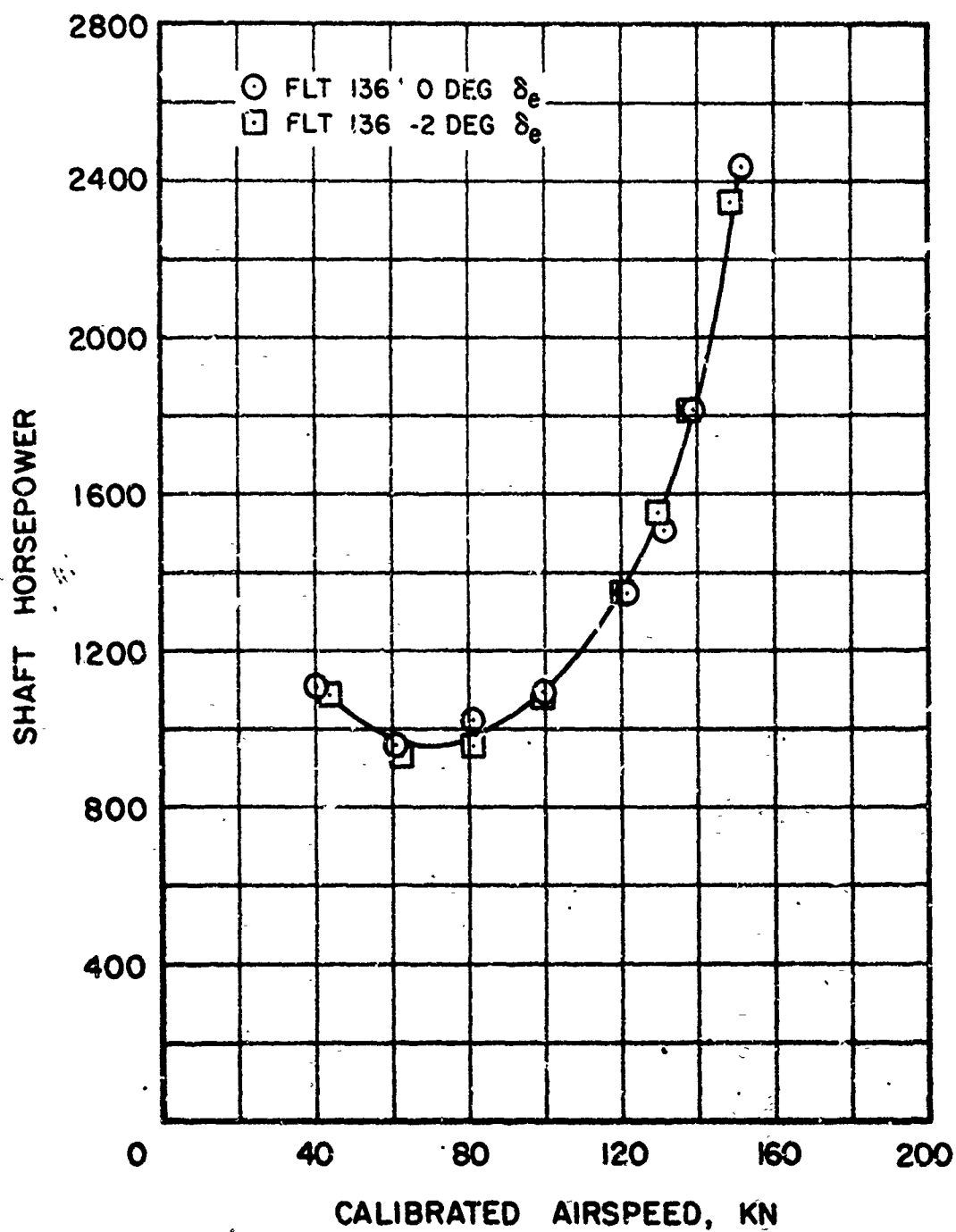
(e) WITHOUT WINGS, WITH JET PODS, SIX MAIN ROTOR BLADES, -4 DEGREES TWIST, VARIOUS  $\delta_e$ , ZERO DEGREE  $i_{HT}$

FIGURE 7. Continued.



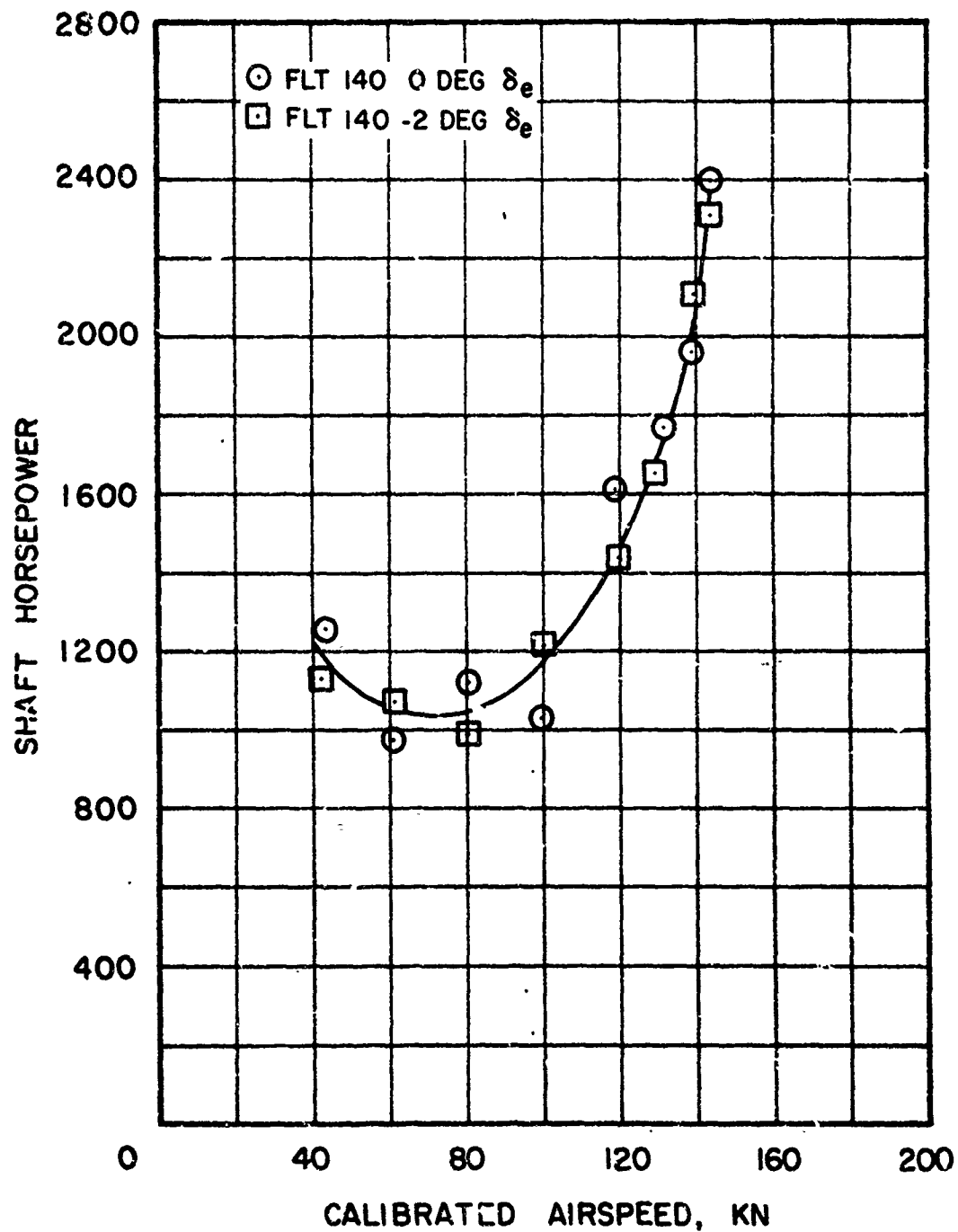
(f) WITHOUT WINGS, WITH JET PODS, 6 MAIN ROTOR BLADES, -8 DEGREES TWIST, VARIOUS  $\delta_e$ , ZERO DEGREE  $i_{HT}$

FIGURE 7. Continued.



(g) WITHOUT WINGS, WITHOUT JET PODS, FIVE  
MAIN ROTOR BLADES, -8 DEGREES TWIST, VARIOUS  
 $\delta_e$ , ZERO DEGREE  $i_{HT}$ , VARIABLE COLLECTIVE

FIGURE 7. Continued.



(h) WITHOUT WINGS, WITHOUT JET PODS, FIVE MAIN  
 ROTOR BLADES, -4 DEGREES TWIST, VARIOUS  $\delta_e$ ,  
 ZERO DEGREE  $i_{HT}$ , VARIABLE COLLECTIVE

FIGURE 7. Concluded.

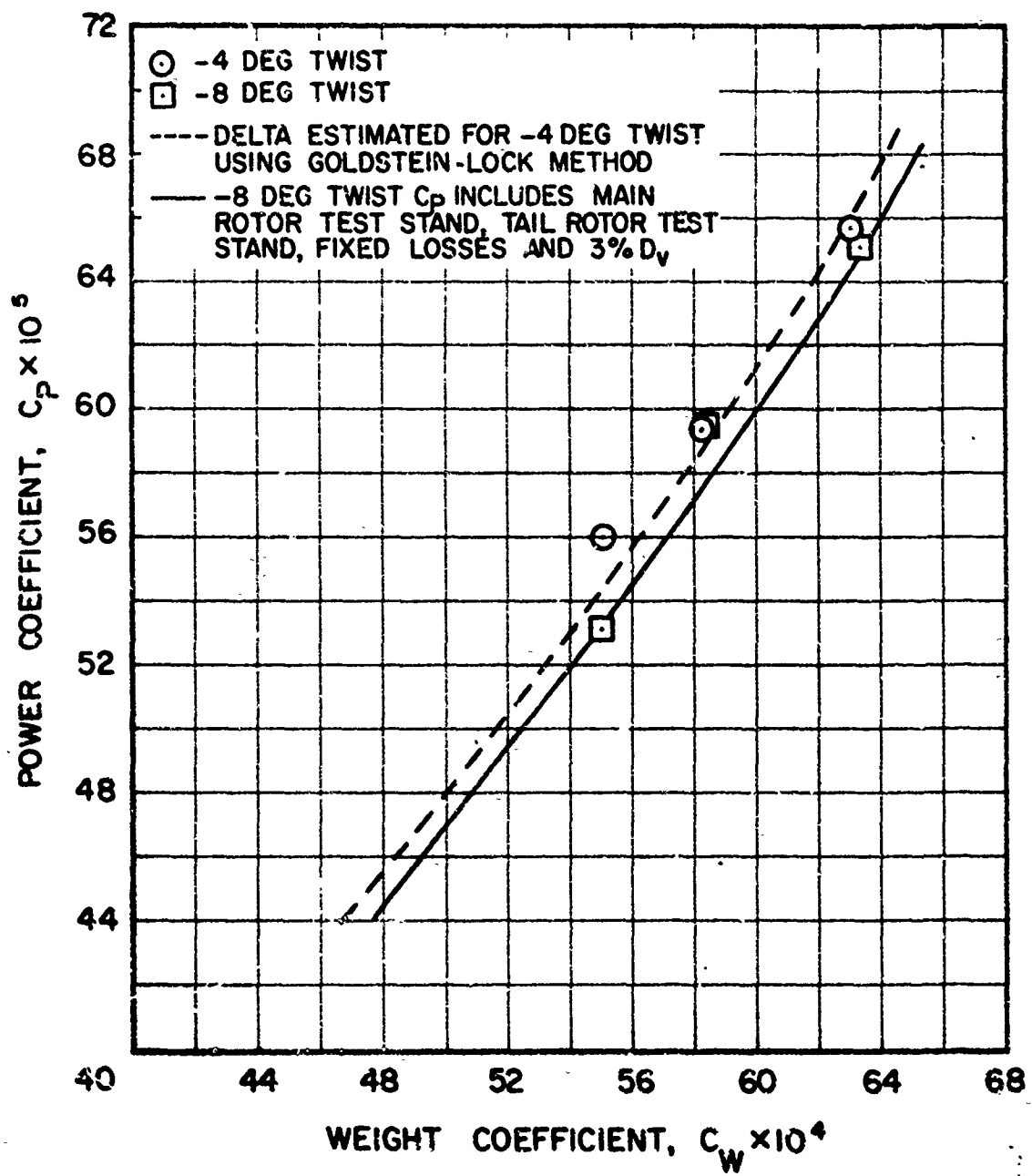


FIGURE 8. HOVER PERFORMANCE, EFFECT OF BLADE TWIST ( BASIC HELICOPTER, FIVE MAIN ROTOR BLADES).

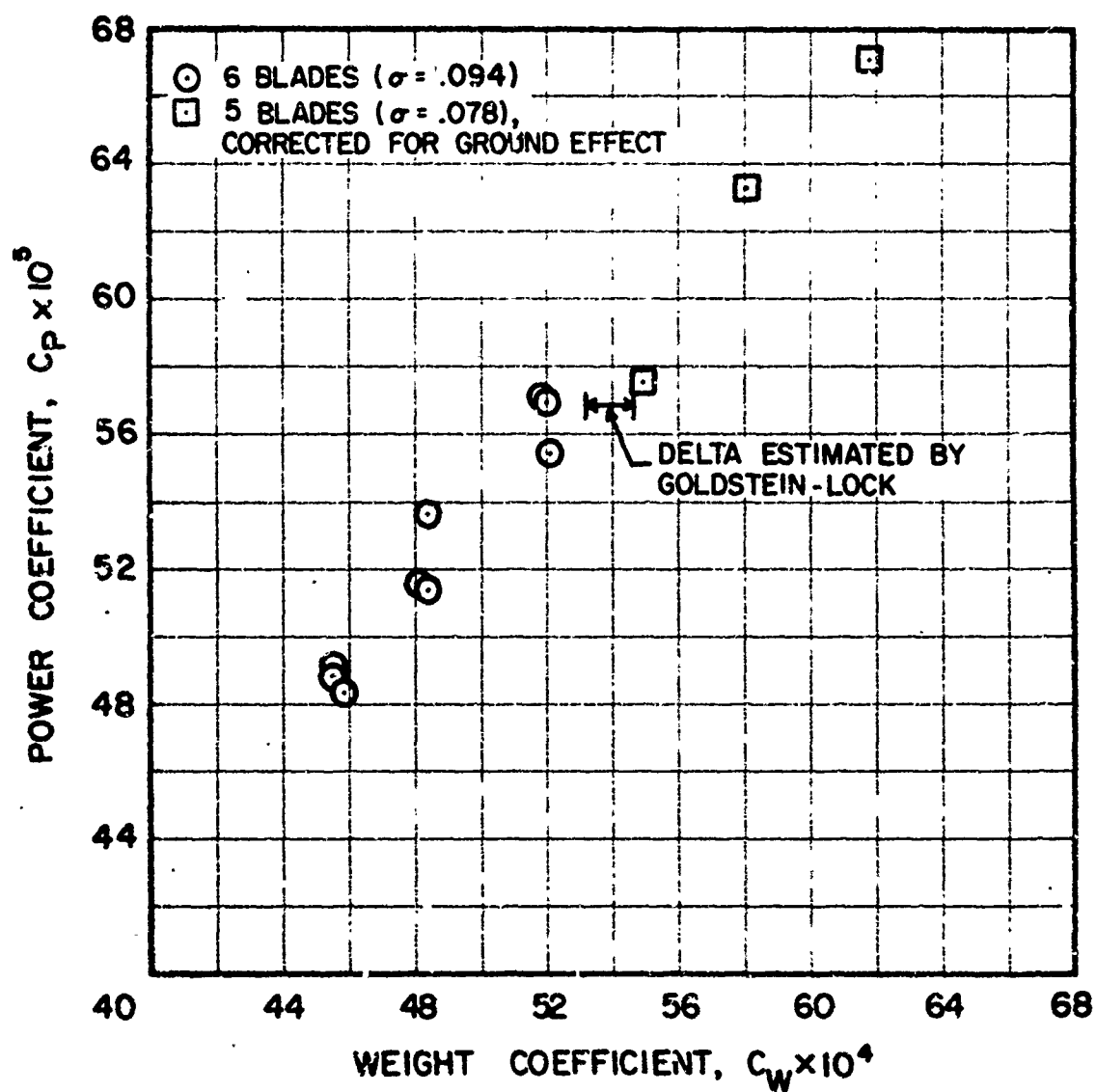


FIGURE -9. HOVER PERFORMANCE, EFFECT OF ROTOR SOLIDITY (-4 DEGREE TWIST, WITH JET PODS).

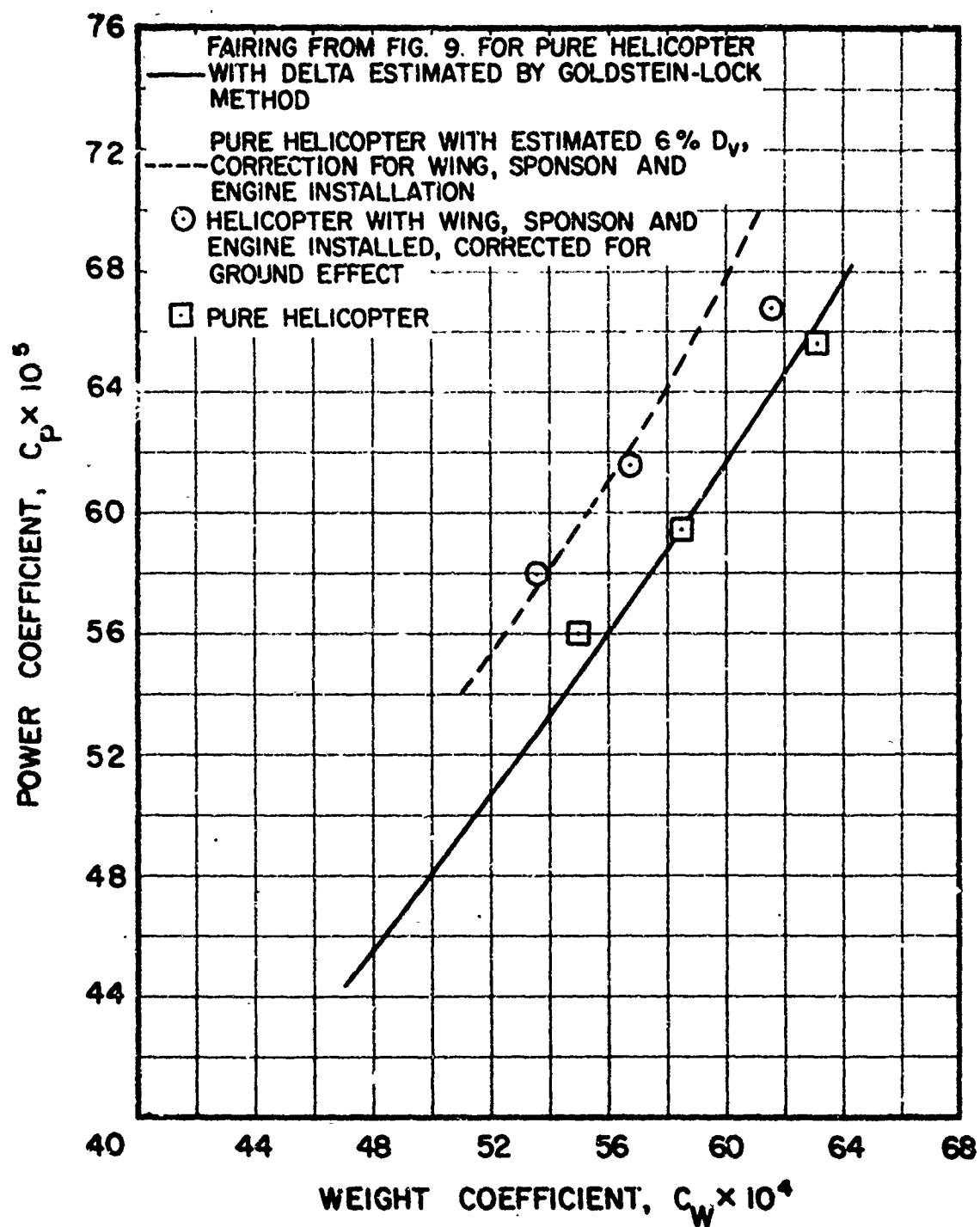
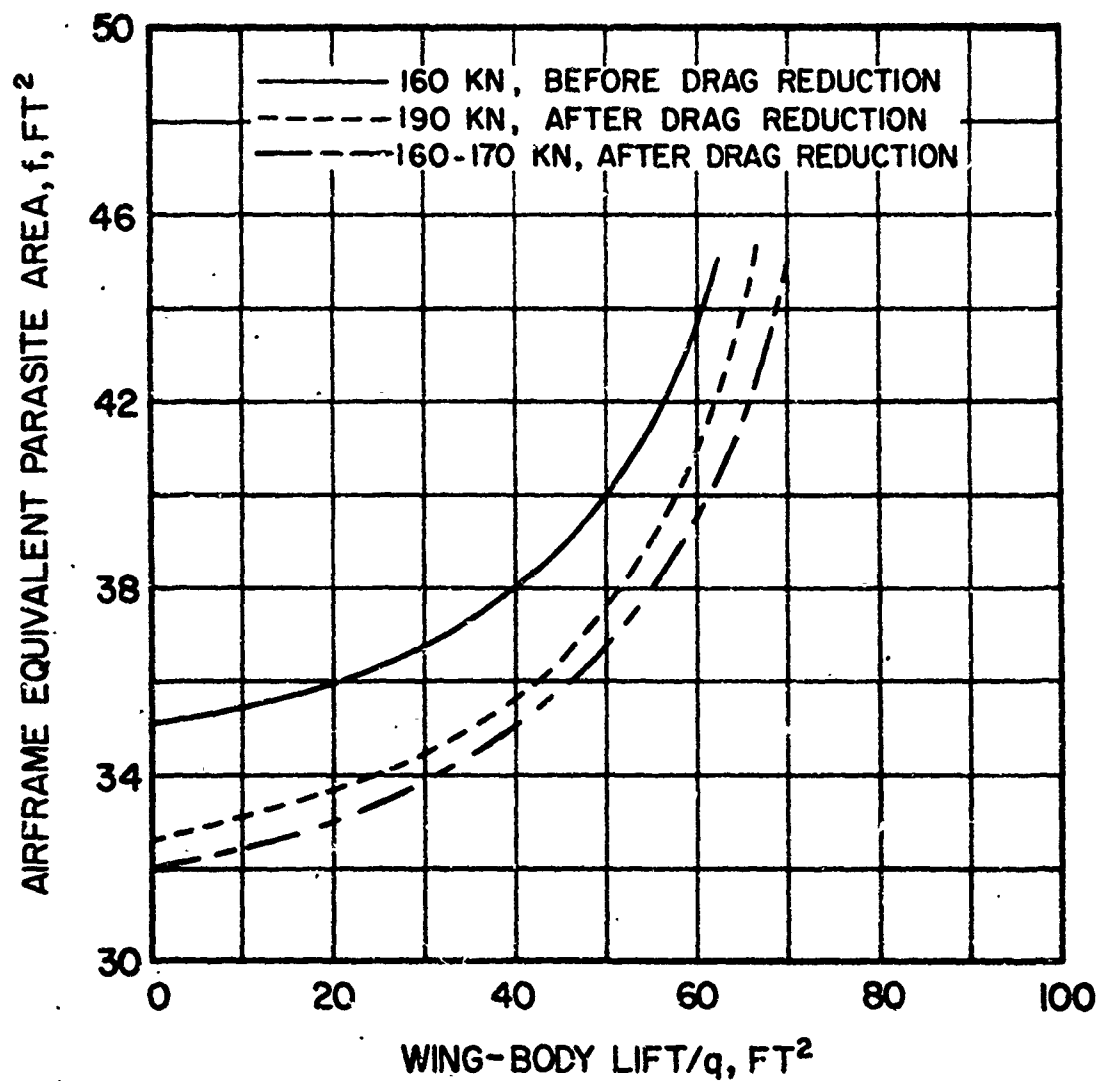


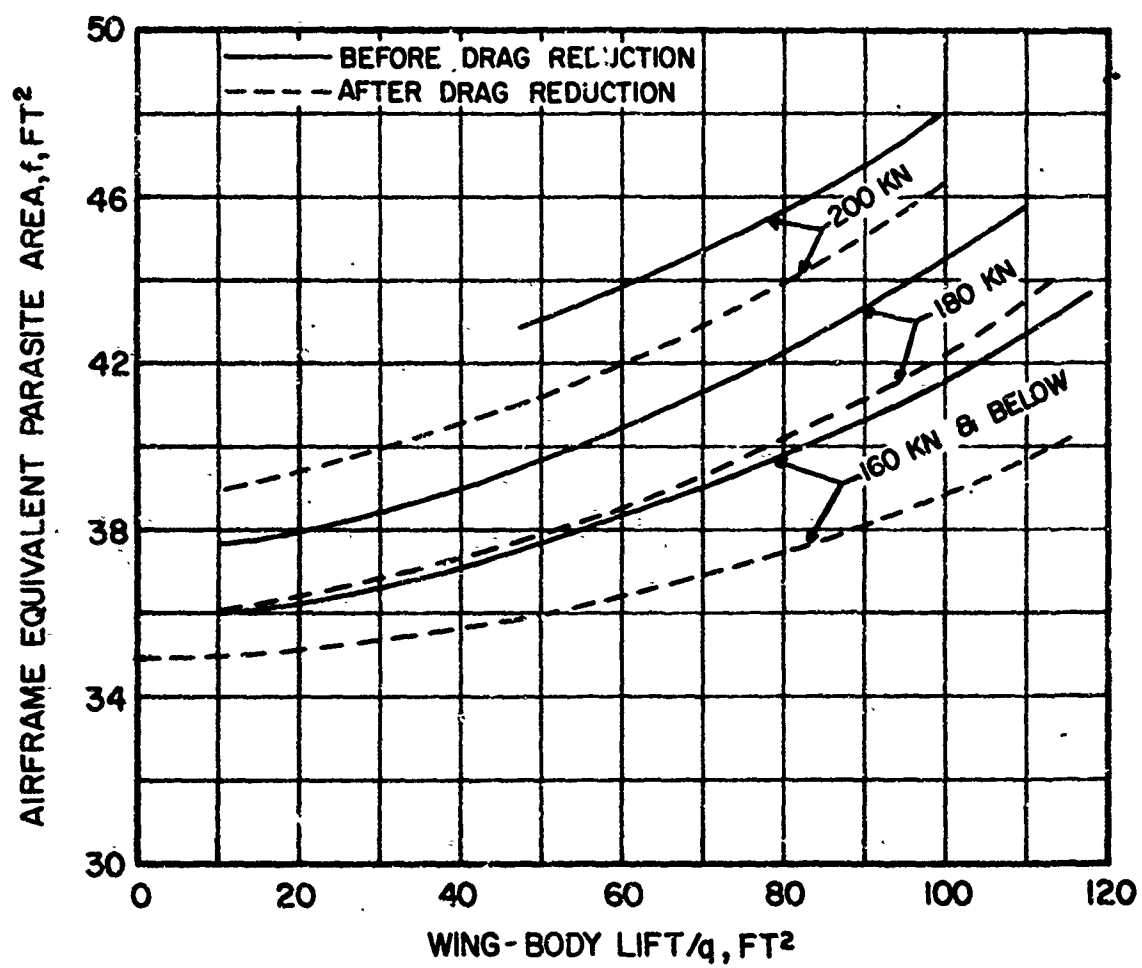
FIGURE 10. HOVER PERFORMANCE, EFFECT OF WING INSTALLATION (FIVE MAIN ROTOR BLADES, -4 DEGREES TWIST).



(a) WITHOUT WINGS, WITH JETS

FIGURE 11. LIFT DRAG POLARS.





(b) WITH WINGS, WITH JETS

FIGURE 11. Concluded..

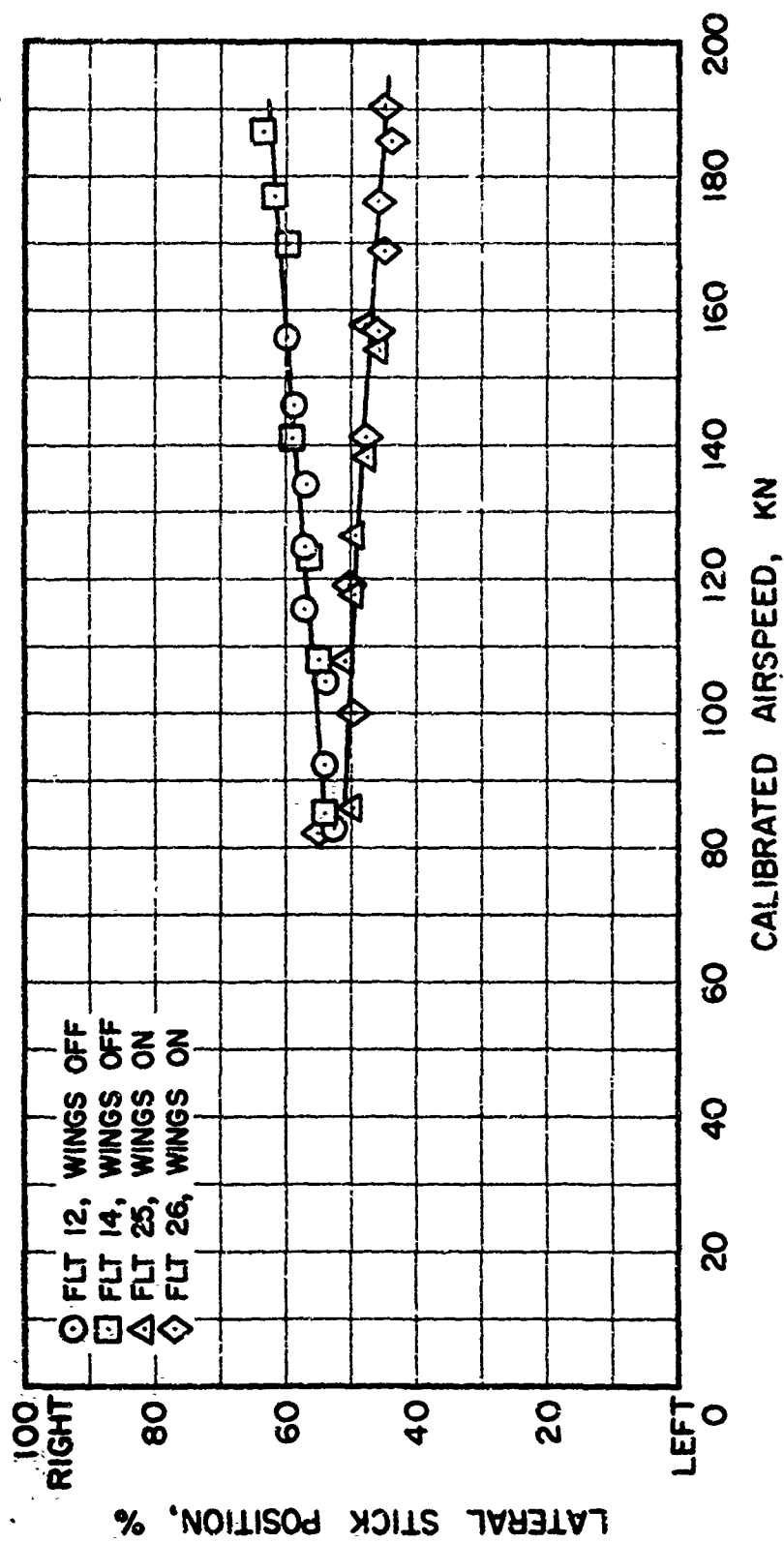


FIGURE 12. LATERAL CONTROL POSITION VERSUS AIRSPEED.

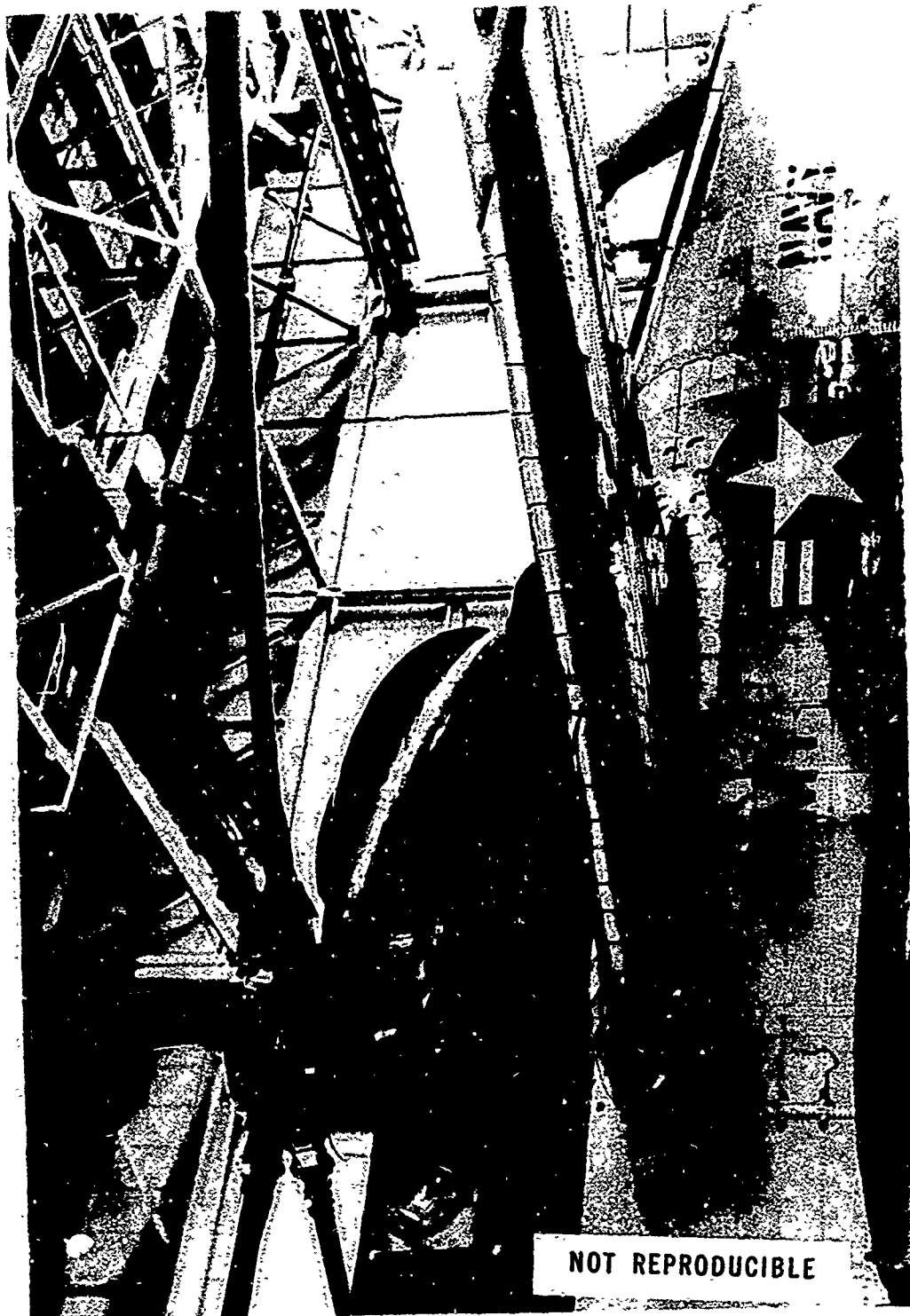
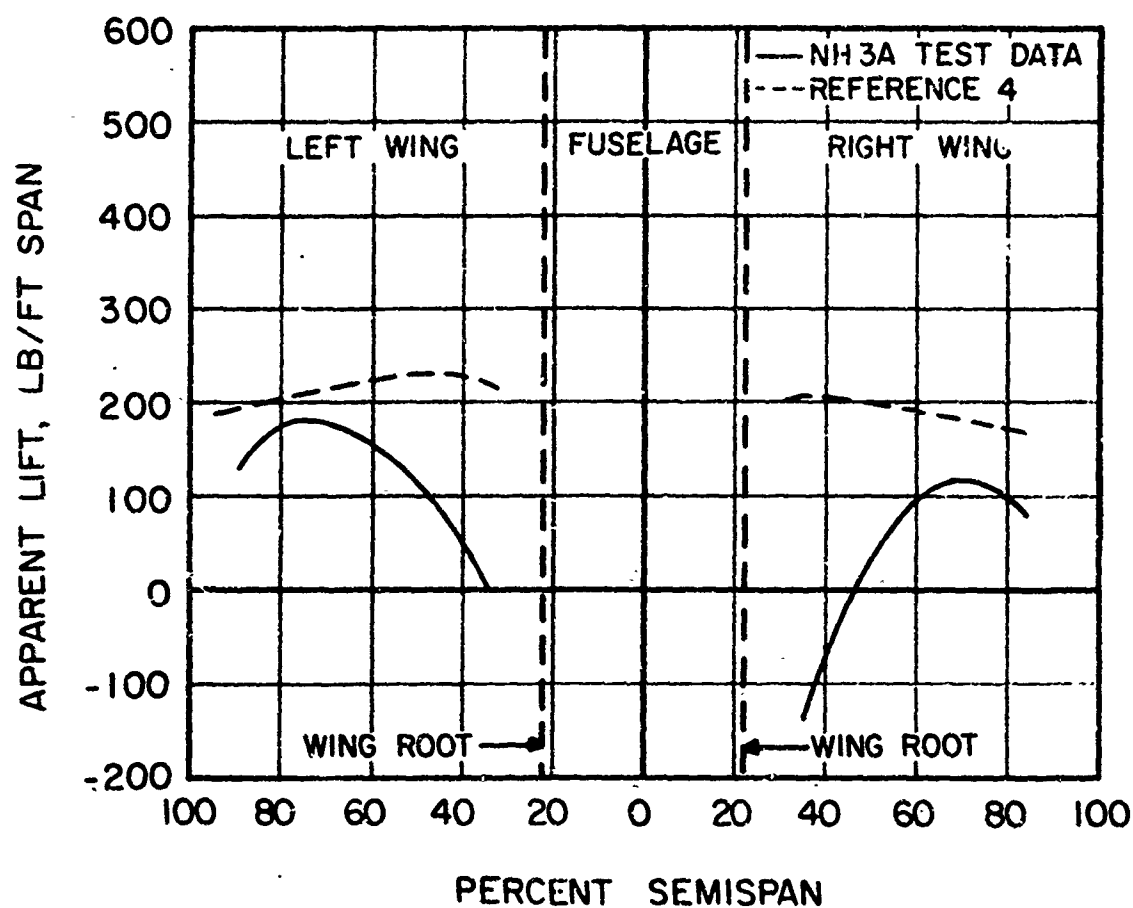
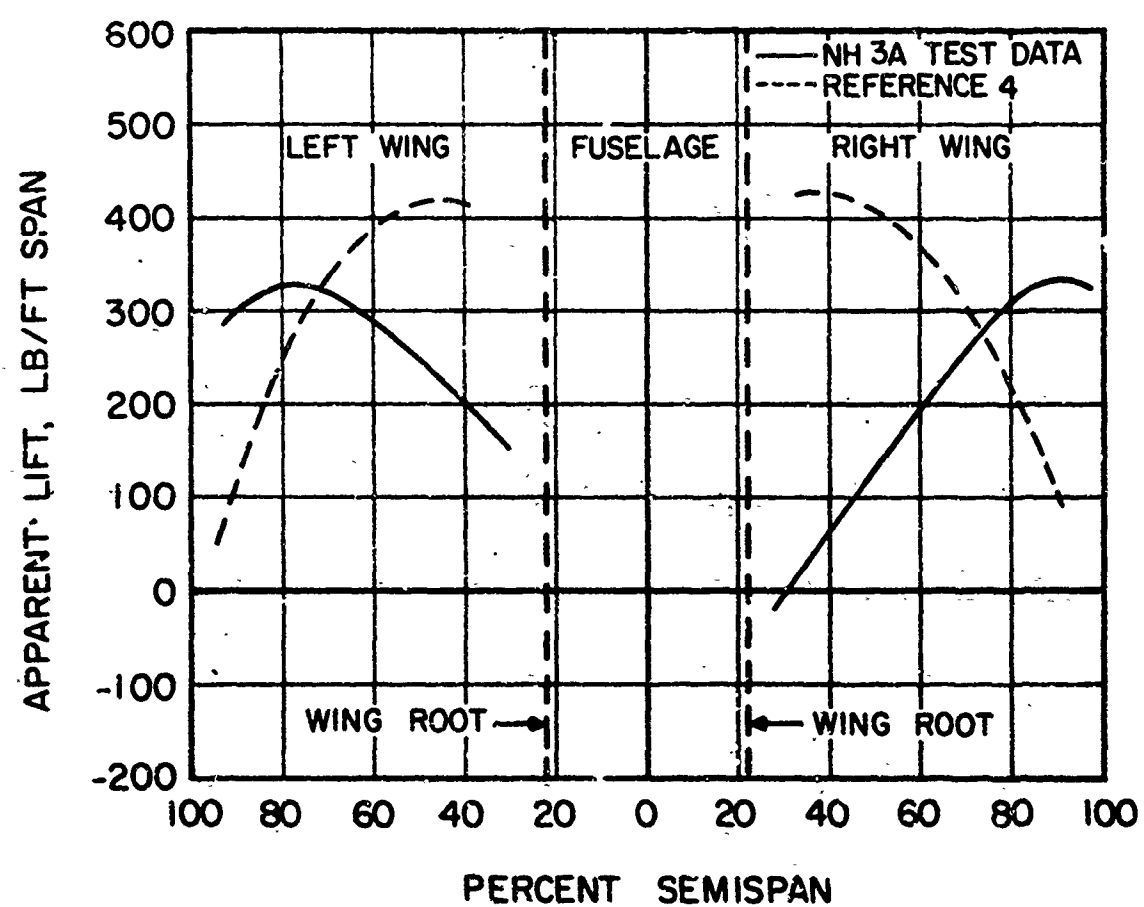


Figure 13. Differential Wing Lift Test Installation.



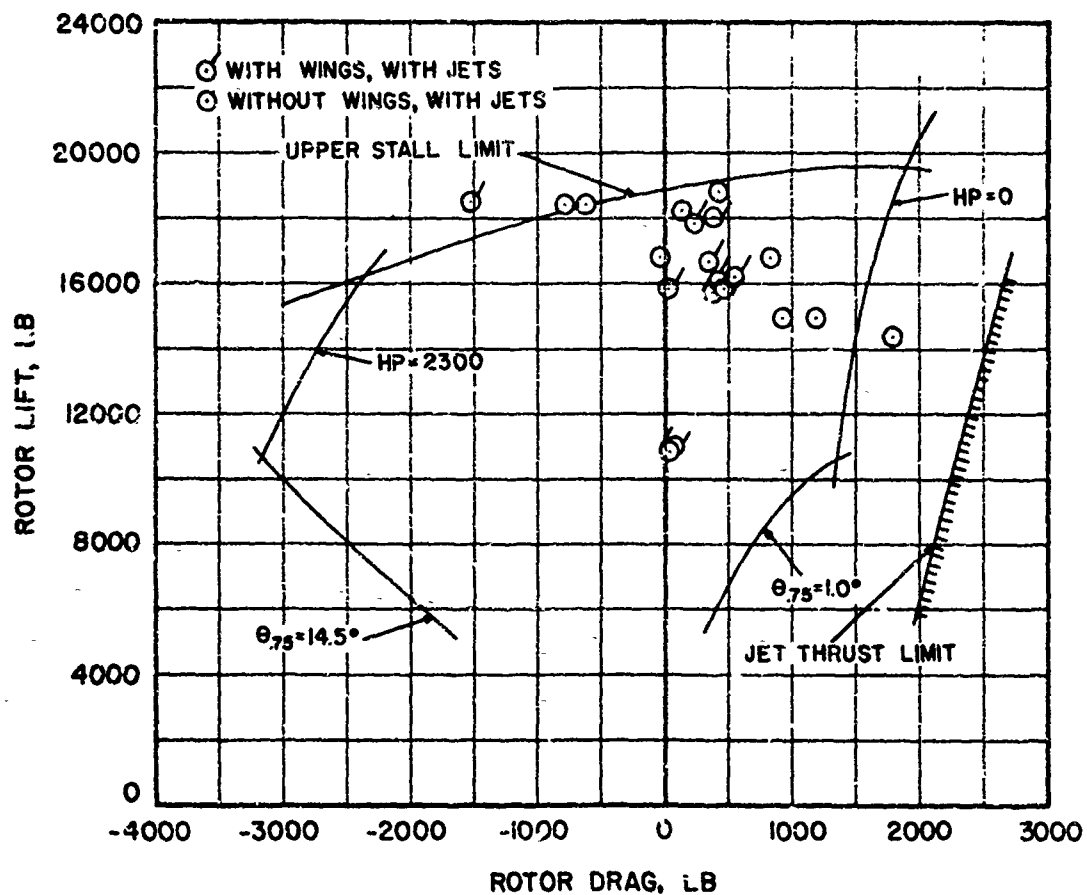
(a)  $V = 120$  KNOTS, PITCH ATTITUDE = 1.9 DEGREES,  
YAW ANGLE = -4.2 DEGREES

FIGURE 14. WING LIFT DISTRIBUTION.



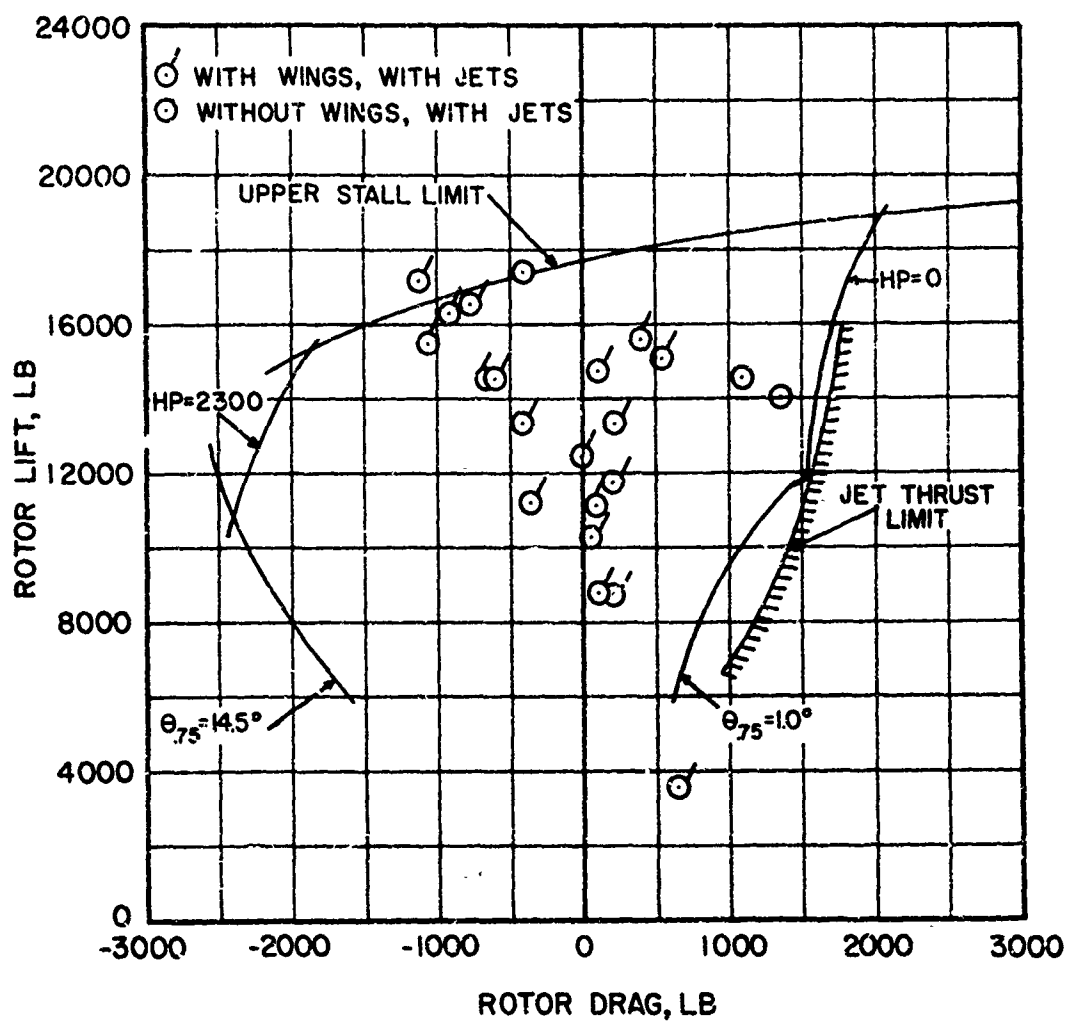
(b)  $V = 164$  KNOTS, PITCH ATTITUDE = 2 DEGREES,  
YAW ANGLE = -3.5 DEGREES

FIGURE 14. (CONCLUDED)



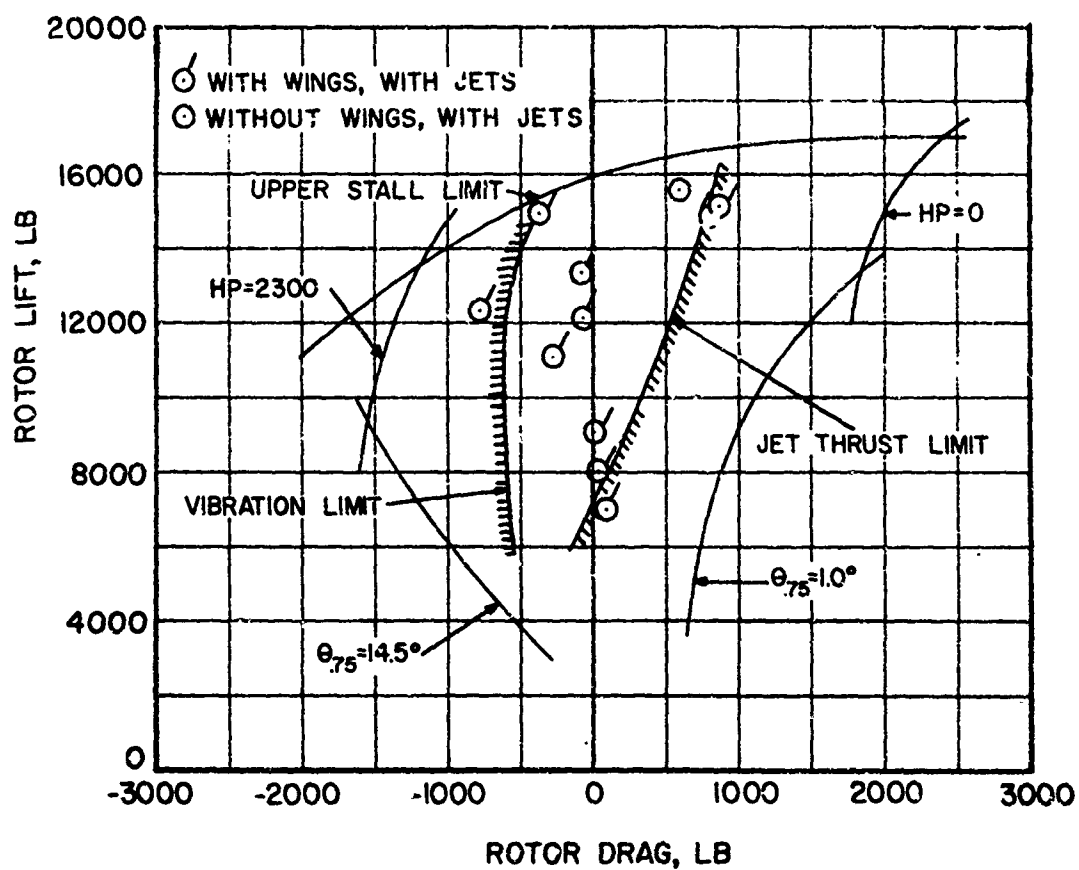
(a) 156 KNOTS ( $\mu = .40$ ), FIVE MAIN ROTOR BLADES,  $-4$  DEGREES TWIST

FIGURE 15. ROTOR OPERATING ENVELOPE FOR VARIOUS AIRSPEEDS AND ROTOR CONFIGURATIONS AND 660 FPS ROTOR TIP SPEED.



(b) 175 KNOTS ( $\mu = .45$ ), FIVE MAIN ROTOR BLADES,  
-4 DEGREES TWIST

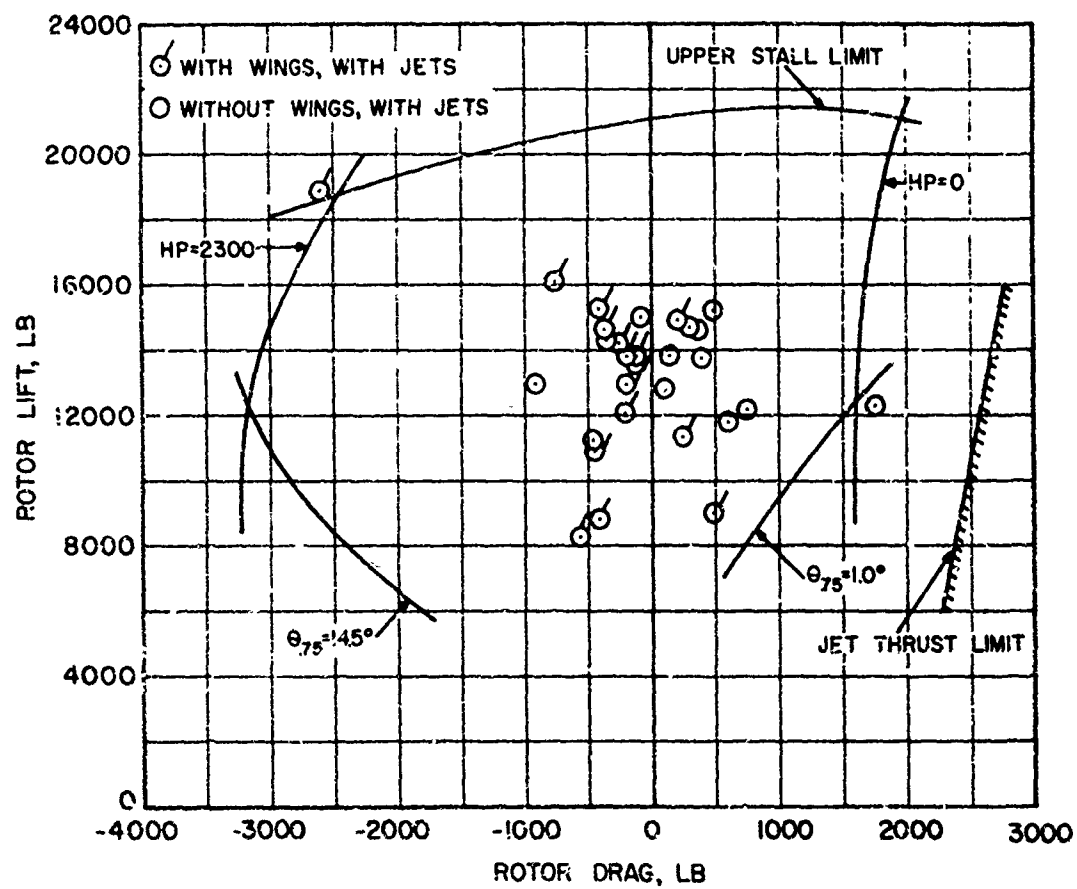
FIGURE 15. Continued.



(c) 195 KNOTS ( $\mu=.50$ ), FIVE MAIN ROTOR BLADES,  
-4 DEGREES TWIST

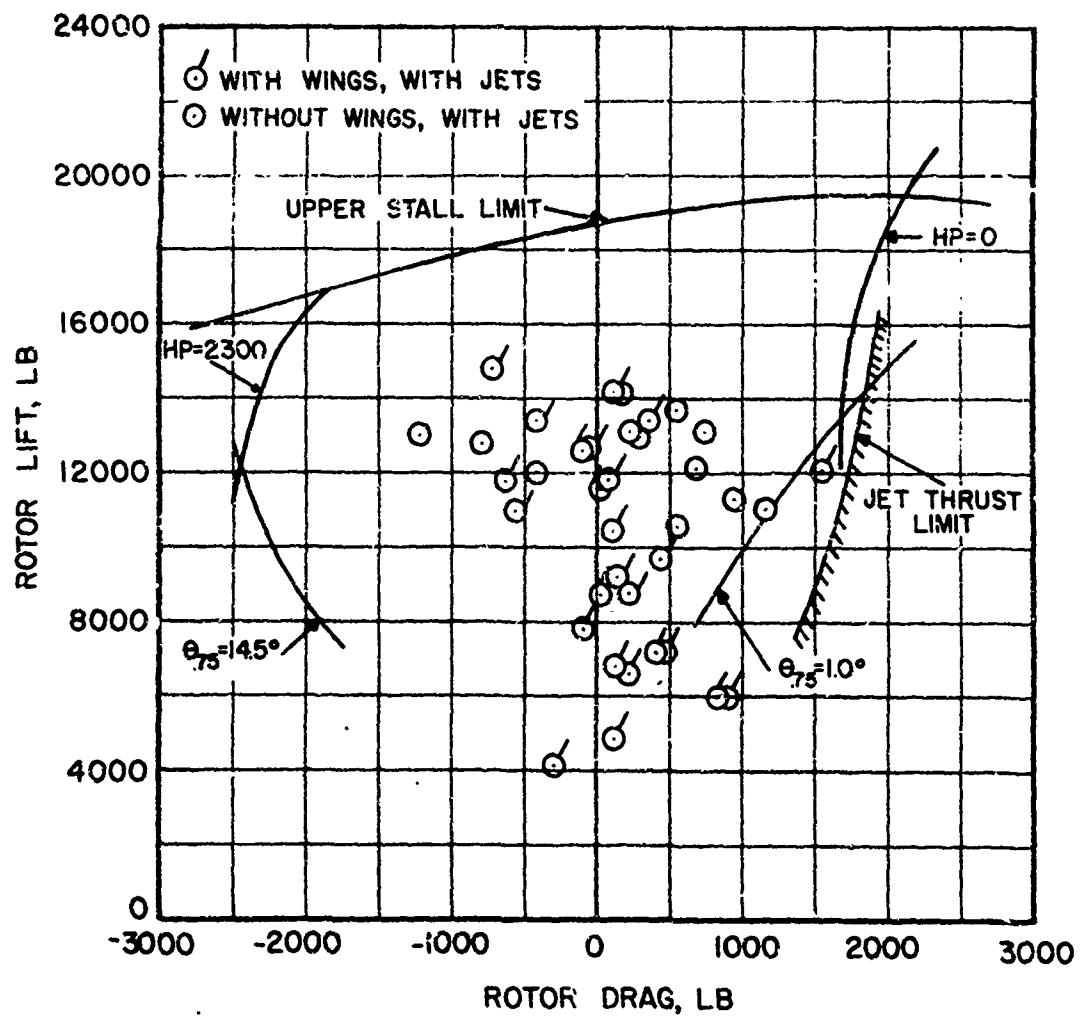
FIGURE 15. Continued.





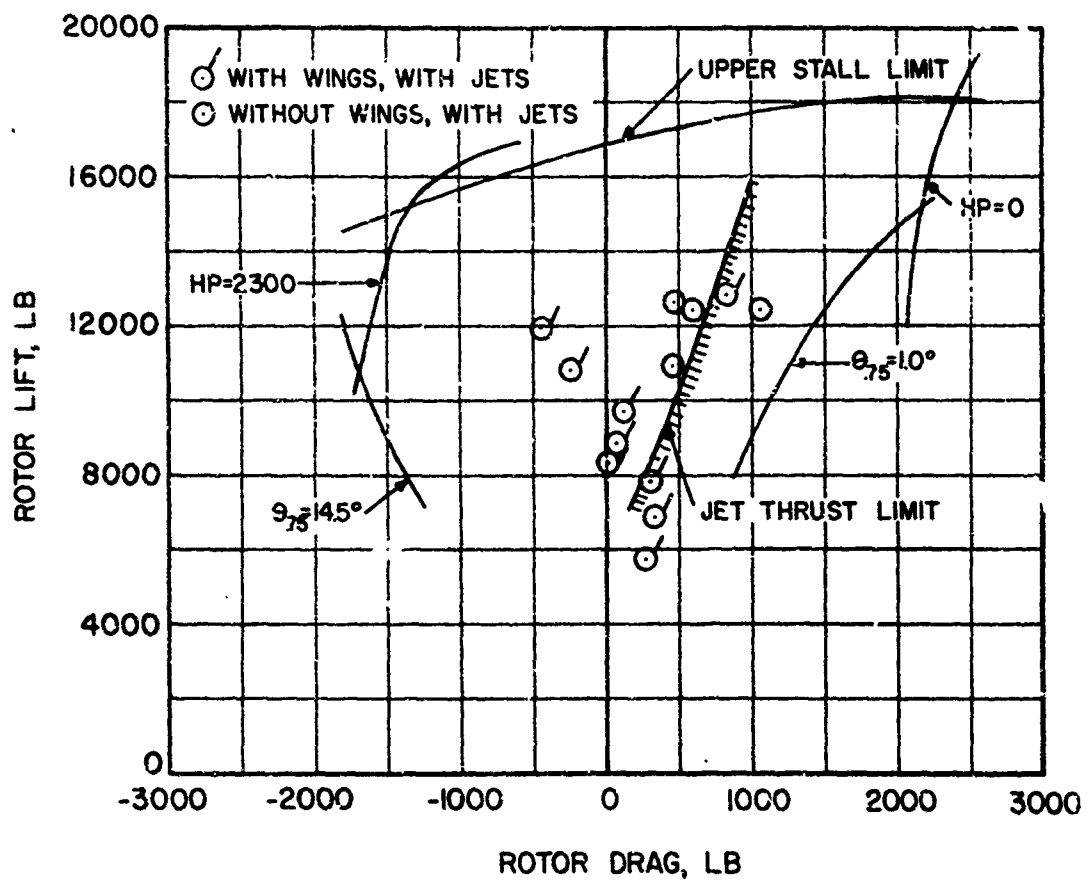
(a) 156 KNOT ( $\mu=.40$ ), FIVE MAIN ROTOR BLADES,  
-8 DEGREES TWIST

FIGURE 15. Continued.



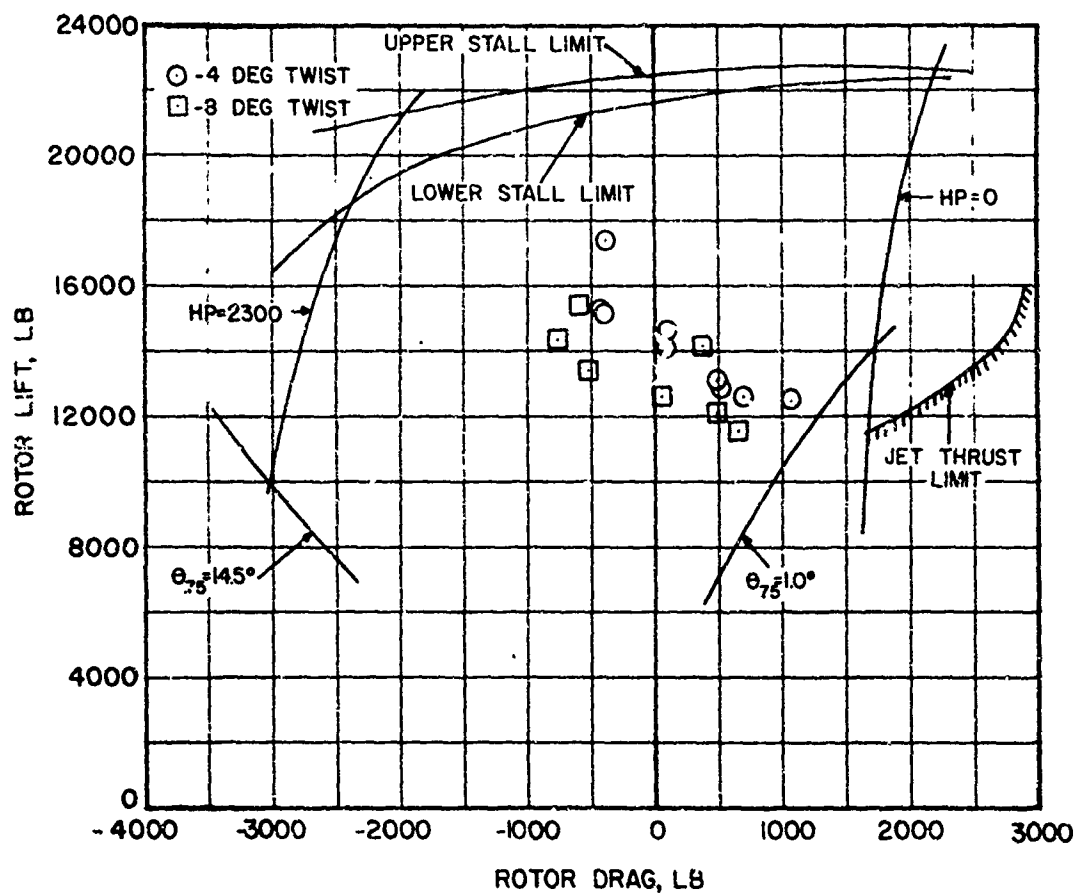
(e) 175 KNOTS ( $\mu = .45$ ), FIVE MAIN ROTOR BLADES,  
-8 DEGREES TWIST

FIGURE 15. Continued.



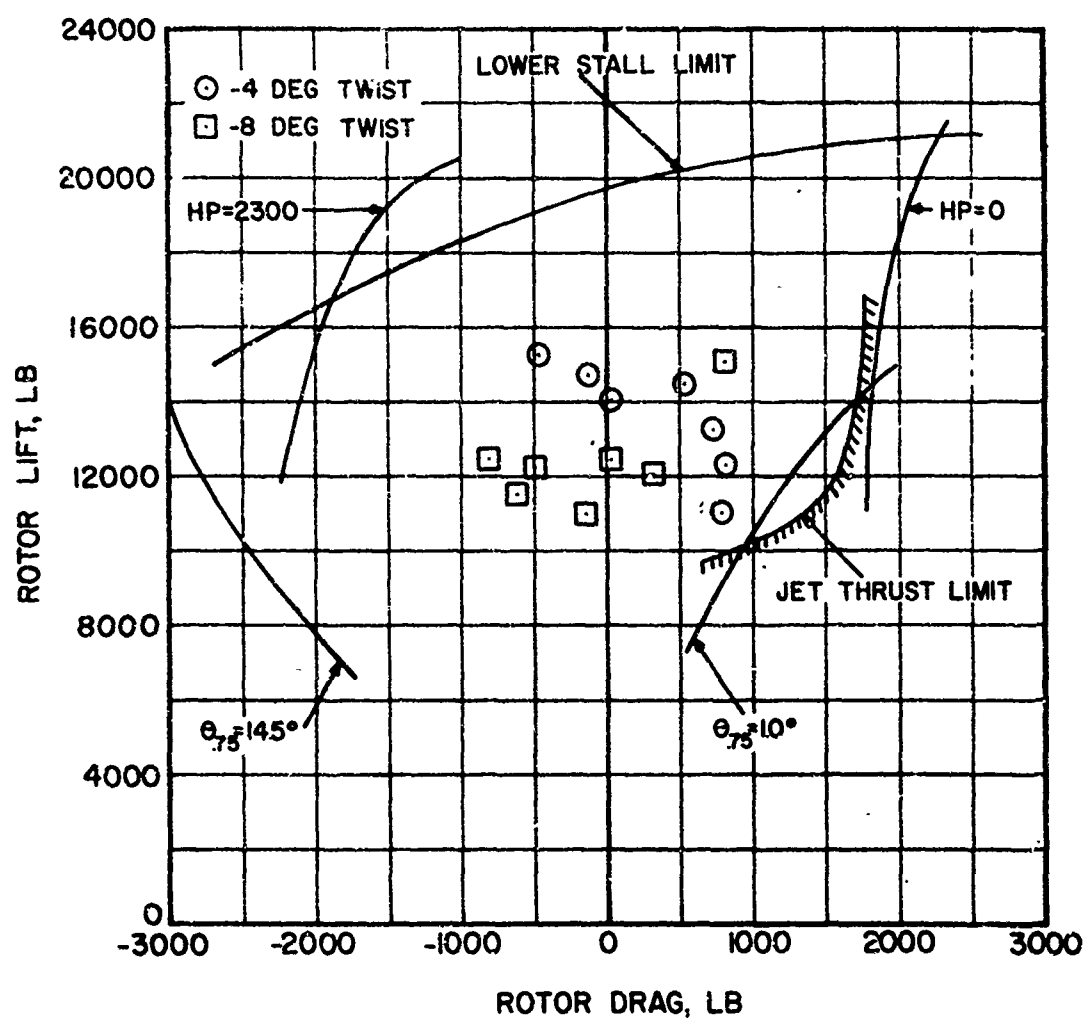
(f) 195 KNOTS ( $\mu=.50$ ), FIVE MAIN ROTOR BLADES,  
-8 DEGREES TWIST

FIGURE 15. Continued.



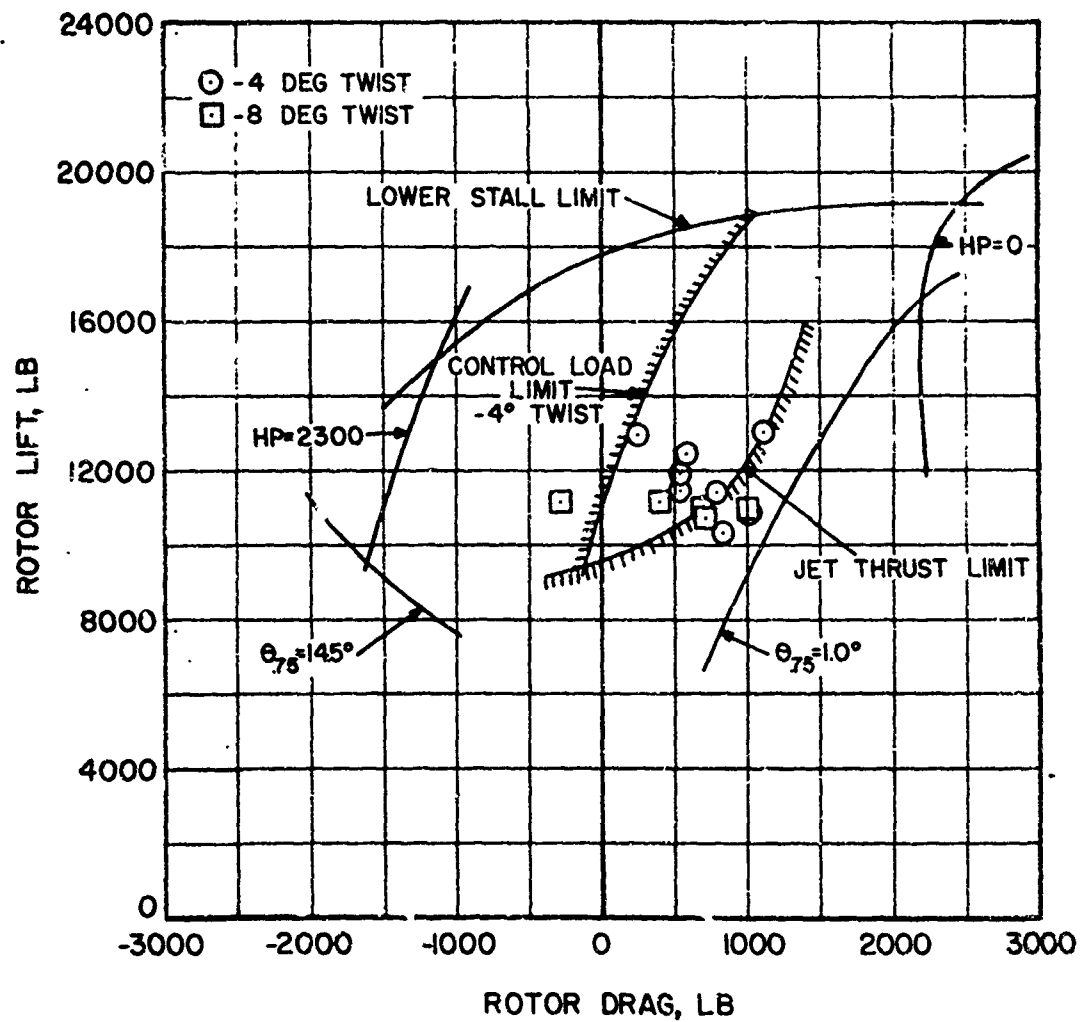
(g) 156 KNOTS ( $\nu = .40$ ), SIX MAIN ROTOR BLADES

FIGURE 15. Continued.



(h) 175 KNOTS ( $\mu = .45$ ), SIX MAIN ROTOR BLADES

FIGURE 15. Continued.



(i) 195 KNOTS ( $\mu=.50$ ), SIX MAIN ROTOR BLADES

FIGURE 15. Concluded.

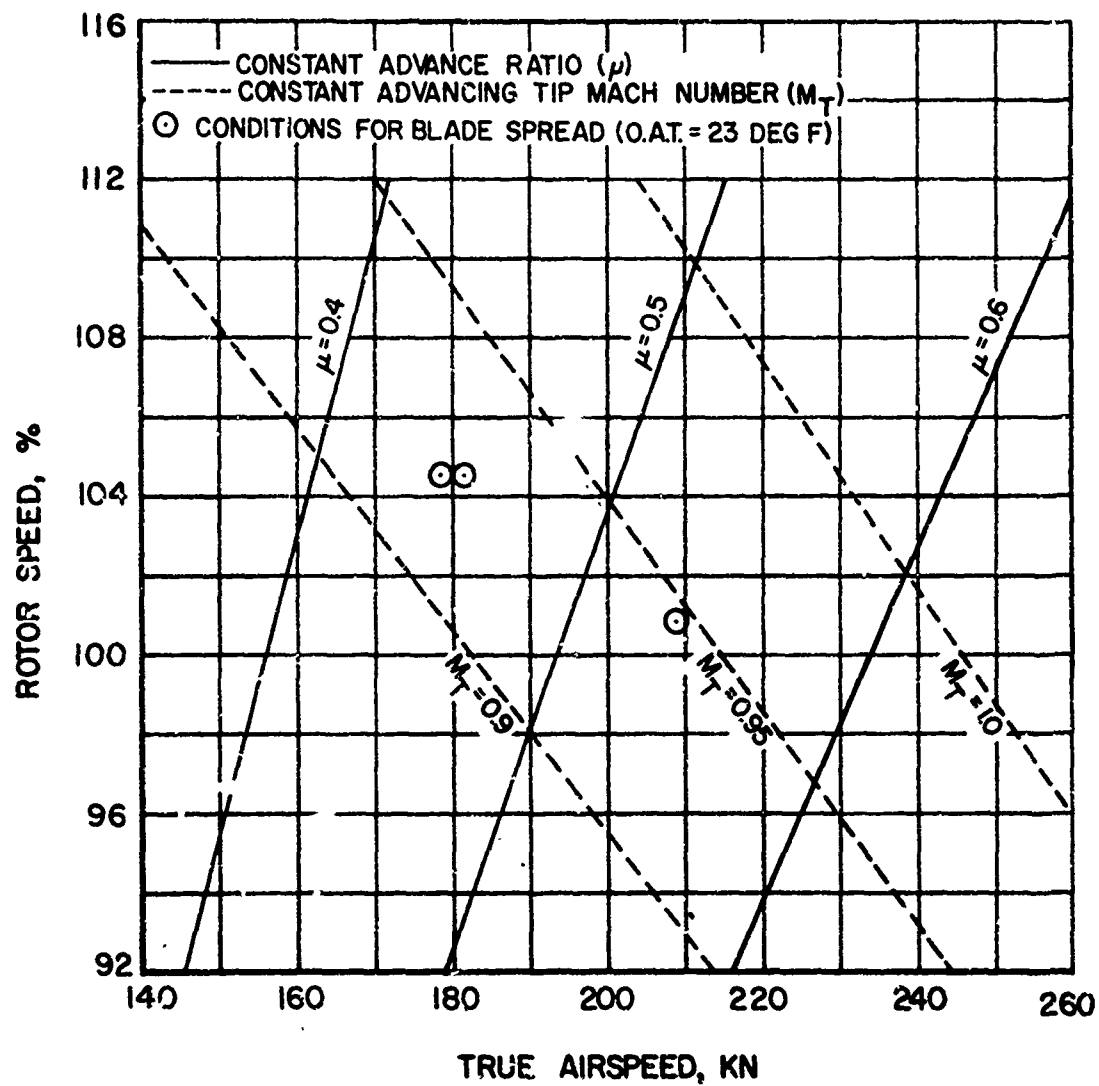


FIGURE 16. COMPRESSIBILITY MAPPING CONDITIONS.

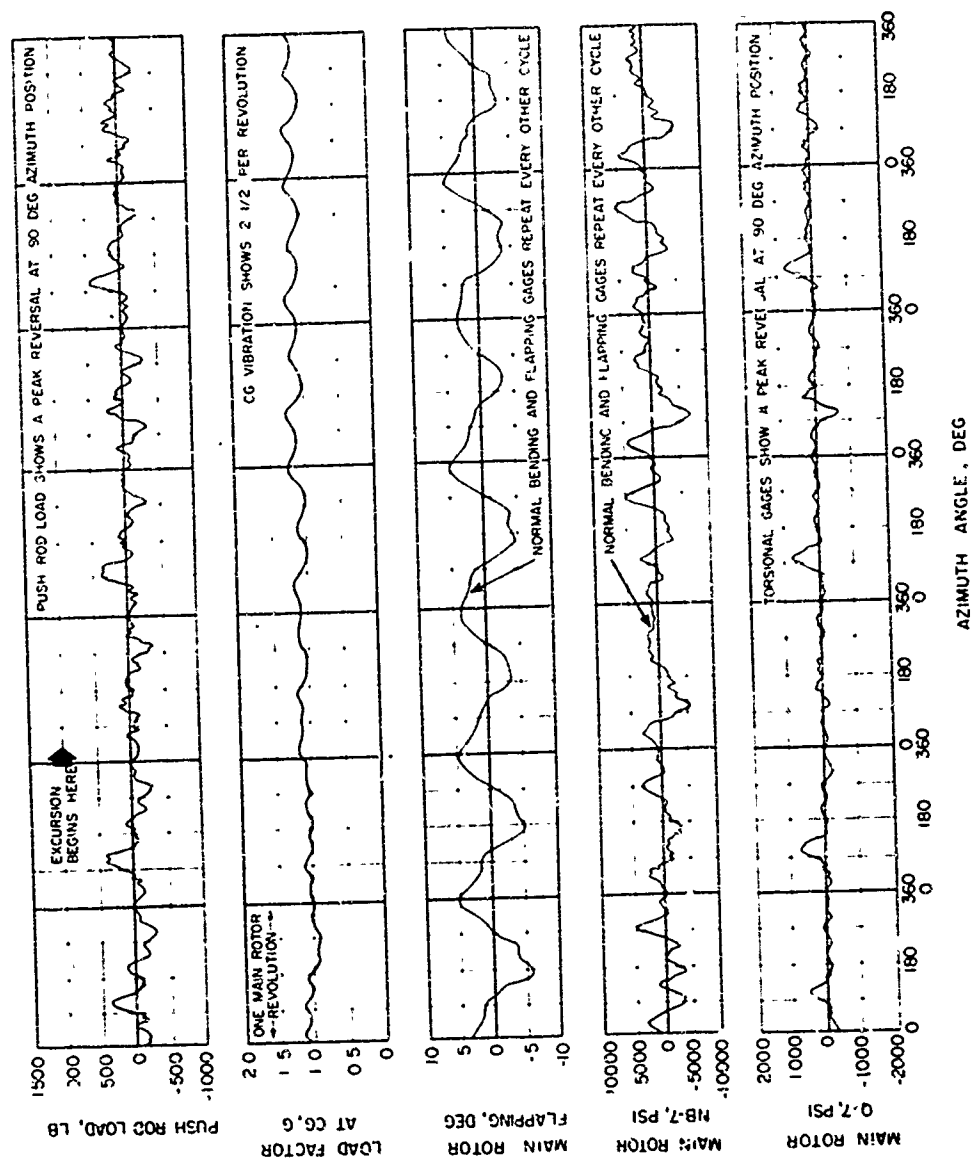


FIGURE 17. DYNAMIC BEHAVIOR DURING BLADE TIP EXCURSION



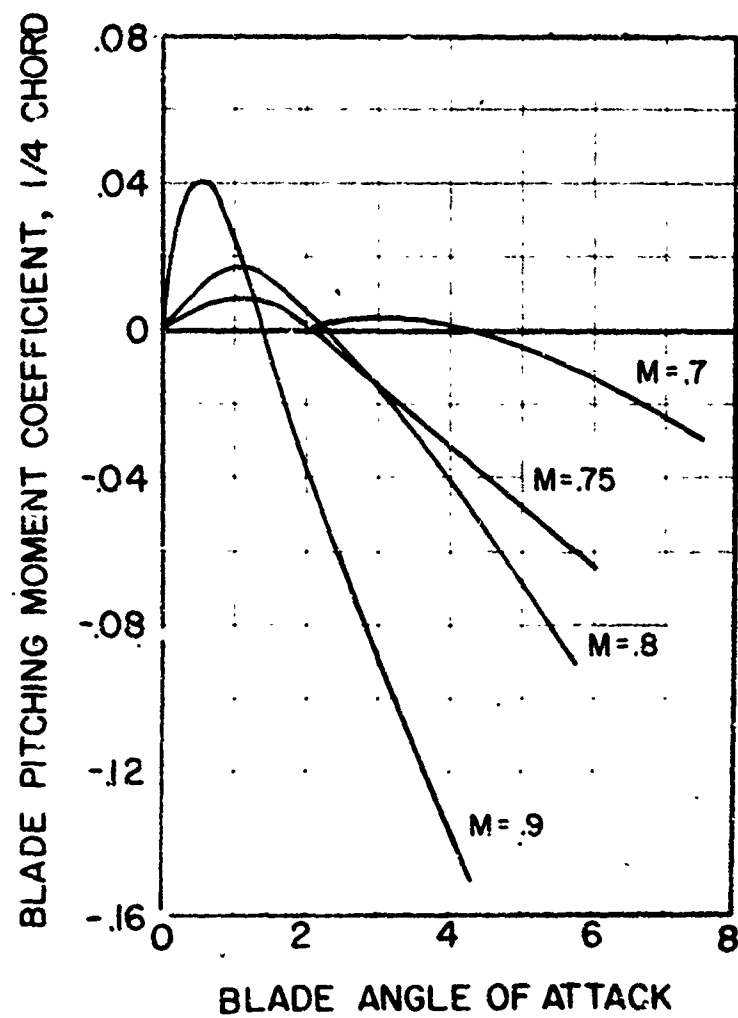


FIGURE 18. BLADE PITCHING MOMENT COEFFICIENT VERSUS ANGLE OF ATTACK AND MACH NUMBER.

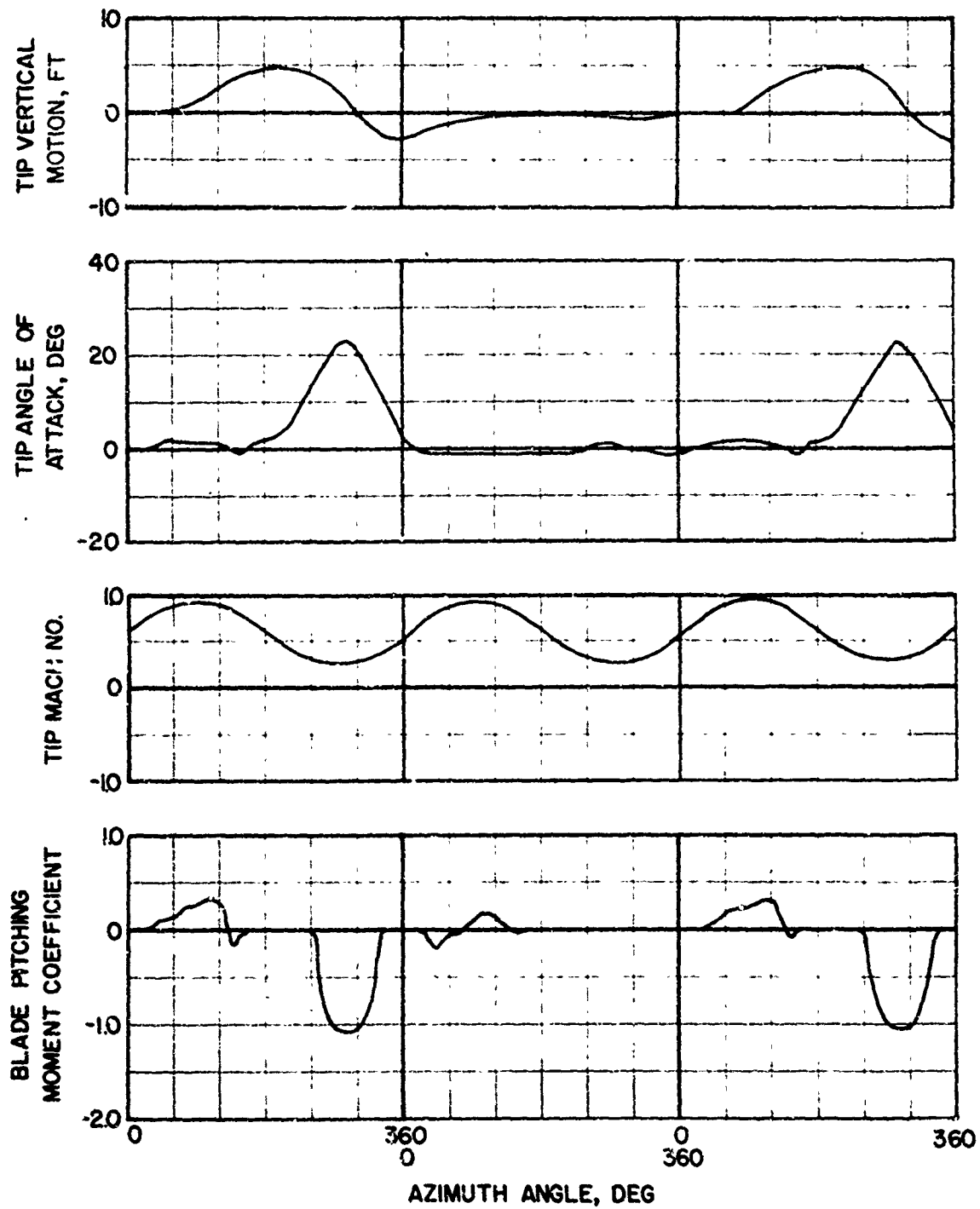


FIGURE 19. ANALYTICAL REPRODUCTION OF BLADE SPREAD.

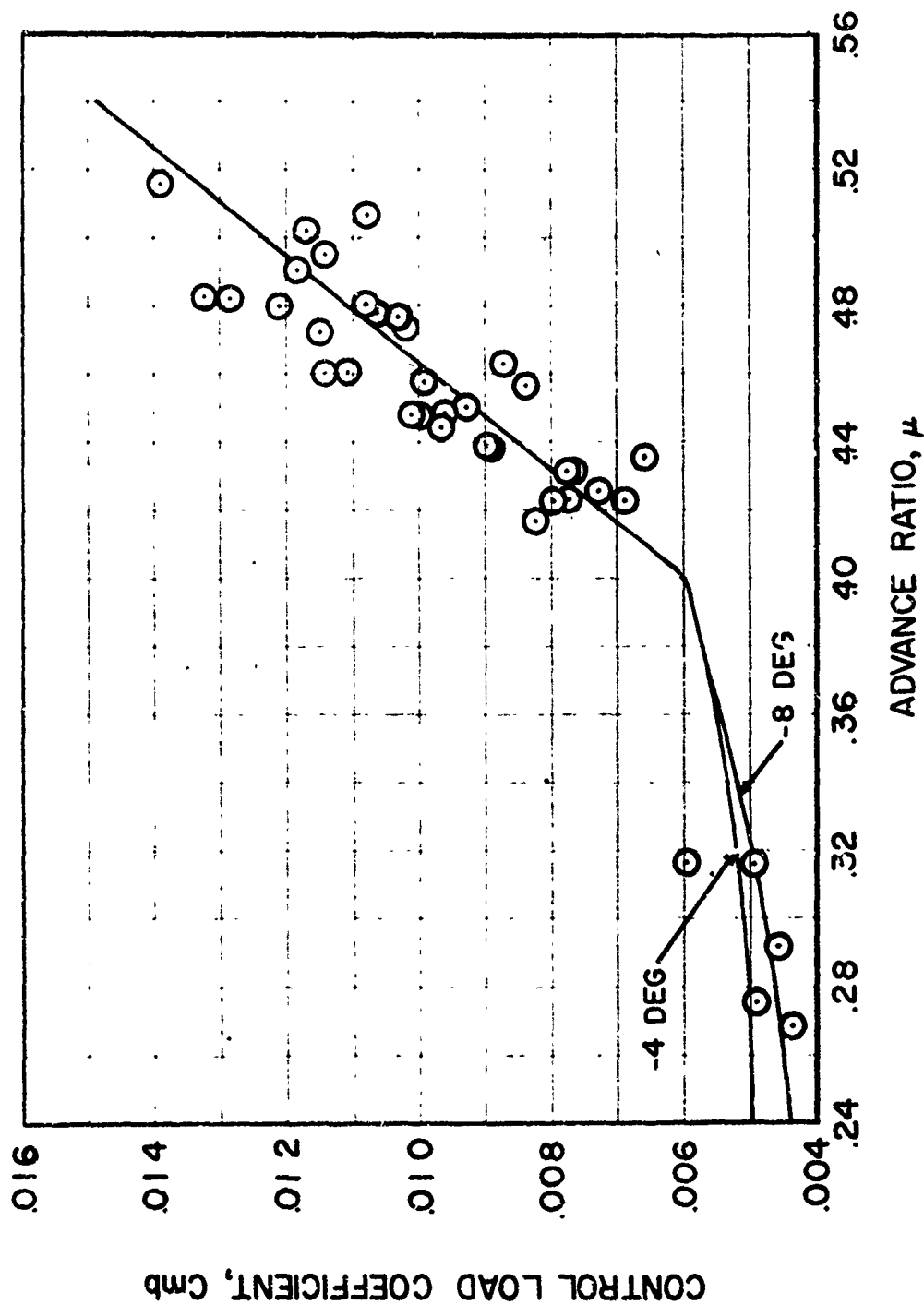


FIGURE 20. CONTROL LOADS AT POINTS BELOW THEORETICAL LOWER STALL LIMIT.

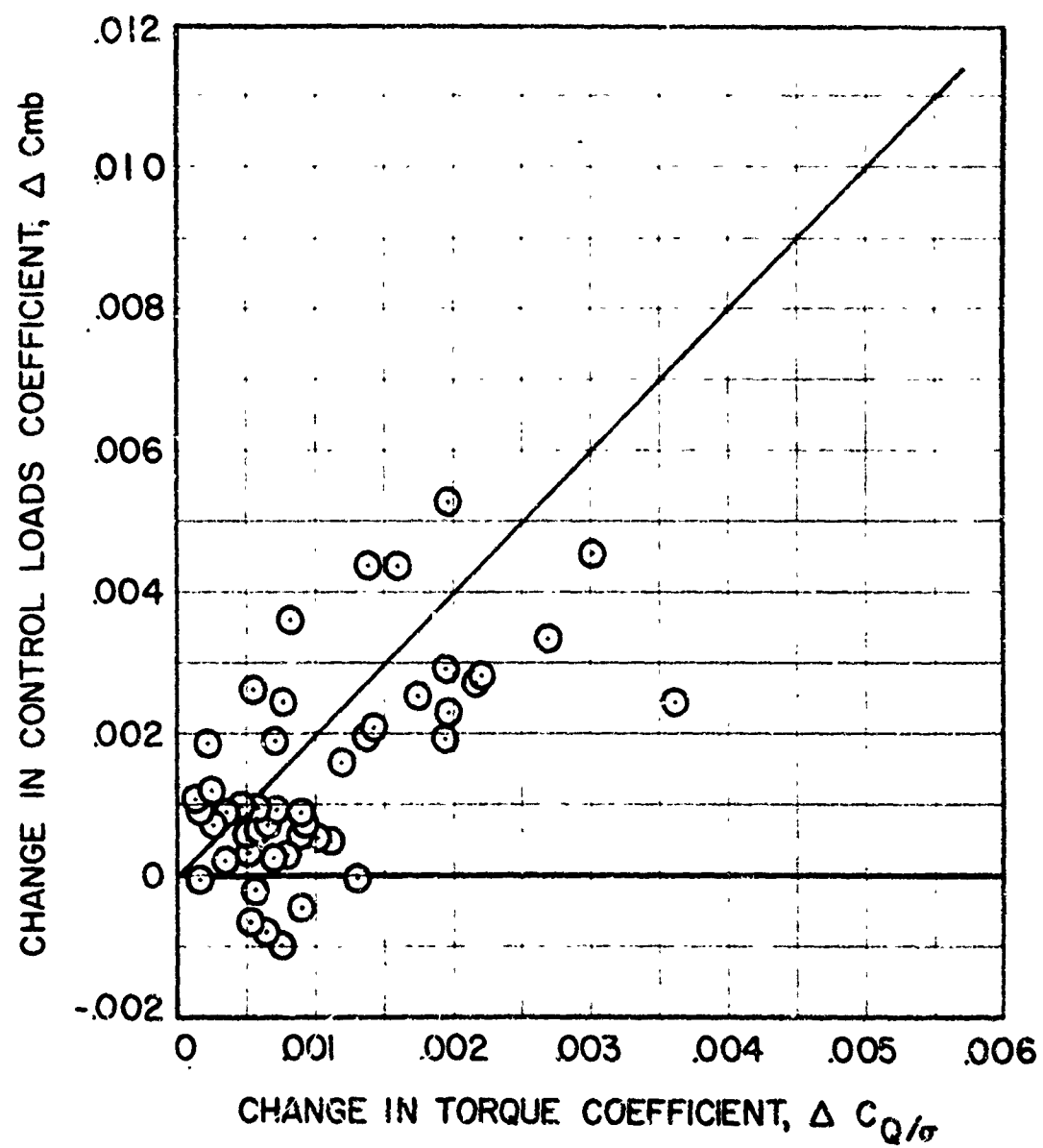


FIGURE 21. CHANGE IN CONTROL LOADS AT POINTS ABOVE THEORETICAL STALL LIMIT.

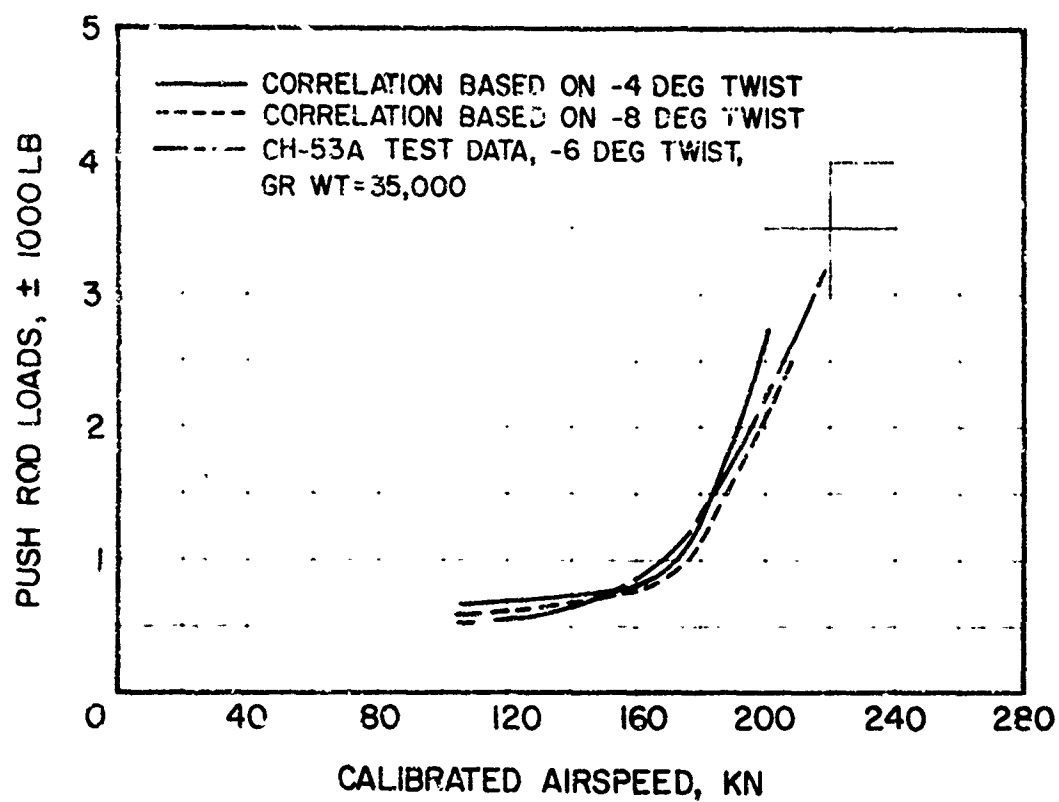


FIGURE 22. CONTROL LOADS CORRELATION WITH CH-53A.

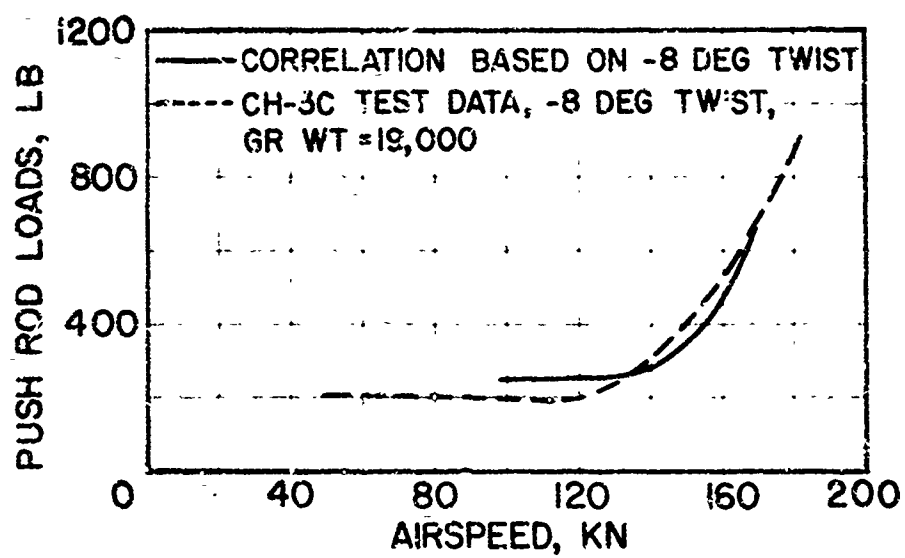


FIGURE 23. CONTROL LOADS CORRELATION WITH CH-3C.

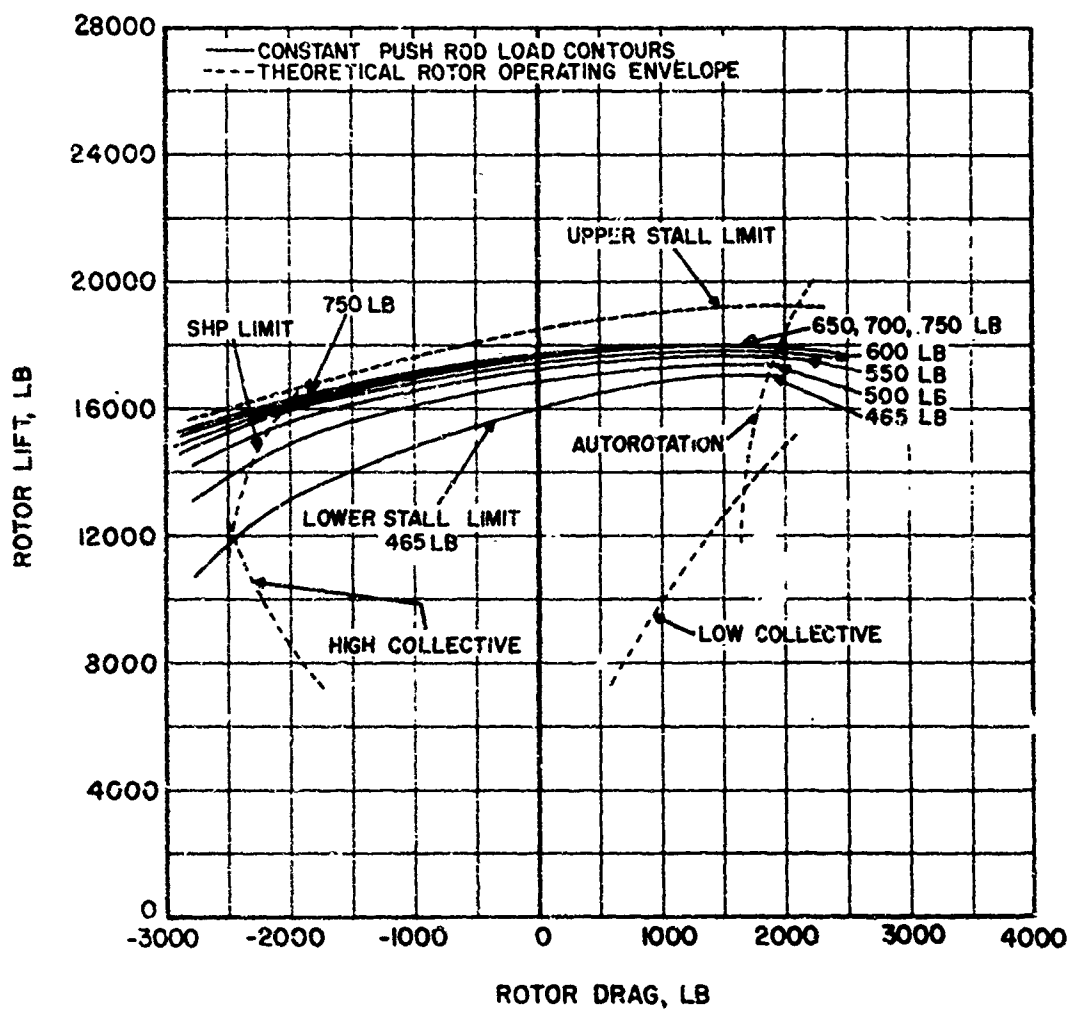


FIGURE 24. CONTROL SYSTEM LOAD CONTOURS AT 175 KNOTS  
(FIVE MAIN ROTOR BLADES, -8 DEGREES TWIST).

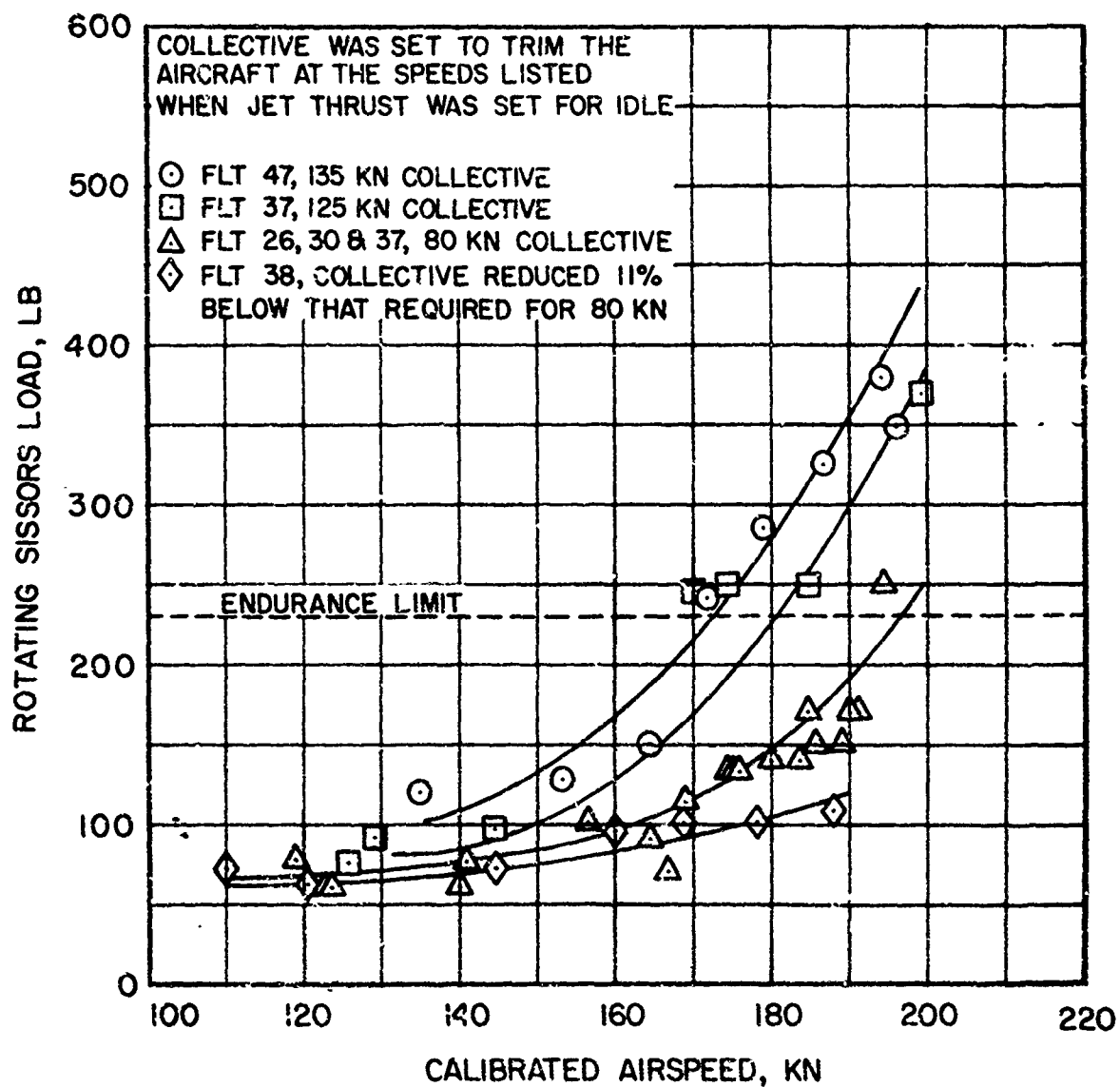


FIGURE 25. MAIN ROTOR OPERATING SCISSORS VIBRATORY LOAD (WITH WINGS AND JETS, FIVE MAIN ROTOR BLADES, -4 DEGREES TWIST, ZERO DEGREE  $i_{HT}$ ).



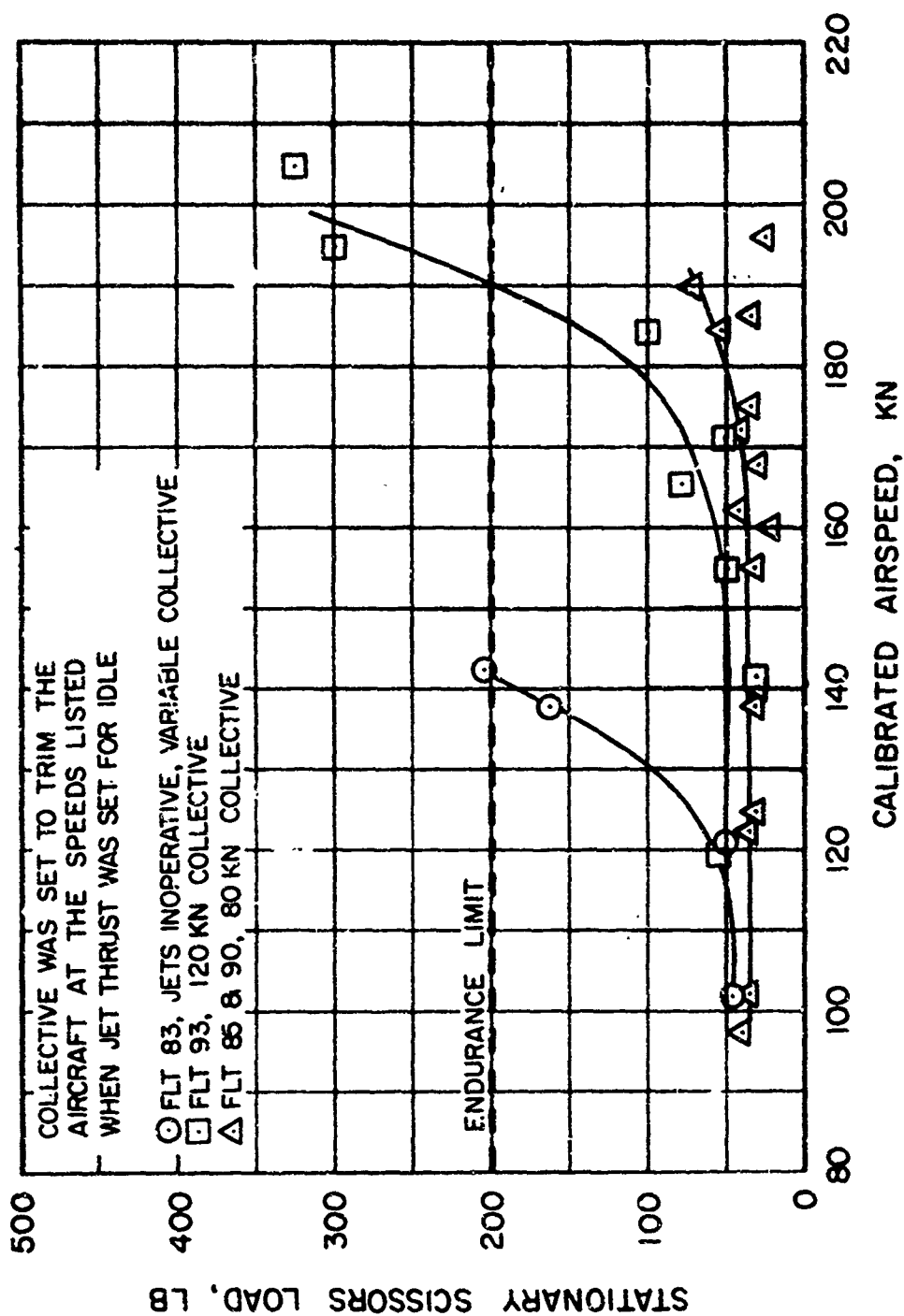


FIGURE 26. MAIN ROTOR STATIONARY SCISSORS VIBRATORY LOAD, (WITHOUT WINGS, SIX MAIN ROTOR BLADES,  $-4$  DEGREES TWIST, ZERO DEGREE  $i_{HT}$ ).

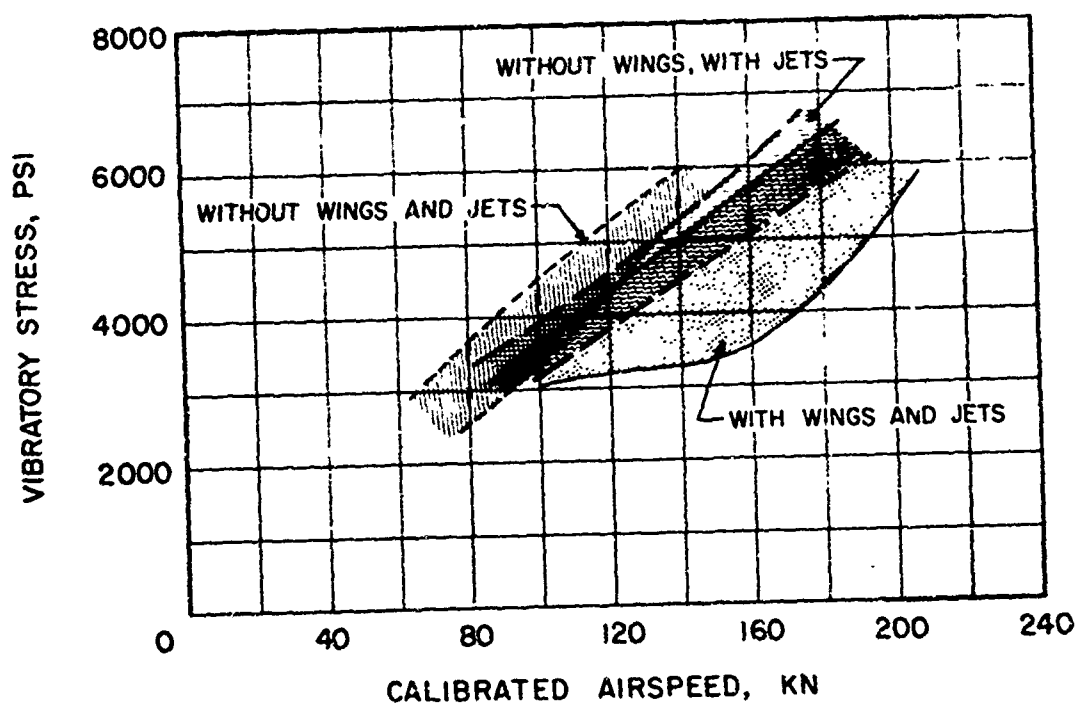


FIGURE 27. BLADE STRESS AT 70 PERCENT RADIUS VERSUS AIRSPEED ( FIVE MAIN ROTOR BLADES, -4 DEGREES TWIST).

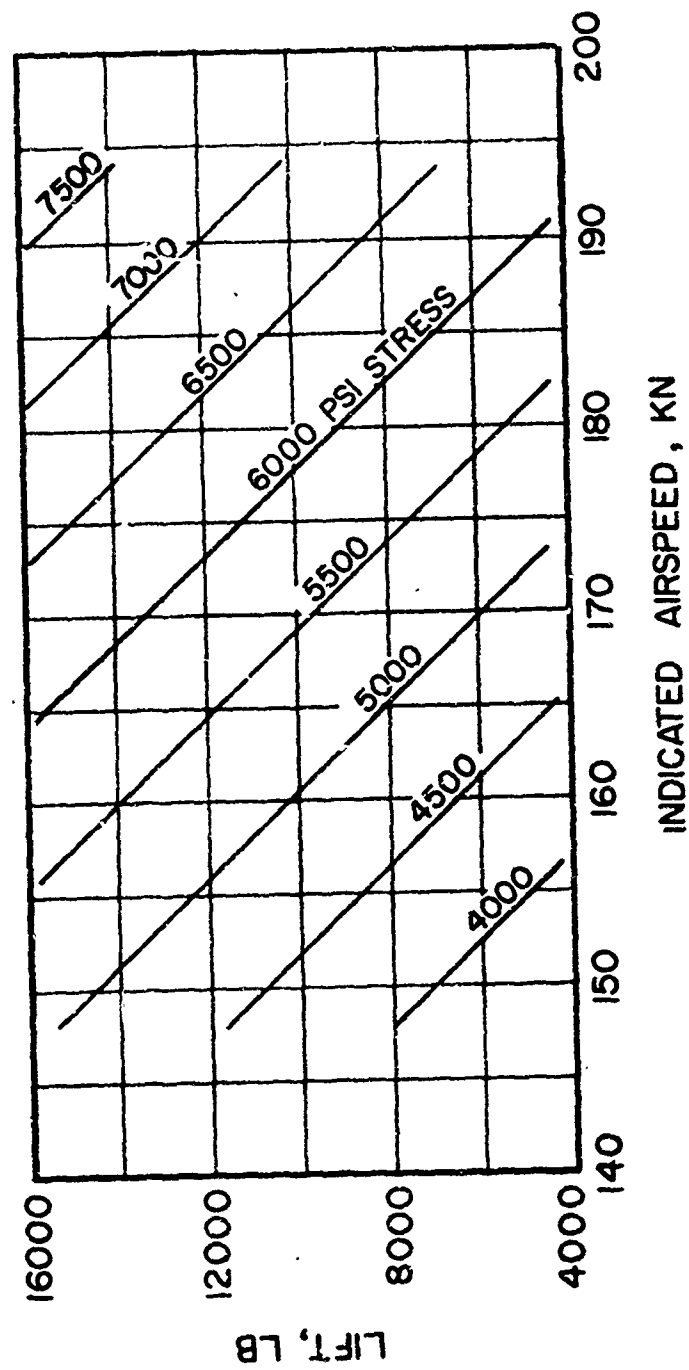


FIGURE 28. EFFECT OF ROTOR LIFT AND AIRSPEED ON BLADE STRESS AT 70 PERCENT RADIUS, (FIVE MAIN ROTOR BLADES, - 4 DEGREES TWIST).

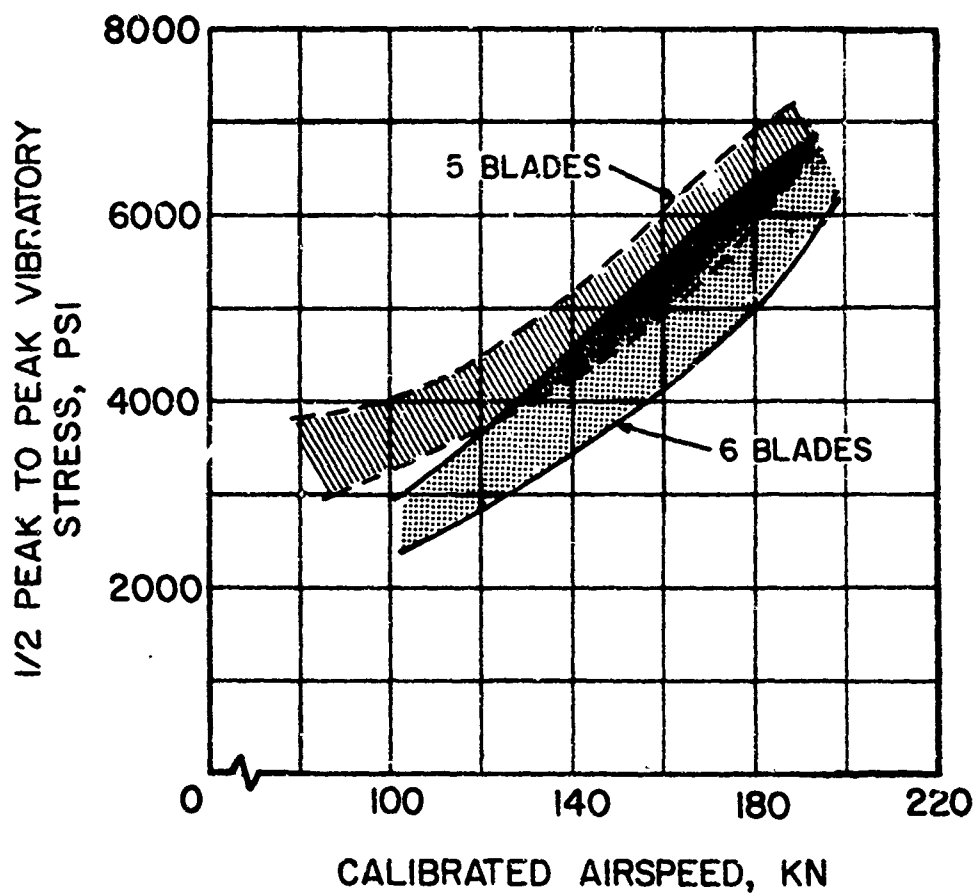


FIGURE 29. EFFECT OF NUMBER OF BLADES ON BLADE STRESS, WITH AUXILIARY PROPULSION, (-4 DEGREES TWIST).

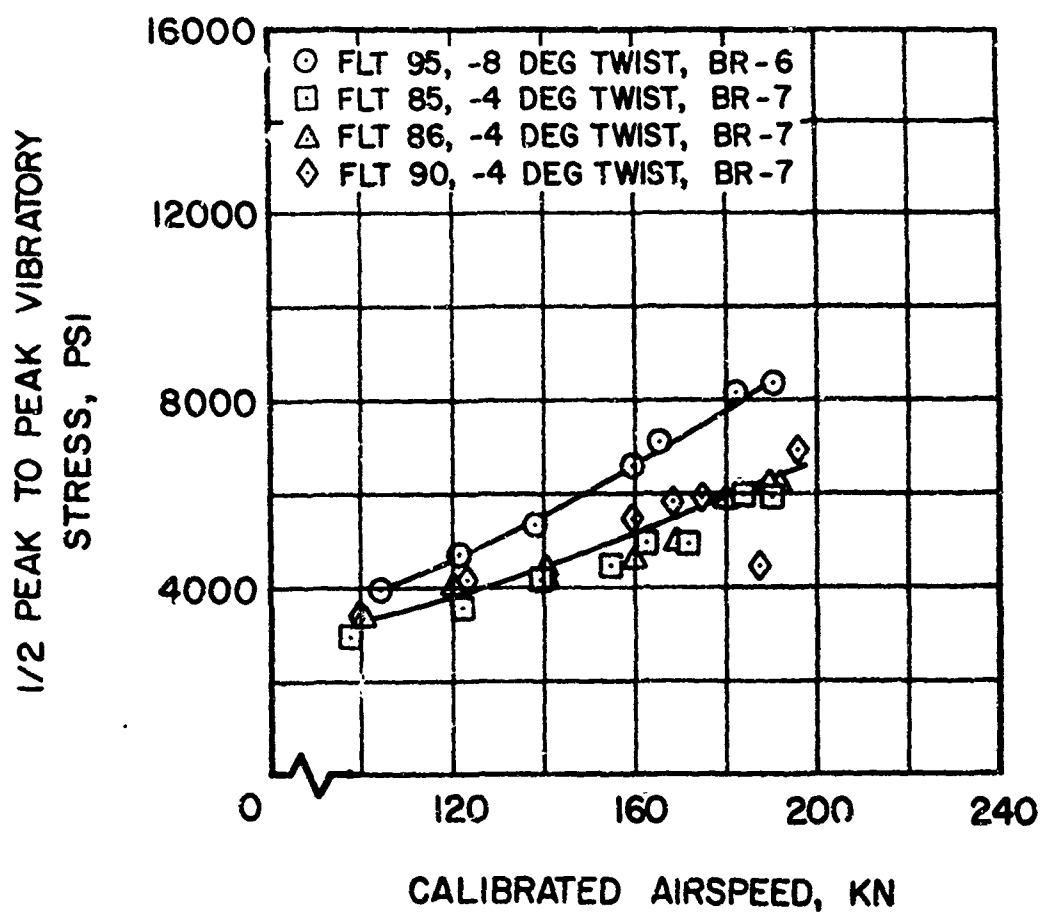


FIGURE 30. EFFECT OF TWIST ON MAXIMUM STRESS, WITH AUXILIARY PROPULSION, (SIX MAIN ROTOR BLADES).

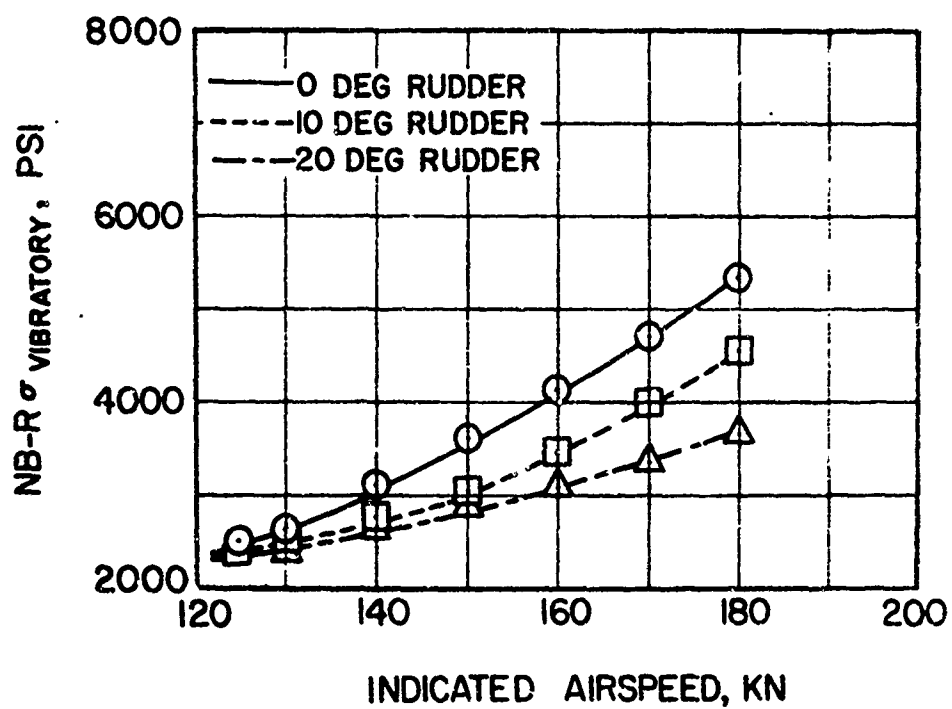


FIGURE 31. EFFECT OF RUDDER DEFLECTION ON TAIL ROTOR STRESSES.

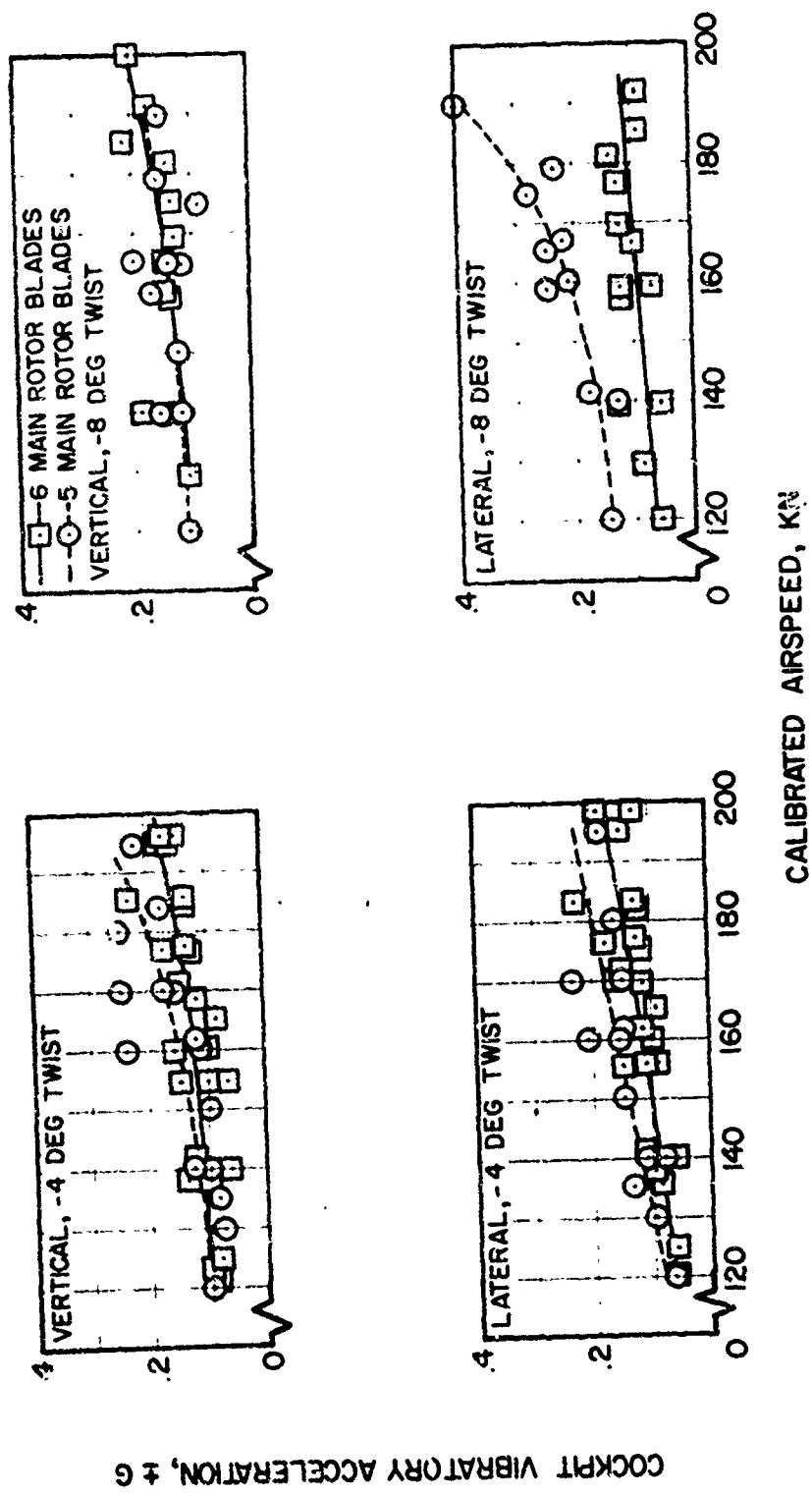


FIGURE 32. EFFECT OF NUMBER OF BLADES AND BLADE TWIST ON FUSELAGE VIBRATION.

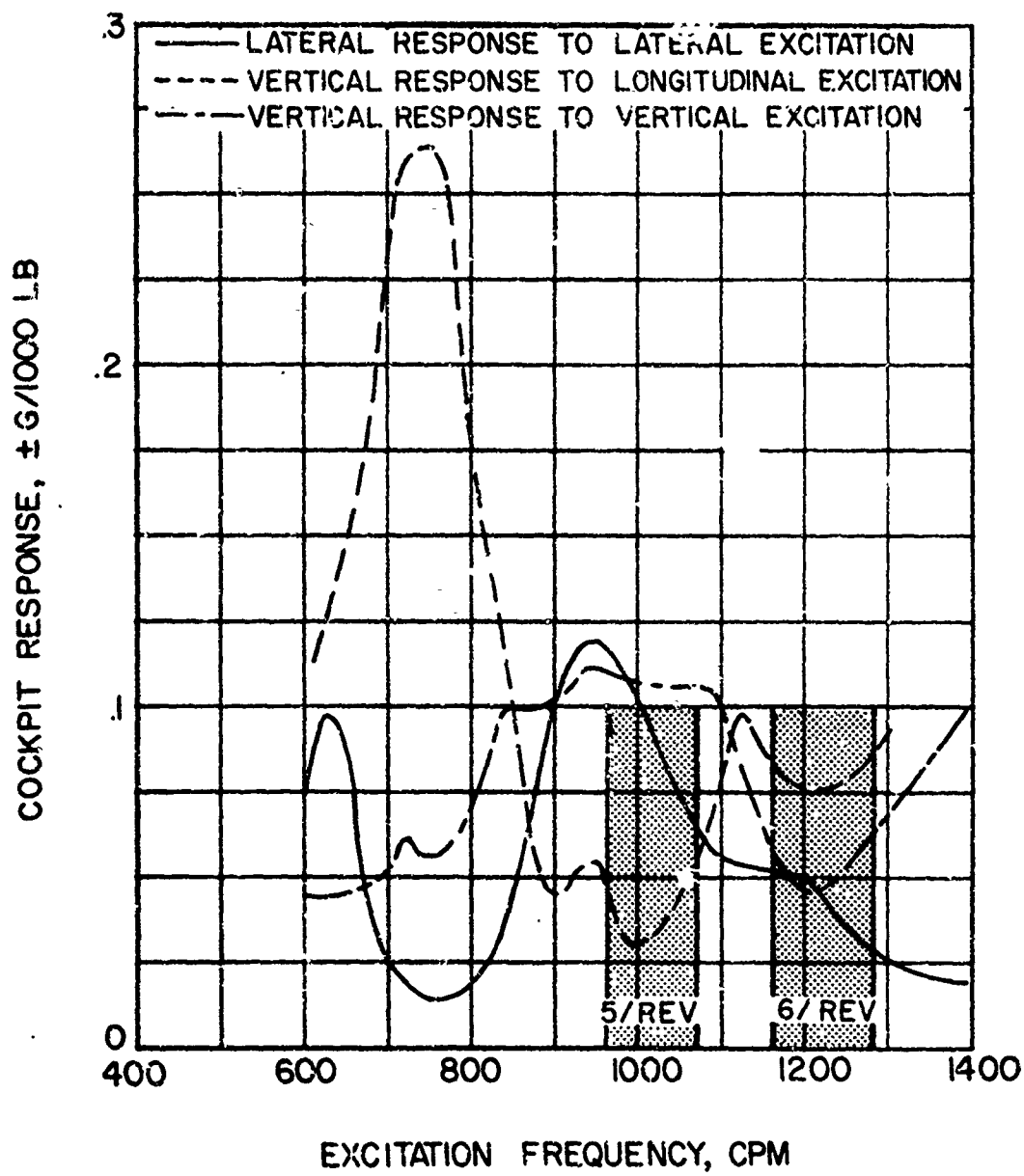


FIGURE 33. NH-3A COCKPIT RESPONSE VERSUS FREQUENCY.



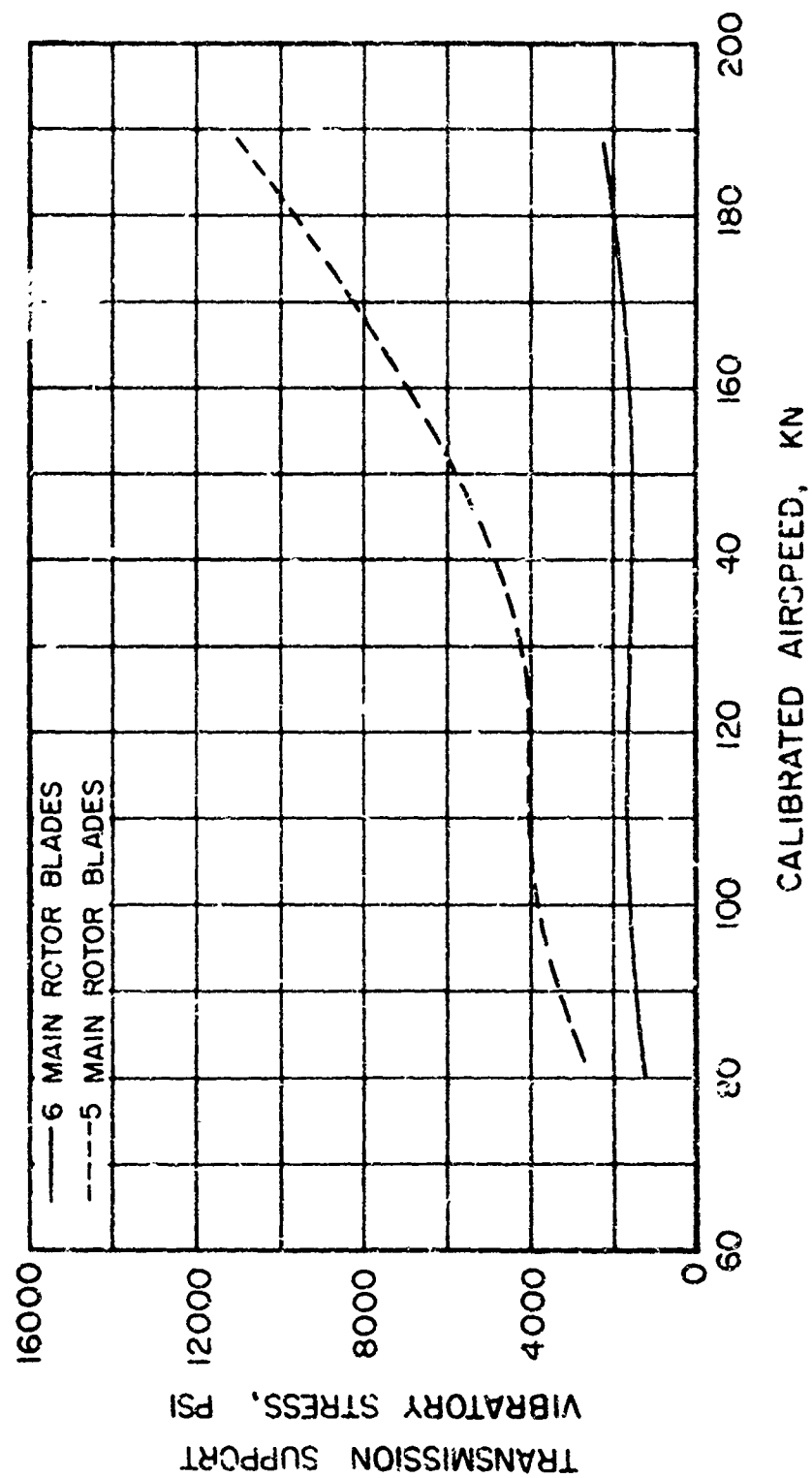


FIGURE 34. EFFECT OF NUMBER OF BLADES ON TRANSMISSION SUPPORT STRESSES AT THE LEFT FORWARD FITTING.

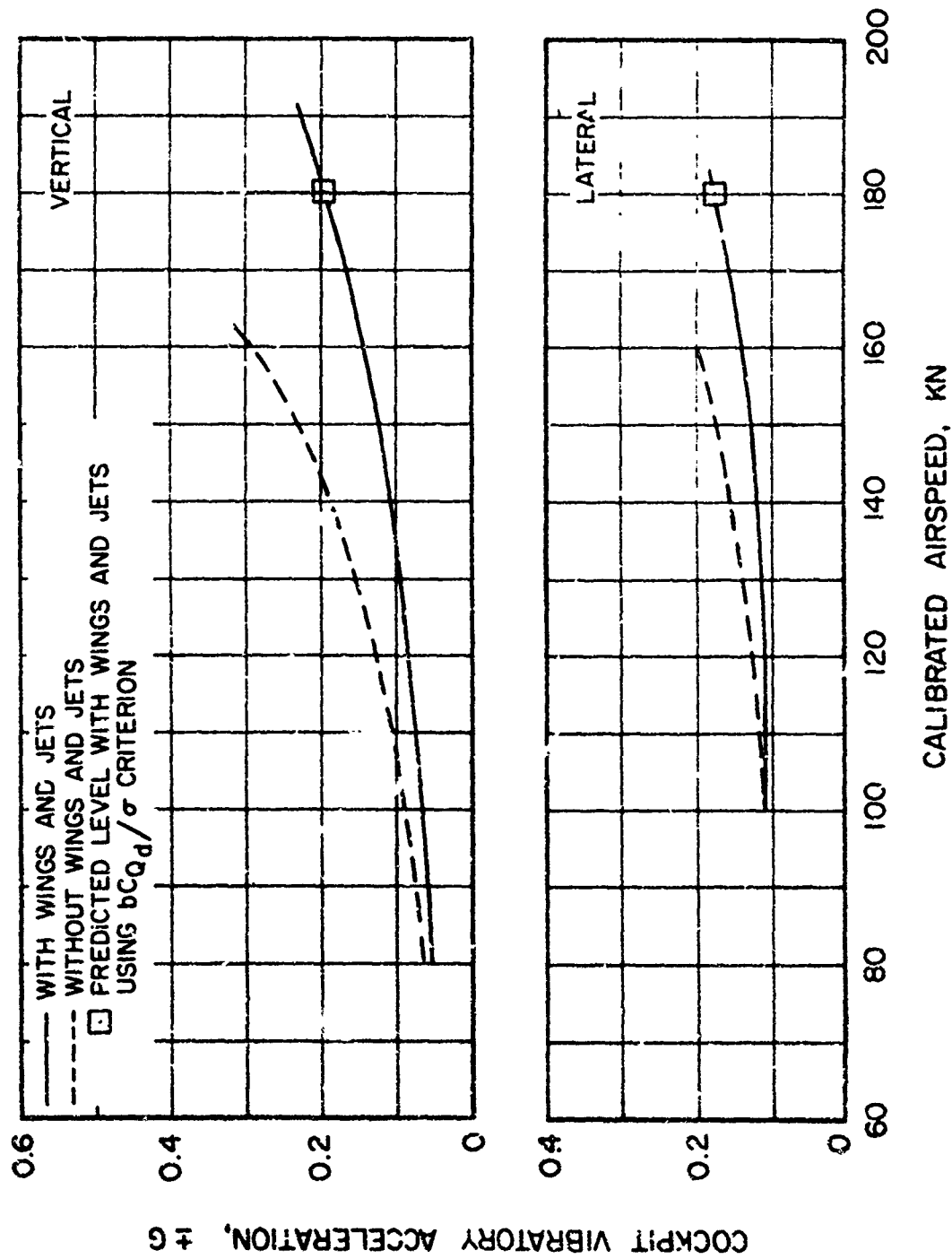
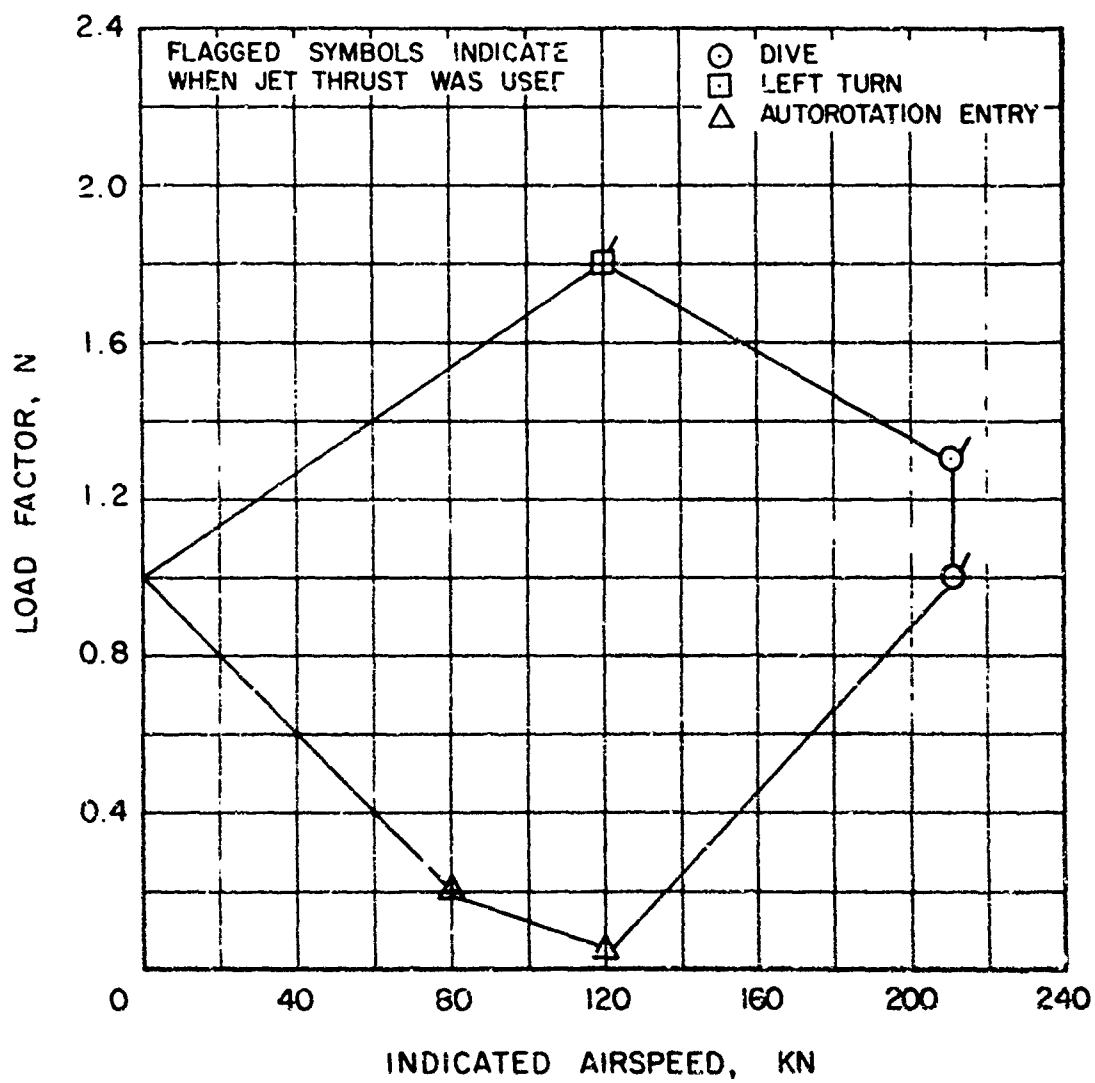
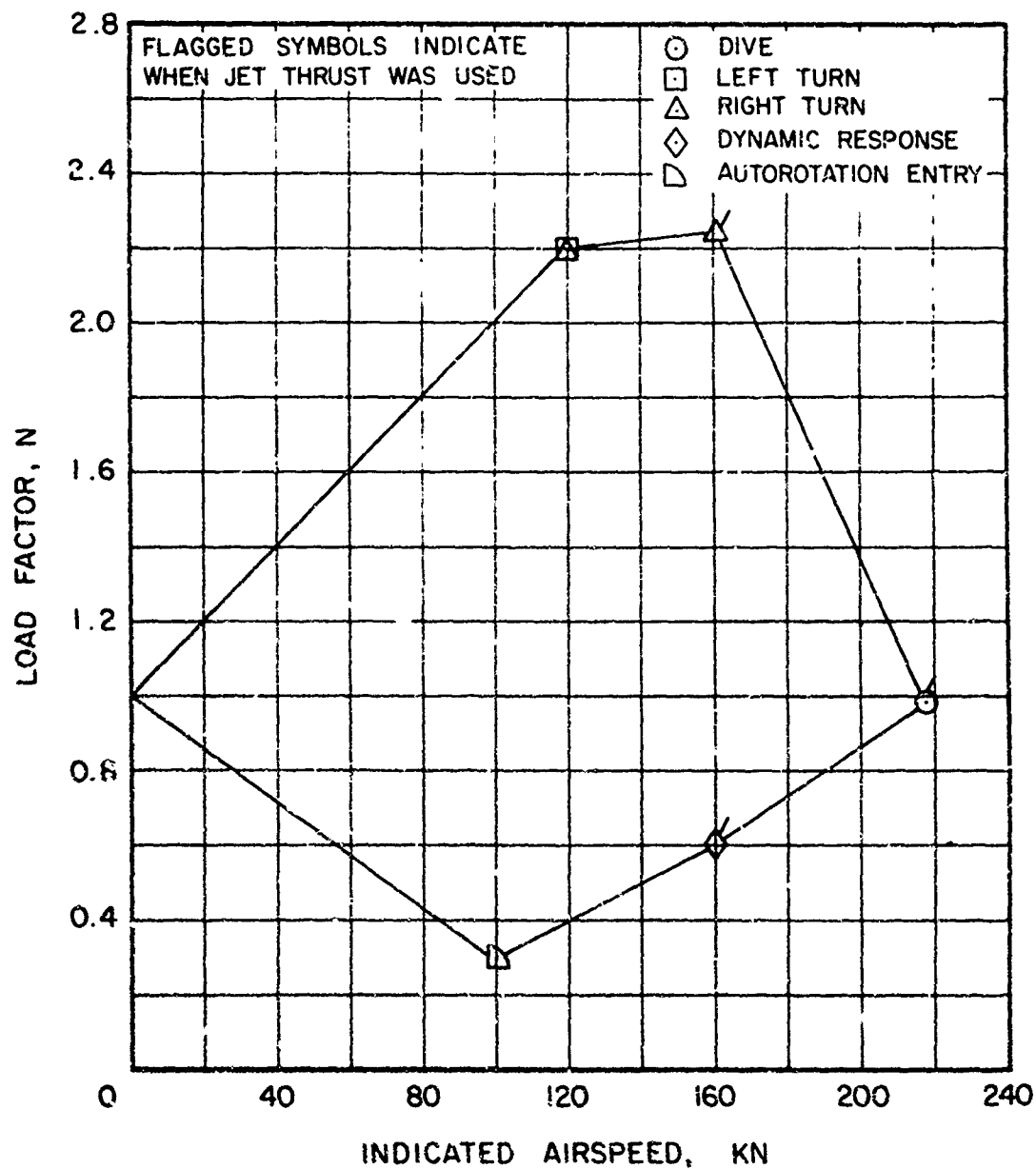


FIGURE 35. EFFECT OF ROTOR UNLOADING ON COCKPIT VIBRATION.



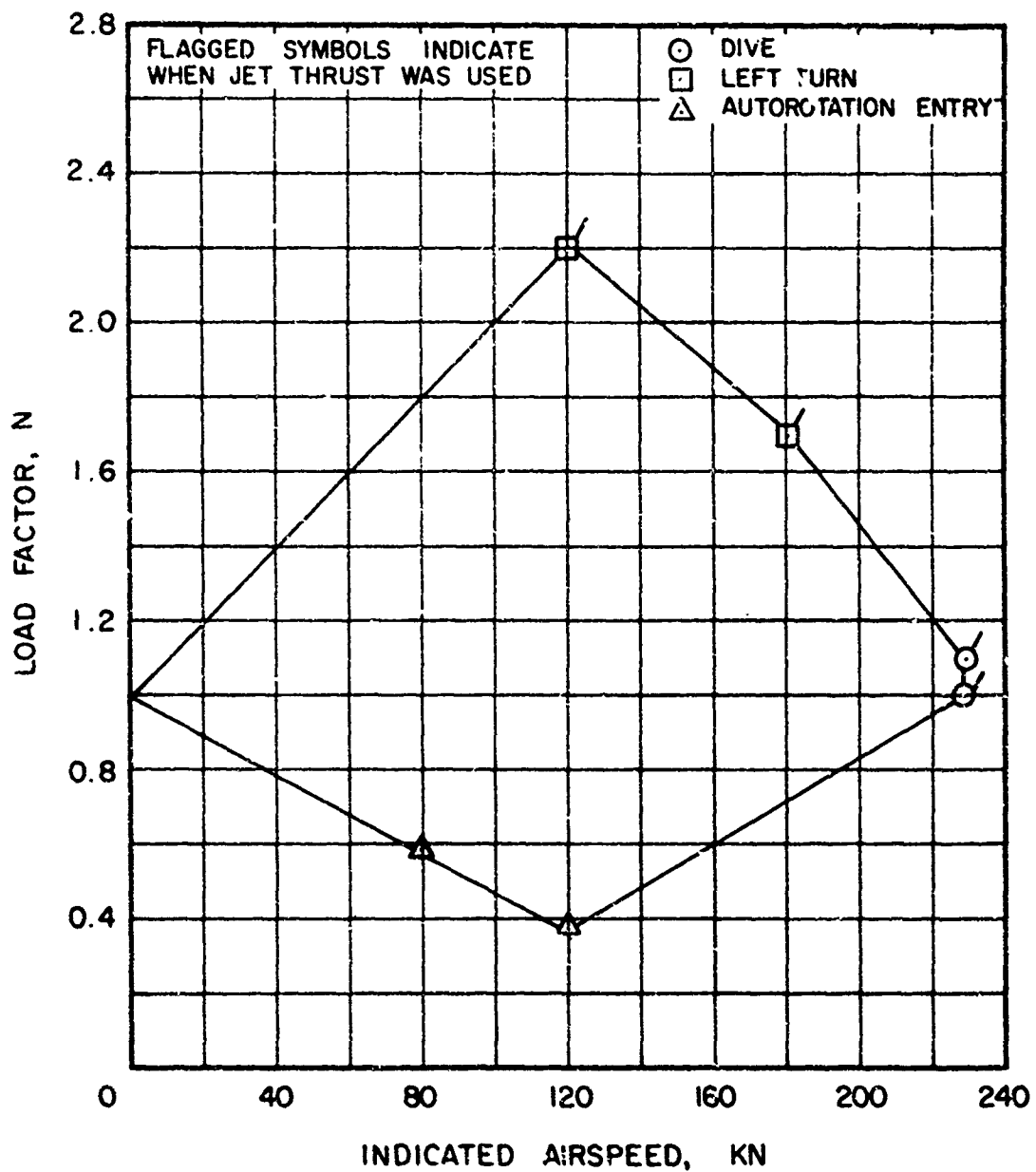
(a) WITHOUT WINGS, WITH JET PODS, FIVE  
 MAIN ROTOR BLADES

FIGURE 36. V-N DIAGRAM FOR VARIOUS AIRCRAFT CONFIGURATIONS.



(b) WITH WINGS, WITH JET PODS, FIVE  
MAIN ROTOR BLADES

FIGURE 36. Continued.



(c) WITHOUT WINGS, WITH JET PODS, SIX MAIN ROTOR BLADES

FIGURE 36. Concluded.

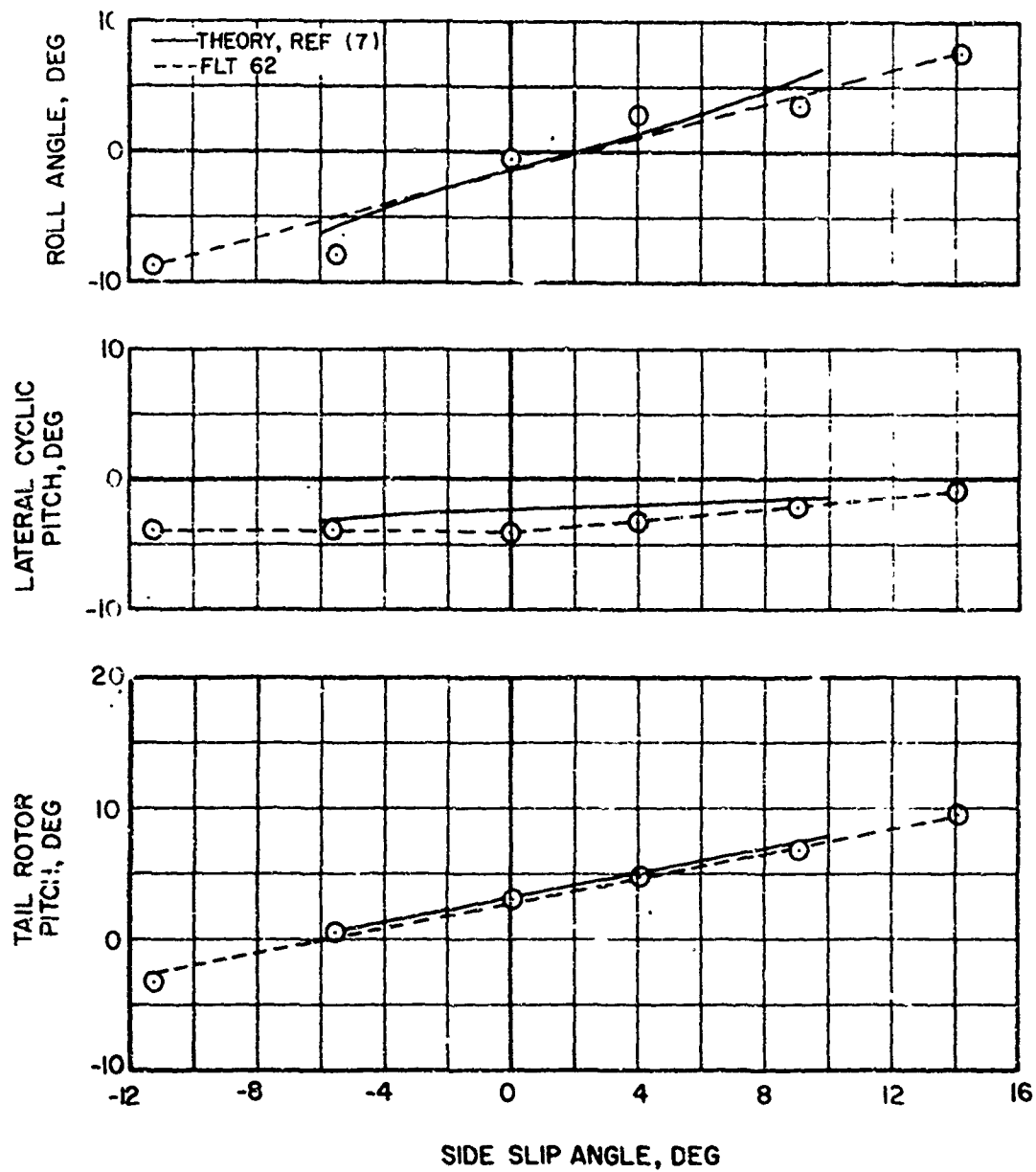


FIGURE 37. LATERAL DIRECTIONAL STATIC STABILITY AT 125 KNOTS, (FIVE MAIN ROTOR BLADES, -8 DEGREES TWIST, ZERO DEGREE  $i_{HT}$ ).

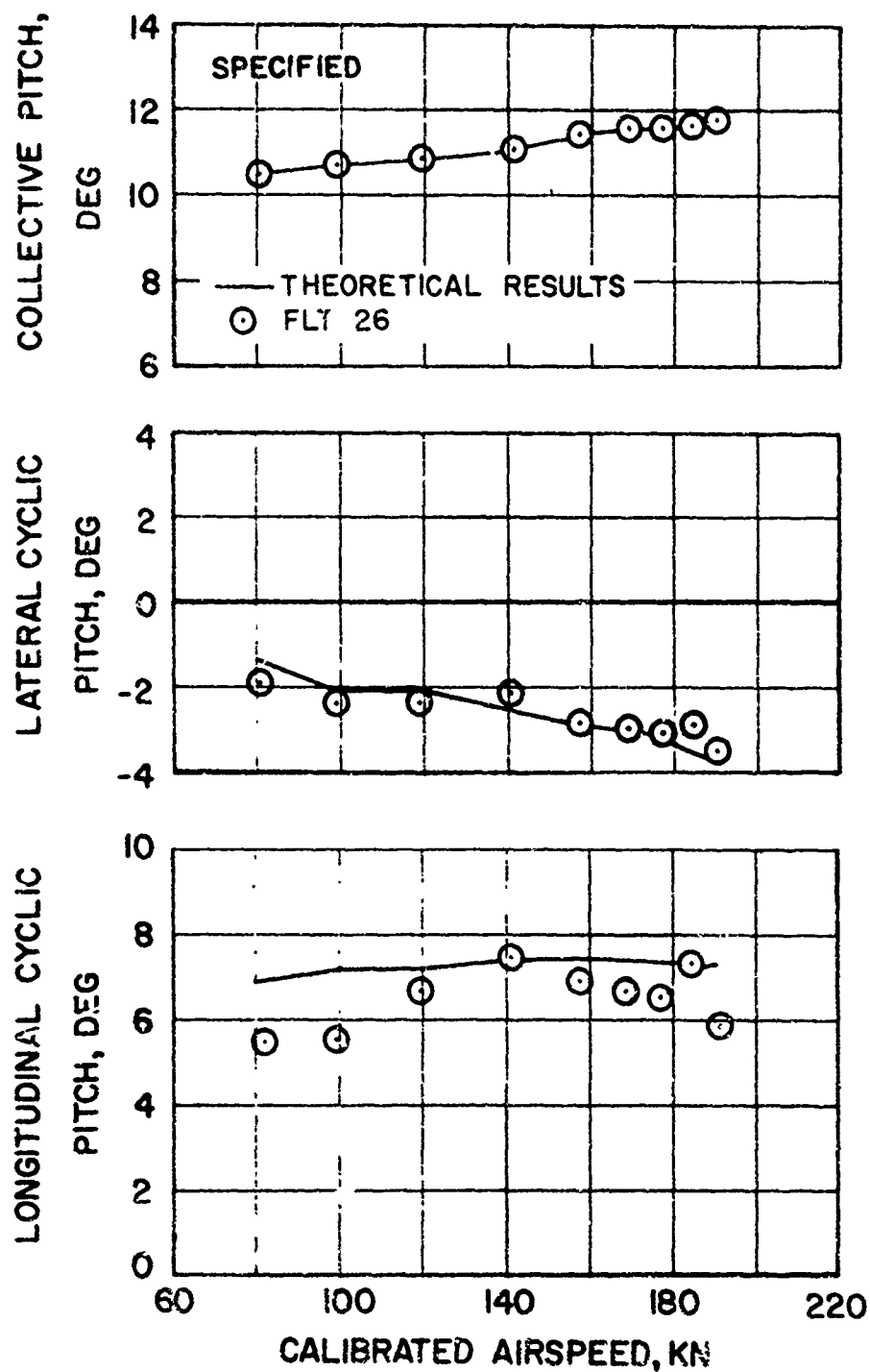
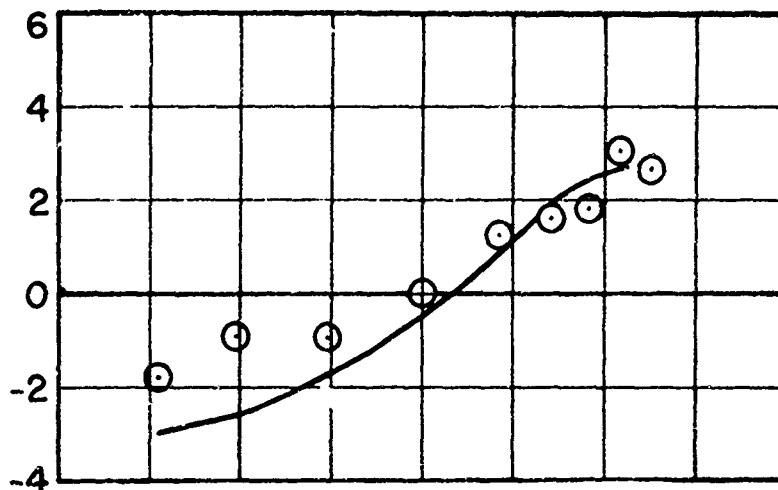
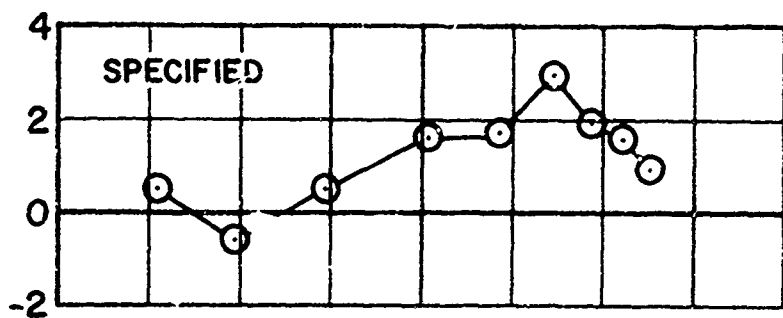


FIGURE 38. CORRELATION OF STEADY STATE FLIGHT PARAMETERS (WITH W. GS AND JETS, FIVE MAIN ROTOR BLADES, -4 DEGREES TWIST, -15 DEGREES  $\delta_e$ , ZERO DEGREE  $\delta_f$ , 5 DEGREES  $i_{HT}$ ).

LONGITUDINAL FLAPPING,  
DEG



ROLL ATTITUDE,  
DEG



PITCH ATTITUDE,  
DEG

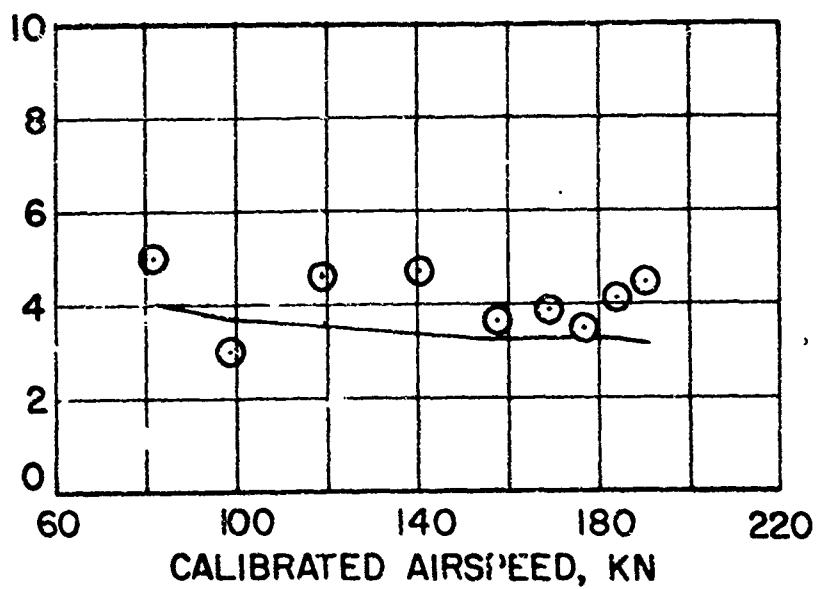
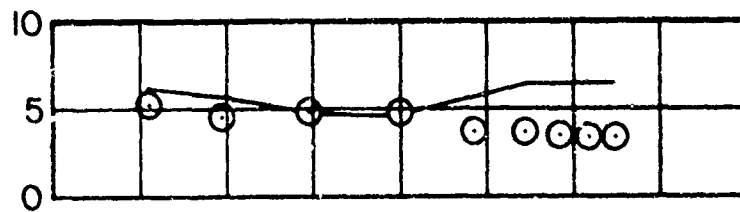


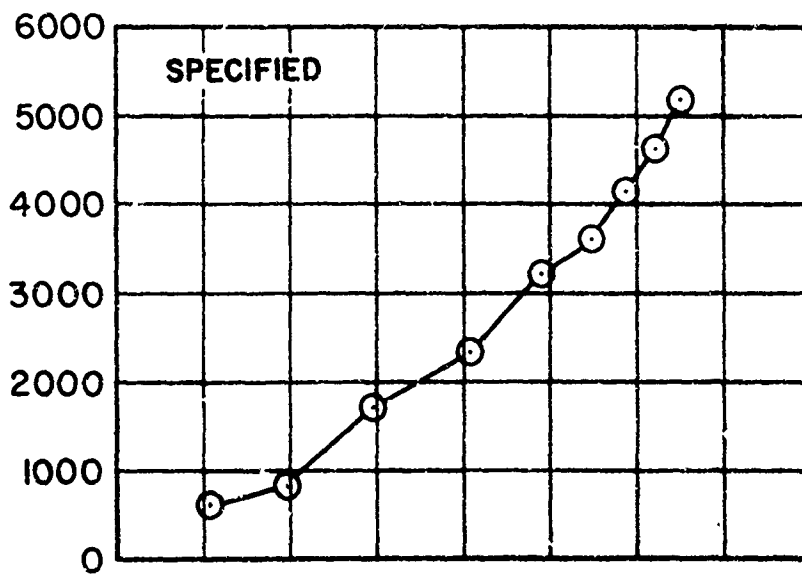
FIGURE 38. Continued.



TAIL ROTOR  
PITCH, DEG



JET THRUST, LB



MAIN ROTOR  
THRUST, LB

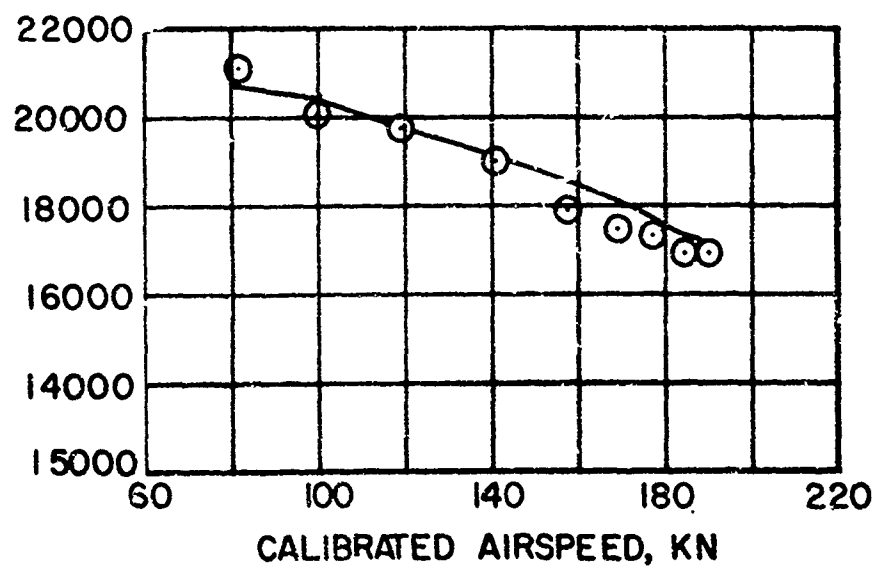


FIGURE 36. Concluded.

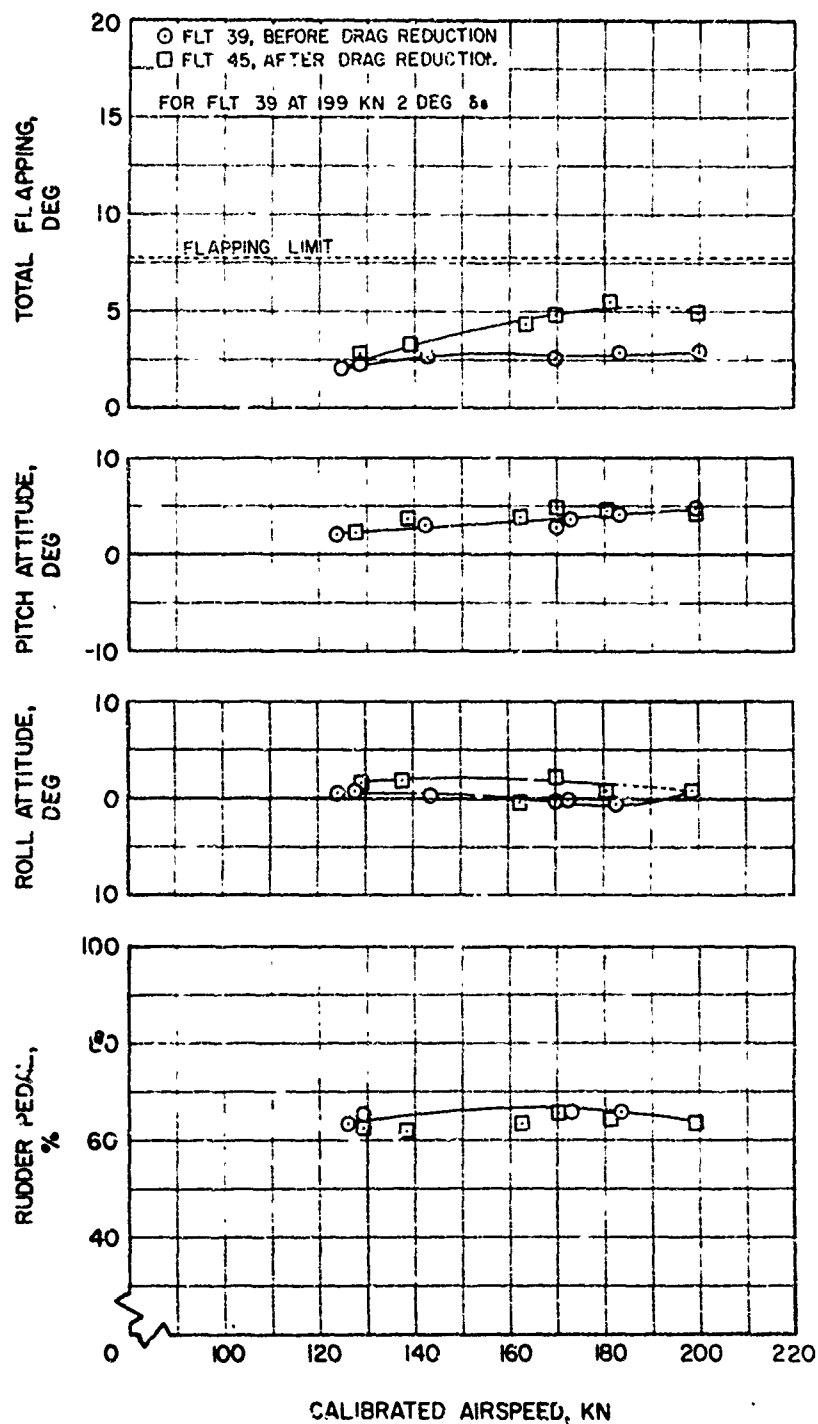


FIGURE 39. EFFECT OF DRAG REDUCTION ON STEADY STATE FLIGHT PARAMETERS, (WITH WINGS AND JETS, FIVE MAIN ROTOR BLADES,  $-4$  DEGREES TWIST, ZERO DEGREE  $\delta_e$ ,  $1$  DEGREE  $\delta_f$ , ZERO DEGREE  $i_{HT}$ ).

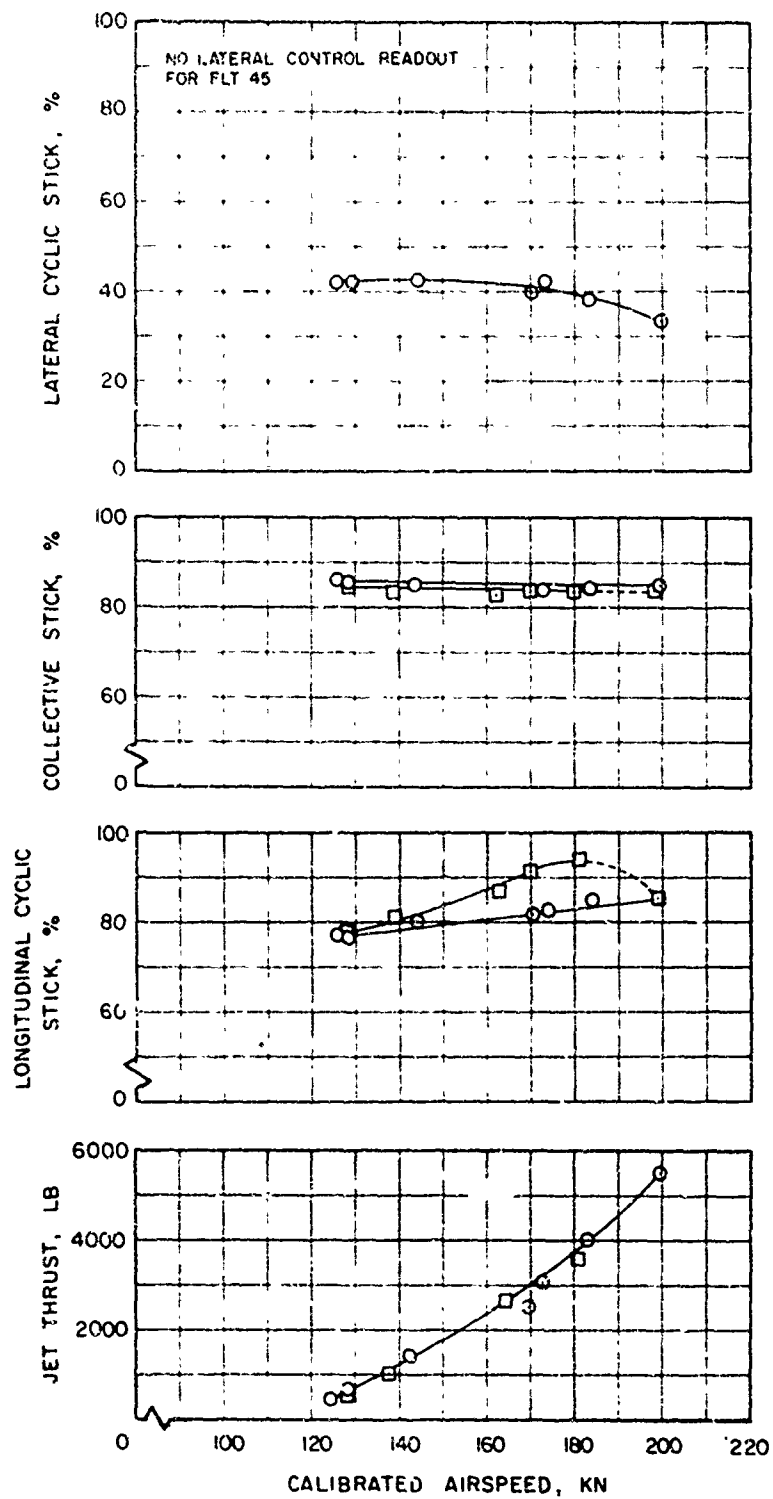


FIGURE 39. Concluded.

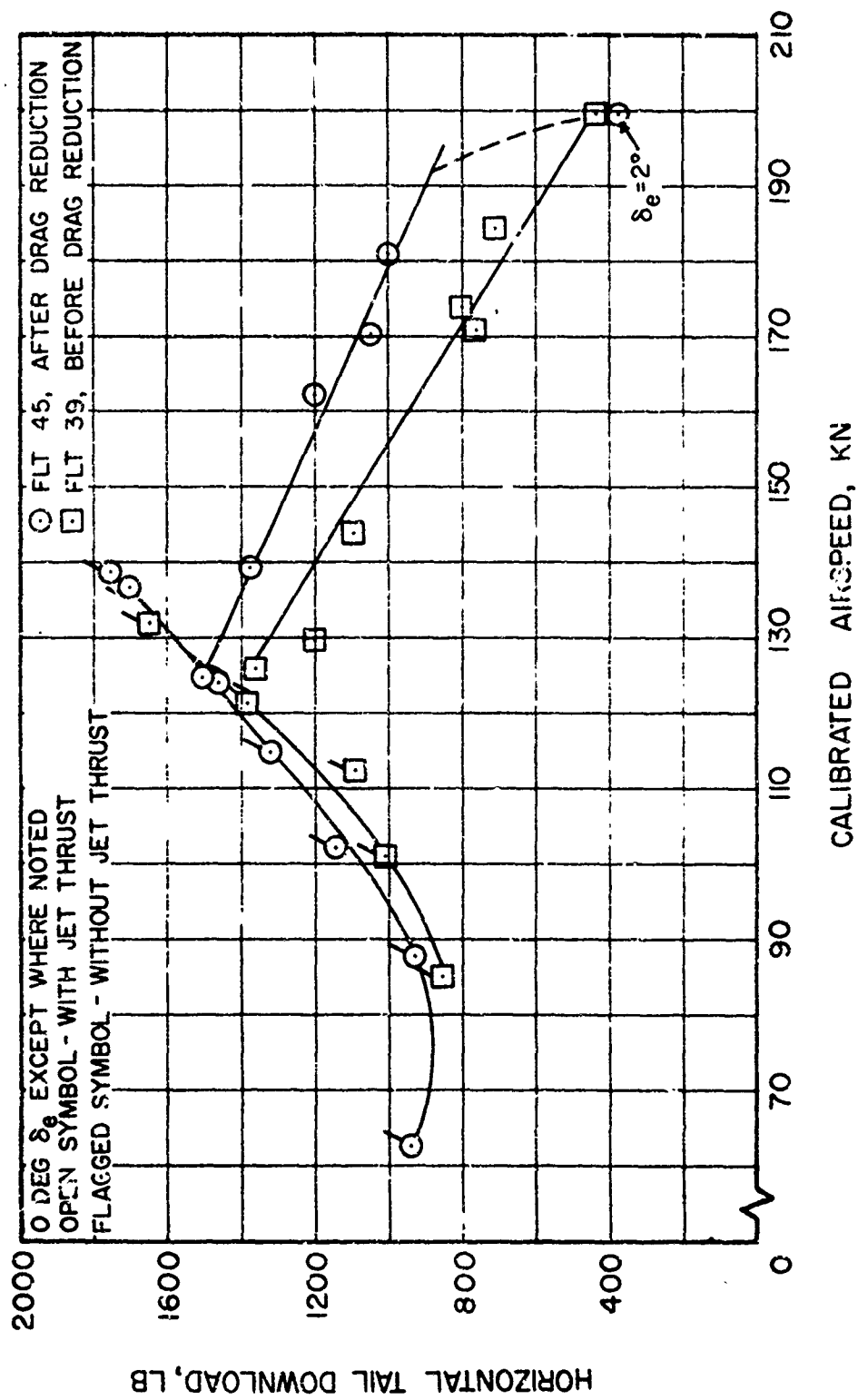


FIGURE 40. EFFECT OF SPEED ON HORIZONTAL TAIL LOADING.

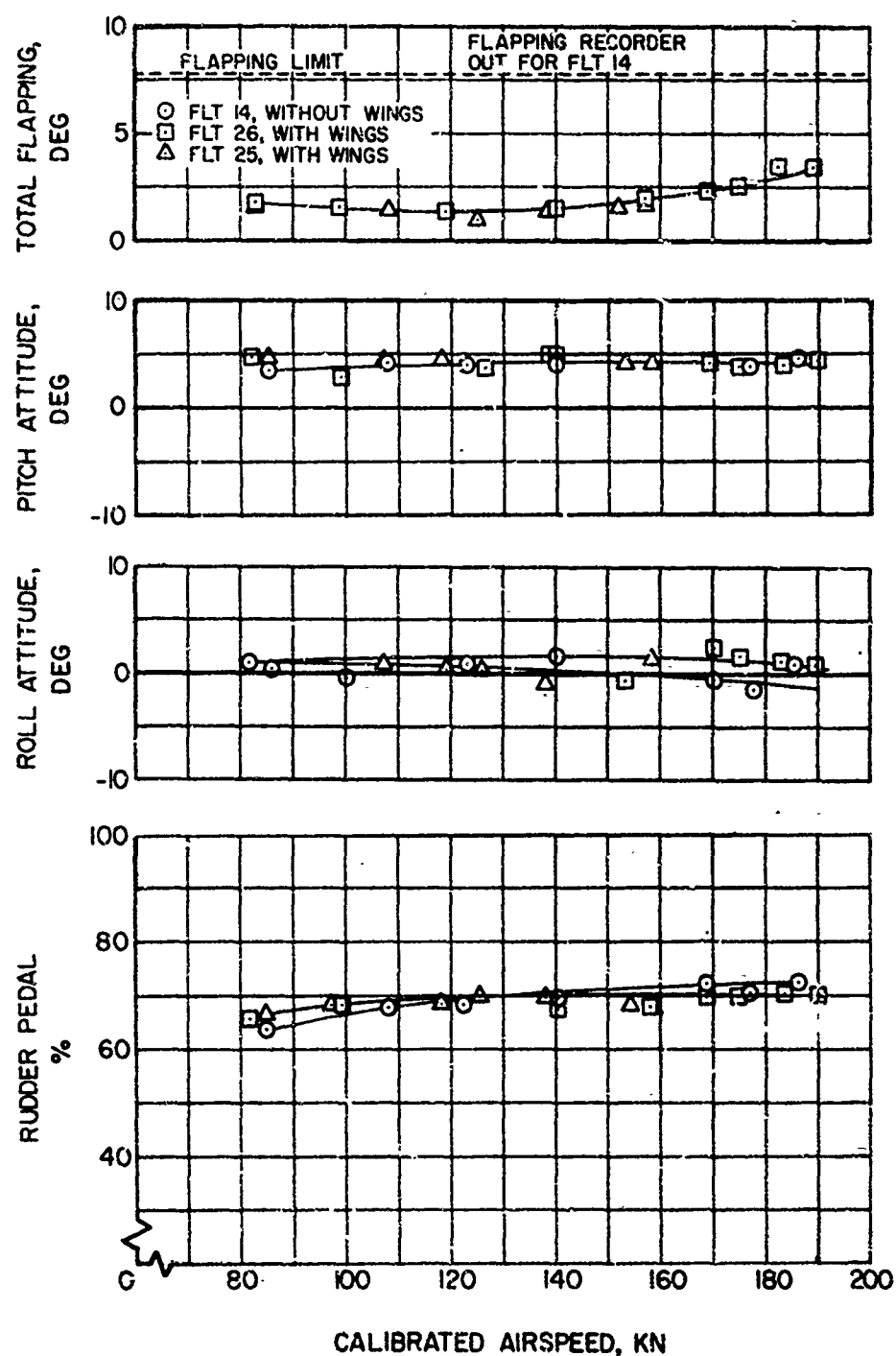


FIGURE 41. EFFECT OF WING ON STEADY STATE FLIGHT PARAMETERS (WITH JETS, FIVE MAIN ROTOR BLADES,  $-4$  DEGREES TWIST, ZERO DEGREE  $\delta_e$ ,  $-1.5$  DEGREES  $\delta_r$ , 5 DEGREES  $i_{HT}$ )

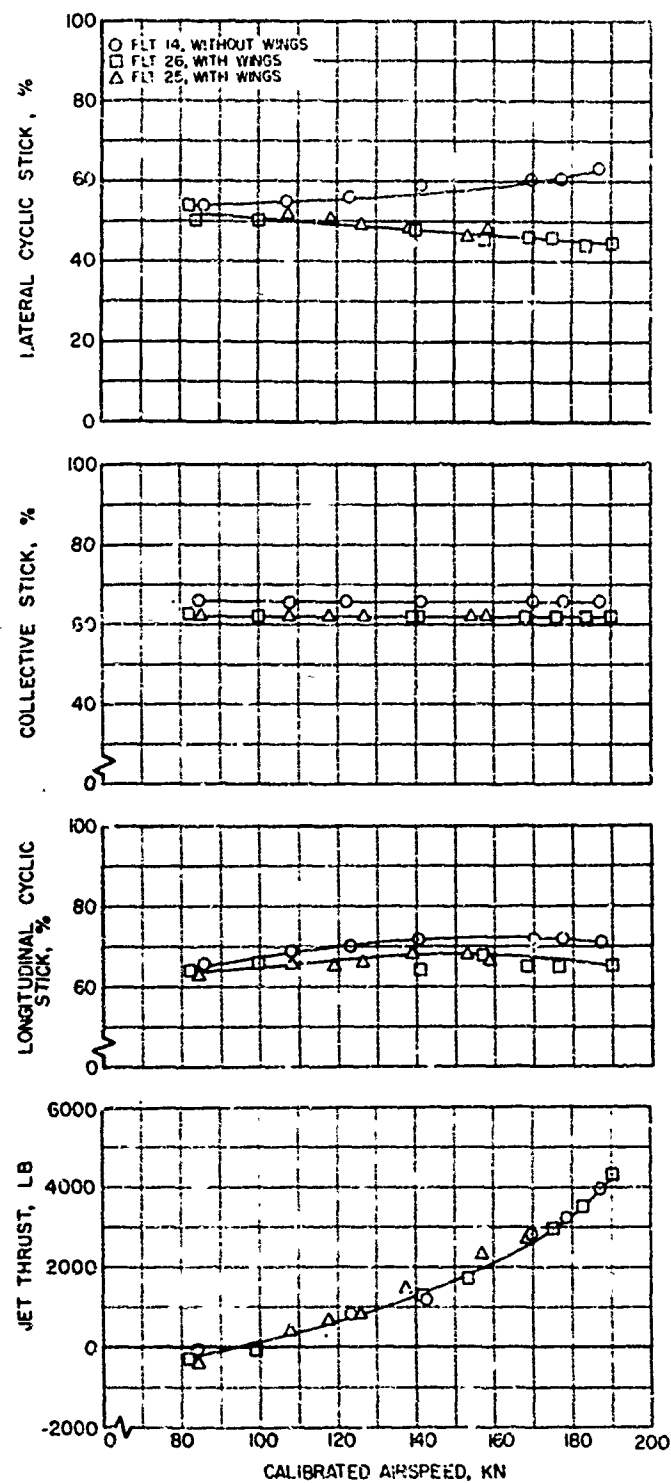


FIGURE 41. Concluded.

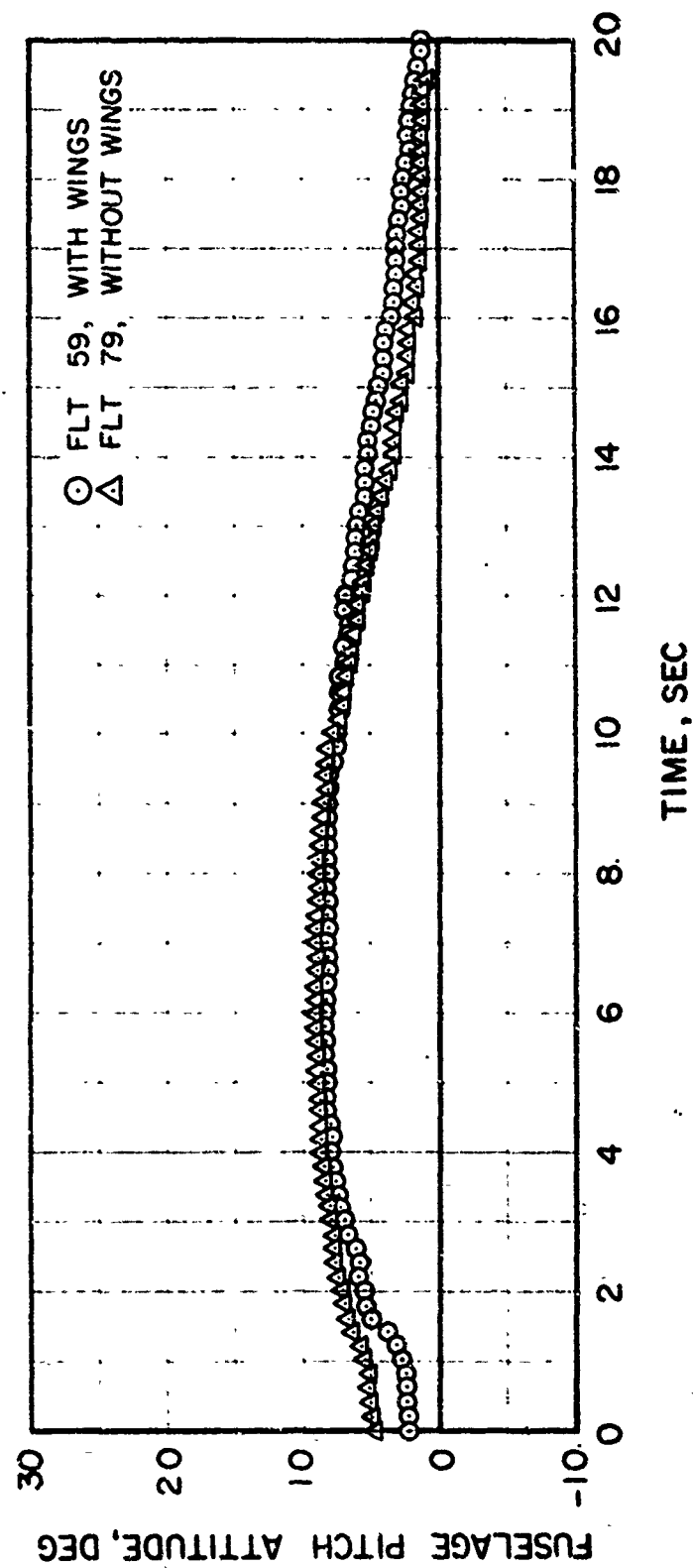
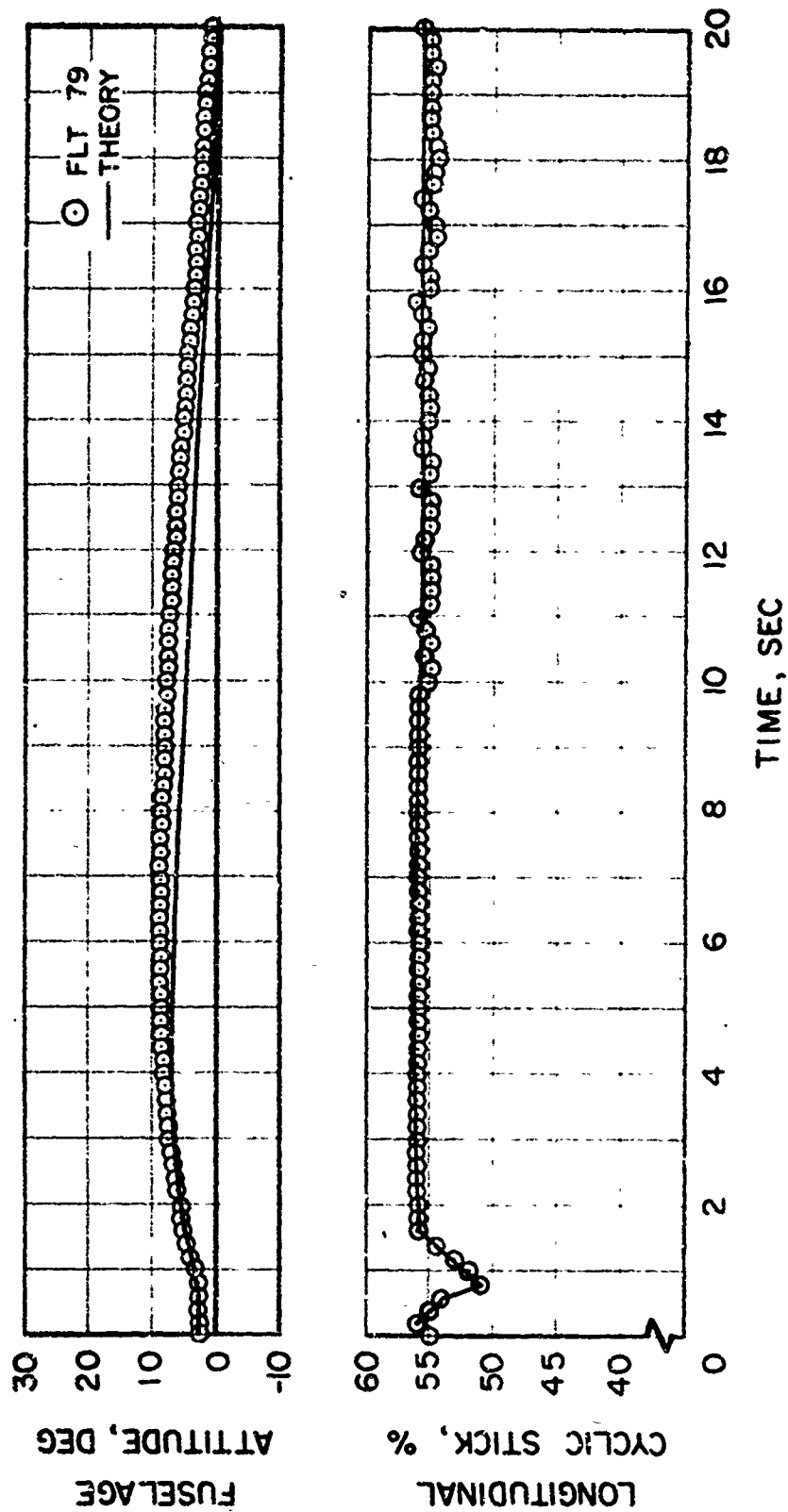


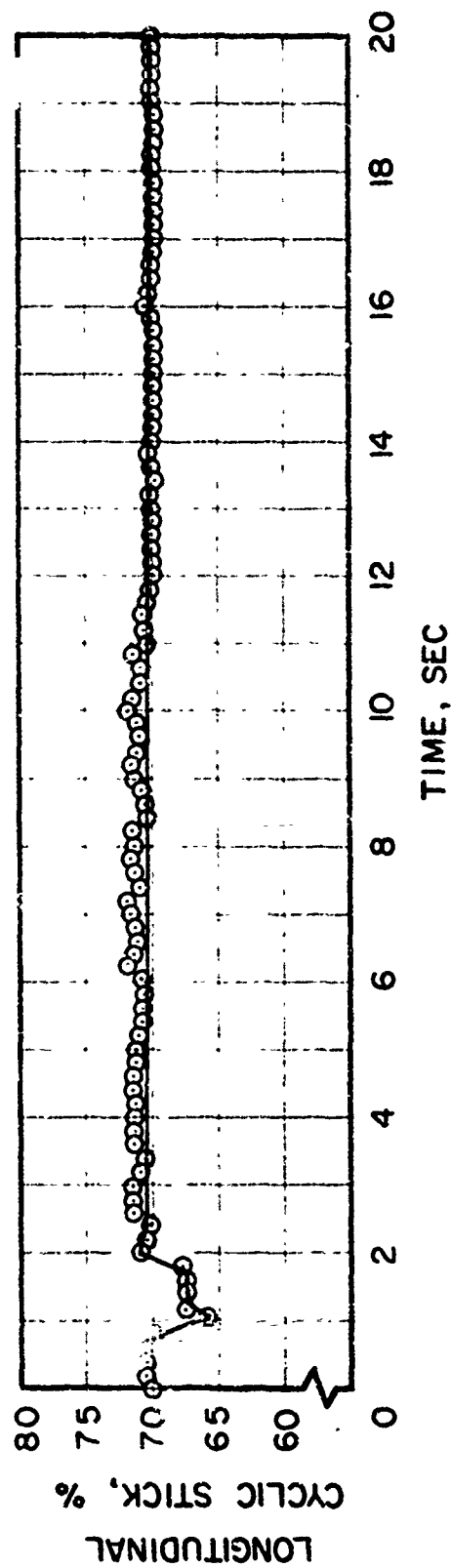
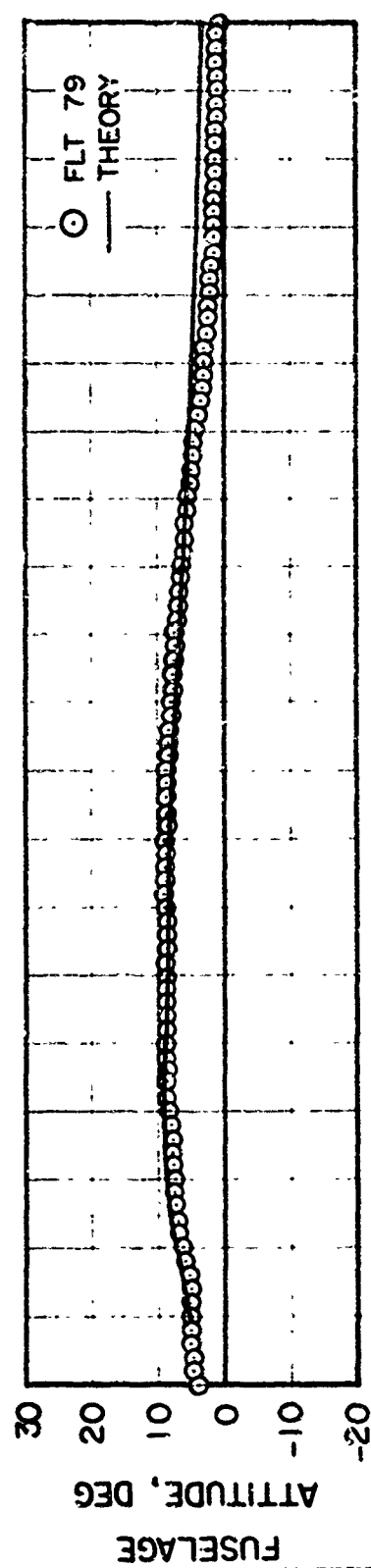
FIGURE 42. EFFECT OF WINGS ON NH-3A DYNAMIC RESPONSE OF FUSELAGE ATTITUDE TO A LONGITUDINAL PULL AND RETURN AT 120 KNOTS, (WITH JETS, FIVE MAIN ROTOR BLADES, -8 DEGREES TWIST, ZERO DEGREE  $\delta_e$ , ZERO DEGREE  $i_{HT}$ ).



(a) WITH WINGS

FIGURE 43. CORRELATION OF DYNAMIC RESPONSE OF FUSELAGE ATTITUDE TO A LONGITUDINAL PULL AND RETURN AT 120 KNOTS, (WITH JETS, FIVE MAIN ROTOR BLADES, -8 DEGREE TWIST, ZERO DEGREE  $\delta_e$ , ZERO DEGREE  $i_{HT}$ ).





(b) WITHOUT WINGS

FIGURE 43. Concluded.

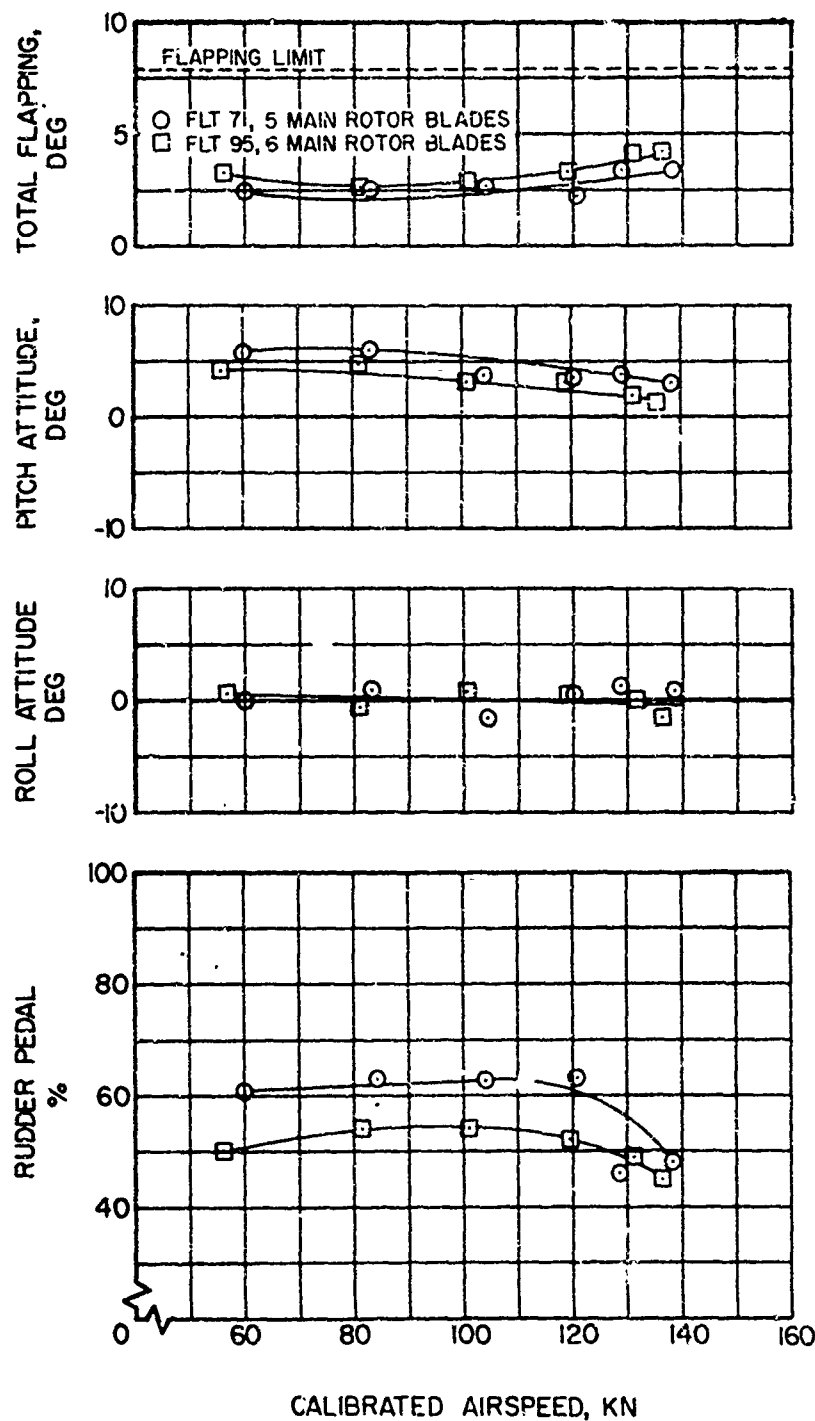


FIGURE 44. EFFECT OF SOLIDITY ON STEADY STATE FLIGHT PARAMETERS (WITHOUT WINGS AND JETS,  $-8$  DEGREES TWIST, ZERO DEGREE  $\delta_e$ , ZERO DEGREE  $i_{HT}$ ).

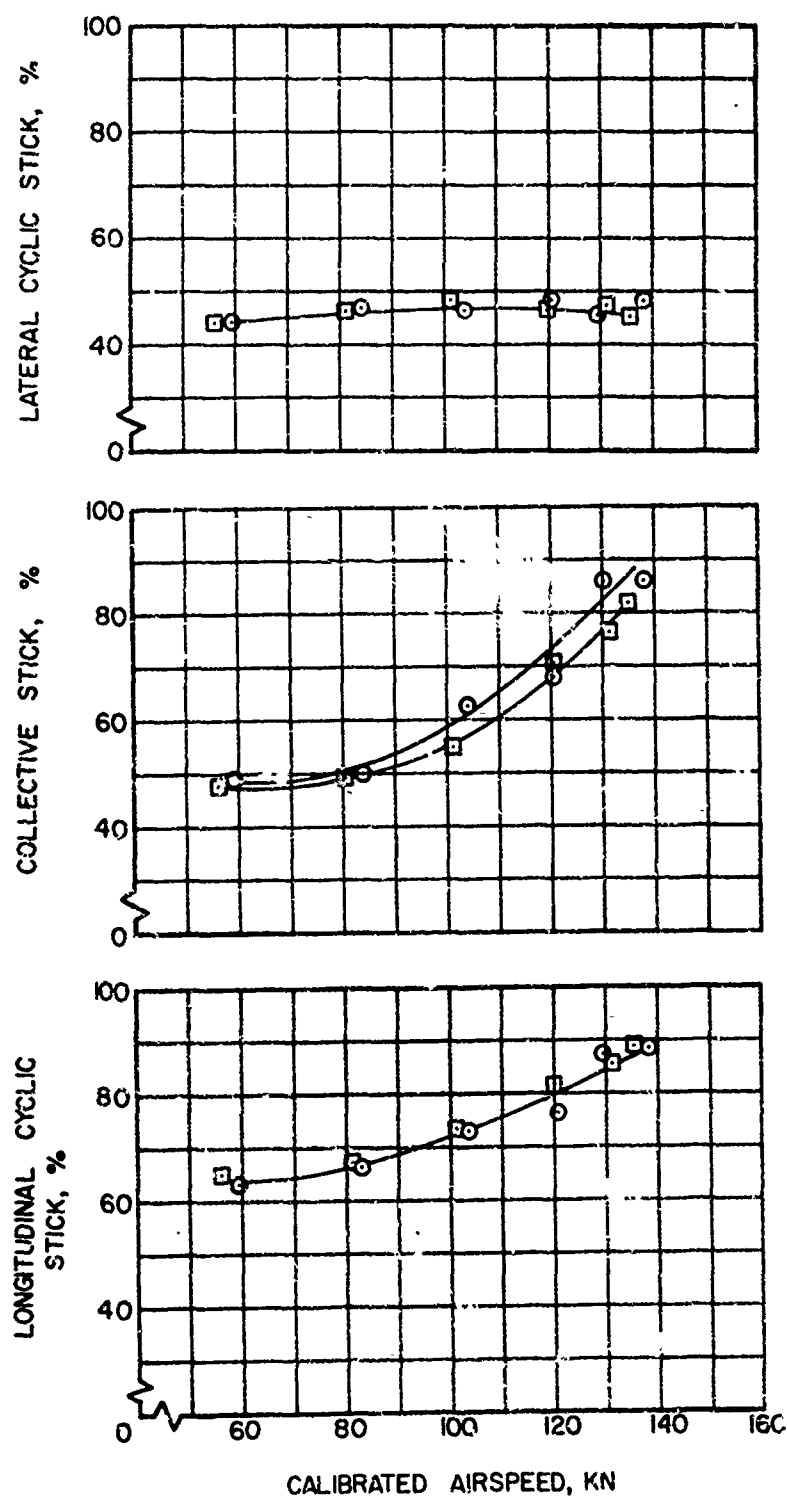


FIGURE 44. Concluded.

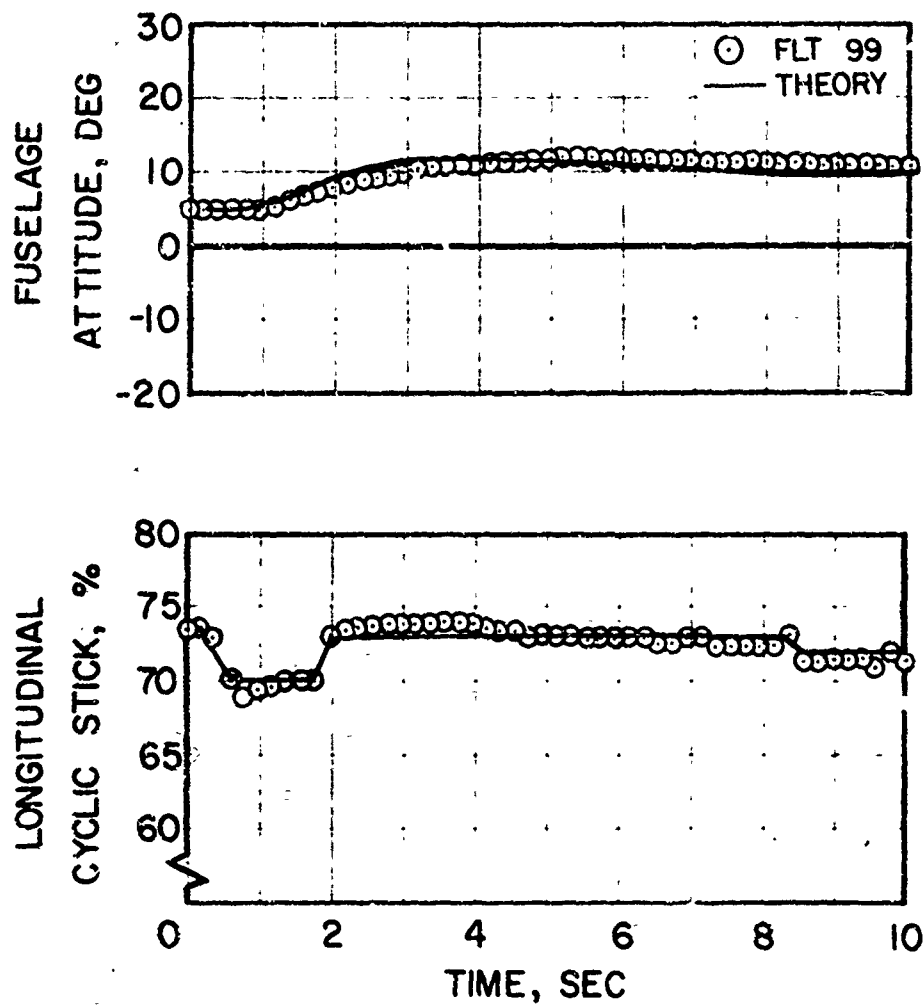


FIGURE 45. CORRELATION OF DYNAMIC RESPONSE OF FUSELAGE ATTITUDE TO A LONGITUDINAL PULL AND RETURN AT 120 KNOTS (WITHOUT WINGS, WITH JETS, SIX MAIN ROTOR BLADES, -8 DEGREES TWIST, ZERO DEGREES  $\delta_e$ , ZERO DEGREE  $i_{HT}$ ).

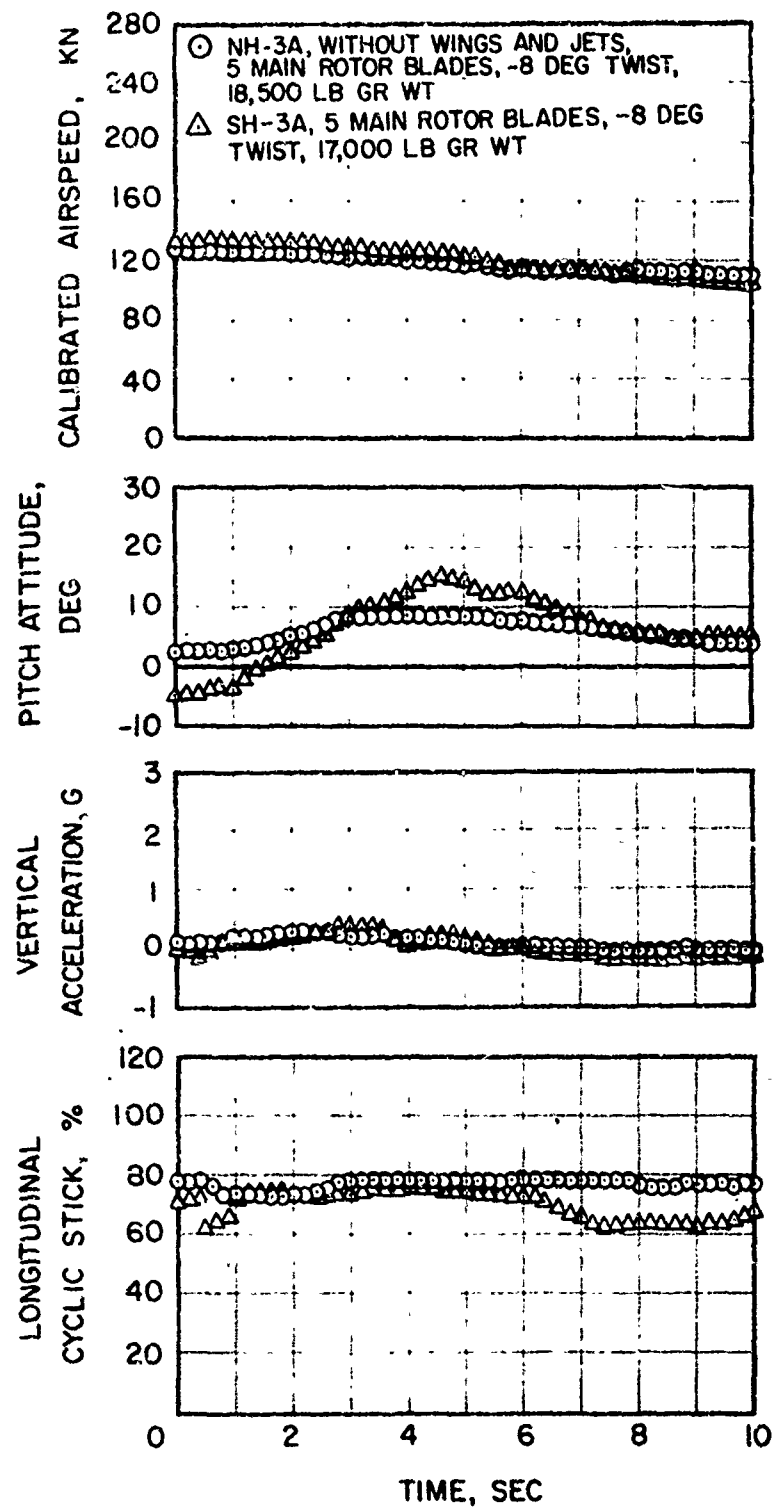
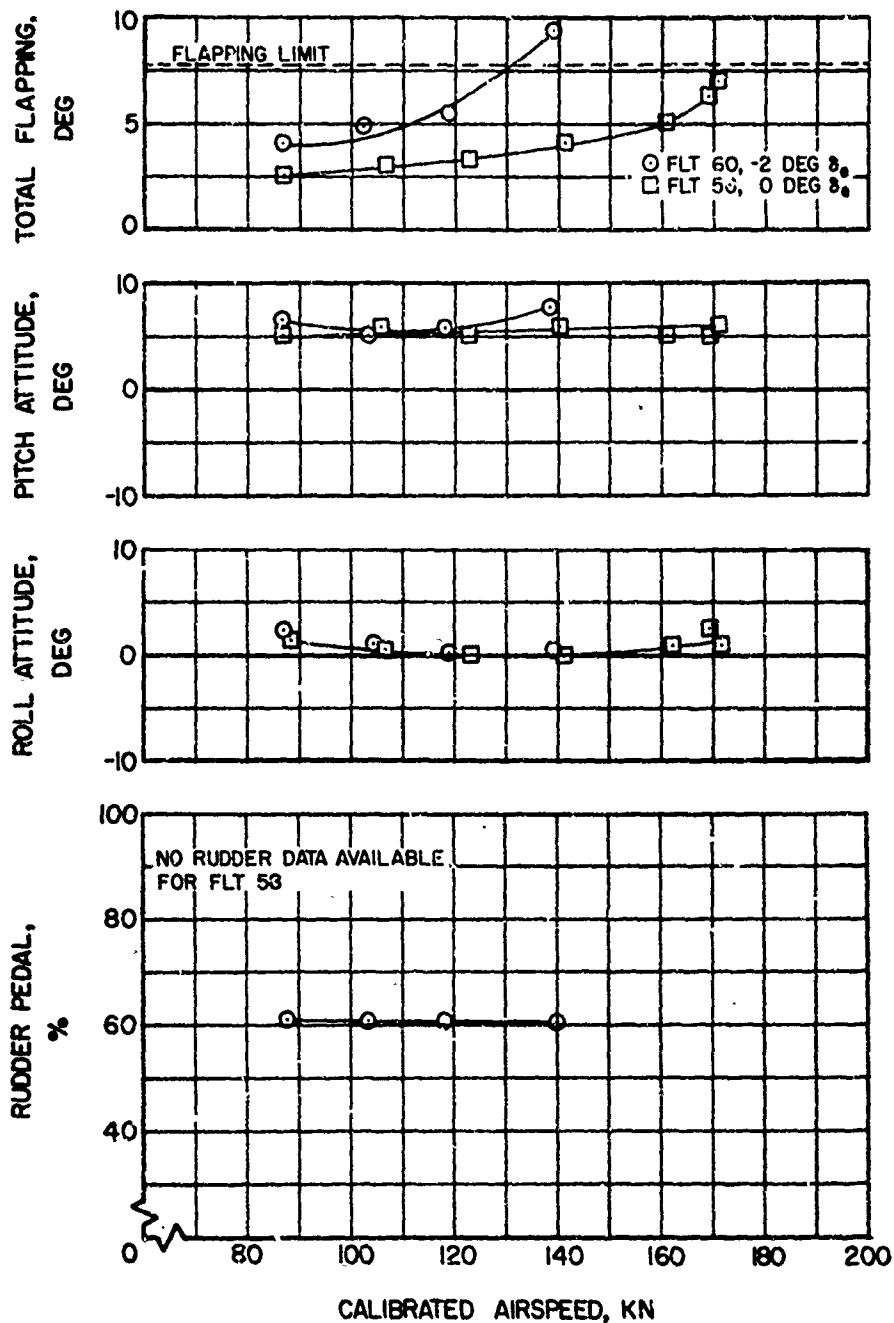


FIGURE 46. COMPARISON OF NH-3A AND SH-3A DYNAMIC RESPONSE.



(a) EFFECT OF NEGATIVE ELEVATOR DEFLECTION

FIGURE 47. EFFECT OF ELEVATOR DEFLECTION ON STEADY STATE FLIGHT PARAMETERS (WITH WINGS AND JETS, FIVE MAIN ROTOR BLADES, -8 DEGREES TWIST, 4 DEGREES  $\delta_f$ , ZERO DEGREE  $i_{HT}$ ).

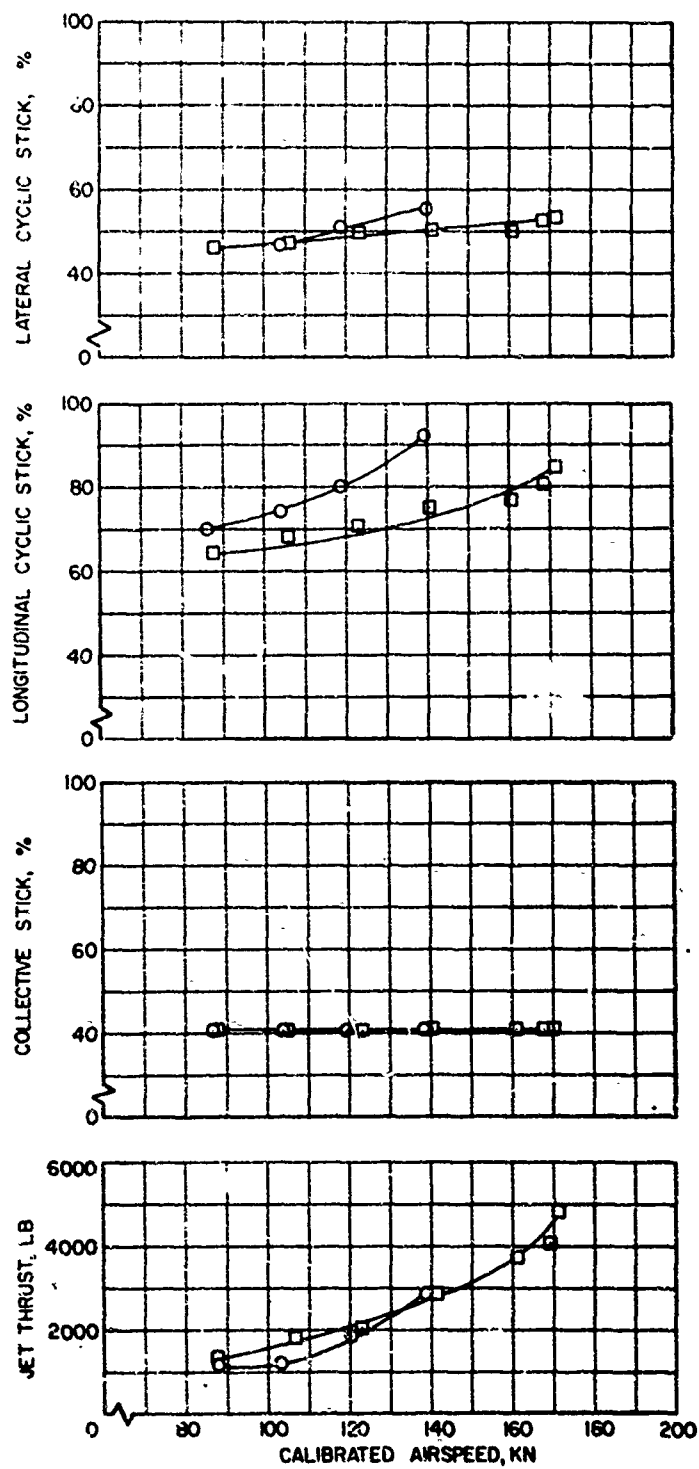


FIGURE 47. (a) Continued.

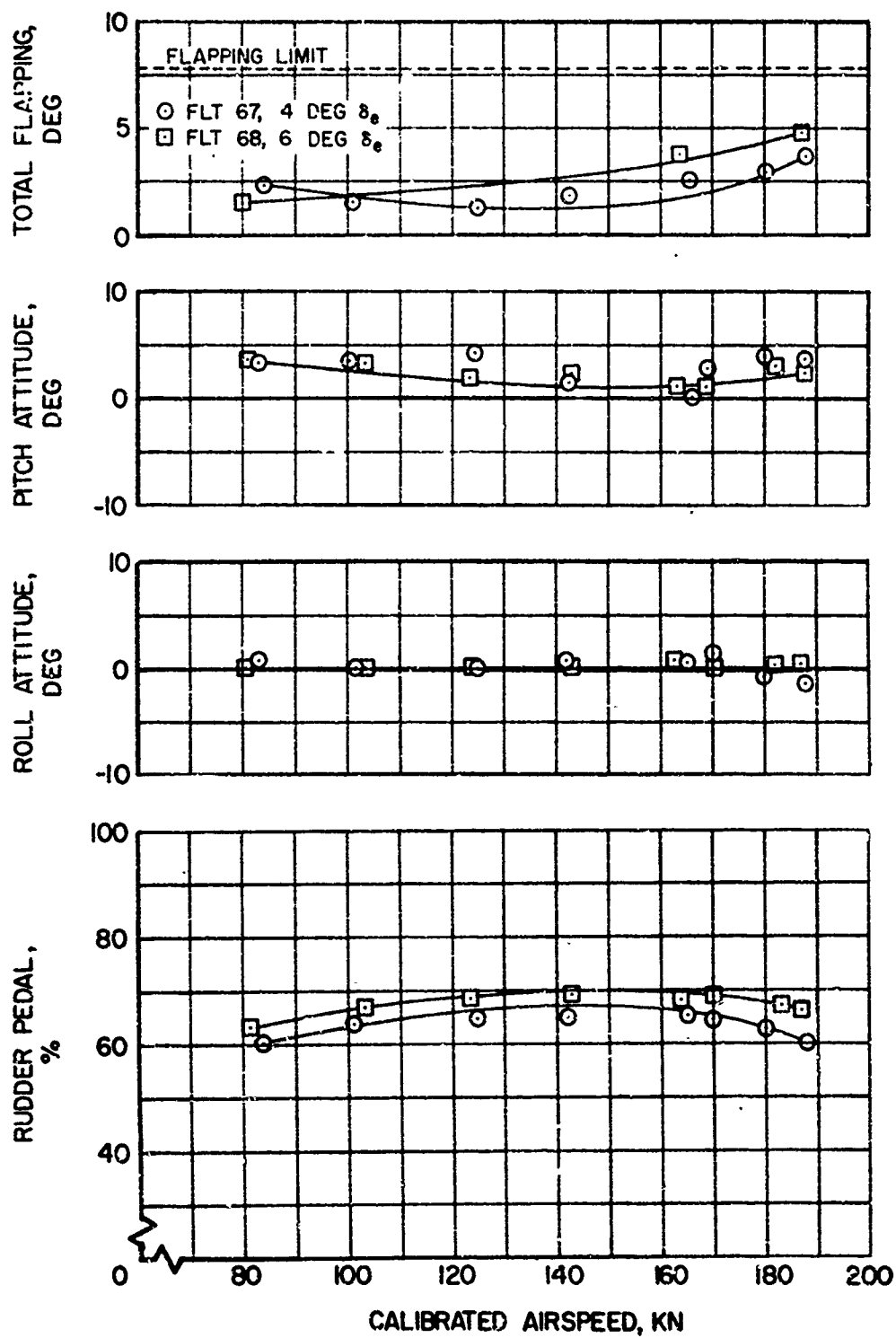


FIGURE 47. (b) EFFECT OF POSITIVE ELEVATOR DEFLECTION



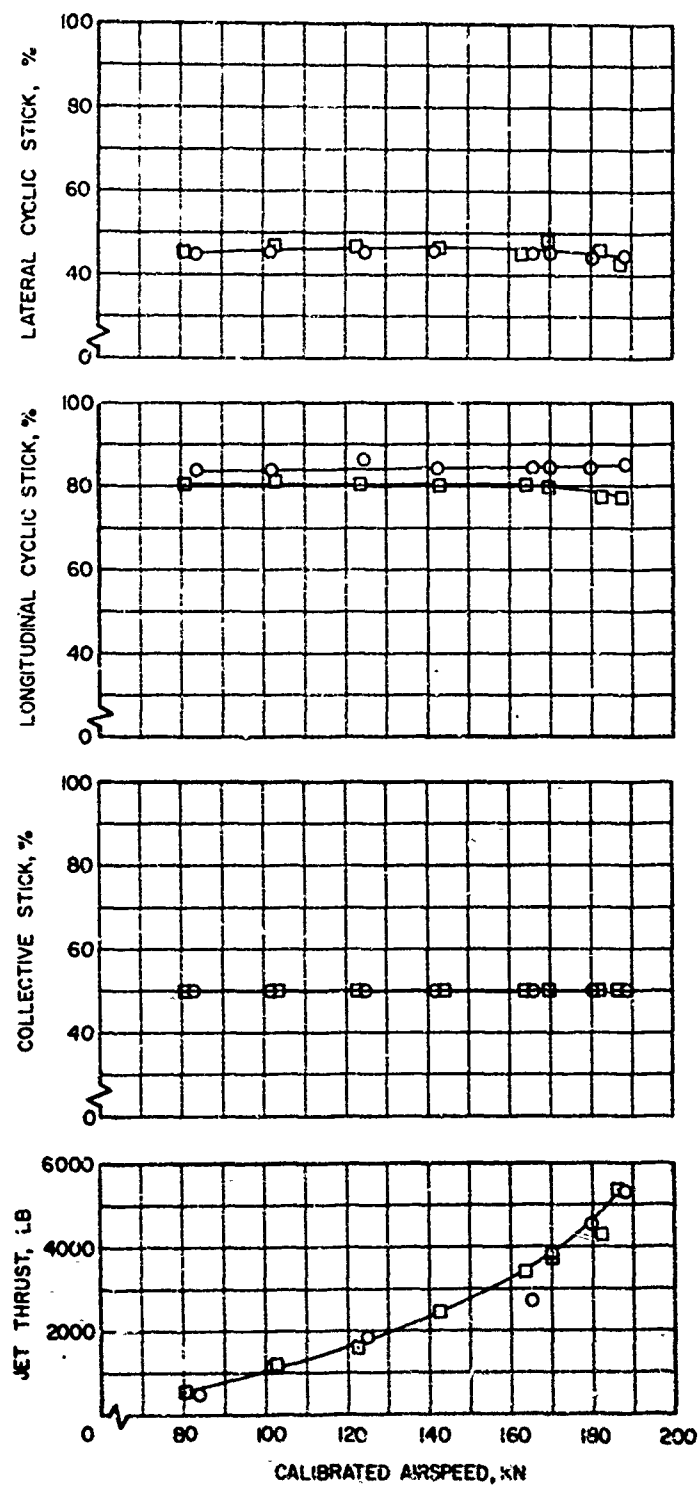


FIGURE 47. (b) Concluded.

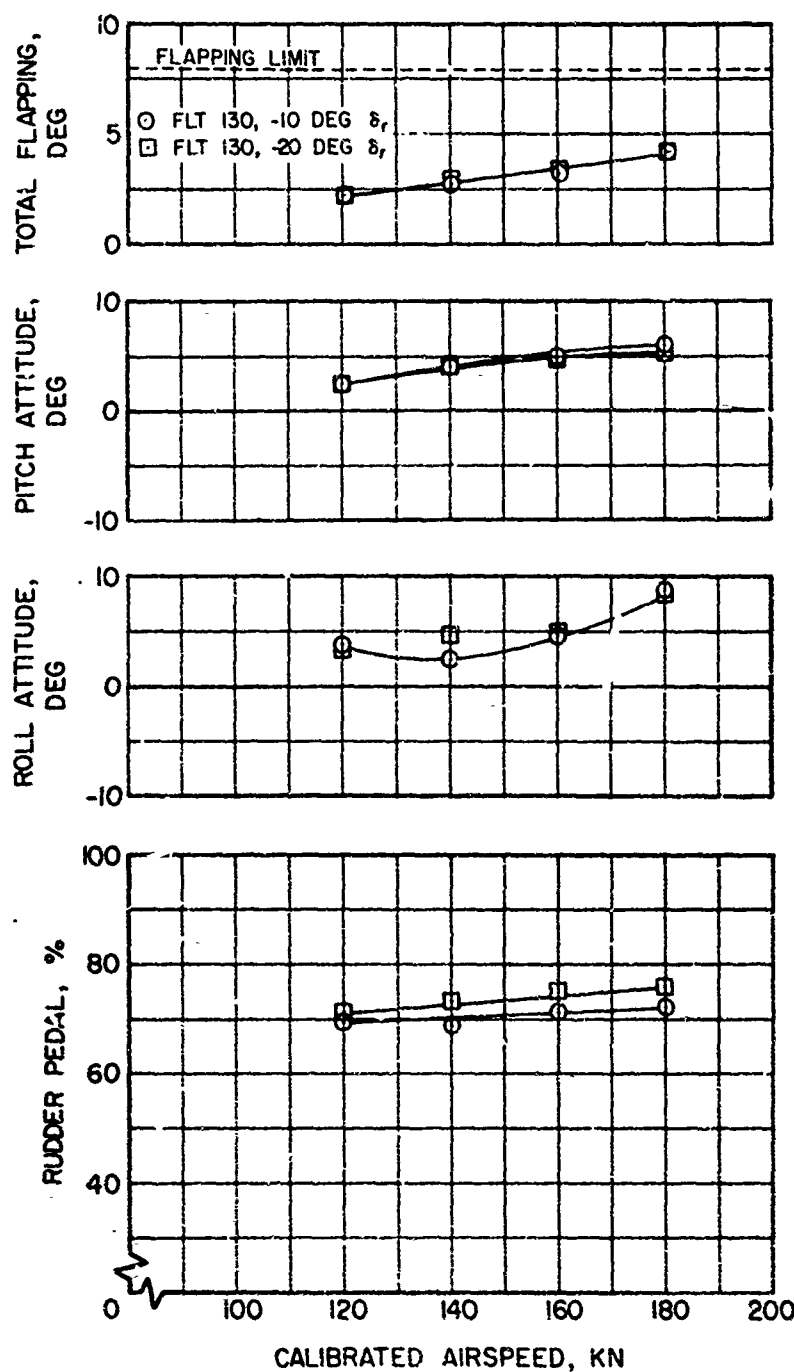


FIGURE 48. EFFECT OF RUDDER DEFLECTION ON STEADY STATE FLIGHT PARAMETERS (WITH WINGS AND JETS, FIVE MAIN ROTOR BLADES, -4 DEGREES TWIST, ZERO DEGREE  $\delta_e$ , ZERO DEGREE  $\delta_r$ , ZERO DEGREE  $i_{HT}$ ).

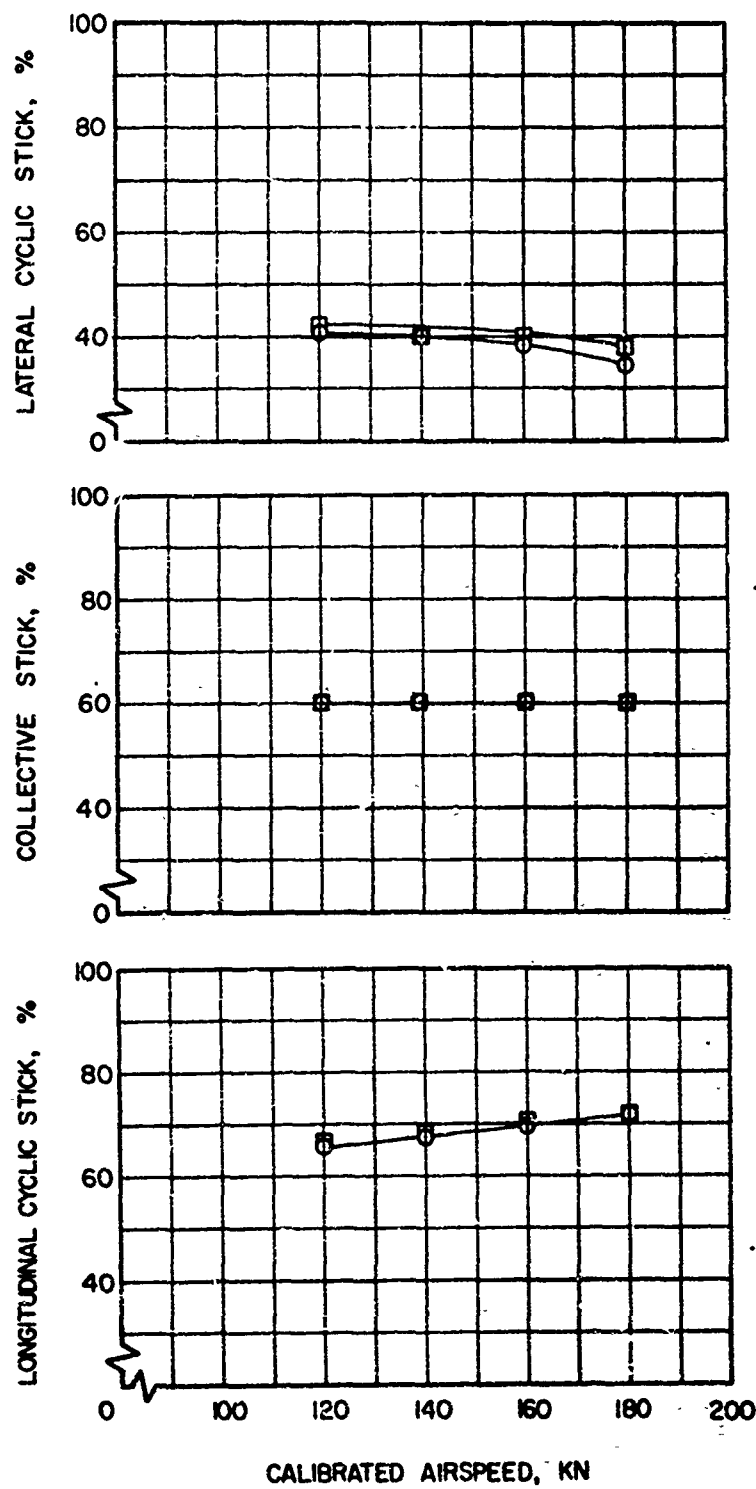


FIGURE 48. Concluded.

## APPENDIX I

### 1/12 SCALE MODEL WIND TUNNEL DATA

Tests of a 1/12 Scale Model of the NH-3A airframe, shown in Figure 49, were conducted in the United Aircraft Corporation 4 x 6 feet Subsonic Wind Tunnel prior to modifying the bailed SH-3A aircraft. Six-component aerodynamic data were obtained over ranges of model pitch and yaw at a constant tunnel dynamic pressure of 25.6 psf, corresponding to a nominal tunnel speed of 100 mph.

This appendix is intended only to provide the most significant data used in evaluation and correlation of the NH-3A flight test results. Data are presented in Figures 50 through 54 in terms of full-scale aircraft forces and moments per unit of freestream dynamic pressure. All quantities are in the wind axis system, through the aircraft c.g., and are corrected for gravity and interference tares. Unless specifically noted, tail incidence, flap deflection and elevator deflection were zero. The model was equipped with a non-rotating simulated rotorhead. Streamlined fairings were incorporated to provide smooth flow about jet inlet and exhaust locations.

Figure 51 presents the effects of the wing and tail upon airframe longitudinal characteristics over a range of angle of attack. Lift, drag and pitching moment parameters are shown for the compound configuration, the helicopter plus jets (compound with wing removed), and the helicopter with jets, but with the horizontal stabilizer removed. The minimum parasite area of the compound configuration was measured as 18.5 square feet. This was initially corrected to 26 square feet to account for protruberances, leakage and details whose drag could not be accurately assessed on the small model. A further discussion of the actual drag was presented in Aircraft Drag, page 15. The pitching moment curve of both configurations, with the stabilizer installed, was highly stable. Figure 51 presents similar data without discussion, showing the effects of flap deflections of 0, 10, 20, and 30 degrees.

Figure 52 presents the effect of elevator deflection and Figure 53 shows the effect of stabilizer incidence upon longitudinal characteristics. The small differences which may appear between data of similar configurations in Figures 50-53 represent the wind tunnel measurement accuracy, because a separate run was conducted in each case.

Figure 54 shows the effect of yaw angle upon side force, rolling and yawing moment parameters. The yawing moment is neutral or slightly unstable at small angles of yaw, probably because of the reduced vertical stabilizer effectiveness in the rotorhead wake. The positive contribution of the tail rotor makes the full scale aircraft directionally stable.

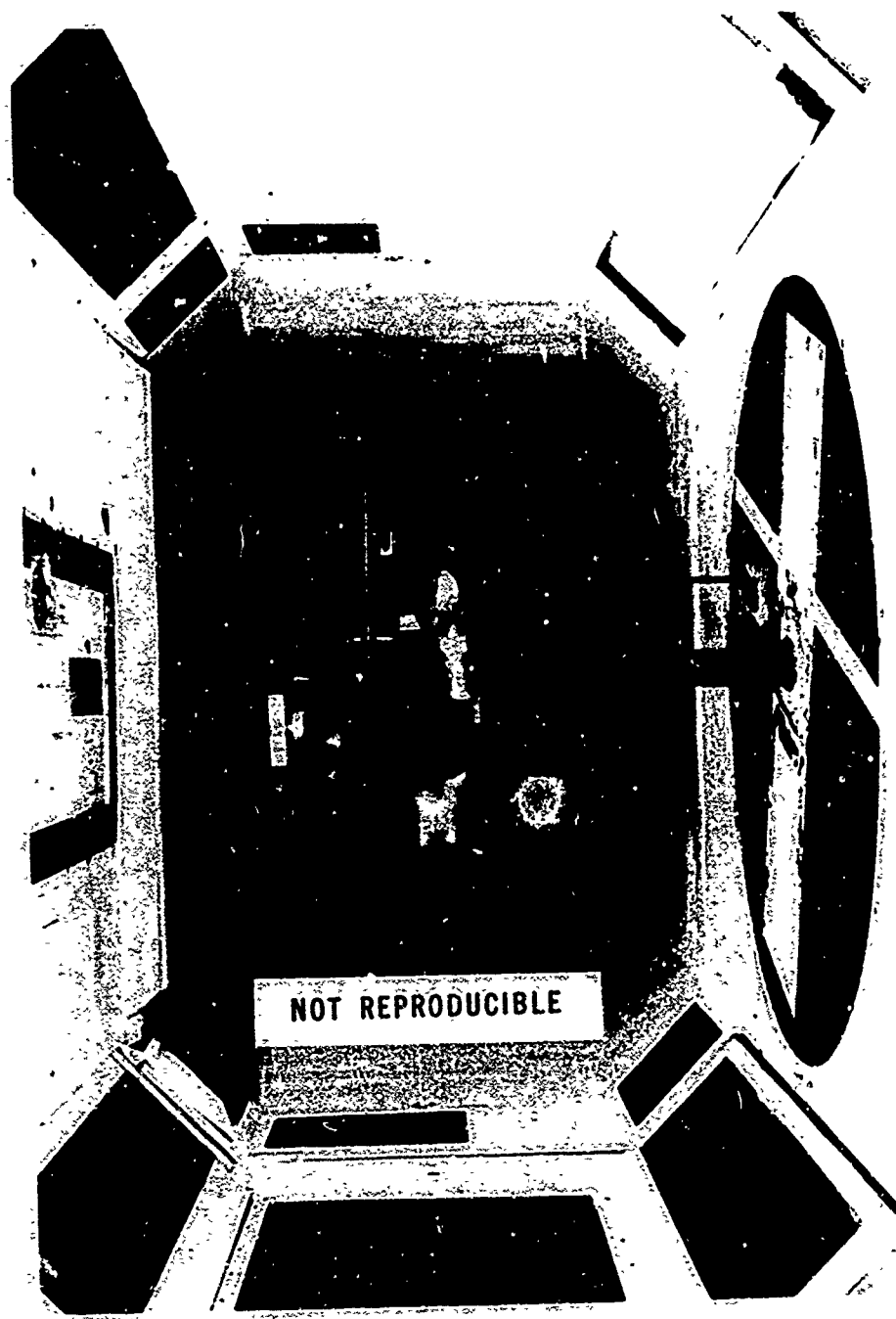


Figure 49. 1/12 Scale Wind Tunnel Model - NH-3A

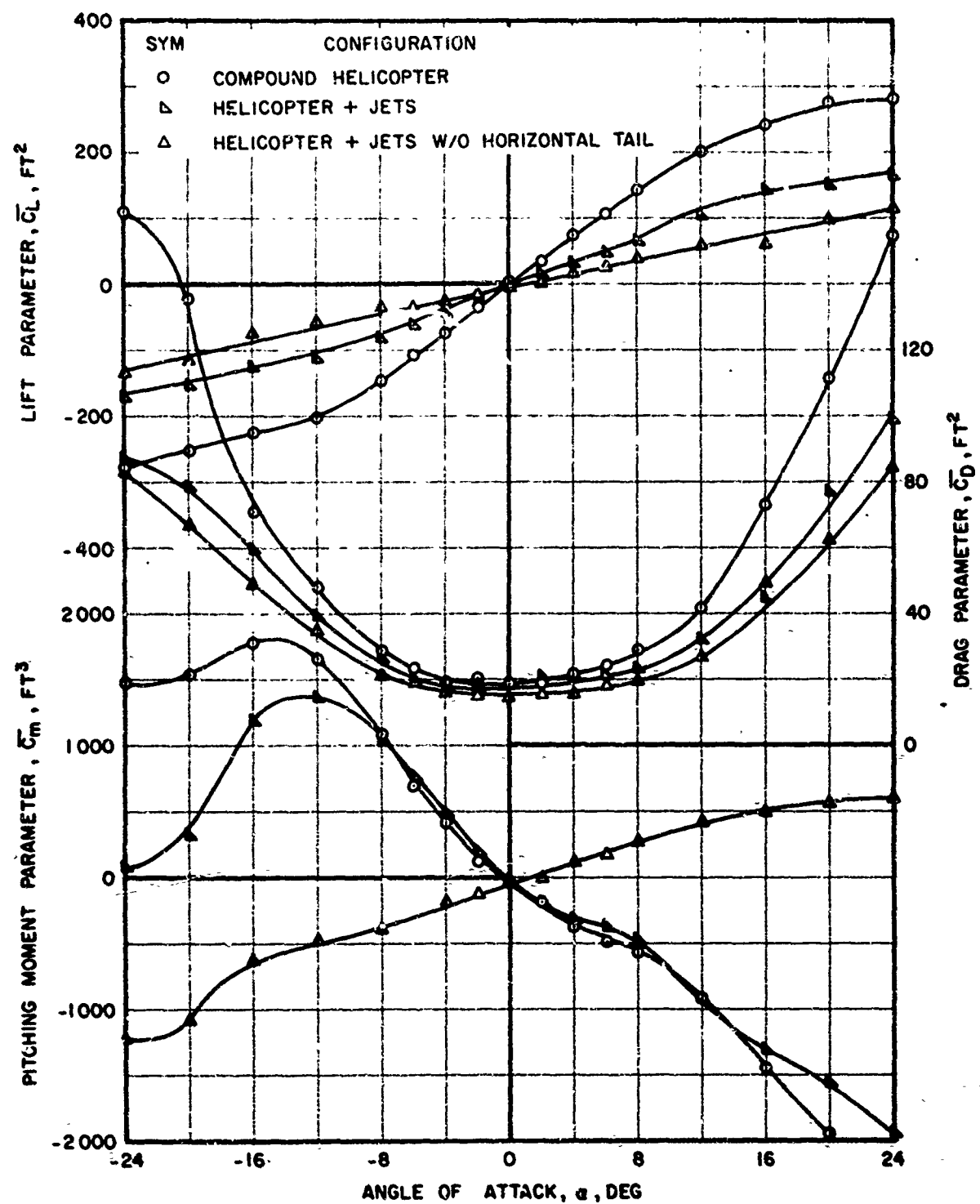


FIGURE 50. EFFECT OF CONFIGURATION ON LONGITUDINAL CHARACTERISTICS, 1/12 SCALE AIRFRAME MODEL.

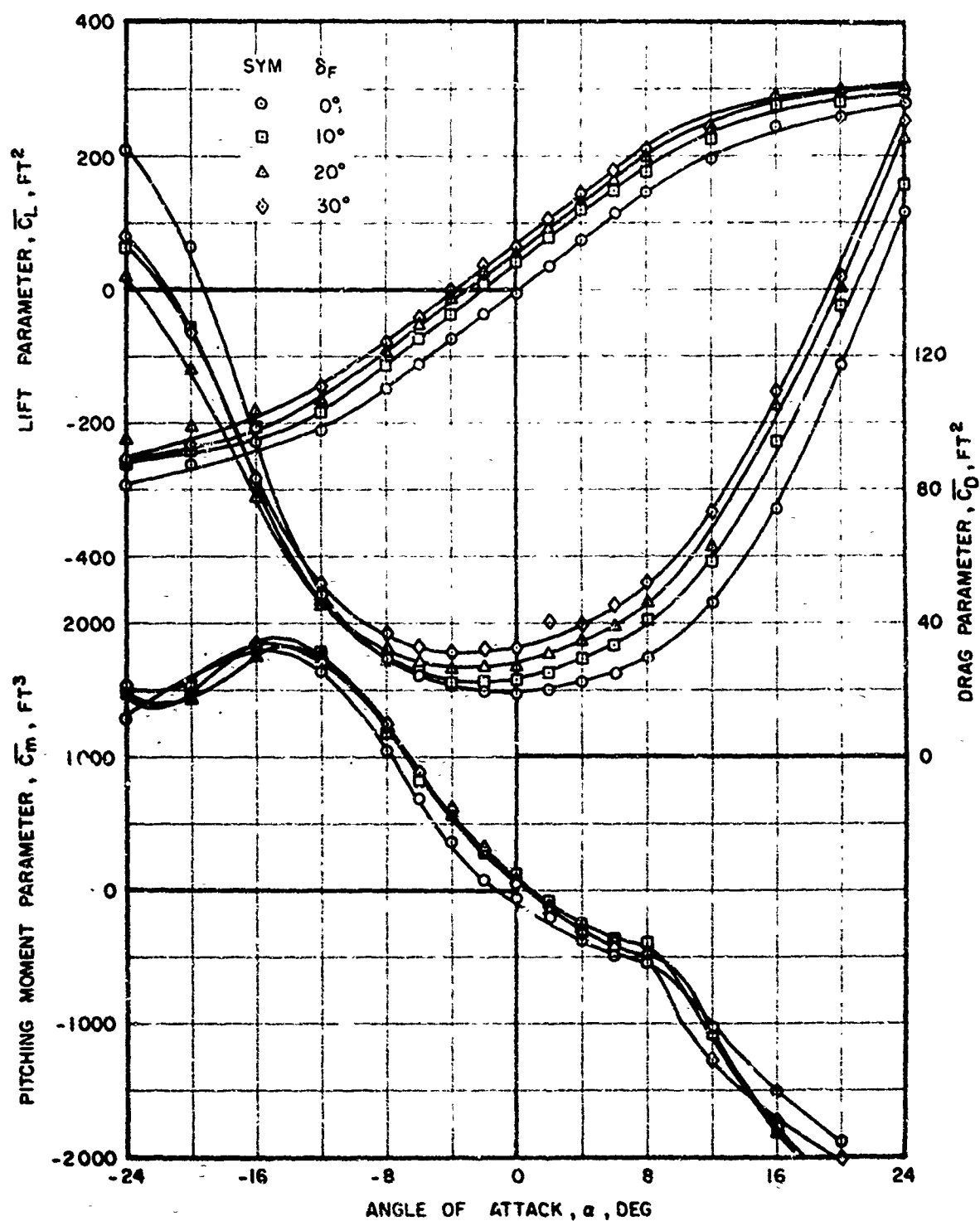


FIGURE 51. EFFECT OF FLAP DEFLECTION ON LONGITUDINAL CHARACTERISTICS, 1/12 SCALE AIRFRAME MODEL.



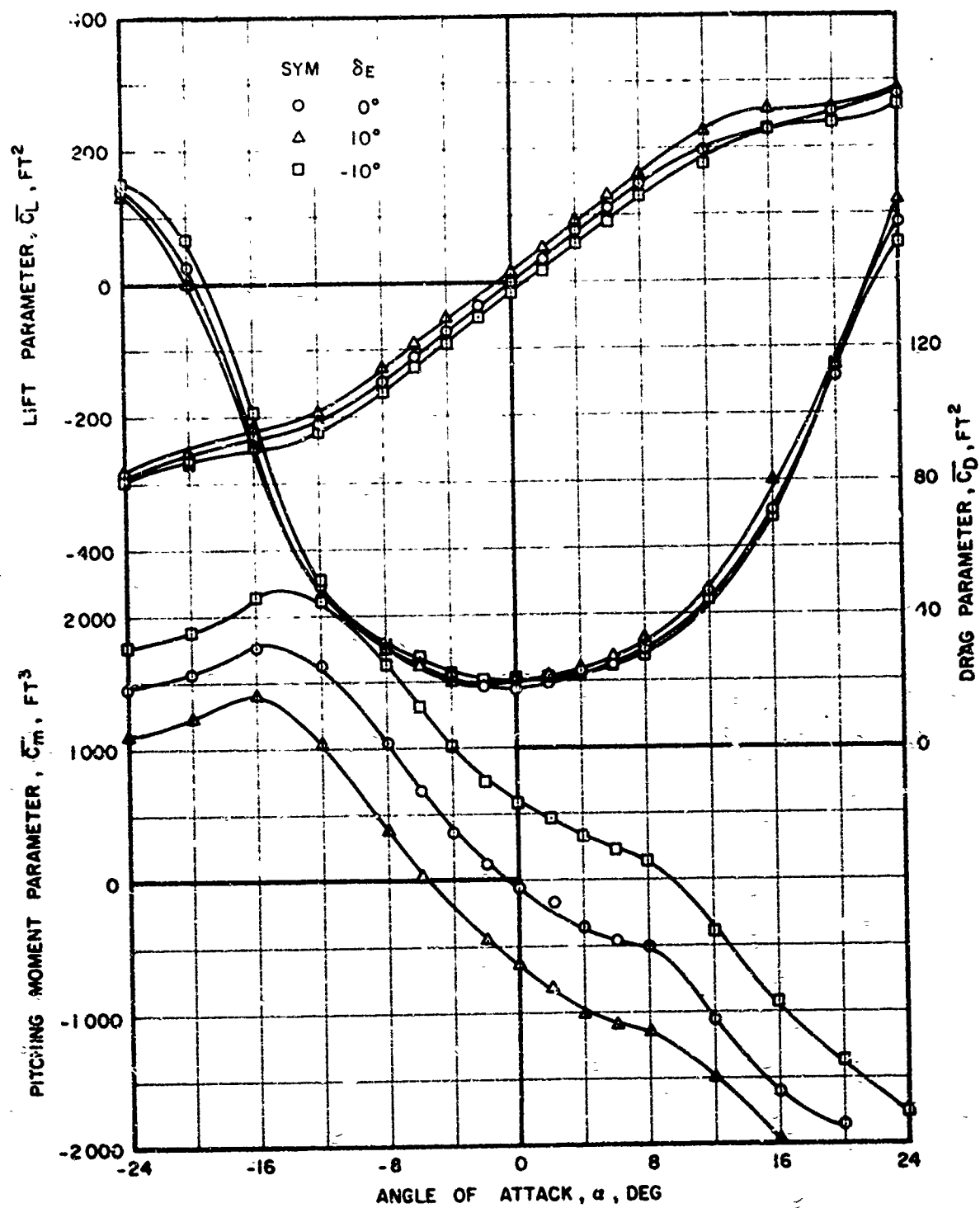


FIGURE 52. EFFECT OF ELEVATOR DEFLECTION ON LONGITUDINAL CHARACTERISTICS, 1/12 SCALE AIRFRAME MODEL.

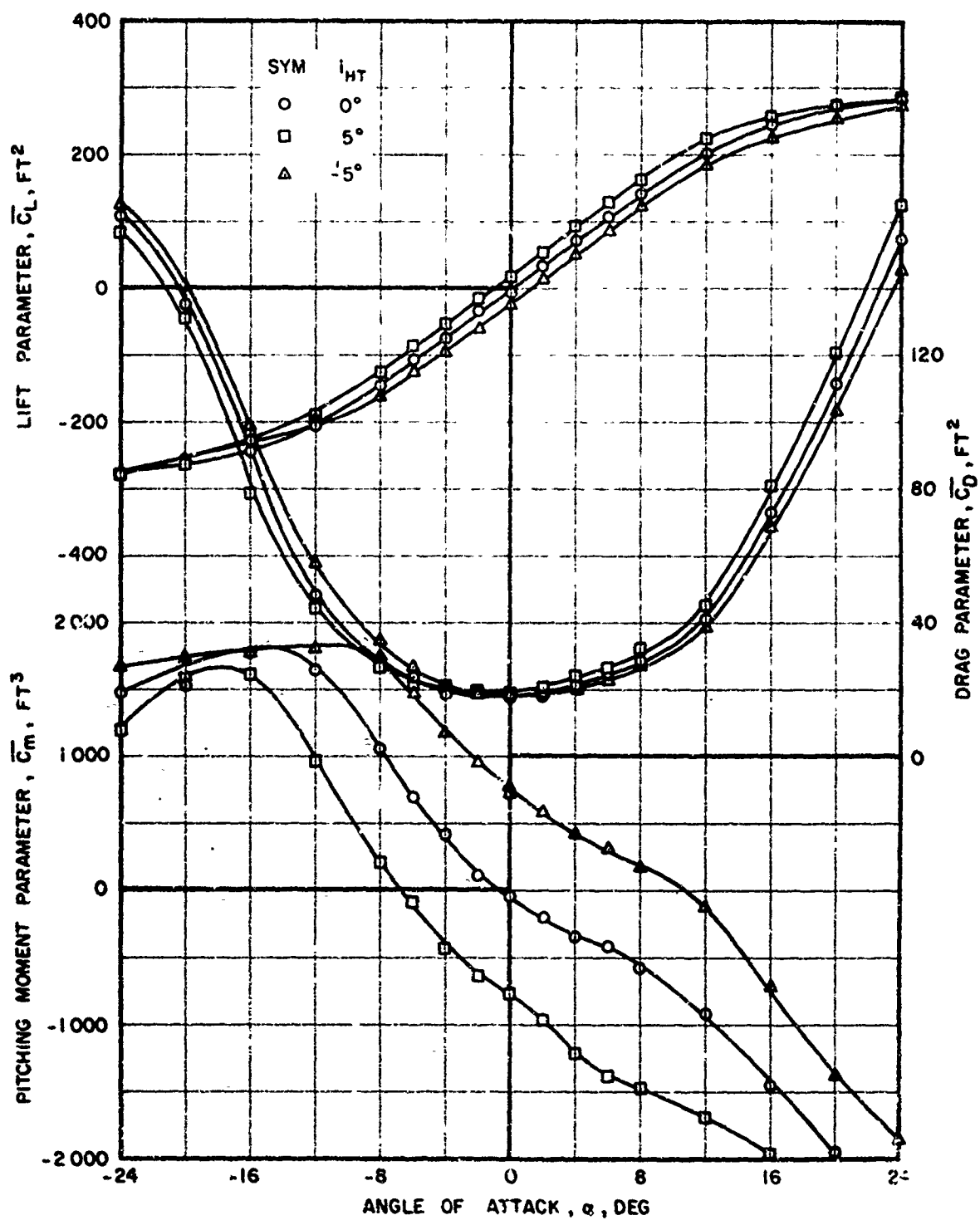


FIGURE 53. EFFECT OF HORIZONTAL TAIL INCIDENCE ON LONGITUDINAL CHARACTERISTICS, 1/12 SCALE AIRFRAME MODEL.

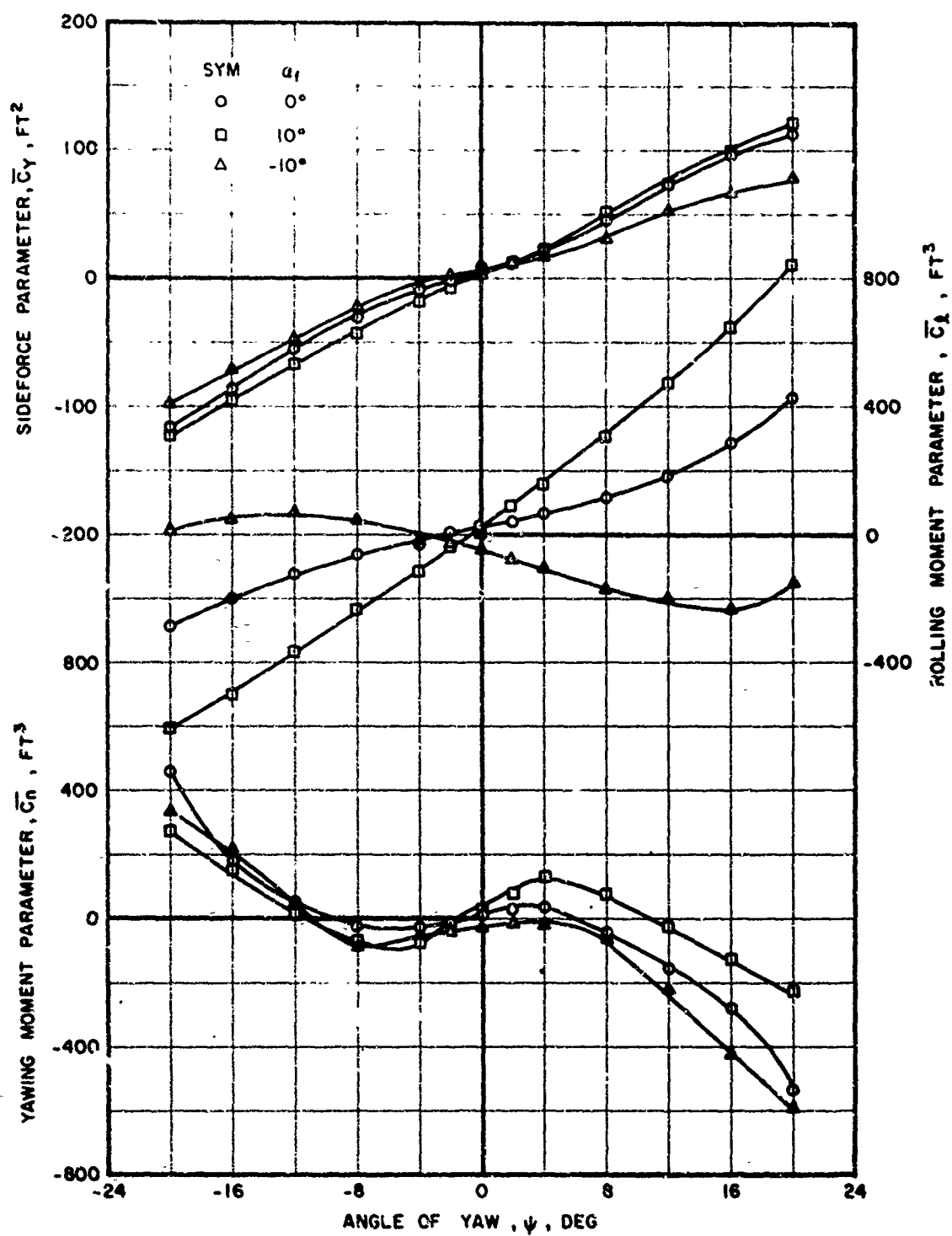


FIGURE 54. EFFECT OF FUSELAGE ATTITUDE ON LATERAL AND ROLL CHARACTERISTICS, 1/12 SCALE AIRFRAME MODEL.

APPENDIX II  
TEST INSTRUMENTATION

Test instrumentation was installed to record flight test data on handling qualities, performance, rotor loads, stress, and aircraft vibration for all configurations investigated. Dual instrumentation was required in some areas to provide simultaneous indications to both the pilot and the oscillograph/photopanel recorders, or to provide back-up for the principal parameters. Instrumentation was also provided to monitor critical structural loads. A description of the basic instrumentation package is provided in the following sequence:

1. Apparatus
2. Calibrations
3. Measurements
4. Accuracy

APPARATUS

Primary recording devices, installed in the cabin area, consisted of two 50 channel light beam photo-recording oscillographs and a 24 hole photopanel, utilizing a variable speed 35 mm camera. Signal conditioning for the transducers was provided by standard bridge balancing modules and potentiometer adapter boxes.

A nose boom was utilized to obtain airspeed, altitude, fuselage angle of attack, sideslip angle, rate-of-climb and static pressure. The original aircraft airspeed system probe was also operational and used as the primary system when the nose boom was removed.

Wire-wound potentiometers were coaxially mounted to sense the angular motions of the longitudinal, lateral, collective, and rudder pedal controls. Similar installations utilizing angulators measured flapping, feathering, and lag angles of the master main rotor blade. Tail rotor flapping and pitch were measured with wire-wound potentiometers.

Vibrations were sensed by velocity pickups and accelerometers. Vertical acceleration at the center of gravity was measured with a load factor type linear accelerometer. Pitch and roll attitudes were measured with a vertical gyro. Pitch, roll, and yaw rates were measured with rate gyros.

Stress and load transducers consisted of electrical strain gages wired as conventional single active gages or as 2 or 4 gage tension or bending bridges. Strain gages normally installed on the leading edge of the main rotor blade spar were removed to the trailing edge to prevent unnecessary drag effects. Internal wiring was provided for the instrumented main rotor blade during fabrication. Wing bending moment measurements were made by strain gaging the fore and aft wing spars at two spanwise locations. Wing lift was determined from the difference in bending moments between these two locations.

#### CALIBRATIONS

Instrumentation items were laboratory calibrated prior to installation on the aircraft. Preflight and post-flight calibrations were made for all oscillograph measurements with the exception of the velocity transducers which only required periodic calibrations. Aircraft rigging checks were made throughout the test program as required by main rotor blade changes. All data presented herein are corrected for instrument and installation errors.

Airspeed position error calibrations were made for the aircraft and nose boom systems to calibrated airspeeds in excess of 200 knots. The calibrations were conducted using the measured speed course method. Results of the airspeed calibrations are shown in Figure 55.

Turbojet thrust determination was made by utilizing the engine manufacturer's test cell calibration data, which included engine pressure ratio, net thrust, corrected fuel flow, and corrected engine speed.

Calibrations of control positions, blade motions, gyros, accelerometers, and pitch and yaw vanes were straightforward and will not be discussed here. The control system rigging is presented in Table III.

Values of main rotor thrust were obtained by direct measurement of axial strain in the main rotor shaft. Laboratory calibrations that included effects of shaft bending and torsion on the thrust showed repeatable, linear results. As testing proceeded, however, it was found that the influence of main rotor gearbox temperature resulted in a shifting of the zero thrust reference. Further investigation of the problem was undertaken with a temperature probe in the main rotor gearbox to establish a relationship between the thrust readings and the temperature gradient. Results of this calibration indicated that five minutes of hovering at moderate temperatures and 10 minutes in cold weather would be sufficient to stabilize the thrust reading and provide a good zero reference. All subsequent flights required an appropriate hover and zero reference calibration prior to the actual data acquisition flight.

Laboratory calibrations of the wing spar bending moments in terms of wing lift, with the center of pressure at various spanwise and chordwise locations, showed repeatable results. However, upon installation of the wing on the aircraft, it was found necessary to replace the attachment bolts with tapered pins to ensure symmetrical distributions of wing loads among the four wing attachments. Even then, a continuing erratic behavior of the wing lift data remained. As a result, the wing/body lift was determined most reliably from the direct measurement of rotor shaft thrust in combination with gross weight.

#### MEASUREMENTS

Oscillograph and photopanel measurements recorded during the test program are given in Tables IV and V. The individual parameters recorded in each of the configurations are noted by an asterisk (\*) in the Tables.

#### ACCURACY

The estimated accuracies of the measurements are presented in Table VI. These accuracies are based on best engineering estimates at the conclusion of the test program.

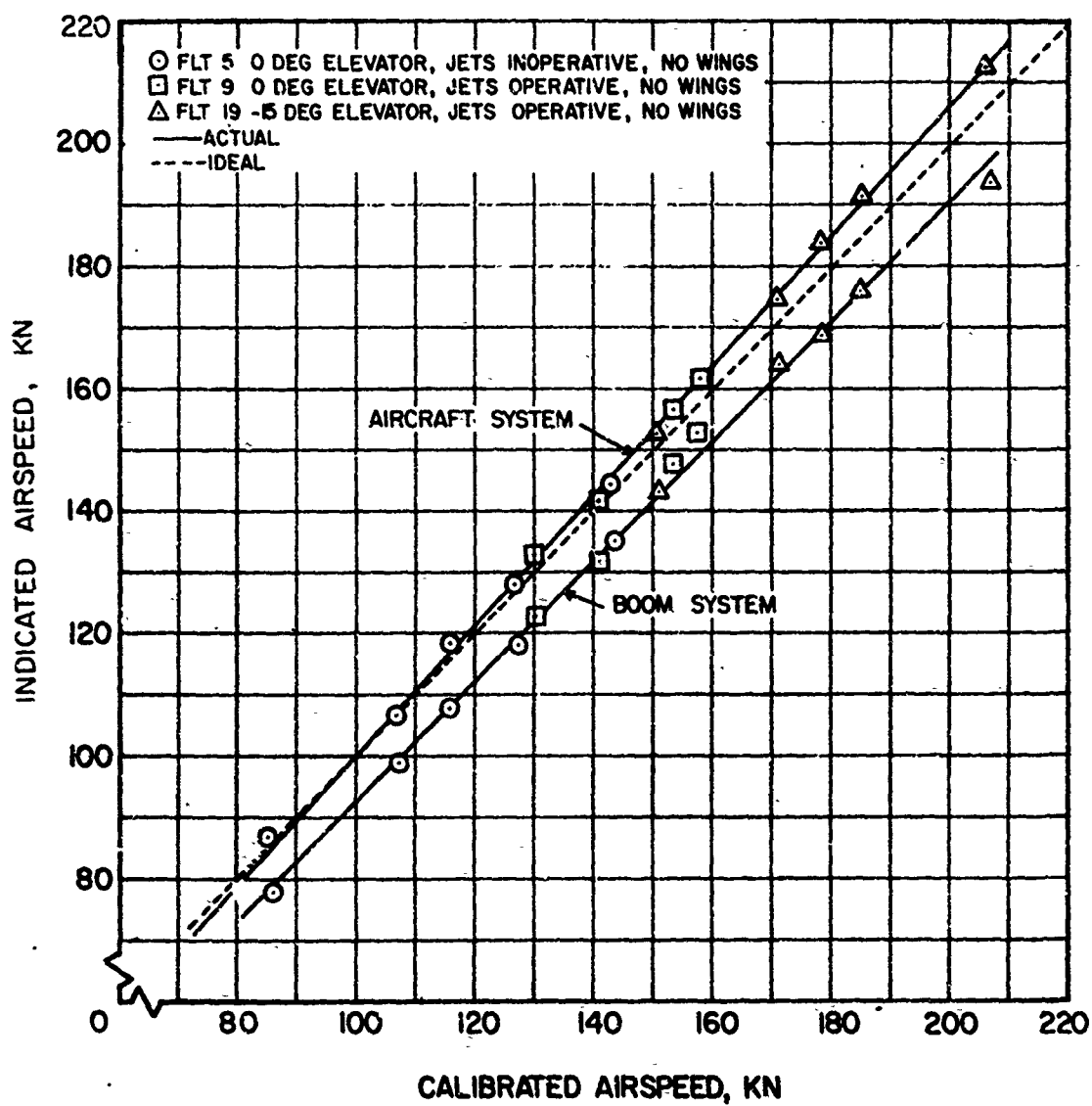


FIGURE 55. AIRSPEED CALIBRATIONS.

TABLE III  
NH-3A CONTROL RIGGING

CONTROL	COCKPIT CONTROL POSITION (%)	CONTROL SURFACE (DEG.)					
		FLT. 14-53	FLT. 56-70	FLT. 71-80	FLT. 95-99	FLT. 104-134	
COLLECTIVE:	$\delta \theta = 100$	18.36	21.94	21.94	22.11	18.64	
	$*\delta \theta_0 = 15$	3.76	7.32	7.32	7.28	3.39	
LONGITUDINAL CYCLIC:	$\delta B_{1S} = 100$	14.50	14.25	14.25	14.30	14.40	
	$\delta B_{1S} = 0$	-10.15	-10.45	-10.45	-10.90	-10.85	
LATERAL CYCLIC:	$\delta B_{1S} = 100$	14.95	15.15	15.15	15.05	14.75	
	$\delta B_{1S} = 0$	-10.30	-10.35	-10.35	-10.60	-10.90	
PEDAL POSITION:	$\delta A_{1S} = 100$	7.20	7.15	7.15	7.10	7.40	
	$\delta A_{1S} = 0$	-7.80	-7.70	-7.70	-8.00	-7.95	
COLLECTIVE	$\delta A_{1S} = 100$	6.60	6.80	6.80	6.75	6.75	
	$\delta A_{1S} = 0$	-8.45	-8.65	-8.65	-8.65	-8.60	
COLLECTIVE	$\delta Ped = 100$	-7.0	-7.0	-6.6	-6.8	-7.0	
	$\delta Ped = 0$	25.0	25.0	24.9	24.0	25.0	
COLLECTIVE	$\delta Ped = 100$	-5.6	-5.6	-4.8	-5.4	-5.6	
	$\delta Ped = 0$	25.5	25.5	25.4	24.9	25.5	

NOTE: \*RELATIONSHIP BETWEEN  $\delta \theta$  AND  $\theta_{CUFF}$  IS LINEAR BETWEEN 15-100% HOWEVER  $\theta_{CUFF}$  REMAINS CONSTANT BETWEEN 0-15%



TABLE IV

OSCILLOGRAPH MEASUREMENTS

## CONFIGURATION

1. Helicopter plus jets, 5 blades,  $-4^{\circ}$  twist.
2. Helicopter plus jets, 5 blades,  $-8^{\circ}$  twist.
3. Helicopter plus jets & wing, 5 blades,  $-4^{\circ}$  twist.
4. Helicopter plus jets & wing, 5 blades,  $-8^{\circ}$  twist.
5. Helicopter, 5 blades,  $-4^{\circ}$  twist.
6. Helicopter, 5 blades,  $-8^{\circ}$  twist.
7. Helicopter plus jets, 6 blades,  $-4^{\circ}$  twist.
8. Helicopter plus jets, 6 blades,  $-8^{\circ}$  twist.

MEASUREMENT	CONFIGURATION							
	1	2	3	4	5	6	7	8
Longitudinal stick position	*	*	*	*	*	*	*	*
Lateral stick position	*	*	*	*	*	*	*	*
Collective stick position	*	*	*	*	*	*	*	*
Rudder pedal position	*	*	*	*	*	*	*	*
Pitch attitude	*	*	*	*	*	*	*	*
Roll attitude	*	*	*	*	*	*	*	*
M. R. blade pitch	*	*	*	*	*	*	*	*
M. R. blade flapping	*	*	*	*	*	*	*	*
M. R. blade lag	*	*	*	*	*	*	*	*
M. R. blade total stress TE-1	*	*	*	*	*	*	*	*
M. R. blade total stress TE-4	*	*	*	*	*	*	*	*
M. R. blade total stress TE-7	*	*	*	*	*	*	*	*
M. R. blade total stress BR-6	*	*	*	*	*	*	*	*
M. R. blade total stress BR-7	*	*	*	*	*	*	*	*
M. R. blade normal bending stress NBR-1	*	*	*	*	*	*	*	*
M. R. blade normal bending stress NBR-3	*	*	*	*	*	*	*	*
M. R. blade normal bending stress NBR-5	*	*	*	*	*	*	*	*
M. R. blade normal bending stress NBR-7	*	*	*	*	*	*	*	*
M. R. blade normal bending stress NBR-9	*	*	*	*	*	*	*	*
M. R. blade torsional stress Q-2	*	*	*	*	*	*	*	*
M. R. blade torsional stress Q-4	*	*	*	*	*	*	*	*
M. R. blade torsional stress Q-7	*	*	*	*	*	*	*	*
M. R. thrust	*	*	*	*	*	*	*	*
M. R. shaft torque	*	*	*	*	*	*	*	*
M. R. shaft longitudinal shear force (X)			*	*				
M. R. shaft lateral shear force (Y)			*	*				
M. R. shaft total shear force							*	*
M. R. shaft longitudinal bending moment (X)			*	*				
M. R. shaft lateral bending moment (Y)			*	*				
M. R. shaft bending stress	*	*	*	*	*	*	*	*
M. R. push rod load	*	*	*	*	*	*	*	*

TABLE IV (Continued)

MEASUREMENT	CONFIGURATION							
	1	2	3	4	5	6	7	8
M. R. stationary scissors load	*	*	*	*	*	*	*	*
M. R. rotating scissors load	*	*	*	*	*	*	*	*
M. R. spindle edgewise bending stress							*	
M. R. spindle flatwise bending stress							*	
Right lateral stationary starload	*	*	*	*	*	*	*	*
M. R. head total stress UP-1							*	
M. R. head total stress UP-2							*	*
M. R. head total stress UP-3							*	
M. R. head total stress VH-1							*	
M. R. head total stress VH-2							*	
M. R. head total stress VHR-2								*
M. R. head total stress VHR-1								*
M. R. head total stress VHR-3								*
T. R. blade pitch	*	*	*	*	*	*	*	*
T. R. blade flapping	*	*	*	*	*	*	*	*
T. R. blade edgewise bending stress LR-TR	*	*	*	*	*	*	*	*
T. R. blade normal bending stress NB-R	*	*	*	*	*	*	*	*
T. R. blade total stress L-1	*	*						
T. R. spindle edgewise bending stress		*	*	*	*	*	*	*
T. R. pitch beam bending load	*	*	*					
T. R. pitch actuator arm load	*	*	*	*	*	*	*	*
T. R. shaft torque	*	*	*	*	*	*	*	*
Tail pylon total stress P-1	*	*	*	*	*	*	*	*
Tail pylon total stress P-2	*							
Tail pylon total stress P-3	*	*					*	*
Tail pylon total stress P-4	*							
Tail pylon total stress P-5	*							
Tail pylon total stress P-6	*	*					*	*
Tail pylon total stress P-7	*	*						
Tail pylon total stress P-8	*							
Tail pylon total stress P-9	*							
Tail pylon total stress P-10	*							
Tail pylon total stress P-11	*	*					*	*
Tail pylon total stress P-12	*							
Tail pylon total stress P-13	*	*					*	*
Tail pylon total stress P-14	*							
Tail pylon total stress P-15	*							
Tail pylon total stress P-16	*							
Tail pylon total stress P-17	*	*					*	*
Tail pylon total stress P-18	*							
Tail pylon web total stress PW-1	*							
Tail pylon web total stress PW-2	*							
Tail pylon web total stress PW-3	*	*					*	*
Tail cone total stress TC-1	*	*	*				*	*
Transmission area total stress WSL-13	*	*	*	*			*	*
Transmission area total stress TLF-160A	*	*	*				*	*
Transmission area total stress TRO-18	*	*	*	*			*	*

TABLE IV (Continued)

MEASUREMENT	CONFIGURATION							
	1	2	3	4	5	6	7	8
Transmission area total stress TLO-18	*				*	*		
Transmission area total stress TRR-160F	*							
Transmission area total stress TRO-16A	*	*					*	*
Transmission area total stress TRO-15A	*							
Transmission area total stress TLFF-6		*			*	*		
Transmission area total stress TLF-160A-2		*			*	*		
Bendix coupling total stress C-1	*	*						
Bendix coupling total stress C-2	*	*						
Jet engine attachment total stress EA-1	*	*					*	*
Jet engine attachment total stress EA-2	*	*					*	*
Jet engine attachment total stress EA-3	*	*					*	*
Stabilizer total stress RST-1	*	*					*	*
Stabilizer total stress RST-3	*	*					*	*
Stabilizer total stress RSB-1	*	*		*	*	*	*	*
Stabilizer total stress RSB-2	*	*					*	*
Stabilizer total stress RSB-3	*	*					*	*
Stabilizer total stress LST-1	*	*					*	*
Stabilizer total stress LST-3	*	*					*	*
Stabilizer total stress LSB-1	*	*		*	*	*	*	*
Stabilizer total stress LSB-2	*	*					*	*
Stabilizer total stress LSB-3	*	*					*	*
Left stabilizer lift	*	*	*	*			*	*
Right elevator moment			*				*	*
Rudder moment								
Right wing lift			*	*				
Left wing lift			*	*				
Right wing flap moment			*	*				
Left wing flap moment			*	*				
Right wing bending stress at root			*	*				
Left wing bending stress at root			*	*				
Right wing total stress BFS-1			*	*				
Right wing total stress TAS-1			*	*				
Left wing total stress BFS-1			*	*				
Left wing total stress TAS-1			*	*				
Yaw rate	*							
Pitch rate	*							
Roll rate	*							
Normal acceleration at c.g.	*	*	*	*	*	*	*	*
Vertical acceleration at pilot (seat)	*	*	*	*	*	*	*	*
Lateral acceleration at pilot (seat)	*	*	*	*	*	*	*	*
Vertical velocity at pilot (seat)		*	*	*			*	*
Vertical velocity at pilot (floor)		*	*	*			*	*
Lateral velocity at #1 J-60	*						*	*
Lateral velocity at #2 J-60	*	*	*	*			*	*
Vertical velocity at #1 J-60	*	*	*	*			*	*
Vertical velocity at #2 J-60	*							
Vertical velocity at #1 T-58							*	

TABLE IV (Continued)

MEASUREMENT	CONFIGURATION							
	1	2	3	4	5	6	7	8
Lateral velocity at #1 T-58							*	
Vertical acceleration at tail rotor gear box	*	*	*	*	*	*	*	*
Lateral acceleration at tail rotor gear box	*	*	*	*			*	*
Vertical acceleration at left stabilizer tip	*	*	*	*			*	*
Vertical acceleration at right stabilizer tip	*	*	*	*			*	*
Vertical acceleration at left wing tip			*	*				
Vertical acceleration at right wing tip			*	*				

TABLE V

PHOTOPANEL MEASUREMENTS

## CONFIGURATION

1. Helicopter plus jets, 5 blades,  $-4^{\circ}$  twist.
2. Helicopter plus jets, 5 blades,  $-8^{\circ}$  twist.
3. Helicopter plus jets & wing, 5 blades,  $-4^{\circ}$  twist.
4. Helicopter plus jets & wing, 5 blades,  $-8^{\circ}$  twist.
5. Helicopter, 5 blades,  $-4^{\circ}$  twist.
6. Helicopter, 5 blades,  $-8^{\circ}$  twist.
7. Helicopter plus jets, 6 blades,  $-4^{\circ}$  twist.
8. Helicopter plus jets, 6 blades,  $-8^{\circ}$  twist.

MEASUREMENT	CONFIGURATION							
	1	2	3	4	5	6	7	8
Main rotor speed	*	*	*	*	*	*	*	*
Rate of climb	*	*	*	*	*	*	*	*
Airspeed (ships system)	*	*	*	*	*	*	*	*
Airspeed (nose boom system)	*	*	*	*	*	*	*	*
Altitude	*	*	*	*	*	*	*	*
Outside air temperature	*	*	*	*	*	*	*	*
Yaw angle	*	*	*	*	*	*	*	*
Fuselage angle of attack	*	*	*	*	*	*	*	*
Elevator position	*	*	*	*	*	*	*	*
Rudder position	*	*	*	*	*	*	*	*
Wing flap position	*	*	*	*	*	*	*	*
No. 1 T-58 free turbine speed	*	*	*	*	*	*	*	*
No. 2 T-58 free turbine speed	*	*	*	*	*	*	*	*
No. 1 T-58 engine torque	*	*	*	*	*	*	*	*
No. 2 T-58 engine torque	*	*	*	*	*	*	*	*
No. 1 J-60 turbine speed	*	*	*	*	*	*	*	*
No. 2 J-60 turbine speed	*	*	*	*	*	*	*	*
No. 1 J-60 fuel flow	*	*	*	*	*	*	*	*
No. 2 J-60 fuel flow	*	*	*	*	*	*	*	*
No. 1 J-60 compressor inlet pressure	*	*	*	*	*	*	*	*
No. 2 J-60 compressor inlet pressure	*	*	*	*	*	*	*	*
No. 1 J-60 turbine discharge pressure	*	*	*	*	*	*	*	*
No. 2 J-60 turbine discharge pressure	*	*	*	*	*	*	*	*
Clock	*	*	*	*	*	*	*	*

TABLE VI

INSTRUMENTATION ACCURACIES

<u>Item</u>	<u>Parameter</u>	<u>Calibration Accuracy</u>	<u>Resolution</u>	<u>Remarks</u>
1.	J-60 Thrust No. 1 Engine No. 2 Engine	+4.0% +4.0%	+0.15% +0.15%	Calibration accuracy reflects difference between test cell curve and aircraft installation.
2.	M.R. Thrust	+1.0%	+500 lb	Calibration accuracy shown is at a constant temperature. Thrust measurements prior to Flight #49 are not valid for the first 10 minutes of flight because of temperature shifts.
3.	M.R. Torque	+1.0%	+250 ft-lb	
4.	M.R. Pitch	+1.0%	+0.25 deg	
5.	M.R. Flapping	+1.5%	+0.25 deg	
6.	M.R. Lag	+1.0%	+0.1 deg	
7.	M.R. Push Rod Load	+1.5%	+25 lb	
8.	M.R. Rt. Lat Star Id.	+1.5%	+50 lb	
9.	T.R. Flapping	+0.5%	+0.25 deg	
10.	T.R. Pitch	+0.5%	+0.25 deg	
11.	M.R. Blade Stress BR-7 NBR-7 TE-7 Q-2	+1.0% +1.0% +1.0% +1.0%	+100 psi +200 psi +100 psi + 50 psi	

TABLE VI (Continued)

<u>Item</u>	<u>Parameter</u>	<u>Calibration Accuracy</u>	<u>Resolution</u>	<u>Remarks</u>
12.	T.R. Blade Stress LE-TR NE-R	+1.0% +7.0%	+100 psi +150 psi	
13.	M.R. Shaft Shear x direction y direction	+50 lb +50 lb	+25 lb +25 lb	Multiple shifts in zero position makes data useless, due to effects of higher harmonics on circuit design.
14.	M.R. Hub Moment x direction y direction	+10 ft-lb +10 ft-lb	+250 ft-lb +250 ft-lb	Multiple shifts in zero position makes data useless, due to effects of higher harmonics on circuit design.
15.	Aircraft Altitude Pitch Roll	+0.5 deg +0.5 deg	+0.25 deg +0.25 deg	
16.	Vertical Acceleration Pilot Seat C.G.	+1.0% +1.0%	+0.1 g +0.1 g	
17.	Lateral Acceleration Pilot Seat C.G.	+1.0% +1.0%	+0.1 g +0.1 g	
18.	Fwd. Trans. Support WSL-L3	+2.0%	+100 psi	
19.	Airspeed (in side slip)	-----	-----	Airspeed calibration flights in yaw are required to determine the system accuracy.

TABLE VI (Continued)

<u>Item</u>	<u>Parameter</u>	<u>Calibration Accuracy</u>	<u>Resolution</u>	<u>Remarks</u>
20.	Angle of Sideslip	$\pm 1.0$ deg	$\pm 0.5$ deg	Elevator positioned with pilots indicator.
21.	Elevator position	$\pm 0.5$ deg	$\pm 0.5$ deg	



# APPENDIX III

## TABLE VII

### TYPICAL FLIGHT TEST DATA

FLIGHT NUMBER	CONFIG. NO.	TAIL INC. $\delta_T$ (DEG)	ELE. DEFL. $\delta_e$ (DEG)	FLAP DEFL. $\delta_f$ (DEG)	CAS (KTS)	SRP	JET THRUST (LBS)	ROTOR THRUST (LBS)	ROTOR DRAG (LBS)	FUS. PITCH ATTITUDE (DEG)	g-TS (%)	LAT. CYC. $A_{1S}$ (%)	LOM. CTC. $P_{1S}$ (%)	FLAPPING $a_{1S}$ (DEG)
8	1	+5	0	No Wing	152.2	877	2930	18200	140	-0.8	66	59	48	7.0
		+5	0		159.4	867	3160	18800	440	-0.8	66	59	46	7.8
12	1	+5	-15		155.4	975	2990	16800	-50	1.2	67	60	73	3.0
14	1	+5	-15		85.8	1040	580	---	---	3.6	66	54	66	
					108.2	1012	1390	---	---	4.0		55	69	
					123.2	959	1800	---	---	3.8		56	70	
					140.5	947	2260	---	---	3.7		59	72	
					169.7	1023	3800	---	---	4.1		60	72	
					176.9	1123	4360	---	---	4.0		61	71	
					186.4	1366	4840	---	---	4.8		63	71	
16	1	+5	-15		85.2	794	1320	---	---	4.9	57	52	63	2.0
					106.5	730	1660	---	---	5.8		55	65	1.1
					128.3	691	2300	---	---	5.7		59	67	.90
					143.3	678	2800	---	---	4.5			67	.40
					157.2	678	3940	16800	930	6.5			65	2.1
					170.2	756	4110	---	---	4.3	58	60	65	2.0
					178.7	787	4370	---	---	3.2	66	63	66	1.2
					188.3	911	4900	15600	570	3.1				
18	1	+5	-15		93.4	485	2410	---	---	5.5	44	57	62	2.1
					132.1	470	3160	---	---	5.2		58	61	1.1
					151	427	3900	15000	905	6.0		61	62	1.7
					161.7	398	4490	15000	1180	7.6		61	61	2.3
					170.6	410	4750	14500	1070	5.6		63	60	3.0
					177	456	5340	14000	1330	7.2		64	60	3.1

\*Indicates peak-to-peak

\*\* CONFIGURATION

1. Helicopter plus jets, 5 blades, -4° twist.
2. Helicopter plus jets, 5 blades, -8° twist.
3. Helicopter plus jets & wing, 5 blades, -4° twist.
4. Helicopter plus jets & wing, 5 blades, -8° twist.
5. Helicopter, 5 blades, -4° twist.
6. Helicopter, 5 blades, -8° twist.
7. Helicopter plus jets, 6 blades, -4° twist.
8. Helicopter plus jets, 6 blades, -8° twist.

TABLE VII (Continued)

FLIGHT NUMBER	CONFIG. NO.	TAIL INC. $\delta_{IT}$ (DEG)	M.E. DEVL. $\delta_e$ (DEG)	FLAP DEVL. $\delta_f$ (DEG)	CAS (KTS)	SEP	JET THRUST (LBS)	ROTOR THRUST (LBS)	ROTOR DRAG (LBS)	FUS. PITCH ATTITUDE (DEG)	0.75 (%)	LAV. CYC. $A_{LS}$ (%)	LOM. CYC. $B_{LS}$ (%)	FLAPPING $\theta_{LS}$ (DEG)
20	1	+5	-15	No Wing	84	1200	0	---	---	3.5	---	54	64	1.7
					105	1300	0	---	---	2.9	---	55	71	1.6
					115.8	1510	0	---	---	2	---	54	74	1.8
					123	1570	0	---	---	1.9	---	53	76	1.6
					135	2200	0	---	---	1.9	---	49	84	1.7
					122.5	1630	520	---	---	2.5	86	52	77	2.1
					133.2	1620	1020	---	---	2.2	---	54	80	2.6
					141.3	1560	1290	---	---	2.7	---	54	79	2.1
					153.5	1540	2030	18400	-780	4	---	52	80	2.2
					161.7	1570	2510	18400	-610	4.9	---	54	81	2.1
24	3	+5	-10	0	167.8	1600	2970	17300	-420	3.8	---	55	80	3.1
					162.3	0	5200	14400	17800	6.7	24	63	46	2.1
					148.5	848	2860	17800	320	1.1	64	46	58	---
25	3	+5	-10	0	158.7	869	3270	18000	390	0.9	65	46	57	---
					153.4	865	2750	15890	10	3.8	62	47	68	---
					157.9	865	3260	15700	370	3.8	---	48	67	---
					158.5	980	3270	10990	40	7.3	---	51	91	---
26	3	+5	-15	0	158.5	827	3240	16650	350	4.8	---	50	68	---
					157	873	3290	16020	410	3.6	62	46	65	1.2
					168.6	871	3640	15820	240	3.9	---	66	66	1.6
					175.9	859	4190	15420	390	3.5	---	55	55	1.8
27	3	+5	-13	0	183.8	503	4730	15000	510	4.2	---	44	64	3.0
					190	910	5290	14950	790	4.5	---	45	65	2.6
					167.4	868	3770	15800	440	4.2	62	OUT	65	---
					181	905	4690	15100	640	4.0	---	---	64	---
					182.6	932	4650	13300	200	3.8	---	---	65	---
					182	965	4630	12400	-40	3.4	---	---	66	---

TABLE VII (Continued)

FLIGHT NUMBER	CONFIG. NO.	TAIL INC. $\delta_{HT}$ (DEG)	ELE. DEFL. $\delta_e$ (DEG)	FLAP DEFL. $\delta_f$ (DEG)	CAS (KTS)	SHIP	JET THRUST (LBS)	ROTOR THRUST (LBS)	ROTOR DRAG (LBS)	POS. PITCH ATTITUDE (DEG)	$\alpha_{TS}$ (°)	LAT. CYC. $\beta_{LS}$ (°)	LOC. CYC. $\beta_{LS}$ (°)	FLAPPING $\alpha_{LS}$ (DEG)
21	3	+5	-13	14	179	1010	1500	11200	-370	3.0	62	OUT	72	
					173.9	933	1490	11700	90	2.0			60	
					179	1008	1470	8000	-160	5.2			93	
					180.6	1018	1480	11800	190	6.2			77	
					188.6	1373	1620	12400	-730	2.9			78	
37	3	0	+5	0	164	842	3440	16200	520	2.7	63	1.6	59	3.4
					173.5	865	4390	16400	782	2.8	63	1.7	58	1.1
					182.6	895	4915	16500	145	3.7	62	1.6	57	1.8
					185.9	962	5110	15200	870	2.3	62	1.8	59	1.8
					190.8	945	5515	15200	805	2.5	61	1.6	56	1.9
					174.8	995	1010	11200	-80	5.0	63	1.6	76	-1.9
					180.2	1007	1460	10300	-30	5.2	63	1.7	76	-2.0
					189	1112	5100	9200	0	5.0	65	1.6	79	-2.5
					110.2	706	1320	----	----	5.4	52	1.7	64	
					120.8	675	1880	----	----	7.1		1.8	56	
38	3	0	0	+4	145.2	722	3130	11000	50	5.4		1.8	68	
					159.6	737	3550	11000	50	5.2		1.7	67	
					168.8	782	4265	8800	70	6.4		1.7	69	
					177.8	816	4640	8800	70	6.0		1.7	70	
					180	887	5445	----	----	5.5	0	1.7	70	
					171.8	348	5465	3600	635	8.0		1.7	46	
					125.8	1667	490	----	----	2.1	85	1.3	77	
					128.8	1638	660	----	----	2.1	84	1.2	77	
					144.2	1614	1515	----	----	3.0		1.3	40	
					170.5	1590	2515	15400	-1085	2.8		1.4	82	
39	3	0	0	+4	173.9	1608	3110	14500	-880	3.7		1.2	83	
					184	1602	4025	----	----	4.2		1.2	85	
					199.3	1668	5485	11200	-595	5.0	0	1.3	86	
					139	121	5360	----	----	9.0		1.6	29	

TABLE VII(Continued)

FLIGHT NUMBER	CONFIG. NO.	TAIL INC. $\delta_{IT}$ (DEG)	ELE. DEFL. $\delta_e$ (DEG)	FLAP DEFL. $\delta_f$ (DEG)	CAS (KTS)	SHIP	JET THRUST (LBS)	ROTOR THRUST (LBS)	ROTOR DRAG (LBS)	FUS. FITCH ATTITUDE (DEG)	8.75 (%)	LAT. CYC. $\alpha_{LS}$ (%)	LONG. CYC. $\beta_{LS}$ (%)	FLAPPING $\alpha_{LS}$ (DEG)
45	3	0	0	+4	63.4	1138	---	---	---	5.4	66	OUT	62	
					84.5	1105	---	---	---	4.2	65		65	
					105.2	1268	---	---	---	3.1	72		70	
					115	1465	---	---	---	2.9	76		74	
					124.1	1607	---	---	---	2.1	81		77	
					146.6	2100	---	---	---	1.7	96		84	
					148.8	2210	---	---	---	1.6	102		86	-1.5
					170.1	1558	2930	14400	-630	1.5	87		90	-4.2
					199.3	1642	5420	12200	-80	4.5	83		86	-4.2
					135.2	2045	510	---	---	1.2	91	4.8	93	-2.2
47	3	0	+2	+1	153	1958	1240	15500	-1520	0.9	91	4.8	91	-2.2
					163.0	1970	1820	---	---	1.7	97	4.2	87	2.3
					171.8	1982	2370	17000	-1130	1.8	102	4.2	84	2.5
					178.8	2005	2950	16200	-930	2.0	39	3.9	85	1.1
					187	2005	3670	---	---	1.7	40	4.0	84	1.0
					194.2	2037	4500	15000	-360	3.8	34	3.5	84	2.0
					197.3	1982	5200	13400	-60	3.1	33	3.3	73	-1.2
					80.3	992	---	---	---	2.6	49	4.2	62	
					102	1118	---	---	---	1.4	55	4.4	67	
					111	1282	---	---	---	0.8	60	4.3	70	
56	4	0	0	+4	120	1454	---	---	---	0.9	68	4.2	77	
					131	1620	---	---	---	0.5	74	4.1	80	
					143	2180	---	---	---	-0.3	83	4.1	84	
					149	2350	2620	18800	2620	-0.1	80	4.4	84	
					104.4	954	1420	---	---	2.1	67	4.4	67	
					123	916	1740	---	---	1.4	67	4.4	67	
					142.2	926	2470	---	---	3.3	70	4.7	70	
					164.2	984	3030	12400	-230	2.1	71	4.7	71	
					169.5	978	3740	11900	60	3.7	71	4.5	71	
					180	1050	4560	---	---	3.1	74	4.5	74	

TABLE VII(Continued)

FLIGHT NUMBER	CONFIG. NO.	TAIL INC. $\delta_{IT}$ (DEG)	ELE. DEFL. $\delta_e$ (DEG)	FLAP DEFL. $\delta_f$ (DEG)	CAC (KTS)	3HP	JET THRUST (LBS)	ROTOR THRUST (LBS)	ROTOR DRAG (LBS)	FUS. PITCH ATTITUDE (DEG)	$\epsilon_{75}$ (%)	LAI. CYC. $\epsilon_{LC}$ (%)	LOS. CYC. $\epsilon_{LC}$ (%)	FLAPPING $\epsilon_{LC}$ (DEG)
56	4	0	+2	+4	186.5	1114	4960	9000	60	3.0	48	45	74	
					190	1176	5500	8000	340	3.4		44	77	
					143.9	303	4650	19800	2620	8.0	0	49	58	
					171.4	418	5210	5000	840	6.0		52	59	
					174.5	413	5490	5000	890	6.3		49	59	
					161.1	684	3500	11300	280	3.1	40	45	68	
					181.5	752	4910	8800	210	3.7		45	70	
					188.7	750	5500	4000	310	3.5		44	71	
					105.2	1142	600	----	----	OUT	58	48	OUT	
					121	1094	1170	----	----			47		
57	4	0	+2	+4	148.8	1068	2250	15200	-430			47		
					161.7	1112	2970	13800	-240			48		
					171	1128	3060	1270	-50			47		
					179.6	1112	4190	----	----			45		
					187.8	1180	5110	9800	140			46		
					194	1260	5430	8500	20			45		
					124	1328	600	----	----	0	65	47	72	
					141.9	1286	1340	----	----	1.3		47	75	
					160.8	1292	2660	----	----	1.8		45	77	
					177.8	1342	3720	----	----	1.8		43	79	
58	4	0	+2	+4	185.2	1395	4220	----	----	2.4		42	79	
					195.1	1517	5490	----	----	3.6		37	80	
					163.5	913	3060	13800	-180	1.4	44	46	57	
					163	932	3070	13500	-150	3.2		48	58	
					164.7	897	3030	14200	-260	0.6		42	55	
					166.8	880	3010	14600	-370	2.0		37	54	

TABLE VII(Continued)

FLIGHT NUMBER	CONFIG. NO.	TAIL INC. $i_{HT}$ (DEG)	ELE. DEFL. $\delta_e$ (DEG)	FLAP DEFL. $\delta_f$ (DEG)	CAS (KTS)	SHP	JET THRUST (LBS)	ROTOR THRUST (LBS)	ROTOR DRAG (LBS)	FUS. PITCH ATTITUDE (DEG)	6.75 (%)	LAT. CYC. $A_{1S}$ (%)	LCN. CYC. $B_{1S}$ (%)
60	4	0	+2	+4	81	497	2100	---	---	7.8	30	46	60
					101.2	490	2160	---	---	5.9		47	62
					119.7	502	2590	---	---	5.2		48	64
					138	522	3090	---	---	4.5		47	62
					162	555	3950	9000	460	4.4		48	64
					172.3	602	4530	1250	410	4.5		50	65
					178	659	4850	7300	370	3.2		49	64
					189	768	5520	5900	260	4.8		44	64
					112.5	76	3920	---	---	10.2	0	45	53
					98.5	36	3390	---	---	10.5		47	52
64	4	0	+2	+4	88.4	40	3860	---	---	12.4		45	54
					135.3	1722	550	---	---	---			
					143.8	1722	990	---	---	---			
					153.5	1700	1280	---	---	---			
					163.2	1680	1860	12000	-220	---			
					172.8	1730	2870	10900	-460	---			
					179.5	1737	3380	5300	-560	---			
					187.3	1808	4260	7900	-100	---			
					198.0	1888	5440	9200	130	---			
					167.4	987	3580	9700	-442	2.4	50	42	72
67	4	0	+2	+10	176.8	1025	4600	9300	-10	3.4		40	74
					182.5	1083	5330	6700	240	5.2		39	76
					160.8	947	3440	8800	-110	3.8		42	74
					170.2	972	4330	6900	130	4.2		44	78
					176.8	1008	5270	4900	110	4.0		44	81
					182	1058	5330	4200	-270	3.6		42	81
					165.9	908	2780	11800	-640	0.8		46	64
					160.8	942	3800	10500	100	3.0		45	64

TABLE VII(Continued)

FLIGHT NUMBER	CONFIG. NO.	TAIL INC. $\delta_{HT}$ (DEG)	ELE. DEFL. $\delta_e$ (DEG)	FLAP DEFL. $\delta_f$ (DEG)	CAS (KTS)	SHP	JET THRUST (LBS)	ROTOR THRUST (LBS)	ROTOR DRAG (LBS)	FUS. PITCH ATTITUDE (DEG)	$\epsilon$ 75 (\$)	LAT. CYC. $A_{1S}$ (\$)	LOX. CYC. $B_{1S}$ (\$)
70	1	0	+2	+4	160	1450	2340	16000	-790	3.7	69	43	77
					168.2	1411	2750	14800	-720	2.8		41	72
					179.9	1418	3430	13400	-420	3.7		41	78
					193	1495	4760	12600	-420	3.6		41	81
					193.4	1587	5080	11000	-230	5.7		42	82
71	2	0	0		84	956	IDLE	---	---	4.5	49	46	66
					102.1	940	1100	---	---	5.0		48	69
					123.4	890	1550	---	---	4.3		49	71
					141.5	893	2590	---	---	7.8		51	77
					153	935	3160	14750	270	8.0		55	77
					158.8	940	3650	14200	200	6.7		55	78
					173.3	958	4210	13600	520	6.9		55	79
					186.3	1065	4880	12700	490	6.6		48	67
					83.5	965	IDLE	---	---	4.5		49	69
					101.9	913	1300	---	---	5.9		51	72
					122.4	861	2050	---	---	7.2		52	72
					141.6	855	2230	---	---	6.0		54	74
					157	875	3360	15250	470	6.1		56	76
					163.8	922	3710	13700	380	7.2		51	74
					173	874	3980	1300	270	6.6		51	74
72	2	0	+2		187.2	1042	4940	12500	600	8.1		51	74
					160.7	1052	3370	14640	310	5.8	55	52	73
					178.5	1140	4640	13170	740	4.5	55	53	76
					166.5	679	4210	12200	680	5.4	40	56	68
					176	770	4950	12280	920	9.3		70	70
					184	817	5470	11060	1120	9.0		70	70

TABLE VII (Continued)

FLIGHT NUMBER	CONFIG. NO.	TAIL INC. HT (DEG)	ELE. DEFL. $\delta_e$ (DEG)	FLAP DEFL. $\delta_f$ (DEG)	CAS (KTS)	SHF	JET THRUST (LBS)	ROTOR THRUST (LBS)	ROTOR DRAG (LBS)	FUS. PITCH ATTITUDE (DEG)	$\delta_1$ 75 (%)	LAT. CYC. $\delta_1$	LOM. CYC. $\delta_1$
73	2	0	0		101.1	1130	550	---	---	4.6	56	49	72
					119	1090	1130	---	---	4.8		49	75
					139	1065	1840	---	---	5.1		51	78
					162.8	1100	3040	15000	-100	7.0		53	85
					164.2	1140	3500	13800	130	7.1		53	87
					179	1178	4200	13200	220	7.0		50	
					196.2	1338	5540	11000	400	7.3		47	
					165.5	1160	4010	12000	120	13.8	95	54	100
					172.2	1035	5050	10600	520	13.1	50	54	
					147.2	1003	3170	12800	90	11.6	51	56	
					102	1120	0	---	---	4.7	51	44	66
75	2	0	0		102	1112	0	---	---	4.2	58	47	72
					108.5	1315	0	---	---	3.5	60	46	75
					121	1565	0	---	---	3.5	70	47	80
					130.5	1654	0	---	---	2.4	73	45	81
					138	1830	0	---	---	1.7	79	45	85
					142.5	2360	0	---	---	2.1	89	42	92
					85.4	0	4280	---	---	15.5	0	46	55
					105.8	0	4180	---	---	13.6		51	56
					122.6	0	3915	---	---	10.3			55
					141.3	0	4805	---	---	11.1			55
					167	22	5490	8400	0	10.5			58
76	2	0	0		120	1372	150	---	---	3.7	66	47	76
					139	1343	1310	---	---	4.4		50	82
					159.6	1340	2330	1300	-940	4.9		51	87
					165.3	1332	2685	12800	-755	4.9		51	86
					177.8	1379	3745	11000	-565	5.3		49	89



TABLE VII (Continued)

FLIGHT NUMBER	CONFIG. NO.	TAIL INC. HT (DEG)	ELE. DEFL. 5° (DEG)	FLAP DEFL. 5° (DEG)	CAS (KTS)	SNP	JET THRUST (LBS.)	ROTOR THRUST (LBS.)	ROTOR DIAG (LBS.)	FUS. PITCH ATTITUDE (DEG)	9.75 (°)	LAT. CYC. A <sub>25</sub> (°)	LOG. CYC. P <sub>15</sub> (°)
77	2	0	+2		157.5	389	4490	1100	110	7.7	30	54	60
		0			164.7	407	4500	1180	60	8.9	30	55	60
79	2	0	+2	0	158	41	5570	12400	1730	5.0	0	52	47
					178.2	34	5620	12000	1520	8.3	0	55	49
					175.3	962	2634	13000	-1242	3.5	51	55	77
					156	721	3400	11200	-1090	5.9	41	53	74
					176.7	722	3520	12000	-1130	6.8	41	54	74
83	7	0	0		59.7	1221	---	---	---	5.6	54	44	63
					61.9	1182	---	---	---	4.1	52	46	63.5
					101.9	1328	---	---	---	4.0	57	47	71
					120.5	1210	---	---	---	1.5	79	45	83
					130	2150	---	---	---	1.2	83	44	83
90	7	0	+1		141.6	3400	---	---	---	0.7	52	42	58
					93.2	1062	521	---	---	3.4	52	42	58
					102.1	1030	1174	---	---	4.2	52	42	58
					123.7	970	1391	---	---	2.8	52	42	58
					140.2	951	2518	---	---	4.5	52	42	58
					159.5	942	3130	14500	70	3.2	52	42	58
					168.3	915	3890	14400	540	5.0	52	42	58
					174.8	965	4510	13000	730	4.2	52	42	58
					187.2	976	5380	13000	1100	4.3	52	42	58
					196.7	1025	5650	11500	760	4.3	52	42	58
					85	750	1950	---	---	3.8	52	42	58
					100.9	738	1766	---	---	4.9	41	46	58
					119.5	685	2300	---	---	6.0	46	46	58
					138.4	642	2813	---	---	5.2	49	49	58
					156.4	646	3630	1300	1730	5.8	51	51	61

TABLE VII (Continued)

FLIGHT NUMBER	CONFIG. NO.	TAIL INC. $\delta_{HT}$ (DEG)	ELE. DEFL. $\delta_e$ (DEG)	FLAP DEFL. $\delta_f$ (DEG)	CAS (KTS)	SP <sup>2</sup>	JET THRUST (LBS)	ROTOR THRUST (LBS)	ROTOR DRAG (LBS)	FUS. PITCH ATTITUDE (DEG)	$\theta$ .75 (%)	LAT. CYC. $A_{LS}$ (%)	LONG. CYC. $B_{LS}$ (%)
90	7	0	+4		164.7	662	3880	12900	495	3.7	4.1	51	58
					177.3	703	5090	11000	790	4.4		52	58
					186.0	752	5590	10800	970	3.8			59
					190.5	775	5690	10400	830	4.2			60
91	7	0	+4		84.5	503	3130	---	---	10.7	29	47	58
					100.3	458	2502	---	---	7.4		47	56
					121.4	448	2189	---	---	6.2		48	54
					140.7	438	3480	---	---	5.0		49	55
					154.1	440	4030	12500	640	5.2		52	55
					164.5	445	4570	12400	1030	5.3		53	54
					176.7	470	5040	12300	815	5.0		53	53
					183.2	492	5670	11200	290	5.0		46	50
					85	0	4320	---	---	15.0	0	46	46
					99	0	4250	---	---	12.8		51	
					140.9	0	4720	---	---	10.0			
					99.1	1318	550	---	---	2.8	62	49	66
92	7	0	+4		122.5	1260	864	---	---	0.6		50	67
					136.0	1222	1622	---	---	1.7		49	67
					154.6	1190	2398	15000	442	2.5		49	67
					164.4	1178	3334	14000	54	3.7		52	69
					174.4	1152	3640	14000	20	2.3		52	
					185	1170	4370	---	---	3.2		49	
					196.5	1210	5460	12500	560	4.2		52	
					151	0	5360	---	---	6.9	0	53	44
					158.4	0	5520	---	---	7.2		51	42
					163.7	0	5510	---	---	6.5		53	42

TABLE VII (Continued)

FLIGHT NUMBER	CONFIG. NO.	TAIL INC. $\delta_{IT}$ (DEG)	ELE. DEVL. $\delta_e$ (DEG)	FLAP DEVL. $\delta_f$ (DEG)	CAS (KTS)	SRP	JET THRUST (LBS)	ROTOR THRUST (LBS)	ROTOR DRAG (LBS)	MUS. PITCH ATT. (DEG)	$\alpha_{.75}$ (°)	LAT. $A_{LS}$ (°)	LOM. CYC. $B_{LS}$ (°)
93	7	0	+4		154	1330	2275	1127	---	2.3	68	18	72
					165.5	1315	2830	1335	---	2.4			72
					171	1295	3315	1386	---	2.2			71
					194.5	1302	4810	1793	---	2.4			72
					204.5	1390	5690	1950	---	3.5			73
95	8	0	0		81.5	1127	---	---	---	4.9	49	46	67
					101	1284	---	---	---	3.0	49	48	73
					120	1688	---	---	---	3.0	70	47	81
					171	1945	---	---	---	1.9	76	47	85
					136	2211	---	---	---	1.5	82	45	89
96	8	0	+4		85.8	900	1240	---	---	6.2	42	46	63
					101.8	859	1830	---	---	6.5		49.5	64
					120.7	825	1876	---	---	4.5		49	63
					138	830	2330	---	---	5.3		50.5	63
					158.1	740	3170	14000	350	4.6		54.5	64
					168	762	3780	12500	30	2.9		55	64.5
					174.2	750	4370	12000	320	3.8		54	63.5
					187.7	745	5380	---	---	4.5		55.5	63.5
					192.3	775	5630	11000	730	3.8		55.5	64
					101.2	1100	552	---	---	2.0	50	47	63.5
					121.2	1059	1178	---	---	2.0		48.5	66.5
					140.1	1012	1920	---	---	2.9		50.5	67
					158.1	914	3210	12000	450	3.7		52.5	69
					164.8	984	3320	11500	620	3.3		54	69
					173.9	990	4100	11000	150	4.2		53	68.5
					187.3	947	4260	11100	290	3.8		56	68
					194.8	975	5600	10800	700	4.2		55	68.5

TABLE VII  
(Concluded)

FLIGHT NUMBER	CONFIG. NO.	TAIL INC. $\delta_{it}$ (DEG)	ELE. DEVL. $\delta_e$ (DEG)	FLAP $\delta_f$ (DEG)	CAS (KTS)	SRP	JET THRUST (LBS)	ROTOR THRUST (LBS)	ROTOR DRAG (LBS)	FWS. PITCH ATTITUDE (DEG)	$\theta$ .75 (%)	LAT. CYC. $A_{15}$ (%)	LONG. CYC. $B_{15}$ (%)
97	8	0	+4		120.8	1435	491	---	---	2.1	63	47	72
					138	1370	1570	---	---	2.2		50	74
					157	1300	2294	14200	-7.6	2.0		50	
					164.5	1280	2916	13300	-564	2.8		52	
					175	1370	3545	12200	-135	3.0		51	15
					182.5	1240	3550	12400	-800	2.6		51	74
					201.2	1262	5580	11200	390	3.2		52	75
					101.0	587	1994	---	---	7.2	32	46	58
					119	563	2406	---	---	5.8		49	58
					110	523	2393	---	---	4.6		52	57
					156	515	3795	---	---	4.8		53	53
					165.2	532	4290	---	---	5.7		55	60
					173.5	543	4790	---	---	5.1		56	60
					184.3	532	5500	---	---	4.8		57	59
99	8	0	+4		187.2	570	5515	---	---	5.2		57	58
					127.8	0	4360	---	---	8.0	0	51	51
					135.1	0	4200	---	---	9.6		52	49
					159.6	0	5370	---	---	6.3		54	44
					158.8	1040	2280	15200	-640	3.2	54	52	66
					171.1	1005	4180	15000	830	6.3	53	53	69